Dissertation

Great River Wood Dynamics in Northern Canada

Submitted by

Natalie Kramer

Department of Geosciences

In partial fulfillment of the requirements

For the Degree of Doctor of Philosophy

Colorado State University

Fort Collins, Colorado

Summer 2016

Doctoral Committee:

Advisor: Ellen Wohl

Sara Rathburn
Stephanie Kampf
Stephen Leisz

Copyright by Natalie Kramer 2016

All Rights Reserved

Abstract

Great River Wood Dynamics in Northern Canada

Downed wood is a resource easily utilized by plants and animals from the forests to the sea and is essential for many ecosystems. The diverse benefits that wood brings to streams and riparian corridors are well documented by river scientists and wood re-introduction is commonly used as a river restoration tool. However, much of the existing work investigates the short-term impact of wood rather than its variability through time and legacy on the landscape. In this dissertation, I use the Slave River (water discharge=2-7 x10^3 m^3s^{-1}, channel widths=300-2000 m, drainage area=6x10^5 km^2), and its receiving sedimentary basin, the Great Slave Lake (surface area=27^3 km^2, depths 20-600 m, volume 1000-2000 km^3), in northern Canada to better understand wood transport dynamics of a major river basin across varied timescales from minutes to centuries and the influence of driftwood on shoreline landscape evolution. The four primary contributions of this work are: a comprehensive literature review and synthesis of wood transport in rivers worldwide (Chapter 1), new methods for monitoring and quantifying wood flux with timelapse cameras (Chapter 2), description of processes among driftwood, sediment, and vegetation that result in shoreline features that I have coined "driftcretions" (Chapter 3), and expansion of wood transport research into multiple timescales with a focus on how flow history impacts magnitude of wood flux (Chapter 4).

In Chapter 1, I: qualitatively summarize existing transport research around flow, wood and reach characteristics, quantitatively consolidate and analyze wood mobility field data in relation to increasing channel size, identify disconnects between driving processes and how mobility is measured, and constrain and conceptualize thresholds between wood dynamic

regimes. In Chapter 2, I introduce a cheap, useful and fast way to monitor and estimate wood flux with timelapse photography through the use of the metric $\hat{p}$, the probability of seeing wood within a timeframe, and I provide statistical methods to estimate appropriate sampling intervals to minimize bias and variance. In Chapter 3, I describe processes and rates by which pulsed driftwood export are delivered and accreted to shorelines and I discuss how these processes influence rates of carbon sequestration, sediment storage and habitat formation. In Chapter 4, I use a variety of methods centered around repeat photography and anecdotes to assess temporal variability of pulsed driftwood flux through the Slave River in the past century.

Findings in this dissertation provide useful information for understanding pulsed wood flux, shoreline dynamics and landforms in marine and terrestrial water bodies before widespread historical deforestation, damming of rivers, and wood removal along major waterways. I not only synthesize and link existing work on wood mobilization, transport and deposition to an intriguing case study, but challenge existing wood transport premises, provide new conceptual models describing processes of wood transport through drainage networks, and present new approaches and methods for quantifying and analyzing the variability in wood flux and influence of wood deposits on landforms. My descriptions of wood transport and shoreline processes prior to development of river corridors will be an invaluable resource to groups who seek to identify environmental impacts of dams and to scientists who are investigating the impact that past and future development of river corridors has had or will have on ecosystems.

Acknowledgements

This dissertation was primarily funded by the Edward M. Warner Graduate Grant awarded by the CSU Geoscience Department and additional departmental funds. Supplemental field support was given by National Geographic CRE Grant 9183-12 (summer 2012), Colorado Water Institute (summer 2014) and the Geological Society of America (2013 and 2014), and Charles Blyth (summer 2012). Special thanks to Robin Reich for his knowledge and support regarding sampling and statistics and to Stephen Leisz for helping me get started using object identification and provided me a lab in which to work. I'd like to thank all the undergraduates who were involved with varying aspects of data analysis: Brooke Hess-Homeier for the log raft data collection and analysis, Jay Merrill and John Harris for Pelican Island data extraction, Aaron Brown for Pelican Island georeferencing, and Madeline Egger, Matthew Suppes, Eva Hanlon, Landry Brogdon and Jake McCane for timelapse image categorization.

A big shout out to my northern network: CBC North Radio show, the Water Survey Canada and the Geoscience offices in Yellowknife, the Fort Smith Pelican Advisory Circle, Parks Canada in Fort Smith, The Yellow House, Blyth and Bathe, Inc., Smith's Landing Band, ENRTP Program at Aurora College, Aurora Research Institute, and the Slave River Delta Coalition. This project would not be the same without these northern folks who went out of their way to help me and share their thoughts: Herb Norwegian of the Deh Cho, Megan Wohlberg of the Northern Journal, Dave Oleson of Hoarfroast River Huskies Ltd., Sean Buckley of Great Slave Lake tours, Erin Palmer of NWT Geosciences office, John McKinnon of Parks Canada, Jacques Van Pelt of the Pelican Advisory Circle and Gord Beaulieau and Karl Cox of Environment Natural Resources. Also thanks to all those who

helped me gather data in the field, it was fun: Ellen Wohl, Gen Cote, John Blyth, Chuck Blyth, Robyn Brown, Jessica Reimer, Helen Panter, Leif Anderson, Brooke Hess-Homeier, Cole Conger-Smith and Don Jaque.

The Fluvial Flamily at Colorado State University was integral for providing a supportive, enthusiastic and exciting community in which to work and think through ideas. Thanks to my committee for being there when I needed you and for being extremely available and easy to schedule. I am deeply grateful for the constructive and well thought out reviews on submitted manuscripts from Edward Schenk, Francesco Comiti, Brett Eaton and other anonymous reviewers. I particularly enjoyed the support of my brother, Russell Kramer, for log research chats over the phone, providing a soundboard for ideas and to talk about research and life in general. Most of all, thanks to my husband, Leif Anderson for making me go kayaking. As a result, I maintained enthusiasm and interest in my project throughout.

Last but not least, I am eternally greatful for the mentoring and long leash that my advisor, Ellen Wohl, gave me during this project. She provided me just enough guidance to expore my topic efficiently while at the same time giving me the freedom to take the project in new directions (while pursuing competition level kayaking and travel). She has certainly shaped who I am as a scientist.

This dissertation is typset in LaTeX using a document class designed by Leif Anderson.

Table of Contents

There is probably no lake in North America which receives anything like the amount of driftwood which is poured into the Great Slave Lake, chiefly through the Slave River - *E.M. Kindle* (1919, pg. 358).

DISSERTATION OUTLINE

This dissertation is centered around the theme of large wood dynamics in rivers, with field case studies on the Slave River ($Q \sim 10^3 m^3/s$, $10^5 ft^3/s$) and the Great Slave Lake in the Northwest Territories and northern Alberta. Following this Introduction (which includes background material on the influence of wood on landscape morphology, wood dynamics, and the study site), this dissertation is comprised of four chapters of re-printed stand-alone papers. The first chapter is a long review paper on wood transport. Chapters 2-4 are three case study papers on the Slave River and Great Slave Lake that highlight wood dynamic processes at varying timescales. Figure 0.1 locates the geographic focus for each case study paper.

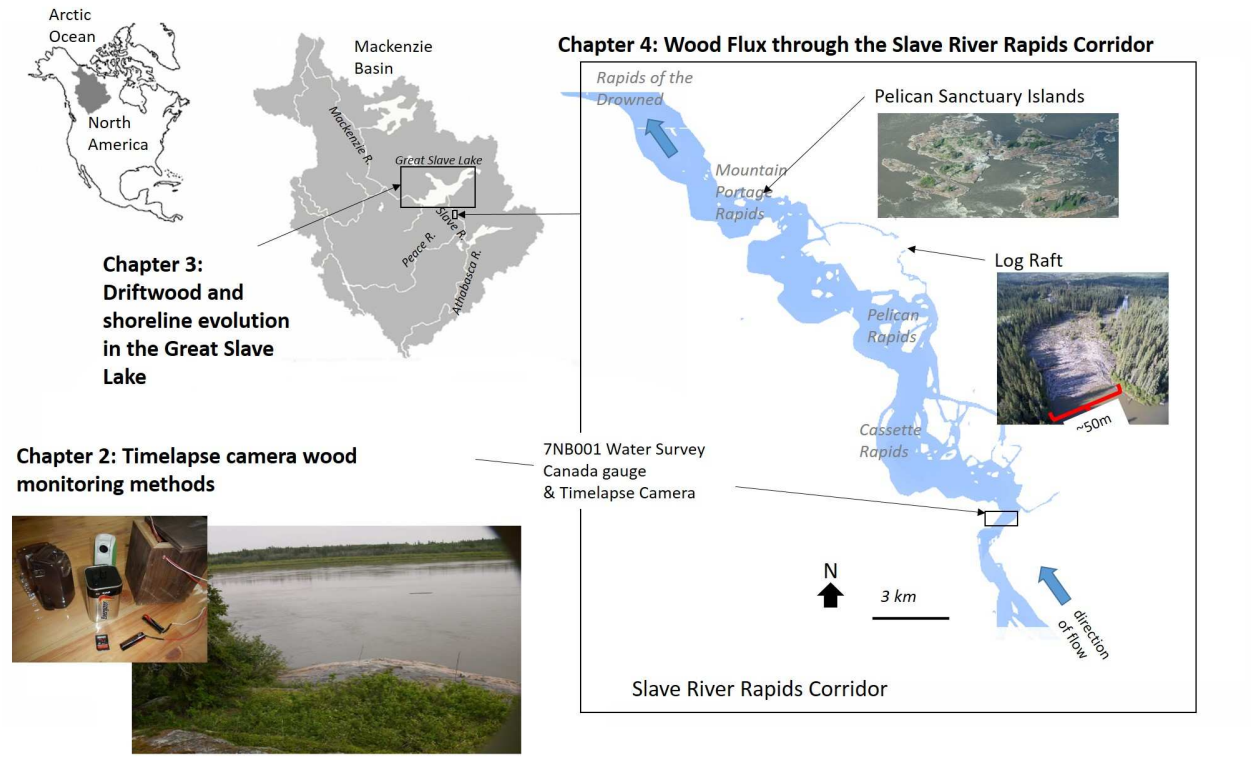

FIGURE 0.1. Geographic location of Chapters 2, 3 and 4

Below, I briefly summarize each chapter and provide the appropriate citation for each of the four articles. Because each paper presented here was either already published or in the review process prior to completion of this dissertation, after this introductory chapter

I use the pronoun "we" rather than I, as published. Rather than a bibliography after each chapter, I have included one bibliography at the end of the dissertation.

Chapter 1. Kramer, N and Wohl, E. (accepted), **Rules of the Road: A quantitative and qualitative review of driftwood transport through drainage networks**, *Gemorphology.*

In this review paper, we conduct an exhaustive literature search to qualitatively and quantitatively review field-based studies of wood transport.

Chapter 2. Kramer, N and Wohl E. (2014), **Estimating fluvial wood discharge using timelapse photography with varying sampling intervals**, *Earth Surfaces Processes and Landforms*, 39(6), 844-852, doi: 10.1002/esp.3540

In this methods paper, we develop new techniques for collecting and computing wood flux from timelapse cameras.

Chapter 3. Kramer, N. and Wohl, E. (2015), **Driftcretions: The legacy impacts of driftwood on shoreline morphology**, *Geophysical Research Letters*, 42(14), 5855-5864, doi:10.1002/2015GL064441.

In this research paper, we report the volume and distribution of driftwood along shorelines, the morphological impacts of sustained driftwood delivery throughout the Holocene, and rates of driftwood accretion for the Great Slave Lake.

Chapter 4. Kramer, N and Wohl, E., Hess-Homeier, B. and Leisz, S. (in review), **The pulse of driftwood for multiple timescales in a great northern river**, *Water Resources Research*

In this research paper, we use timelapse cameras, remote aerial imagery, and historical accounts to characterize driftwood transport and thresholds on the Slave River over time intervals from days to decades.

BACKGROUND

The following text includes introductory information with literature references on the impact of river driftwood on landscapes and ecology, in-stream wood dynamics and the study location (the Great Slave Lake and Slave River).

0.1. Driftwood in the Landscape

Driftwood greatly facilitates biogeomorphic plant succession in a dynamic, high-disturbance setting: the interface between land and water. Biogeomorphic succession expands upon the traditional concept of vegetation succession by incorporating physical disturbance and landform development (*Corenblit et al.*, 2007). Figure 0.1 diagrams how driftwood is utilized in ecosystems and Figure 0.1 conceptualizes the feedbacks among driftwood, sedimentation, and plant succession. In landscapes with high amounts of driftwood, these interactions lead to major alteration of physical and ecological states similar to the actions of an engineer species.

For example, high wood loads are shown to play a major role in maintaining: step-pool and multi-thread channels in low gradient mountain alluvial valleys (*Polvi and Wohl*, 2013); vegetated island-braided rivers (*Gurnell and Petts*, 2002); large expanses of alluvial old-growth forests on floodplains (*Collins et al.*, 2012); semi-stable multi-thread, wide distributary channels in deltas (*Phillips*, 2012); stable sand dunes and steeper gravel berms on beaches (*Kennedy and Woods*, 2012); habitat patchiness and bio-available nutrients in estuaries; mid-ocean food webs (*Gonor et al.*, 1988); and biologic hotspots on the nutrient- and energy-poor deep ocean floor (*Knudsen*, 1970). Without driftwood, these landscapes revert to a simpler design that supports less life. Mountain channels revert to plane bed with single channels; larger rivers no longer have vegetated islands; alluvial floodplains are narrower without old-growth forest patches; and beach dunes are more mobile and drier. In sum, landscapes that contain driftwood have more habitat patchiness and thus are much more biologically productive than they would be without driftwood.

Driftwood plays a major role distributing water-borne nutrients and organic particulates, including carbon, into broader areas than would otherwise be readily available. For example, wood jams in rivers substantially increase sedimentation of organics within the channel and on the floodplain (*Wohl*, 2013a; *Beckman and Wohl*, 2014). There are large amounts of carbon per unit area stored in sediments from pools behind channel-spanning jams in headwater channels, and in floodplains and riparian wetlands (*Walter and Merritts*, 2008; *Cierjacks et al.*, 2010; *Wohl*, 2011a). In addition to physically enhancing the deposition of water-borne nutrients and particulates, driftwood is an important food and carbon source in itself (Figure 0.1). For example, fecal pellets from wood-boring crustaceans provide an important food source for near shore environments (*Gonor et al.*, 1988), and the episodic delivery of vast quantities of wood from uplands and river corridors during tropical storms

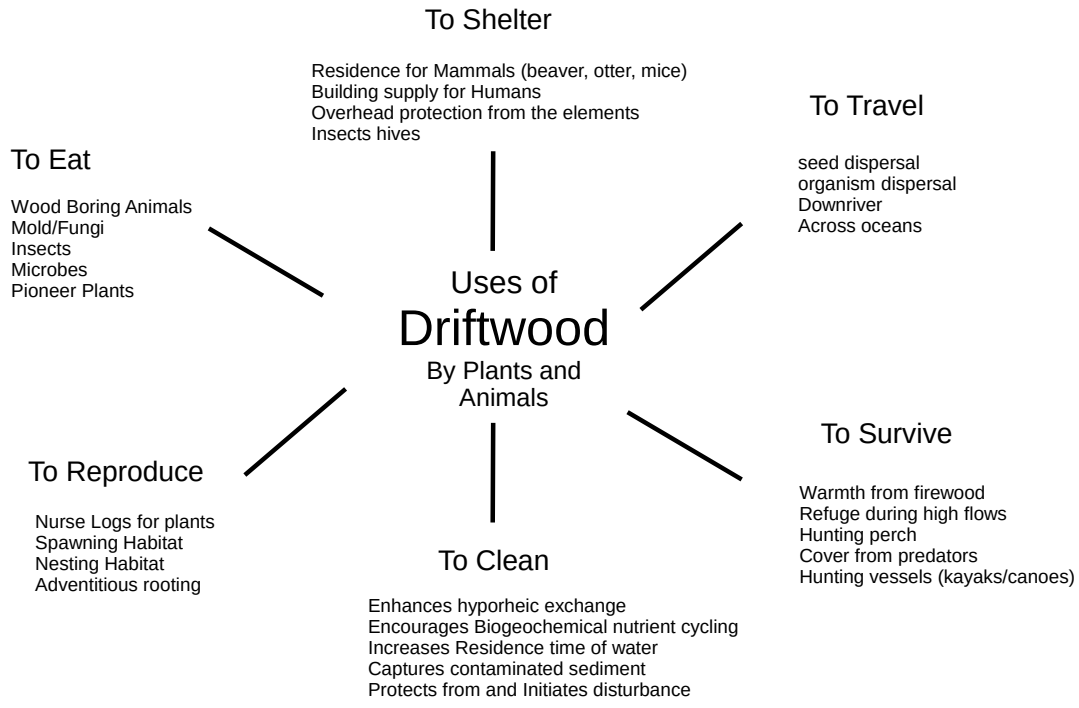

FIGURE 0.2. Examples of how driftwood is utilized by plants and animals

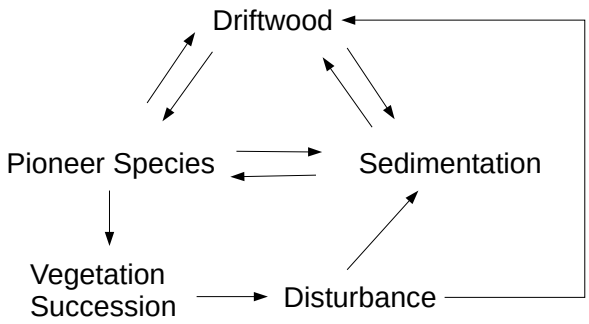

FIGURE 0.3. Conceptualization of the feedbacks among driftwood, sedimentation, plant succession, and disturbance

provides a highly concentrated flux of carbon and nutrients that represents a significant transfer of terrestrial biomass to oceans (*West et al.*, 2011).

Despite high-profile papers emphasizing the role of rivers in the global carbon cycle (*Eglinton*, 2008; *Battin et al.*, 2008, 2009; *Aufdenkampe et al.*, 2011), research examining the processes that create and maintain instream and floodplain complexity or facilitate organic carbon storage is just beginning. To date, much of the work has focused on monitoring and quantifying dissolved and particulate organic carbon (e.g., *Holmes et al.*, 2012) or describing the impact that driftwood jams have on sedimentation, hydrology, and/or biogeochemical processing of nutrients (*Montgomery and Piégay*, 2003; *Wohl et al.*, 2012). Research that investigates the long-term storage and decay of drift piles and their legacy impact on landform, food webs, and carbon cycling is rare. Historical accounts of enormous volumes of wood on rivers in the temperate zone (*Triska*, 1984; *Maser et al.*, 1988; *Wohl*, 2014a) describe a scenario that has largely vanished. Deforestation, flow regulation, channelization, levees, snagging (wood removal from rivers), and other activities have removed so much wood that most rivers (*Montgomery and Piégay*, 2003; *Collins et al.*, 2012; *Wohl*, 2014a),

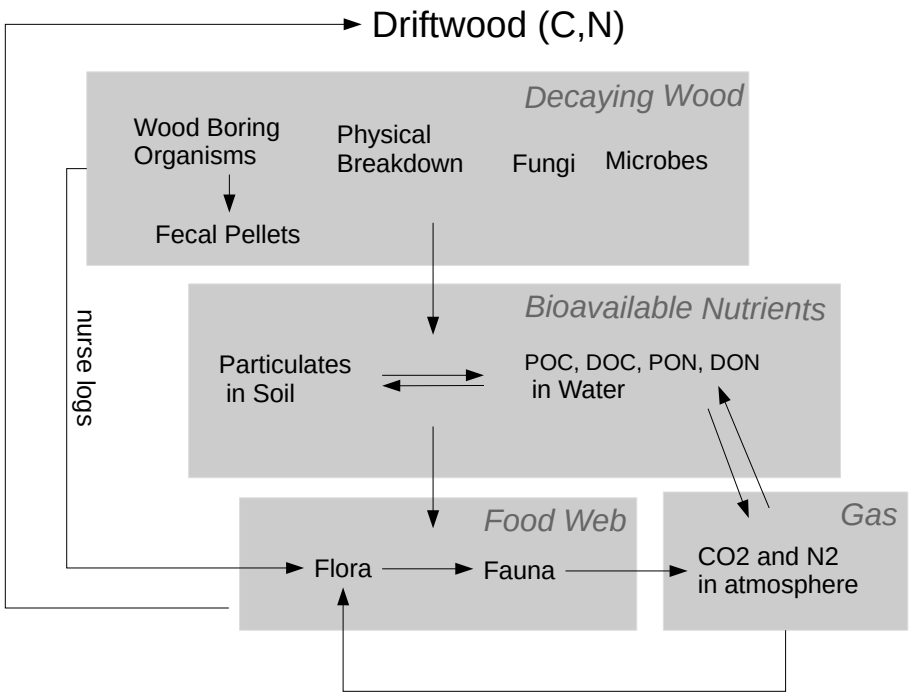

FIGURE 0.4. Conceptual model showing how carbon and nitrogen from driftwood enter global cycles

and by consequence shorelines (*Maser et al.*, 1988), are severely wood-impoverished relative to their condition prior to intensive human settlement. Thus, stable landforms that we see today along river corridors and lakes may reflect past processes when driftwood was more abundant. In the absence of modern wood, studying these processes, let alone connecting vestige landscapes to driftwood processes, is difficult.

In a state of the science report, *Reinhardt et al.* (2010) suggest that the co-evolution of landforms and biological communities should be a central theme to motivate future research, and note that identifying rates of biological and geomorphological processes and how they interact to generate landforms is of primary importance. Recently, in the emerging field of biogeomorphology, much focus has been on how, given enough time, small-scale biotic processes can influence the evolution of the landscape and ecosystems (*Dietrich and Perron*,

2006). Over long time scales, actions by engineer species create unique and patchy ecosystems with high biodiversity by modulating resources to other species (*Corenblit et al.*, 2011). A good example of these processes is the formation of extensive wet meadows in mountain alluvial valleys, which have been dubbed the beaver meadow complex due to the importance of beaver dams in maintaining the wetland ecosystem (*Ives*, 1942; *Westbrook et al.*, 2011). *Gibling and Davies* (2012) suggests that the meandering river form is a physical expression of the existence of life because it co-evolved with vascular land plants. Without riparian vegetation and driftwood stabilizing river banks, they postulate that the meandering planform would not exist.

0.2. Wood Dynamics

Wood dynamics refers to the processes governing recruitment, storage and transport of large wood[1] through catchments. The main drivers behind research into wood dynamics in rivers are to understand the role that wood plays in the ecology and health of riparian corridors; to understand the influence wood has on shaping the morphology and sediment regime of channels; to better constrain the global biogeochemical cycles by describing how large wood influences nutrient fluxes from the land to the oceans; and to predict and plan for hazards associated with wood clogging of engineered structures during high flows.

The existing framework for conceptualizing large wood dynamics is usually presented as a wood budget in which the change in storage (ΔS) along any given reach (Δx) for a given time frame (Δt) is equal to wood inputs minus wood outputs. Below is a wood budget equation by *Benda and Sias* (2003) .

$$\Delta S = [L_i - L_o + \frac{Q_i}{\Delta x} - \frac{Q_o}{\Delta x} - D]\Delta t$$

[1]My Note on Terminology: Unless otherwise noted, large wood is defined to be greater than 10 cm in diameter and 1 meter in length. I also use the term "driftwood" in place of "large wood" because I discuss floating wood in a lake and along a very wide river that is about 15 to 30 times wider than the longest pieces of wood. In these situations, wood is drifting through the water and washes up on shorelines, thus the term driftwood is appropriate. "Large wood", "wood" and "driftwood" are more universally applicable than the commonly used term, "instream wood", to both rivers and lakes. Thus, I limit my use of "instream wood" to only those scenarios where I am referring specifically to reach-scale locations on a river rather than the drainage basin as a whole.

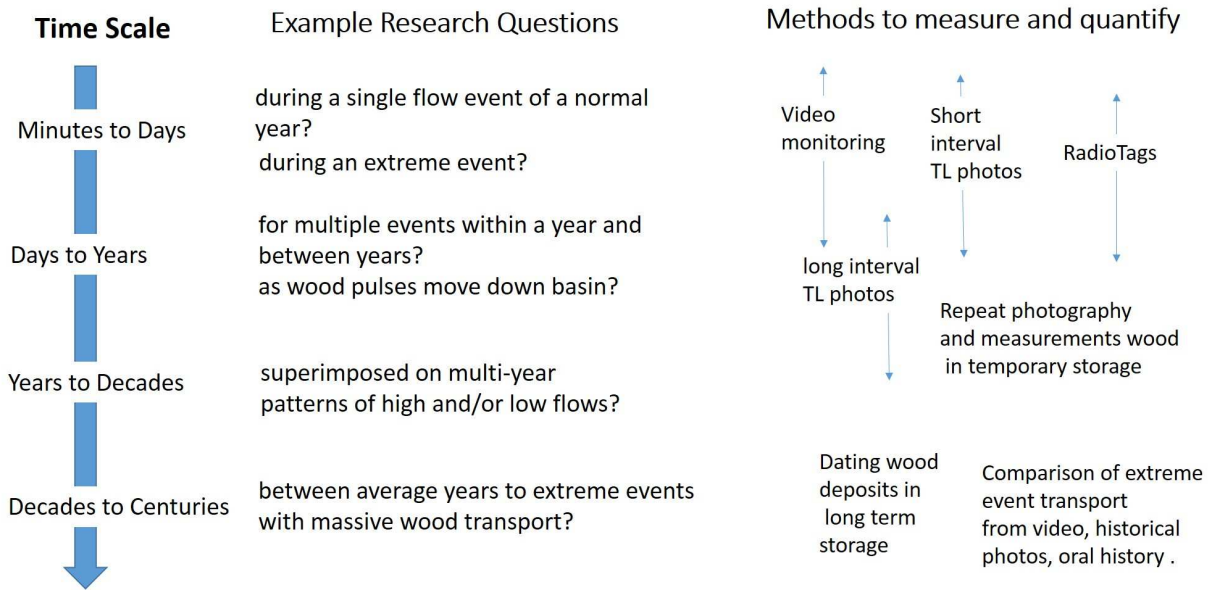

FIGURE 0.5. Conceptualization of transport questions and appropriate methods to answer them at varying timescales.

In the above equation, wood inputs are from lateral recruitment and exhumation (L_i) and fluvial transport from upstream (Q_i). Wood outputs are from lateral deposition and burial (L_o), fluvial export downstream (Q_o), and decay (D). This equation has been used to back-calculate wood flux based on reach-scale field measurements of storage and recruitment *Martin and Benda* (2001, e.g). However, recent research monitoring wood flux with video cameras (*MacVicar and Piégay*, 2012) has shown that wood flux estimates derived from wood budget equations may be underestimating wood flux by as much as four times.

I hypothesize that part of the problem may be from extrapolation of reach-scale metrics on short timescale (<2 yrs) to basin-scale processes that occur over decades. Figure 0.5 is a conceptualization of types of research questions and appropriate methods at varying timescales. Rather than focusing on wood recruitment and storage, this dissertation assesses the variability in wood export (Q_o) from the Slave River drainage basin to the Great Slave Lake on varying timescales from days to centuries using a variety of methods including timelapse photography, repeat photography, dating wood deposits and historical anecdotes. By focusing on the outlet of a large basin rather headwater catchments, I can assess the cumulative patterns of wood flux from the entire basin through time.

0.3. The Slave River and Great Slave Lake

The Slave River and Great Slave Lake (GSL) are uniquely situated in the middle of the Mackenzie Basin, effectively dividing the basin in half (Figure 1.3). Water draining the southern Canadian Rockies and the boreal forests to the south makes its way north into the GSL. GSL water eventually becomes the source water for the Mackenzie River, which flows north into the Arctic Ocean.

A recent international report (*Vaux*, 2013) emphasized that the Mackenzie Basin is still one of the most intact large-scale ecosystems in North America, but it is at risk from a warming climate and development from exploitation of hydrocarbon, minerals, and hydroelectric power. The Basin is recognized as a resource that affects the welfare of people globally, but it is not well monitored and less well studied than other major river basins. The Mackenzie River of Canada exports large amounts of driftwood to the Arctic Ocean that can be found and identified as far away as Scandinavia (*Eggertsson*, 1994). The Mackenzie River stands out from other circumpolar Arctic rivers as having notably low dissolved organic matter yields to the Arctic Ocean because the GSL efficiently processes and retains constituents transported to the lake from the upper watershed (*Holmes et al.*, 2012; *Gibson et al.*, 2006).

The Slave River has a mean annual flow of 3432 m^3s^{-1} and provides 74% of the inflow to the Great Slave Lake. The remaining inflow is from catchments surrounding the lake (21%) and from precipitation (5%) (*Gibson et al.*, 2006). Sediment and wood delivered to the lake mostly originate from catchments on the southern shore. Rivers along the north shore carry negligible amounts of wood and sediment to the lake because they drain the Canadian Shield or low relief wetlands. Yearly influx of wood is associated with rapid rise and fall of river flows from mechanical break up of river ice and freshet high flows that float stranded wood on river banks (*Kramer and Wohl*, 2014; *Brown*, 1957). Episodically, vast carpets of wood are delivered when summer freshet flows are much higher than previous years (*Kramer et al.*, in submission).

The GSL has a surface area of $28,568$ km^2 and a catchment area of $949,000$ km^2 (*Gibson et al.*, 2006). It is one of the deepest lakes in the world, reaching a maximum depth of 620 m

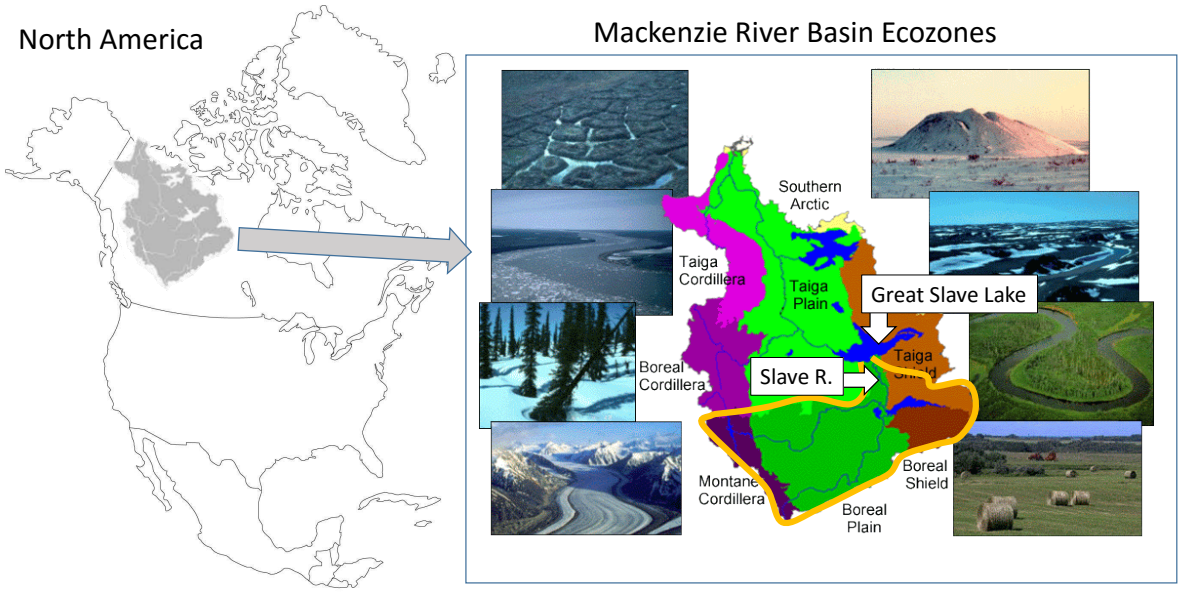

FIGURE 0.6. The Slave River Basin (outlined in yellow) as situated in the Mackenzie River Basin of North America. Ecozone inset figure was adapted from the Mackenzie River Basin Impact Study (*Cohen*, 1997) and re-printed with permission.

in the east arm where subglacial meltwater from the Continental Laurentide ice sheet pooled along faults (*Christoffersen et al.*, 2008). While the east arm was formed underneath the ice, the main body of the lake formed marginal to the retreating ice sheet (*Vanderburgh and Smith*, 1988; *Lemmen*, 1990) and is much shallower ($10 - 90$ m) (*León et al.*, 2007). The lake is underlain by till of mostly limestone boulders and cobbles from Paleozoic sedimentary rocks of the Interior Plains Platform (*Lemmen*, 1990). Granitic boulders and cobbles increase towards the contact with the Canadian Shield along the eastern margin of the lake (*Lemmen*, 1990) (Figure 1.3). Originally, the main body of GSL was a part of Glacial Lake McConnell, which also included modern-day Lake Athabasca to the south and Great Bear Lake to the north (Figure 1.3). Due to isostatic rebound and drainage, Glacial Lake McConnell separated into three lakes, and the Slave River was formed connecting Lake Athabasca to the Great Slave Lake around 8300 BP (*Smith*, 1994). Buried driftwood in Slave River deltaic sediments has been used to estimate progradation of the Slave River Delta into the GSL from 8070

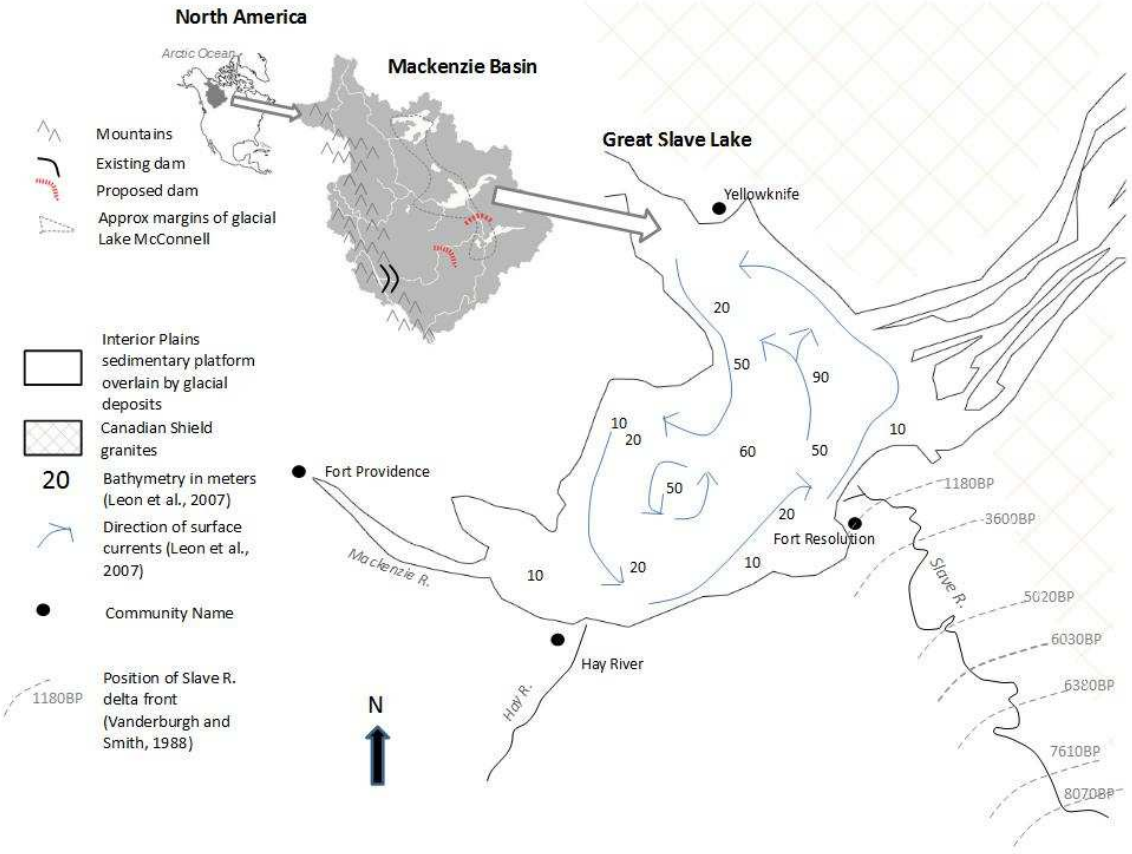

FIGURE 0.7. The Great Slave Lake, its location, and some background information.

to 1180 BP (*Vanderburgh and Smith*, 1988), highlighting that wood delivery to the lake has been occurring since de-glaciation. Based on the elevation of dated driftwood from 6960 to the present, an estimate for the modern rate of isostatic rebound is $0.2cm/year$ (*Vanderburgh and Smith*, 1988).

The GSL is considered hydrologically active, with an average residence time for a water molecule of 16 years (*Gibson et al.*, 2006). Based on data from 2002-2009, GSL is, on average, completely frozen for 186 days per year and has some ice present for 193 days per year (*Kang et al.*, 2012). Ice break up occurs May-June and freeze-up in November-December (*Kang et al.*, 2012). During ice break up in years of high river discharges, wind can push blocks of drift ice up onto exposed shorelines, effectively bulldozing large boulders, cobbles, and wood into raised beach ridges (*Philip*, 1990; *Lemay and Bégin*, 2012). During the ice-free

late summer (July and August), seiches (rapid fluctuations in lake levels) develop from high, steady winds stacking surface waters at the downwind shore. Seiches on the Great Slave Lake < 0.15 m in height are common due to long fetch distances and occur on average $10 - 14$ times per year (*Gardner et al.*, 2006). The largest seiches ($0.15 - 0.40$ m), which account for less than 10% of all recorded events from 1938 to 2000, raft driftwood high enough onto the shoreline to be unaffected by smaller events (*Gardner et al.*, 2006). Seiche-forcing winds on the north shore come from the SE and on the south shore from the NW (*Gardner et al.*, 2006).

Mean surficial lake currents flow in a counterclockwise direction (*León et al.*, 2007). When driftwood enters the lake, it circulates in this direction on calm days and is pushed up against shore on windy days (personal observation). Lake currents are weak near the mouth of the Mackenzie River and thus wood entering the lake tends to not be exported downstream, but rather stored permanently along shorelines, in river deltas, and in nearshore lake sediments. This is corroborated by local residents of Fort Providence, who have noted the lack of wood floating down the Mackenzie at that location. The GSL supports a high level of biodiversity of both plants and animals (*Condon*, 2013). There are two ecological regions mapped on the lake, Taiga Plains and the Taiga Shield, which correspond to underlying geology of sedimentary (Interior Plains Platform) versus crystalline rock (Canadian Shield) (*Ecosystem Classification Group*, 2007, 2009). Driftwood is primarily stored on shores in the Taiga Plains ecoregion due to its much lower relief along shorelines and erodible boundaries. Shoreline vegetation is composed of mostly sedges (*Cyperaceae*), willow (*Salix*)-alder (*Alnus*) shrublands, balsam poplar (*Populus balsamifera*), spruce (*Picea*), quaking aspen (*Populus tremuloides*), and tamarack (*Larix laricina*). These species interact with the driftwood to trap fine grained sediment as well as stabilize sand bars, beaches, and ice-pushed gravel and cobble berms (*English et al.*, 1997).

Decaying driftwood is especially important as nurse logs for the germination of spruce (*Berger*, 2002; *Timoney and Robinson*, 1996). The GSL contains sustainable populations of high quality commercial fisheries of whitefish, trout, pickerel, northern pike, and inconnu

(*Rundle et al.*, 2005). The GSL serves as a major staging and rearing area for migratory birds because it is located on the Atlantic, Mississippi, and Central flyways (*Milburn et al.*, 1999). Stranded and decaying wood pieces along shorelines are commonly used as perches by both shore and migratory birds. Bird species diversity is declining and is at high risk from climate and up-basin development (*Condon*, 2013). Moose, muskrat, mink, and beaver are mammals that thrive in the nearshore wetlands and are important culturally for local indigenous communities (*Milburn et al.*, 1999).

Many studies have looked at how the construction of the W.A.C. Bennett Dam $>$ 1500 km upstream (see Figure 1.3) on the Peace River in the late 1960s has impacted the ecology and geomorphology of the Slave River Delta (SRD). The Bennett Dam and nearby Peace Canyon dam together have a hydro capacity of 3400 MW and Williston reservoir behind the Bennett Dam is the ninth-largest man-made lake in the world (*Vaux*, 2013).

- *English et al.* (1997) showed that the biological productivity and diversity of the SRD is closely linked to flooding and sediment delivery from the Slave River, which sustains extensive shoreline habitat. They also showed that upstream damming has shifted the delta to a drier environment and growth of the outer delta has slowed or stopped.
- *Milburn et al.* (1999) investigated aquatic animals that could be used as ecosystem indicators to monitor and predict response to various development scenarios that impact hydrologic regimes. They identified muskrat and mink as the best indicators due to their dependence on changes in hydrology, small geographic range limited to the SRD, and importance for local food and trade.
- *Prowse et al.* (2006) found that because of the small water surface slope of the SRD, small lake level changes from upstream hydroelectric development have the potential to alter large areas of the main active delta. A reduction of lake levels by 0.05-0.2 m during spring and summer flooding or during seiche activity would likely lead to decreased flooding and drying of wetlands in the delta.

- *Beltaos et al.* (2006) found that the ice jam flood have occurred less frequently on the Peace River (the primary tributary to the Slave River) after construction of the W.A.C Bennett Dam due to supressed water levels in the Spring.
- *Gibson et al.* (2006) related dam regulation to water levels in the GSL. Regulation has increased discharge from the Slave River in the winter and reduced flows during the spring and summer, impacting lake levels in a similar manner. The highest lake level years correspond to wetter than average years that also had large releases from the W.A.C Bennett Dam.
- *Brock et al.* (2010) analyzed flood frequency variability in the SRD for the past 80 years using paleolimnological analysis of perched basins prone to flooding during high water years. They found decadal scale intervals of high and low flood frequency, with the driest years pre-dating construction of Bennett Dam. They emphasize that changes in climate and precipitation in headwater catchments have greater impact on flooding than regulation from the existing dam.

Many communities along lake shores still follow a traditional lifestyle and have a culture that is closely tied to the health of the ecosystem (*Wolfe et al.*, 2007). However, the ecosystem is under threat from climate and development-driven change. During the exceptionally dry summer of 2014, an unprecedented 3.5 million hectares of land burned in the Northwest Territories, much of it near the Great Slave Lake (K. Johnson, pers. comm ., September 2014). The hydropower potential for the Mackenzie Basin is thought to equal the rest of Canada combined (*Vaux*, 2013). Although no more dams are currently approved for construction, dam projects are currently proposed on the Peace River (site C), Slave River, and on the Athabasca. Much of the hydropower will be used by oil shale and other mining operations. There is potential for structural failure of tailing ponds from hydrocarbon development to contaminate water and sediment delivered to the Slave River Delta.

In the past decade, community groups have expressed concern over how climate change, fires, land use change, and upstream damming will impact the water quality and health of the

ecosystem. In response, the Slave River and Delta Partnership (SRDP) was formed to coordinate research, monitoring, and planning efforts among communities, government agencies, aboriginal governments, non-governmental organizations, and academic institutions. This study provides baseline data on the importance and quantity of driftwood delivery to the shoreline ecosystem for groups such as the SRDP to use as they plan for the future.

CHAPTER 1

Rules of the Road: A quantitative and qualitative review of driftwood transport through drainage networks

Summary

To effectively manage wood in rivers, we need a better understanding of how and when wood moves through river networks. Building from an extensive literature search, we qualitatively and quantitatively review field-based studies of wood transport. We distinguish small, medium, large, and great rivers based on wood piece dimensions relative to channel and flow dimensions and dominant controls on wood transport. We suggest that designating wood transport regimes, such as piece-dominated, jam-dominated, high-flow-dominated, and burial-dominated, is a useful way to characterize spatial-temporal network heterogeneity and to conceptualize the primary controls on wood mobility in diverse river segments. We draw analogies between wood and bedload transport, including distinguishing Eulerian and Lagrangian approaches, exploring transport capacity, and quantifying thresholds of wood mobility, which can be expressed as a ratio of flow stage to stage at incipient wood motion, or as a fraction of bankfull flow. We identify mobility envelopes for re-mobilization of wood with relation to increasing peak discharges, stream size, and dimensionless log lengths. Wood transport in natural channels exhibits high spatial and temporal variability, with discontinuities along the channel network at bankfull flow and when log lengths equal channel widths. Although median mobilization rates increase with increasing channel size, maximum mobilization rates are greatest in medium-sized channels. Most wood is transported during relatively infrequent high flows, but flows under bankfull can transport up to 30% of stored wood and the highest flows may not transport any wood. We use a conceptual model of dynamic equilibrium of wood in storage, a conceptual model of spiralling wood transport paths through drainage networks, and a metaphor of traffic on a road to explore how discontinuous

wood movement through a river network reflects the characteristics of river flow, the wood pieces, and the channel boundaries. We note a disconnection between how mobilization is measured and the processes that drive mobilization. The primary limitations to describing wood transport are inappropriate time scales of observation and lack of sufficient data on mobility from diverse rivers and regions. Improving models of wood flux on local and regional scales requires better characterization of average step lengths within the lifetime travel path of a piece of wood. We suggest that future studies focus on: (i) continuous or high-frequency monitoring of wood mobility; (ii) monitoring changes in wood storage at known retention sites at varying time scales; (iii) using wood characteristics to fingerprint wood sources; (iv) quantifying volumes of wood buried within channels and floodplains; (v) using remote sensing to assess changes in wood storage over large spatial scales; (vi) obtaining existing or new data from unconventional sources, such as citizen science initiatives, (vii) creating online interactive data platforms for facilitation of data synthesis, and (viii) further consolidation and review of residence time and basin wood flux.

1.1. Motivation

There is a strong need to understand large wood transport dynamics in the context of flooding hazards (e.g., *Mazzorana et al.*, 2012; *Ruiz-Villanueva et al.*, 2013, 2014; *Lucía et al.*, 2015) and global nutrient fluxes (*Bilby*, 1981; *Elosegi et al.*, 2007; *Hilton et al.*, 2008; *West et al.*, 2011; *Wohl et al.*, 2012). By wood dynamics, we mean the processes associated with the recruitment, storage, and transfer of dead wood through drainage basins. Specifically, we focus on the transport of large wood ($\geq$ 1 m in length and 10 cm in diameter).

Conceptual and quantitative models of river adjustment typically rely on two primary driving variables, water and sediment (*Knighton*, 1998). However, instream wood can be as important for channel change as sediment (e.g., *Massong and Montgomery*, 2000; *Brooks and Brierley*, 2002; *Montgomery and Abbe*, 2006; *Le Lay et al.*, 2013). Early scientific and historical writings on wood were mainly inspired by awed observations of immense volumes of wood and associated channel change (*Kindle*, 1919, 1921; *Bevan*, 1948; *Triska*,

1984). Reviews of historical accounts document the enormous quantities and landscape-scale impacts of wood from headwater channels to large rivers prior to extensive wood removal (*Triska*, 1984; *Sedell et al.*, 1988; *Wohl*, 2014a) and most forested or historically forested catchments have vegetation or wood-driven morphologies (*Hickin*, 1984; *Collins et al.*, 2012; *Gibling and Davies*, 2012; *Polvi and Wohl*, 2013; *Gurnell et al.*, 2015).

Despite this evidence for the importance of wood as a driving geomorphic variable, descriptions of geomorphic effects of wood on channel processes were largely absent in the mid 1900s (*Hickin*, 1984), when researchers were building foundational conceptual models (*Grant et al.*, 2013; *Wohl*, 2014b) - such as graded rivers (*Mackin*, 1948) and Lanes balance (*Lane*, 1955)), and quantitative understanding of river systems - such as hydraulic geometry relations (*Leopold and Maddock Jr*, 1953). The large-scale removal of wood from rivers during the 20th century (*Montgomery and Piégay*, 2003; *Wohl*, 2014a) likely led to a neglect of the geomorphic effects of wood on river process and form during this formative period of fluvial geomorphology.

As long as rivers are wood-depleted, models of river form adjusting primarily to sediment and water are adequate for managing rivers. However, in order to improve valued ecosystem services such as de-nitrification, sustainable fisheries, improved water quality, and enhanced physical and mental health of human communities (e.g., *Wohl et al.*, 2015), managers now focus on re-introducing wood as engineered structures (*Abbe and Brooks*, 2011; *Gallisdorfer et al.*, 2014), leaving mobile un-engineered wood in place on the floodplain (*Piégay et al.*, 2005; *Wohl et al.*, 2015), and managing riparian forests to increase the amount of wood that can be recruited (*Kail et al.*, 2007; *Wohl et al.*, 2015).

In Europe, afforestation of river corridors (*Liébault and Piégay*, 2002) has led to increased wood in transport, resulting in wood impoundments against bridge piers during floods (e.g., *Lucía et al.*, 2015), increasing flood levels, and forcing large-scale channel changes beyond what can be predicted through existing models (*Piégay et al.*, 2005). Inability to plan for the impacts and hazards of large wood on channels is a management concern and stems largely

from the fact that current models of river form and process used by managers do not include wood dynamics.

In the past few years, substantial progress in numerical simulation of wood transport has come from flume studies (*Bertoldi et al.*, 2014; *Davidson et al.*, 2015) and incorporation of wood modules into computer simulations, such as the *Reach Scale Channel Simulator* for habitat modelling (*Eaton et al.*, 2012; *Davidson and Eaton*, 2015) and *Woody Iber* for hydrodynamic modelling of wood transport (*Ruiz-Villanueva et al.*, 2014, 2015a). Simulations from these models have led to better understanding of wood-related flooding hazards, channel change, and aquatic habitat. However, models are simplified versions of the complex interactions found in the field and they require information from field studies to constrain variables and assess reliability of scenario responses (*Ruiz-Villanueva et al.*, 2015b). Recent rapid growth in numerical and modelling publications on wood transport is not matched by equivalent growth in field studies (Figure 1.1).

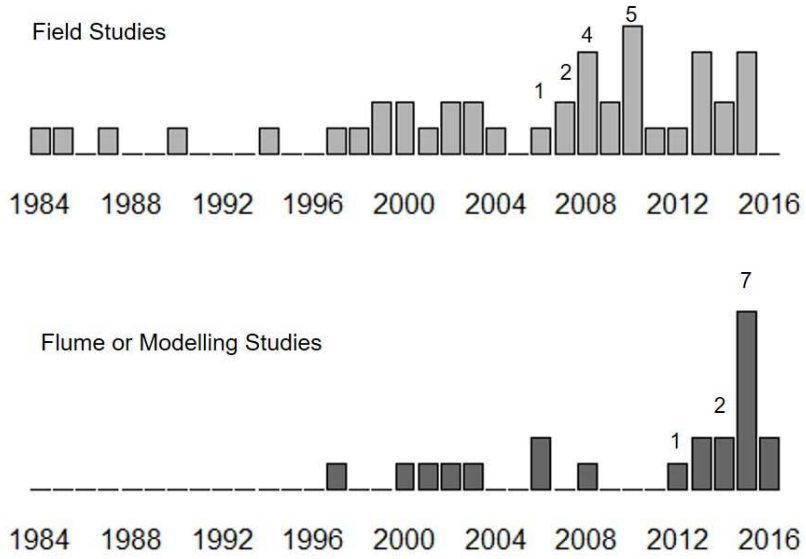

FIGURE 1.1. Comparison of field and modelling publications that report direct measurement of wood transport by year. Bar heights equal total number of articles found.

In this paper, we first qualitatively and then quantitatively summarize, analyze, and synthesize literature on wood transport within the framework of a functional classification of small, medium, large, and great rivers (Table 1.1, Figure 1.2). We focus on presenting a thorough review of case studies that have directly measured wood transport. We examine existing transport premises, present new conceptual frameworks of wood transport through drainage networks, and make suggestions for avenues of further research.

Although other reviews have included wood transport as a subcategory (*Keller and Swanson*, 1979; *Harmon et al.*, 1986; *Sedell et al.*, 1988; *Gurnell*, 2003; *Le Lay et al.*, 2013; *Wohl*, 2016), this is the first review of which we are aware that focuses solely on transport. We intend the review to be a thorough summary to acquaint new wood researchers with the existing literature; a compilation of field-based constraints to compare to future numerical models; and as a collection of thought-provoking ideas intended to push researchers to develop new, testable hypotheses, thus rapidly advancing wood transport research.

Table 1.1: Functional classification of river size based on wood dynamics. Categorization based on characteristic dimensions of wood pieces relative to channel size and patterns of recruitment, storage, and transport of wood.

Small rivers	
Size	1st to 2nd order; key piece wood length > channel width; diameter of logs > flow depth
Recruitment	Characteristics of riparian woodland of overriding importance; hillslope instability, blowdown, snow avalanches, individual riparian tree mortality
Storage	Individual wood pieces form stable features that control sediment deposition, channel morphology, and gradient; pieces typically span and are suspended above the active channel; jams may be present, but most wood stored as individual pieces; distribution of wood close to random and governed by sites of input; wood causes local widening where channel boundaries are erodible; wood condition depends on input mechanisms and forest disturbance history; low mobility can result in high levels of wood decay
Transport	Wood not reorganized or transported except during unusual floods or debris flows with recurrence intervals > decadal; large pieces mostly immobile; long residence times regulated by decay and physical breakdown rather than fluvial transport
Medium rivers	
Size	2nd to 4th order; log diameter $\sim$ flow depth; length of key logs > or $\sim$ channel width

Table 1.1(continued)

Recruitment	Hillslope, riparian, and bank source areas; tributary inputs; transport from upstream
Storage	Wood commonly stored in non-random, spatially discontinuous jams that partly or completely span the channel; jams comprised of mixed sizes of wood pieces, with larger key pieces trapping smaller, more mobile pieces; jams form at roughness elements such as boulders and planform irregularities; jams force bank erosion and avulsion, can create multithread planform; high inter-reach variation in wood loads; wood regulates sediment transport
Transport	Hydrologic regime is dominant control; drives periodic transport of stored and newly recruited pieces during high flows; key pieces and jams remain in place during smaller floods, accumulating smaller pieces; larger, more infrequent floods break up and rearrange jams
Large rivers	
Size	>5th order; log diameter << depth of flooded channel; all wood lengths < channel width; transition between medium and large rivers at channel widths ∼20-50 m wide because longest wood piece lengths are in this range
Recruitment	Transport of wood from upstream, lateral channel erosion; exhumation of previously buried wood on floodplains
Storage	River morphology dictates wood storage sites; wood generally has less decay because of greater mobility; wood influences bar and channel sedimentation and regulates formation of secondary channels, channel planform, and widening of valley floor; reaches with greater sinuosity, more bars, and lower gradients typically have higher wood loads; wood accumulates within active channel at sites such as apex of bars, outer upstream-facing margins of channel bends, backwaters, bank benches, and as individual pieces along channel margins during flood recession; large proportion of wood may be buried in floodplains and channel bars; wood accumulates on upstream side of living vegetation and influences morphologic evolution of stable vegetated islands and formation of multithread planform; wood does not form channel-spanning jams, but can form channel-spanning, dynamic wood rafts that persist for decades and cause channel avulsions
Transport	Wood exported downstream, laterally onto floodplains, or buried; wood exported regularly during high flow; amount of wood transfer highly variable and largely dependent on pattern of antecedent peak flows; high variability in water levels during flooding creates many opportunities for wood sequestration in long-term storage on the floodplain, causing large variability in wood residence time
Great rivers[a]	
Size	$\sim 10^6$ km^2 or larger; mean annual discharge $> 10^3$ m^3/s; perennial flow; commonly have vast, seasonally inundated floodplains, great hydraulic diversity, large fine sediment loads, and deep channels
Recruitment	Mostly via inputs from upstream; local inputs include lateral exchange with floodplain, exhumation of buried wood, inputs from bank failures, and mass recruitment such as during hurricanes (*Phillips and Park*, 2009)

Table 1.1(continued)

Storage	Pieces stranded along banks during receding flows; larger wood loads downstream from tributary junctions that deliver wood; floodplain accumulations at long lateral distances from channel; accumulations commonly decay in place or are partly buried; rafts that completely plug the channel are rare except where a multithread planform occurs
Transport	During most flows, rapid transfer of wood to deposition zones such as deltas, estuaries, or the ocean; lesser fluctuations in discharge than occur in large rivers, creating fewer opportunities for trapping of wood within channel or overbank deposition as a result of fluctuating stage; wood transfer largely controlled by the spatial distribution and timing of wood recruitment from large tributaries; floodplain wood likely transported and redeposited within the floodplain rather than transported to main channel; wood buried within channel bed may be transported downstream annually as part of the bed load

a. Very little study has been done on wood in great rivers. This summary is based on our current understanding of wood dynamics in great rivers from personal field experience. The ideas presented should be tested and refined with further study.

1.2. Qualitative Summary

Wood in storage is commonly referred to as instream wood. However, once wood becomes mobile, researchers tend to prefer the terms floating wood or drift wood (*MacVicar et al.*, 2009; *MacVicar and Piégay*, 2012; *Kramer and Wohl*, 2014; *Ruiz-Villanueva et al.*, 2014). Considering wood as floating or drift wood makes sense in the context of drainage networks, especially in scenarios when the same piece of wood is referenced in the context of river networks and non-channelized settings such as lakes, estuaries, or oceans (*Kramer and Wohl*, 2015). Within rivers, it is useful to investigate the processes that enable instream wood to float and how far the wood is likely to travel downstream.

Wood flux is governed by the unique interactions among hydraulics, wood pieces, and channel morphology, across space and time (*Gurnell et al.*, 2015; *Ruiz-Villanueva et al.*, 2015a). Thus, we summarize the existing knowledge of wood transport from field and numerical studies in three categories: flow characteristics (Section 1.2.1, Table 1.2), wood characteristics (Section 1.2.2, Table 1.3) and reach characteristics (Section 1.2.3, Table 1.4). Tables 1.2-1.4 are used to summarize the literature. In the following text, we propose a series of ideas, hypotheses, and suggested future research directions based on the findings from the

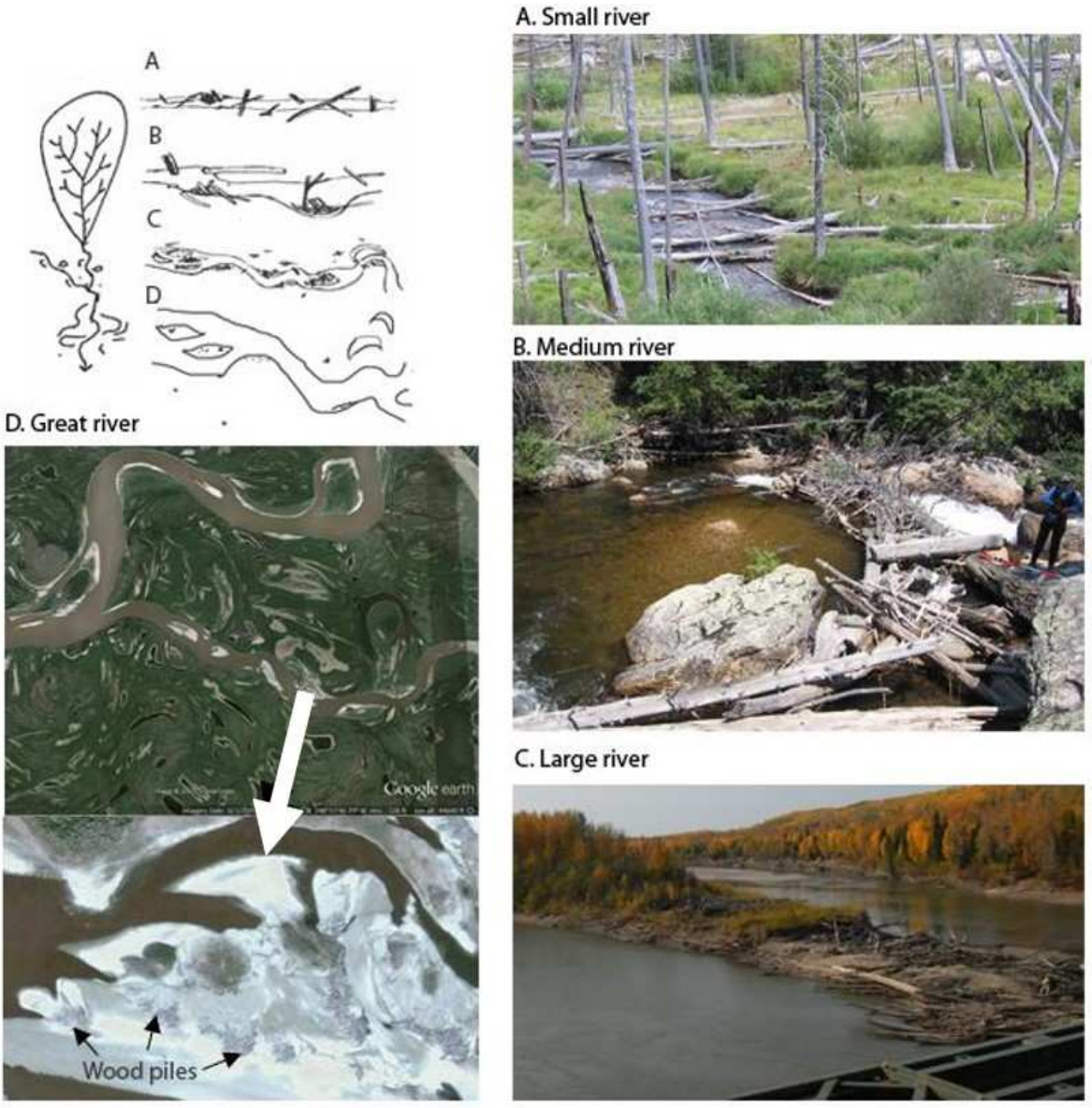

FIGURE 1.2. Stream size with relation to wood storage patterns in a fluvial system. Schematic after *Naiman et al.* (2002),*Keller and Swanson* (1979), *Le Lay et al.* (2013) and *Schumm* (1977). A. Random distribution of pieces on Ouzel Creek, Colorado through a burned area ($\sim$ 6 m channel width, average piece length is 2.7 m with maximum pieces > width of channel) B. Log jamming on North St. Vrain Creek, Colorado ($\sim$25 m channel width and average piece length is 3.3 m, maximum piece size < channel width). C. Wood accumulations and vegetated island formation in Hyland River, British Columbia (channel width is $\sim$100 m wide). D. Burial of wood accumulations on side bars of the Yukon River, Alaska. ($\sim$ 500 m channel width at 66.18510 N, -148.11925 E)

papers presented in Tables 1.2-1.4. We summarize some of the main hypotheses presented in the following text in Table 1.5.

1.2.1. FLOW CHARACTERISTICS. The primary flow characteristics that influence wood mobilization and transport include general shape of the hydrograph magnitude, duration, and rate of rise and fall and the sequence of flows through time (Table 1.2). Flow magnitude influences the areas inundated and the hydraulic roughness and retention capacity of the flooded area. Although wood discharge generally increases with water discharge on the rising limb, the relationship is nonlinear and highly variable (*MacVicar and Piégay*, 2012; *Kramer and Wohl*, 2014; *Ruiz-Villanueva et al.*, 2014; *Ravazzolo et al.*, 2015a). This is logical, given the potential for multiple and complex interactions among piece size and shape, hydraulic forces, and channel characteristics such as boundary irregularities that can trap wood.

Table 1.2: Synthesis of main findings and references for influence of flow characteristics on wood transport

Flow Characteristics
Magnitude
• Flow magnitude strongly influences whether wood is in transport because it dictates the flooded cross-sectional area, velocity, and depth of flow • The largest wood fluxes on rivers of all sizes occur during infrequent high flows • Background wood mobility rates under 30% exist for wood movement initiation in ordinary floods for many rivers • Wood transport responds non-linearly to increases in flow magnitudes and is highly variable • Hysteresis in wood transport: flows of equal magnitude transport much less wood on the rising limb than the falling limb • Wood mobilization threshold exists at magnitudes less than bankfull; before this transport is negligible, after this transport is possible and increases linearly with discharge until an upper wood transport threshold associated with overbank flows is reached, at which point wood transport suddenly decreases or levels off • Most wood is deposited near peak flow magnitude • Floods strand wood at discrete elevations and locations depending on stage height; elevations of stored wood can be used indirectly to assess wood flux for particular flows • Newly recruited wood can re-organize into jam stable states after only one bankfull flow; jams are re-mobilized and re-organized during exceptional flows • Wood transport velocity is more significantly related to log volume than magnitude of floods

Table continued on next page

Table 1.2(continued)

Duration

- The amount of time between initiation of wood transport and peak flow is a better predictor of wood displacement downstream than magnitude of flow alone
- Wood recruited during floods moves farther distances downstream than previously recruited wood

Rising and falling limbs

- Mobilization of wood occurs on the rising limb and is comparably negligible on the falling limb
- New wood on the falling limb originates from morphological changes of the channel
- Wood in transport on the falling limb is rapidly retained and entrapped
- Flashier, more steeply rising hydrographs mobilize more wood
- Transport and storage patterns respond nonlinearly to wood input rates (rate of rising limb), with a threshold input rate governing transition between congested and uncongested transport and corresponding depositional pattern as jams or single pieces (high or low wood loads)
- Shorter pieces (i.e., broken pieces and branches) are transported earlier on the rising limb and follow a consistent relation with discharge; larger pieces are mobilized after small pieces and do not correlate well with discharge
- Short pieces are transported on the rising and falling limbs, whereas the largest pieces are mainly transported on the rising limb

Flow History

- The amount of wood available for transport for any flood is a function of past flow history and non-fluvial recruitment since the last wood transporting flow
- Flood peaks of similar magnitude will have varying wood loads based on their position in a sequence of floods
- In small streams, the frequency of extreme events governs wood transfer downstream, with cycling of wood storage related to recurrence intervals of debris flows
- In medium rivers, low recurrence, yearly flows re-organize individual pieces of wood into jam stable states, whereas exceptional floods re-organize jams
- Newly recruited wood is less stable than previously transported wood
- In large rivers, reach-scale wood storage can be highly variable year to year, and depends on flows during prior years

Field References: *Keller and Swanson* (1979); *Lienkaemper and Swanson* (1987); *Berg et al.* (1998); *Keim et al.* (2000); *Haga et al.* (2002); *Angradi et al.* (2004); *MacVicar et al.* (2009); *Angradi et al.* (2010); *MacVicar and Piégay* (2012); *Bertoldi et al.* (2013); *Turowski et al.* (2013); *Kramer and Wohl* (2014); *Schenk et al.* (2014); *Iroumé et al.* (2015); *Jochner et al.* (2015); *Ravazzolo et al.* (2015b,a)
Modelling References: *Braudrick et al.* (1997); *Bertoldi et al.* (2014); *Ruiz-Villanueva et al.* (2014); *Davidson et al.* (2015); *Ruiz-Villanueva et al.* (2015a, 2016a)

The rate of discharge increase may be important for estimating wood transport rates and rapid changes in the hydrograph may account for much of the variability in wood discharge on the rising limb (*Braudrick et al.*, 1997; *Angradi et al.*, 2004; *MacVicar et al.*, 2009). Some of the observed variability in wood transport may reflect wood input rates associated with processes such as bank erosion, floating of previously stable pieces, and piece-to-piece

interactions among wood in transport (*Braudrick et al.*, 1997; *Keim et al.*, 2000; *Bertoldi et al.*, 2014; *Wohl*, 2016). Thus, we propose that transport distance will be more limited for flashier floods because more wood will be mobilized in shorter amounts of time, leading to congested transport and increased wood deposition, especially as jams (*Braudrick et al.*, 1997; *Bertoldi et al.*, 2014). Higher densities of jams deposited near peak flows then limit transport distance of uncongested single pieces on the falling limb (*Davidson et al.*, 2015).

We hypothesize that the duration of flows near or just under bankfull exerts the greatest influence on wood transport distance in meandering rivers. Transport capacity is likely maximized near bankfull when smaller-scale channel roughness features occupy a smaller proportion of the total flow and overbank roughness and wood trapping are not yet factors. Longer duration floods just under bankfull may also result in greater bank erosion due to maximization of stream power directed at banks during these flows. Catastrophic bank failures during floods mostly occur on the falling limb (*Rinaldi et al.*, 2008) or between long duration moderate floods (*Luppi et al.*, 2009) from erosion of the bank on the outside of a bend (*Pizzuto*, 2009). Wood that enters the river from these bank collapses falls directly into the thalweg and moves longer distances downstream than previously fluvially deposited instream wood (*MacVicar and Piégay*, 2012). Consequently, transport distances may also be longer for flows with longer duration of stage just under bankfull on the falling limb.

Although larger wood transport rates have been observed when water levels increase rapidly (*MacVicar et al.*, 2009; *Ruiz-Villanueva et al.*, 2016a), not enough studies have focused on wood transport rates in relation to hydrograph characteristics, specifically rates of hydrograph rise and fall, to provide robust constraints, or thresholds for, initial, downstream, or lateral mobility. Thus, uncertainty remains regarding what types of flood hydrographs facilitate the greatest downstream versus lateral movements of wood and whether there are threshold rates of change in water discharge that dictate how and where wood will be deposited for different channel types. Also, more work should be done to characterize the variability in speed of wood transport related to piece type and flow magnitude for diverse rivers. Although *MacVicar and Piégay* (2012) found that uncongested transport of logs

moved at approximately the surface velocity of the water in a single-thread, meandering channel, *Ravazzolo et al.* (2015a) found that wood moved at approximately half the celerity of peak flow for a gravel-bed river.

Although higher floods mobilize wood that remains stable during lower floods (*MacVicar and Piégay*, 2012), the relationship between flood magnitude and large wood flux is highly variable (*Kramer and Wohl*, 2014; *Iroumé et al.*, 2015) and depends on flow history (*Haga et al.*, 2002). The lack of consistent relations between flow magnitude and large wood flux because of the influence of prior flows is analogous to the lack of consistent correlations between flow magnitude and channel morphologic change (*Harvey*, 1984; *Desloges and Church*, 1992; *Cenderelli and Wohl*, 2003). Because wood deposition mostly occurs near peak water discharge (*MacVicar and Piégay*, 2012; *Ravazzolo et al.*, 2015a), we suggest that prior patterns of flood peak magnitudes may have high predictive power regarding how much wood is available for downstream transport in future floods. We hypothesize that the frequency of wood redistribution within the channel banks is largely scale-dependent, such that wood is redistributed more frequently with increasing river size. We predict that further research will reveal a discontinuity in transport flux through drainage networks simply because the frequency of re-distribution and delivery is dissimilar between river types and sizes.

Turowski et al. (2013) has shown that for the steep, step-pool headwater Erlenbach river in Switzerland, coarse particulate organic matter (CPOM) transport rates (including finer material such as twigs, leaves, and large wood) consistently scales with discharge. Furthermore, they suggest that consistent power relations exist for transported piece size distributions of all organic matter and that if transport rates of finer fractions of CPOM can be monitored, transport rates of large wood could be estimated and vice versa. This idea holds some promise, as *MacVicar and Piégay* (2012) found that smaller pieces of large wood followed consistent relations with discharge on the rising limb of a flood, whereas larger pieces did not. *Turowski et al.* (2013) may have found more consistent relations between wood transport and discharge magnitudes compared to other large wood studies (*MacVicar and Piégay*, 2012; *Kramer and Wohl*, 2014) because they included the more abundant finer

fraction of CPOM and/or because a stronger relation between discharge and wood export exists in steep headwater channels with limited floodplains. We suggest further testing the broad applicability of estimating wood discharge based on monitoring subsets of smaller size fractions that have consistent relationships with flood magnitudes, and then back-estimating quantity of larger wood based on known transported size distributions for a particular river.

1.2.2. WOOD CHARACTERISTICS. Five characteristics of wood pieces exert an important influence on wood mobilization and transport: anchoring, length, diameter, orientation, and tree type (species, which governs decay rates, abrasion intensity, density, and branching complexity) (Table 1.3). There is widespread agreement that burial is the most important anchoring mechanism (*Berg et al.*, 1998; *Wohl and Goode*, 2008; *Merten et al.*, 2011) and that rootwads are substantially less mobile than pieces without rootwads (e.g., *Braudrick and Grant*, 2000; *Bocchiola et al.*, 2006a; *Daniels*, 2006; *Cadol and Wohl*, 2010; *Welber et al.*, 2013; *Davidson et al.*, 2015; *Iroumé et al.*, 2015), but anchoring thresholds are not yet well understood. Information is very limited, for example, on the amount of burial needed to effectively keep pieces stationary for floods of variable magnitude and the stability of different types of rootwads. Surprisingly, *Davidson et al.* (2015) recently found that small pieces with simplified square rootwads in flumes were actually more stable than longer pieces with rootwads. We suggest further exploring the relative stabilizing effect and likelihood of subsequent jam formation for different types of rootwads from different species with varying levels of complexity and varying bole lengths because rootwads are commonly used in stream restoration projects. Managers could use information on the minimum degree of root complexity and length required to meet stability criteria because of preference for smaller, less complex pieces that can more easily pass built structures if mobilized. Detailed field measurements of rootwads coupled with 3D printing technology could be used to more accurately simulate wood characteristics in future flume experiments to test anchoring processes.

Table 1.3: Synthesis of main findings and references for influence of wood characteristics on wood transport.

Wood Characteristics

Anchoring

- How well a piece of wood is anchored is the most important variable governing initial wood mobilization; anchoring types include burial, bracing against other pieces or in-stream obstructions, ramping or bridging onto banks, roots of living vegetation growing from logs, rootwads
- The single most important anchoring mechanism for initial mobilization of non-rooted pieces is burial
- Bracing by other pieces of wood is more common and more effective at limiting mobilization than bracing against other in-stream elements, such as boulders
- Wood loads and jams are related to spacing of mobile ramped pieces

Rootwads

- Presence of a rootwad limits travel distance and initial mobilization
- Shorter pieces with rootwads may travel the shortest distances
- Rootwads influence log steering in transport and pivoting during entrainment and entrapment

Length

- A length mobility threshold exists near or above bankfull width; wood less than bankfull width is more easily mobilized and travels farther
- Piece length is a better predictor for whether a piece will move out of a reach than volume or diameter for non-braided rivers
- Shorter pieces (i.e., broken pieces and branches) are transported earlier on the rising limb because they are preferentially transported longer distances on the falling limb of previous floods and deposited at lower elevations
- Shorter pieces of wood may not always move before longer pieces of wood due to shielding and bracing against larger pieces
- In medium rivers, shorter pieces generally travel longer distances than longer pieces but there are instances when the longest pieces travel the longest distances
- In large rivers, there is no consistent relation between transport distance and length of wood
- In braided rivers, medium sized logs travel the farthest distances

Diameter

- A threshold for transport exists when flow depths = a critical floating depth related to the diameter and density; this is 0.5 log diameter
- Diameter is important for controlling the timing and elevation of wood deposition, especially in streams where inundated depth contracts rapidly with small changes in discharge, such as in broad braided rivers or floodplains
- There is weak predictive power between log diameter and distance travelled in single thread channels and high predictive power in braided channels
- Most instream logs float more than half way under water and are denser than in the forest environment

Table continued on next page

Table 1.3(continued)

Orientation

- Single pieces with rootwads are commonly deposited oriented parallel to flow with the rootwad on the upstream side, which can then entrap more wood
- Flume studies indicate perpendicular pieces are mobilized sooner than parallel pieces, while field studies indicate the opposite; natural complexities in piece shapes and anchoring are likely the source of the discrepancy.
- Wood travels parallel to flow: unless interacting with other pieces (then perpendicular), ruddering from branches or rootwads, or travelling through velocity heterogeneities
- Despite smaller forces acting on the parallel pieces, they are more mobile during floods than perpendicular or oblique pieces, which are commonly anchored or braced against other wood or banks
- Loose unanchored pieces originally stored oriented at an angle to flow travel farther distances, most likely because once mobile they ferry across the current away from snags on the bank and enter the swifter velocities of the thalweg sooner

Species (also Decay, Density and Branching Complexity)

- Tree species is a master variable that governs many other mobility predictors (i.e., length, breakage, density, branching complexity, shape, rate of decay)
- Field studies find species to be the best predictor of variance in transport distances
- Travel distance decreases with increasing density
- Density and shape strongly influence travel speed and entrapment during flood recession
- Newly recruited green wood moves differently than fluvial wood due to differences in abrasion, water absorption, and buoyancy

Field References: *Harmon et al.* (1986); *Lienkaemper and Swanson* (1987); *Gippel et al.* (1996); *Piégay and Gurnell* (1997); *Berg et al.* (1998); *Jacobson et al.* (1999); *Keim et al.* (2000); *Haga et al.* (2002); *Lassettre and Kondolf* (2003); *Daniels* (2006); *Millington and Sear* (2007); *Warren and Kraft* (2008); *Wohl and Goode* (2008); *MacVicar et al.* (2009); *Cadol and Wohl* (2010); *Iroumé et al.* (2010); *Merten et al.* (2011); *MacVicar and Piégay* (2012); *Bertoldi et al.* (2013); *King et al.* (2013); *Merten et al.* (2013); *Beckman and Wohl* (2014); *Dixon and Sear* (2014); *Schenk et al.* (2014); *Shields et al.* (2006); *Iroumé et al.* (2015); *Ravazzolo et al.* (2015b,a)
Modelling References: *Bocchiola et al.* (2006b,a); *Braudrick and Grant* (2000, 2001); *Welber et al.* (2013); *Bertoldi et al.* (2014); *Davidson et al.* (2015); *Ruiz-Villanueva et al.* (2015c, 2016b)

Variability in results relating wood size to mobility likely result from: (1) Equal mobility conditions when small pieces are shielded from movement by larger instream structures (such as boulders and larger logs or logjams). This scenario is similar to the concept of armouring in gravel- and cobble-bed streams (*Parker and Toro-Escobar*, 2002). (2) Local anchoring or bracing of pieces in natural channels exerting greater controls on wood mobilization than size (*MacVicar and Piégay*, 2012). (3) Smaller pieces preferentially transported earlier on the rising limb of floods because they are transported longer during the falling limb of prior floods and stranded at lower bank heights (*MacVicar and Piégay*, 2012). (4) Flashy hydrographs mobilizing wood in short time intervals, potentially reducing any significant differences in

initial mobilization between large and small pieces (*Ravazzolo et al.*, 2015a). (5) Variability in piece shapes and densities (*Merten et al.*, 2013). (6) Local and reach scale variability in channel retentiveness and characteristics (*Wyżga and Zawiejska*, 2005; *Wohl and Cadol*, 2011).

Flume studies indicate that pieces perpendicular to flow are less stable than those oriented parallel to flow (*Bocchiola et al.*, 2006b), but this relationship is unclear in the field (*Iroumé et al.*, 2015). In natural channels, individual loose pieces of wood are commonly deposited along channel margins parallel to flow, whereas wood oriented perpendicular is usually anchored or braced. This complicates field mobility studies on log orientation. If flow is sufficient to float most loose, un-jammed wood on the channel margins, a greater amount of wood oriented parallel may be floated simply because there are greater amounts of loose, easily transported pieces with this orientation.

The influence of floating wood piece orientation on travel distance is not well characterized in the field. Video monitoring of a large river found that uncongested wood transport is oblique to flow, commonly zig-zagging across the channel (*MacVicar et al.*, 2009). This is in disagreement with flume studies that show uncongested transport parallel to flow (*Braudrick and Grant*, 2001; *Welber et al.*, 2013). Flume studies typically use smooth dowels, whereas wood pieces in natural channels have irregularities in shape which could work as passive rudders, making parallel travel less likely in natural settings.

We could not find any studies that investigated travel orientation in small to medium channels. We hypothesize that, for these channels, orientation and position of wood in the river are not dominant explanatory variables for travel distance because they are likely to be overshadowed by the influence of flood magnitude and reach-scale roughness elements which can deflect pieces. However, if orientation does play a role in these streams, we hypothesize that wood which spends a longer portion of time oriented parallel to flow will travel longer because the wood is less likely to become lodged or braced en route. This may be one reason why shorter wood travels longer distances; shorter wood pieces are generally more similar

to cylindrical rods and their small size allows them to spend more time travelling parallel to flow and less time being deflected by instream roughness elements.

Species and level of decay dictate how prone driftwood pieces are to breaking en route and can impact travel distances by changing the size and shape of pieces (*Lassettre and Kondolf*, 2003; *Wohl and Goode*, 2008; *MacVicar and Piégay*, 2012; *Merten et al.*, 2013). Preliminary findings from the few studies to explicitly look at influences of density, tree species, and shape on travel distance suggest that tree type is one of the best predictors of downstream transport distance (*Merten et al.*, 2013; *Schenk et al.*, 2014; *Ravazzolo et al.*, 2015a; *Ruiz-Villanueva et al.*, 2016b). We hypothesize that tree type is the most important global predictor variable for how wood moves downriver and through drainage networks, explaining variance associated with transport distance, residence times, travel paths, and depositional patterns.

Recent advances have been made in understanding how wood density relates to water content and buoyancy (e.g., *Ruiz-Villanueva et al.*, 2015c) and how variation in buoyancy among and within different species relates to travel distance (*Ruiz-Villanueva et al.*, 2016b). However, more work is needed on how water content of logs changes as they travel through drainage networks and how this relates to depositional patterns such as the probability of becoming buried, which can lead to longer residence times. We hypothesize that, for a particular tree species, increasing density (due to increasing water content) correlates positively with residence time and negatively with travel distance. In relation to wood type, we also hypothesize that wood pieces recruited from tree species that maintain a more complex, branched shape during river transport have lower mobility than pieces that tend to approximate cylinders.

Case studies conducted on small to large rivers have found that longer pieces are either less likely to be moved during floods or are mobilized at higher discharges (*Jacobson et al.*, 1999; *King et al.*, 2013). A threshold for piece mobility exists based on the ratio of piece length to bankfull width, with logs less than bankfull width substantially more mobile than logs greater than bankfull width (*Lassettre and Kondolf*, 2003; *Shields et al.*, 2006; *Warren and Kraft*,

2008; *Wohl and Goode*, 2008; *Merten et al.*, 2011; *MacVicar and Piégay*, 2012; *Dixon and Sear*, 2014). Longer pieces are more likely to be braced or buried against channel margins, form key pieces in jams, and be anchored by rootwads, all of which give the longer pieces greater stability (*Merten et al.*, 2011). However, there is much variability. For example, wood shorter than bankfull width does not always move when larger pieces become mobile (*Warren and Kraft*, 2008), and tracking studies of loose wood in large rivers have noted no relationship between size of wood and whether a piece is mobile during a flood (*Schenk et al.*, 2014) or the timing of mobilization (*Ravazzolo et al.*, 2015a). This lack of relationship between wood size and mobilization in large rivers is matched by observations in the flume that length does not influence threshold movement for logs shorter than bankfull width (*Braudrick and Grant*, 2000).

Transport distance can be easily assumed to increase with decreasing piece size because, in general, case studies on medium rivers show that wood pieces shorter than bankfull width travel greater distances than longer pieces (e.g., *Lienkaemper and Swanson*, 1987; *Berg et al.*, 1998; *Daniels*, 2006; *Millington and Sear*, 2007; *Warren and Kraft*, 2008; *Iroumé et al.*, 2010; *Dixon and Sear*, 2014). However, transport distances are highly variable and the longest logs are capable of travelling the farthest distance despite their size (*Dixon and Sear*, 2014). Also, this relationship between piece length and travel distance does not consistently hold true for large rivers. Even though bigger pieces are less likely to be moved by floods (*Jacobson et al.*, 1999), once mobilized, there is commonly no consistent relation between transport distance and piece size (*Jacobson et al.*, 1999; *MacVicar and Piégay*, 2012; *Schenk et al.*, 2014; *Ravazzolo et al.*, 2015a). Confusing matters, a flume study simulating a large river showed that mobilization and travel distance actually increase with length (*Davidson et al.*, 2015). Another flume study showed that travel distance peaks with medium sized logs which are long enough to steer off obstacles and have enough momentum to scrape past shallow depositional zones, but are short enough not to be deflected by banks (*Welber et al.*, 2013).

Existing observations leave several questions unanswered: If larger logs are mobilized later and are trapped sooner than shorter logs (*MacVicar and Piégay*, 2012), why can they

have equal or longer transport distances? Is this solely because they travel at faster velocities or could this be a result of sampling bias because it is easier to tag, track, and identify larger pieces? Is there a threshold of piece size for which equal downstream mobility arises? Does this threshold vary by stream and wood type? How does piece length impact the effectiveness of hydraulic steering to avoid obstacles and remain in swift current?

Diameter is more easily measured in the field than wood density and thus is commonly used in field studies of mobilization as a surrogate for flotation depth (i.e., buoyant) depth, which flume studies indicate is an important variable in predicting wood mobilization and entrapment (*Braudrick and Grant*, 2000). For single pieces, diameter controls the timing and elevation of deposition on the falling limb of floods, especially for braided reaches or floodplains where the inundated depth alters rapidly with small changes in river stage (*Bertoldi et al.*, 2013). As depths decrease, larger diameter pieces are slowed and stopped earlier on the receding limb (*Bertoldi et al.*, 2013).

Although diameter can be the most important variable for mobility in braided channels (*Welber et al.*, 2013), in headwater, single-thread mountain and meandering channels, wood diameter is a good predictor of mobilization only in the absence of other, more primary predictor variables such as anchoring and length (*Haga et al.*, 2002). Field observations of natural wood in medium mountain and meandering channels have found no significant relationship (*Iroumé et al.*, 2010) or weak predictive power (*Dixon and Sear*, 2014) between log diameter and distance travelled. Thus, although diameter appears to be important as a secondary threshold condition for initial mobilization, its influence on travel distance in these channels may be limited to conditions in which greater proportions of flow depth are similar to log diameter, such as during low flows, and through shallow braided or unconfined reaches.

The importance of diameter during low or average flows is supported by work in headwater rivers of Chile, which shows that pieces that move during average floods are not only shorter than average bankfull width, but also have diameters less than half bankfull depth *Iroumé et al.* (2015). During braided flume studies, (*Welber et al.*, 2013) also found that

wood mobility decreased at threshold flows equal to half of the diameter. Thus, we hypothesize that diameter is a stronger predictor variable for wood mobility in reaches with high depth variability during wood-transporting flows and that diameter becomes increasingly significant with greater proportion of flow depths near half the diameter. Although half-diameter appears to be equivalent to the flotation depth of wood, recent experiments of relationships between water saturation, density, and buoyancy for instream wood suggest that most logs actually float more than halfway underwater (*Ruiz-Villanueva et al.*, 2016b). Thus, the half-diameter threshold for wood mobility identified in the field and flume (*Welber et al.*, 2013; *Iroumé et al.*, 2015) may be more closely related to conditions when flow depths are slightly less than flotation depths.

1.2.3. REACH CHARACTERISTICS. Although there are general patterns that relate hydrology (see Section 1.2.1) and wood characteristics (see Section 1.2.2) to wood mobility, these relations are highly variable (*Welber et al.*, 2013; *Iroumé et al.*, 2015) and significant differences in mobility and deposition exist among contrasting channel types, sizes, and forest disturbance regimes (*Young*, 1994; *Wyżga and Zawiejska*, 2005). Much of this variability is likely related to local channel and floodplain characteristics that promote reach-scale retention (*Braudrick and Grant*, 2001; *Wyżga and Zawiejska*, 2005; *Pettit et al.*, 2006) because, during floods, wood is preferentially deposited and stored in hydraulically rougher (*Ruiz-Villanueva et al.*, 2015b), unconfined (*Dixon and Sear*, 2014; *Lucía et al.*, 2015) reaches.

The degree of channel roughness is commonly described using relationships between wood characteristics and channel morphology (*Braudrick and Grant*, 2001), abundance of dead wood and jams (*Beckman and Wohl*, 2014), and presence of live-wood within the flow (*Jacobson et al.*, 1999). Forest history governs the recruitment of new wood (*King et al.*, 2013) and catastrophic events can drastically change wood loads, channel morphology, and distribution of live wood (*Johnson et al.*, 2000; *Pettit et al.*, 2006; *Oswald and Wohl*, 2008). Thus, we have grouped reach-scale characteristics that govern wood transport into five categories: channel morphology, wood abundance and jams, live wood, and forest disturbance history (Table 1.4).

Table 1.4: Synthesis of main findings and references for influence of reach characteristics on wood transport.

Reach Characteristics

Channel Morphology

- Wood will be routed more quickly and stored for less time in reaches that are confined versus unconfined, multi thread versus single thread, higher slopes versus lower slopes, flow regulated versus unregulated, smaller variability in channel depths of the flooded cross-section
- Best predictors for wood mobility and transport distance change based on channel type; in reaches with high connectivity to floodplains, wood characteristics are better predictors, whereas in channelized reaches, hydrologic variables are better predictors
- Wood transport distances and mobilization are substantially reduced on floodplains versus the main channel
- For steep, coarse substrate, confined channels, roughness during low flows limits transport mobility and distance travelled; as flows overtop roughness elements, transport capacity increases, and wood flux is limited by supply
- For alluvial channels with floodplains where low flow roughness is low, the duration and depth of flow over sand bars and supply of wood limit transport at flows under bankfull, whereas vegetated bars and floodplains limit transport as flows begin to overtop the regularly flooded channel
- Degree of sinuosity may not limit transport distance

Wood Abundance and Jams

- Large wood and wood jams are commonly the dominant entrapment site for fluvially deposited wood
- Wood pieces incorporated into jams are harder to mobilize than individual pieces
- Storage frequency of jams decreases overall reach-scale mobility of wood
- Single pieces of wood can travel past jams during moderate and high flow.
- Channel spanning wood jams may have a limited impact on the travel distance of wood because most wood is transported during very high flows when jams are floated, water flows around them or over them, or the jams are transported
- Log jams are frequently mobile and often exchange pieces or are transported and re-form in the same location with new pieces but similar structure
- Most jams are mobilized by channel change during high flows or failure of key pieces due to breakage or decay
- Jam frequency and location are related to long ramped pieces
- Increased wood abundance in storage relates to increased wood recruitment during floods

Live-Wood

- Living vegetation within the flow (live-wood) is extremely effective at trapping and anchoring wood, especially key pieces that later form jams
- Floods create heterogeneity in riparian vegetation patterns based on locations of deposited wood piles that re-sprout or provide nursery sites for new live-wood

Table continued on next page

Table 1.4(continued)

Forest disturbance history

- Forest disturbance history is closely related to dead and live wood abundance, which in turn influences mobility
- Extreme floods in channels with high wood loads recruit more wood than floods in channels with low pre-flood wood loads
- Wood mobilization is lower in old-growth reaches due to associated increase in channel complexity and supply of large key pieces that form jams
- Wood is more mobile, with higher export rates and greater travel distances, in recently burned versus unburned catchments
- Large, infrequent, catastrophic disturbances re-set the template for wood distribution patterns and channel change in subsequent years
- Peak wood loads occur decades after catastrophic forest mortality events

Field References: *Murphy and Koski* (1989); *Benke and Wallace* (1990); *Young* (1994); *Piégay and Gurnell* (1997); *Berg et al.* (1998); *Jacobson et al.* (1999); *Johnson et al.* (2000); *Gurnell* (2003); *Wyżga and Zawiejska* (2005); *Shields et al.* (2006); *Pettit et al.* (2006); *Millington and Sear* (2007); *Oswald and Wohl* (2008); *Curran* (2010); *Sear et al.* (2010); *Iroumé et al.* (2010); *Wohl and Goode* (2008); *Wohl and Cadol* (2011); *Collins et al.* (2012); *MacVicar and Piégay* (2012); *King et al.* (2013); *Le Lay et al.* (2013); *Beckman and Wohl* (2014); *Dixon and Sear* (2014); *Boivin et al.* (2015); *Jackson and Wohl* (2015); *Lucía et al.* (2015); *Wohl* (2016)
Model References: *Braudrick et al.* (1997); *Braudrick and Grant* (2001); *Bertoldi et al.* (2014, 2015); *Davidson et al.* (2015); *Ruiz-Villanueva et al.* (2015b, 2016a)

Wood pieces that are not travelling in the thalweg, are long compared to bankfull width, or that have a diameter larger than flow depth, are more likely to interact with in-channel obstructions, channel margins, and the floodplain, limiting mobility and transport distances (*Braudrick et al.*, 1997). The proportion of wood carried in the thalweg versus near-bank regions for different levels of flow and diverse river types is unknown. Preliminary studies suggest that, in large and great rivers, wood is predominantly carried in the thalweg for flows less than bankfull (*MacVicar et al.*, 2009; *MacVicar and Piégay*, 2012; *Kramer and Wohl*, 2014). However, as water levels reach overbank flows, wood is quickly routed to and trapped on the floodplain (*MacVicar and Piégay*, 2012). For flows which exceed bar heights on gravel bed braided rivers, GPS tracking of log paths during transport showed that most logs are transported above bars rather than travelling in the thalweg and, as flows begin to recede, wood is quickly deposited (*Ravazzolo et al.*, 2015a).

Reach characteristics contributing to wood retention change as flood magnitude increases (*MacVicar and Piégay*, 2012; *Ruiz-Villanueva et al.*, 2015b) because deposition is dominantly controlled by the availability and type of trapping sites at peak flow (*Millington and Sear*,

2007; *MacVicar and Piégay*, 2012). For steep, confined, small to medium sized, mountain channels, retentiveness is highest at lower flows and decreases as flood magnitude increases (*Wohl and Goode*, 2008; *Wohl and Cadol*, 2011). However, floods with peak flows greater than bankfull will be more effective at trapping wood than floods below bankfull because wood is more likely to interact with roughness elements such as riparian vegetation and shallow depths in overbank areas (*Wohl et al.*, 2011; *MacVicar and Piégay*, 2012). For any stream reach, we hypothesize that reach retention capacity is smallest within the range of discharges above wood mobilization thresholds and under bankfull, and retention capacity is greatest for very low and overbank flows.

Retention rates of reaches have been estimated using exponential decay models of transport distances for experimentally introduced leaves (*Larrañaga et al.*, 2003) and small dowels $\leq$ 1.06 m in length and $\leq$ .035 m in diameter (e.g., *Millington and Sear*, 2007). Whether these models can be scaled up to model large wood retention has yet to be tested, but emergent properties such as congested transport (*Braudrick et al.*, 1997) are unlikely to be adequately represented in experimental additions of small materials.

Wood transport dynamics on floodplains are less understood than transport in channels, particularly with respect to the timing and transfer of wood between channels and floodplains. Limited studies suggest that, despite having higher initial mobility, floodplain wood does not move very far and floodplains are a net sink for wood that becomes an important part of the floodplain ecosystem (*Benke and Wallace*, 1990).

Large wood, channel-spanning jams, and wood rafts can be very efficacious at trapping wood and when present are commonly the dominant entrapment site for fluvially transported wood (*Pettit et al.*, 2006; *Millington and Sear*, 2007; *Warren and Kraft*, 2008; *Beckman and Wohl*, 2014; *Dixon and Sear*, 2014; *Wohl*, 2014a; *Boivin et al.*, 2015; *Iroumé et al.*, 2015; *Jackson and Wohl*, 2015). Higher amounts of wood in storage, especially as jams, have been related to higher amounts of wood recruited during floods (*Johnson et al.*, 2000), lower wood export rates (*Bertoldi et al.*, 2014; *Davidson et al.*, 2015), and longer residence times (*Wohl and Goode*, 2008). However, several studies highlight that jams are frequently mobilized,

often re-forming in the same locations with new pieces (*Piégay and Gurnell*, 1997; *Gurnell et al.*, 2002; *Wohl and Goode*, 2008; *Curran*, 2010; *Sear et al.*, 2010; *Collins et al.*, 2012; *Dixon and Sear*, 2014). Pieces that are trapped within and behind jams can be released and replaced by other pieces during high flows, so that the overall architecture of the jam appears similar even though the internal pieces are different (*Lienkaemper and Swanson*, 1987; *Dixon and Sear*, 2014). Direct observations indicate that entire logjams can be floated up and then set back down during high flows (S. Gregory, pers. comm., July 2015) or can break apart as individual basal wood pieces break or are dislodged (*Wohl and Goode*, 2008). Although factors such as proportion of channel cross-sectional area obstructed by the jam, potential for overbank flow and dissipation of hydraulic force (*Wohl*, 2011b), porosity of the jam, and cause of jam formation likely influence the relative stability of individual jams, little is known of the relative importance of diverse processes by which jams become mobile.

Because the storage frequency of large pieces of in-channel wood has a negative relationship to piece mobilization (*Merten et al.*, 2011; *Wohl and Beckman*, 2014; *Davidson et al.*, 2015), channels with more stored wood and greater numbers of jams have so far been assumed to have lower overall wood mobility and to transport wood shorter distances (*Warren and Kraft*, 2008). However, destruction and re-formation of jams in the same location may create the impression that a reach is transport limited because there is a high density of wood in storage, when in fact the site favors repeated formation of jams. Thus, field observations made during low flow of changes in wood storage may not actually reflect how much wood moved during a flood because overall storage values within a reach can remain the same despite high wood flux (*Lienkaemper and Swanson*, 1987; *Keim et al.*, 2000; *Wohl and Goode*, 2008; *Dixon and Sear*, 2014). And, although jams and large key pieces of wood form obstacles, they do not impede the ability of some pieces to flow over, around, or through the jams during high flows (*Lassettre and Kondolf*, 2003; *Millington and Sear*, 2007; *Warren and Kraft*, 2008; *Dixon and Sear*, 2014; *Schenk et al.*, 2014). Several questions remain, such as: what storage density of wood is needed to greatly impact overall wood mobility within

a reach; what is the impact of removing wood from streams on the downstream transport of other pieces of wood; and can turnover of wood can be estimated based on storage density?

The proportion of the channel cross-sectional area obstructed by a jam, as well as the porosity of the jam, likely influences the ability of individual wood pieces to move downstream past the jam. Jams can also cause avulsion during high flow (*Keller and Swanson*, 1979; *O'Connor et al.*, 2003; *Collins et al.*, 2012; *Phillips*, 2012), creating a transport bypass chute for wood. We suggest that presence of jams does not necessarily cap wood transport distances at one to two jam spacing intervals, as previously presumed (*Warren and Kraft*, 2008) and modelled (*Martin and Benda*, 2001; *Lassettre and Kondolf*, 2003). We hypothesize that logjam spacing may only limit transport distances during low flows with limited wood mobility. This is supported by observations by *Lassettre and Kondolf* (2003), who found that jams only impede wood travel distance for floods with recurrence intervals $<$ 6-15 years. Relationships between transport distance and jam spacing remain unclear for varying flow magnitudes and should be an avenue of future research. Complicating analysis of jam mobility and jam influence on piece transport in the existing literature is that the word jam is used to refer to both 2-3 pieces of wood in contact (e.g., *Wohl and Cadol*, 2011; *Bertoldi et al.*, 2013), as well as large, channel-spanning structures (e.g., *Beckman and Wohl*, 2014), and commonly the criteria for designating a jam are not clearly stated.

Of particular importance to trapping efficacy during major floods is the presence of rooted living vegetation (live-wood after *Opperman et al.* (2008)) within the flow and on banks (*Jacobson et al.*, 1999; *Pettit et al.*, 2006; *MacVicar and Piégay*, 2012; *Bertoldi et al.*, 2015; *Ravazzolo et al.*, 2015a). Living vegetation is particularly effective at trapping mobile wood in overbank areas (*Wohl et al.*, 2011) and on mid-channel bars (*Jacobson et al.*, 1999). We hypothesize that during infrequent high flows when most wood is transported, the frequency and length of inundation during which living vegetation obstructs flow is a better predictor of wood transport distance than the downstream spacing of logjams. Furthermore, the abundance and distribution of specific live wood species that are singularly effective trappers (*Jacobson et al.*, 1999) may account for most of the variance. If this is the case, then a

large river with flow paths that route wood over vegetated bars and floodplains and through overbank channels may be more transport limited than medium channels with a high density of logjams, even though channel widths on the large river are greater than log lengths.

We also hypothesize that entrapment of wood by living vegetation may be the reason why wood flux peaks before water flux (*MacVicar and Piégay*, 2012; *Ruiz-Villanueva et al.*, 2016a), because live wood can snare dead wood on the rising limb of the hydrograph before deposition during flood recession due to decreasing flow depths. If this is true, then the lag between the wood flux peak and the discharge peak could be used as a measure of overall entrapment efficiency of that channel for a particular flood.Episodic re-organization of wood and mass deposition of wood from exceptional flooding can have lasting effects on channel morphology and overbanks and greatly impact the availability, mobility, and transport paths of wood (*Oswald and Wohl*, 2008).

Fluvially deposited wood piles create heterogeneity in riparian vegetation patterns by providing nursery sites for new live-wood and by creating hard points, protecting new growth from rapid erosion of banks and bars at lower flows (*Hickin*, 1984; *Collins et al.*, 2012; *Gurnell et al.*, 2015). Even where input and transfer of fluvial wood are rare and wood piles rapidly decay or burn, their influence on vegetation germination can be substantial (*Pettit et al.*, 2006). Thus, flooding disturbance history can have a feedback loop governing forest structure, heterogeneity, and age, which in turn influence wood loading, channel complexity, and wood transport. Flume studies show a threshold response in patterns of wood storage (*Bertoldi et al.*, 2014) and wood transport to input rates of wood (*Braudrick et al.*, 1997). These results suggest the possibility of using estimates of wood input rates from episodic events, such as floods or hillslope failures, to predict different alternate stable states of reach-scale wood transport (congested versus uncongested) and wood storage patterns (single piece versus jam dominated).

Although there is general agreement that channels draining old-growth forests have lower wood mobility than younger forests due to higher wood loads (*Gurnell*, 2003; *Iroumé et al.*, 2010; *Collins et al.*, 2012; *Beckman and Wohl*, 2014; *Jackson and Wohl*, 2015), some field

TABLE 1.5. Hypotheses regarding controls on wood mobilization and transport drawn from the literature review

Hypotheses and associated assumptions
Flow characteristics The duration of flows near bankfull exerts the greatest influence on wood transport • transport capacity is likely maximized near bankfull • transport distances may be longer for flows with longer duration of discharge near bankfull The frequency of wood redistribution within the active channel is scale-dependent, such that wood is redistributed more frequently with increasing river size
Wood characteristics Diameter is a strong predictor variable for wood mobility in reaches with high depth variability during wood-transporting flows. Diameter becomes increasingly significant with greater proportion of flow depths near half the diameter of wood pieces. In small to medium rivers, orientation and position of wood do not strongly influence travel distance. • orientation and position are likely to be overshadowed by the influence of flood magnitude and reach-scale roughness elements that can deflect pieces Wood that spends a greater portion of time oriented parallel to flow in small to medium rivers will spend more time in transport. • wood moving parallel to flow is less likely to become lodged or braced en route Tree type is the most important global predictor variable for how wood moves through drainage networks. • tree type significantly influences piece size, shape, and wood density For a particular tree species, increasing density correlates positively with residence time and inversely with travel distance. Wood pieces recruited from tree species that maintain a more complex, branched shape during river transport have lower mobility than pieces that weather to cylindrical shape.
Reach characteristics Reach retention capacity is smallest within the range of discharges above a wood mobilization threshold and below bankfull stage. Retention capacity is greatest for very low flows and overbank flows. Log jam spacing only limits wood piece transport distance during low flows with limited wood mobility. During infrequent high flows when most wood is transported, the frequency and length of inundation during which living vegetation obstructs flow is a better predictor of wood mobility than the downstream spacing of log jams. Entrapment of wood by living vegetation may explain why wood flux peaks before water flux. • live wood can snare dead wood on the rising limb of the hydrograph before deposition at flood recession due to decreasing flow depths

studies of transport distances in relation to forest history yield mixed results, with *Berg et al.* (1998) documenting greater transport distances in an old-growth watershed compared to a logged watershed and *Young* (1994) and *King et al.* (2013) documenting greater export in burned watersheds compared to unburned watersheds. Differences between disturbance types and subsequent impact on transport dynamics in channels likely influence these contrasting findings.

Legacy impacts from past land use also influence contemporary wood transport. Studies from forest ecology indicate that rates of wood recruitment vary on time frames from decades to centuries (*Murphy and Koski*, 1989; *Wohl*, 2016). Two centuries or more are commonly required to reach old-growth forest conditions and peak wood loads occur decades after catastrophic forest mortality events such as pine beetle outbreaks (*Bragg*, 2000). Consequently, observed wood transport could reflect past rather than current conditions of the watershed (*Wohl and Cadol*, 2011), but the effect on interpretation of wood transport processes remains unclear.

1.3. Quantitative Summary

Field researchers have made advances in understanding wood transfer and transport through natural drainage networks during the last 40 years, but this has been on a case-by-case basis and generalizations have not yet been drawn from the data. In this section, we focus on analyzing and synthesizing field measurements of wood transport in order to highlight general patterns of wood mobility across diverse sizes and types of rivers. This section also provides a summary of field-derived empirical equations.

We conducted a literature search for field studies that measured the mobility of wood via change in storage in a reach (Eulerian) and studies that measured the travel distance of wood pieces (Lagrangian). Henceforth, we use the term "initial mobility" to refer to observations of change in storage, "downstream mobility" to refer to data that record travel distance, and "mobility" to refer generally to both categories. In the literature, the term mobility is used interchangeably when referring to initial mobility of wood in storage and

downstream transport mobility of floating wood. This ambiguity can create confusion. We distinguish between initial and downstream transport mobility because factors that influence initial mobilization may not be as important for transport of the same piece downstream.

We only included studies with direct mobility measurements in the field. We did not include studies that back-calculated mobility from wood budgets or recruitment measurements, or results from numerical models. We located 40 studies with such measurements in a broad range of peer-reviewed publications (17 journals), as well as one technical report and two theses. About 57% of studies came from physical science publications, while about 43% came from ecology- and forestry-related publications. The largest proportion of studies from a single journal was 20% in *Geomorphology*, followed by 10% in both *Earth Surface Processes and Landforms* and *River Resources Research*. Table 1.6 summarizes the studies by continent and by number of data values contributed from each study. Figure 1.3 displays the distribution of the case studies globally with circle size scaled to increasing numbers of data values. We did not conduct a full quantitative analysis on total wood flux because this information was very limited; most flux values were back-calculated rather than directly measured; and reconciling values from different studies proved too difficult because of different reporting metrics. We suggest another review focused on compilation of wood budget fluxes.

Table 1.6: Summary of field studies by location used in the quantitative analysis of wood mobility. $\#T_d$ are the number of downstream travel distances and $\#M_i$ are the number of initial mobiility measurements used from each study at each location.

Location	River	$\#T_d$	$\#M_i$	Study
North America				
California	Central Sierra Streams	2	23	Berg et al. (1998)
California	Soquel Creek	–	2	Lassettre and Kondolf (2003)
California	Sacramento River	6	6	MacVicar et al. (2009)
Colorado	5 Rocky Mountain Streams-Colorado	–	48	Wohl and Goode (2008)
Georgia	Oggeechie River	–	7	Benke and Wallace (1990)
Illinois	Poplar Creek	1	1	Daniels (2006)
Illinois	Upper Mississippi Missouri Ohio Rivers	–	6	Angradi et al. (2010)

Table continued on next page

Table 1.4(continued)

Minnesota	Streams draining into Lake Superior	–	1	Merten et al. (2010)
Minnesota	Streams draining into Lake Superior	1	–	Merten et al. (2013)
Mississippi	Little Topshaw Creek	–	4	Shields Jr. et al. (2008)
New York	Rocky Branch	1	3	Warren and Kraft (2008)
North Carolia	Lower Roanoke	2	1	Schenk et al. (2014)
North Dakota	Upper Missouri	–	1	Angradi et al. (2004)
Oregon	Bark Buttermilk and Hudson Creeks	–	8	Keim et al. (2000)
Texas	San Antonio River	–	1	Curran (2010)
Washington	Salmon Creek	–	4	Bilby (1984)
Washington	Various	–	1	Grette (1985)
Washington	Queets River	1	–	Latterell and Naiman (2007)
Washington	Streams in Lookout Basin	1	5	Lienkaemper and Swanson (1987)
Wyoming	Crows and Jones Creek	2	4	Young (1994)
Central and South America				
Costa Rica	6 Costa Rican Streams	–	12	Cadol and Wohl (2010)
Chile	Vuelta de la Zorra	1	1	Iroiume et al. (2010)
Chile	Vuelta de la Zorra	–	1	Ulloa et al. (2011)
Chile	Buena Esperanza and Tres Arroyos	3	4	Mao et al. (2013)
Chile	4 Chilean Mountain Streams	–	18	Iroume et al. (2015)
Chile	Blanco River	–	4	Ulloa et al. (2015)
Europe				
Basque	12 Iberian Streams	–	19	Diez et al. (2001)
Basque	Agueara Basin	–	4	Elosegi et al. (1999)
England	Highland Water	1	4	Dixon and Sear (2014)
England	Main Highland Water	–	1	Piegay and Gurnell (1997)
England	upper and main Highland Water	–	2	Gurnell (2003)
England	Upper HIghland Water	–	9	Millington and Sear (2007)
France	Ain River	–	11	MacVicar et al. (2009)
France	Ain River	–	4	MacVicar and Piegay (2012)
Italy	Tagliamento River	–	3	Bertoldi et al. (2013)
Italy	Tagliamento River	1	–	Ravazzolo et al (2015a)
Italy	Tagliamento River	–	8	van der Nat et al. (2003)
Italy	Piave River	1	1	Pecorari (2008)
Switzerland	Erlenbach River	1	–	Jochner et al. (2015)
Africa, Asia and Australia				
Namibia	Kuisab River	1	2	Jacobson et al. (1999)
Japan	Oyabu Creek	4	4	Haga et al. (2002)
Australia	Daly and Katherine Rivers	–	1	Pettit et al. (2013)

Wood mobility is typically monitored via tagging pieces or remote sensing of large accumulations along a reach (Δx) and then noting how much and how far this wood moved within a given time frame (Δt), typically one year. Consolidating data from many disparate sources on wood mobility proved difficult. Most studies do not report the same values because study questions differ. For example, some studies investigated jam mobility, whereas others looked

at mobility of loose pieces. Some studies analyzed only wood that was exported, whereas others considered only newly recruited wood.

From each initial mobility study, we recorded what was measured (typically # pieces or volume of wood), as well as the following categories (if reported): the starting amount in storage ("start"), the amount that left the reach ("left"), the amount that entered the reach ("came"), the amount that stayed ("stayed"), and the final value in storage ("end"). For comparison with the widely used wood budget equation (*Benda and Sias*, 2003), "came" is Q_i and/or L_i , " left" is Q_o and/or L_o. "Start", "end" and "re-positioned" are all different forms of S_c. When possible, the stayed variable was subdivided into an amount that stayed but moved within the reach ("re-positioned"), and the amount that was immobile ("immobile"). When studies did not differentiate between pieces that were re-positioned locally versus pieces that were exported downstream, we assumed that the pieces were exported downstream. When a study differentiated between re-positioned pieces and exported pieces, the authors distinguished two populations of mobile wood, one that moved minimal distances and was locally retained and one that was exported longer distances downstream. In most cases, we were able to back-calculate categories not supplied. Sometimes we calculated values based

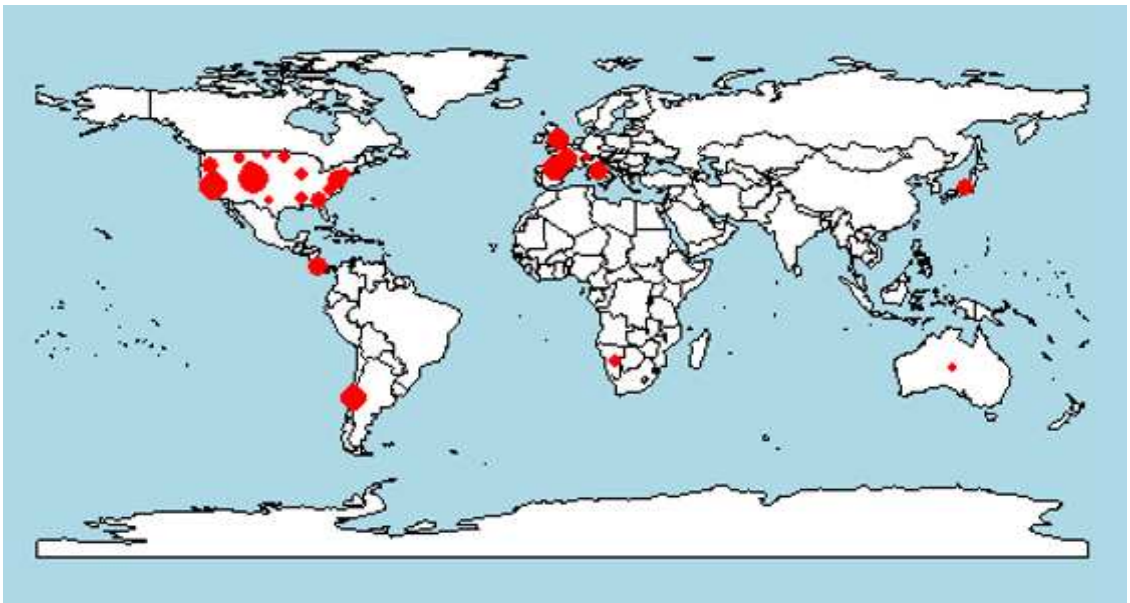

FIGURE 1.3. Location of field data used in the quantitative analysis. Larger circles denote larger numbers of data values used from that region. Table 1.6 lists the studies and rivers used in the analysis.

on a starting value and a reported % mobilized. If we were unable to back-calculate based on given information, the category was left empty.

In addition to these values, we recorded potential explanatory variables: stream width (w), recurrence interval of largest event in Δt (RI), fraction bankfull of largest event in Δt (F_b), maximum log length in storage (L_{max}), study time frame (Δt), and reach length (Δx). We chose not to focus on diameter because the range of flows and channel types would hide any relationships related to diameter. Also, diameter was not as consistently reported as length. When available, we used reported bankfull widths; otherwise, we used reported width, reported mean or median width, or used the center of a given range. We were not overly concerned about the mix of types of width values because the error introduced from this is much smaller than the range of stream widths (1.5 m- 927 m). When possible, we used the fraction bankfull reported for each study. If this value was not reported, we calculated the value based on reported discharge values for floods and bankfull or we estimated the value based on text descriptions, assigning a value of 0.5 for low flows, 1 for near bankfull flows, 1.5 for over bank flows, and 2 for very high flows. In some cases, too little information was given to determine fraction bankfull and this category was left blank. We did not attempt to estimate recurrence intervals and only used values for this category when reported. The final dataset included 36 studies with 229 data entries (Supplemental data file *initialmobility.csv*). Channel widths (w) ranged from 1.5-927 m (median (M)=7.2, n=223), RI from 0.29-50 yr (M=1.5, n=44), F_b from 0.4-5.4 (M=1, n=169), L_{max} from 1-60 m (M=20, n=229), Δt from 0.01-13 yr (M=1, n=211) and Δx from 0.04-240 km (M=100 m, n=193).

We computed dimensionless wood lengths as L_{max}/w (henceforth L^*). L^* values ranged from 0.02-11 (M=3, n=223). Based on data availability, we simply used the maximum length of wood found in storage for the river to calculate L^*. When maximum log lengths were not reported, we used maximum log lengths from other wood studies on the same river or from similar regions. We chose not to use average length of wood, because the size of the largest pieces reflects key pieces for jams and accumulations that moderate wood mobility. Another option would have been to use riparian tree heights, but these are commonly larger

than wood found in the stream because most trunks break during the recruitment process. Maximum wood length might not be the best metric to calculate L^* because maximum length can be highly variable, depending on how many pieces are measured. No studies have thoroughly investigated how L^* should be calculated, so uncertainty remains regarding which log lengths should be used for comparison with stream width to maximize predictive power on wood mobility. Should maximum log length in storage be used, or some other size fraction such as L_{90} or L_{85} (analogous to D_{90} or D_{85} in sediment research)? We recommend that future studies more fully characterize the distribution of log lengths in storage. Additional reporting of other size fractions such as L_{90} and L_{85} might provide better metrics than L_{max} to use in calculations of L^*. Also, channel width is generally assumed to be width at bankfull, but there is no reason to limit L^* to just one width and this metric could be calculated at various stages of flooding.

In order to compare studies, we calculated the % net change in storage ((end-start)/start), re-deposition rate (% end value that came), re-mobilization rate (% start value that left), stability rate (% of start that stayed or was re-positioned), re-position rate (% start value that was re-positioned), and % total mobile pieces (100*(came + left + re-positioned)/(start + came)) in Δt. We suggest that % total mobile pieces as defined here is the best overall metric for mobility because this includes imported, exported, and locally transported wood as a fraction of all the wood that moved through storage during Δt. In many studies, it is unclear whether mobilized pieces were locally mobile or left the reach because no differentiation is made between re-positioned pieces and downstream mobile pieces. The most commonly reported mobility variable was the re-mobilization rate because most studies were focused on exploring factors that influenced the relative stability of wood already in storage, not fluvial re-deposition of previously transported or newly recruited wood.

We analyze transport distance by stream size using all reported values for distance travelled: minima, maxima, means, and medians (Supplemental data file *distance.csv*). We used all reported values in order to assess range of variability within travel and because travel

distance from field data is limited. Although we would have liked to compare transport distance to transported wood lengths and diameters, many studies did not report transported log dimensions separately from stored wood dimensions. Thus, we were unable to extract this information for enough studies to achieve meaningful results.

1.3.1. Results. To obtain an overall sense for initial mobility during varying flows, we plotted % mobility values against fraction bankfull and against recurrence interval (RI) of the highest flow within the study period (Figure 1.4). Most of the data are from flows under twice bankfull. Of the studies that reported RI, most were $\geq$ 1 yr and $<$ 10 yr. There is a strong stepped threshold for maximum mobility at bankfull discharge or the yearly recurrence interval. Below bankfull or for minor floods with less than yearly RI, the maximum possible mobility of stored wood is ~30%. For bankfull or higher discharges, maximum possible mobility jumps to ~80%. These thresholds bound a mobility envelope for stored wood. The outliers not contained within this envelope include mobility measurements after large morphological changes (*van der Nat et al.*, 2003) or measurements of mobilization of newly recruited wood on an actively eroding meander bend (*MacVicar et al.*, 2009) and in a braided river (*Bertoldi et al.*, 2013).

The 30% percent low flow maximum mobility threshold (Figure 1.4) is slightly lower than typical values for % of wood stored as individual pieces and % of wood in the regularly flooded channel (Table 1.7). This is expected because some of the individual pieces are probably above bankfull and some of the pieces below bankfull are probably within stabilizing jams or anchored. Comparing loose, unattached single pieces at varying stage heights to low flow mobility rates would be useful. If a consistent relationship holds, it may be possible to determine yearly, low flow, background wood flux based on wood elevations, akin to base flow on hydrographs.

To relate mobility to change in storage (ΔS), we plotted the % total mobility in relation to net change in storage (Figure 1.5). Our compiled data show that a net change in storage of zero is associated with the widest range in mobility from zero to ~80-90 %. There appears to be a definable lower threshold for % total mobility based on % net change in

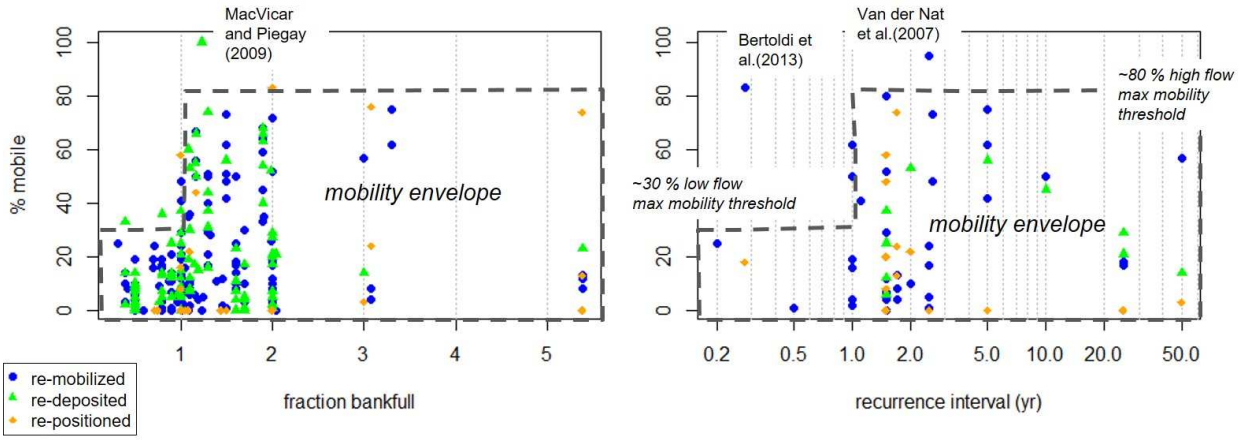

FIGURE 1.4. Mobility of wood in relation to flow. Left: Mobility related to fraction of bankfull from the highest discharge in the study period. Right: Mobility related to highest recurrence interval flood within study timeframes. Dashed lines annotate possible mobility thresholds outlining a mobility envelope. Marked outliers discussed in the text. Data are provided in the supplemental file *initialmobility.csv*.

TABLE 1.7. Case study values for percent pieces in storage that could be potentially mobile in lower flows. %Ind. is the percent of wood surveyed as individual pieces and %ubf is the percent of wood in the regularly flooded channel between low flow and bankfull.

River (Reference)	% Ind.	%ubf
East Fork (*Berg et al.*, 1998)	23	–
Empire (*Berg et al.*, 1998)	<1	–
Lavezolla (*Berg et al.*, 1998)	27	–
Badenaugh (*Berg et al.*, 1998)	2	–
Sagehen (*Berg et al.*, 1998)	25	–
Pauley (*Berg et al.*, 1998)	9	–
Veulta de la Zorra (*Ulloa et al.*, 2011)	50	47
Pichún (*Ulloa et al.*, 2011)		20
Tres Arroyos (*Mao et al.*, 2013)	88	–
Sacramento (*MacVicar et al.*, 2009)	66	40
Kuisab River (*Jacobson et al.*, 1999)	54	–
Lower Roanoke (*Schenk et al.*, 2014)	50	44
Kochino-tani Creek (*Haga et al.*, 2002)	66	–
Crows Creek (*Young*, 1994)	25	55
Jones Creek (*Young*, 1994)	37	41
Upper Missouri (*Angradi et al.*, 2004)	39	–
Upper Missouri (*Angradi et al.*, 2010)	86	30
mean	**43**	**40**
st.dev	**27**	**21**

storage (Figure 1.5). This lower bound resembles a funnel that meets at a point and is nearly symmetrical for negative and positive net change for lower rates of mobility. This means that, on average, rivers are in equilibrium with wood inputs equal to outputs. This observation is also supported by Figure 1.4, which shows that there is little difference in the ranges of % mobility of wood that "came" or "went". However, mobility between 30-80% is more commonly related to larger net gains in storage than net loss (Figure 1.5). This probably reflects the influence that high flows have on recruitment of new wood.

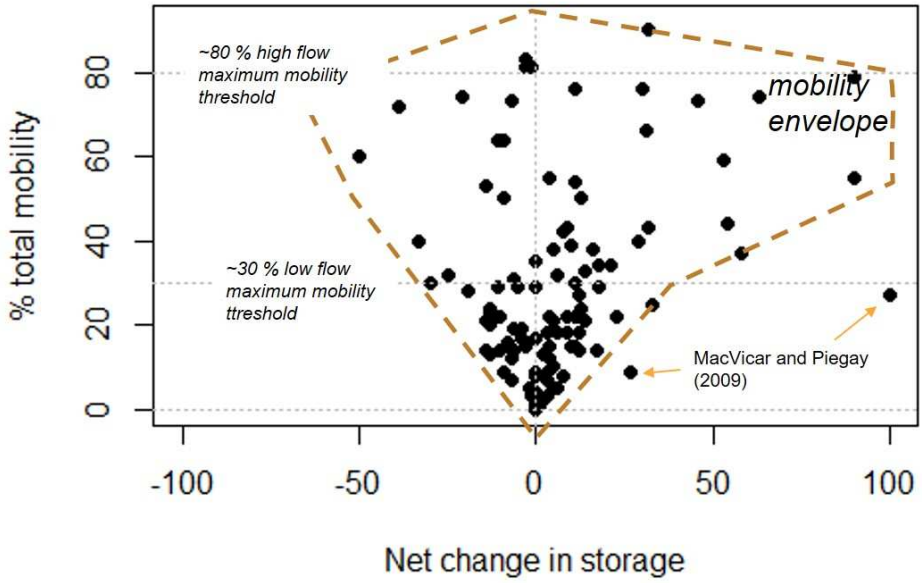

FIGURE 1.5. Total mobility of wood in relation to percent net change in storage. Dashed line defines a mobility envelope, marked outliers are discussed in text. Low and high flow thresholds are from Figure 1.4. Total mobility was calculated as the amount of wood that was mobile (re-deposited, re-mobilized and re-positioned) divided by the total amount of wood in storage within the timeframe (original amount plus the amount that was newly deposited). Data are provided in the supplemental file *initialmobility.csv*.

To understand mobility across stream sizes, we plotted percent initial mobility and transport distance against channel width and L^* (L_{max}/w) (Figure 1.6). The explanatory variables w and L^* were plotted on a log scale as well as untransformed to better display the results from the 900-m range in channel widths. Maximum potential wood mobility (drawn as the upper dashed threshold in Figure 1.6) increases as channels become wider up to ~ 3

m, at which point maximum mobility stabilizes at $\sim$ 80-90% up to $\sim$ 20 m channel width, then decreases until channels are >100 m wide, beyond which mobility likely stabilizes again, although we lack the data to definitively show this.

If L^* is used rather than absolute stream widths, this relationship of increasing maximum mobility from small to medium channels (L^*<5), constant maximum mobility for medium channels ($5 \geq L^* \geq 1$), and then decreasing mobility for large channels (L^*<1) becomes more clear, with fewer outliers (Figure 1.6). Outliers not contained within the mobility envelope (Figure 1.6) are from a study of with re-mobilization of recently recruited wood from a volcanic eruption (*Ulloa et al.*, 2015), mobilization of wood from one actively eroding meander bend (*MacVicar and Piégay*, 2012), and re-mobilization of wood due to large morphological changes in braided rivers (*van der Nat et al.*, 2003; *Bertoldi et al.*, 2013).

The braided river data may be plotting outside mobility envelopes due to inappropriate values for stream width used in the calculation of L^*. The estimated channel width carrying water was not reported for different flows, so we had to use the channel width of the entire valley bottom. Channel widths change substantially with small changes in stage along braided rivers. As a result, many of these outlier values may actually plot closer to a medium sized river for low flows, large river for high flows, and possibly a great river for extremely high flows. Also, diameter is an important mobility variable in braided systems where depth and width change rapidly with small fluctuations in flow (*Welber et al.*, 2013). Thus, similar graphics as in Figures 1.4 and 1.6 that replace L^* with a dimensionless log diameter, D* (Diam/flow depth), may highlight mobility patterns in braided rivers and on floodplains that we were unable to capture in analysis.

Transport distances plotted against channel width and L^* fall into two main groups, which are depicted as two separate shaded boxes on Figure 1.6, corresponding to medium and large rivers. There is a discontinuity between these two groups at channel widths between 20-50 m and L^* between 0.5 and 1 (maximum log lengths $\geq$ half the channel width and $\leq$ the channel width). The mean recovery rate from studies for tracked wood was $\sim$ 50-70 % and ranged as low as 0 % for studies that reported transport distance at reach length.

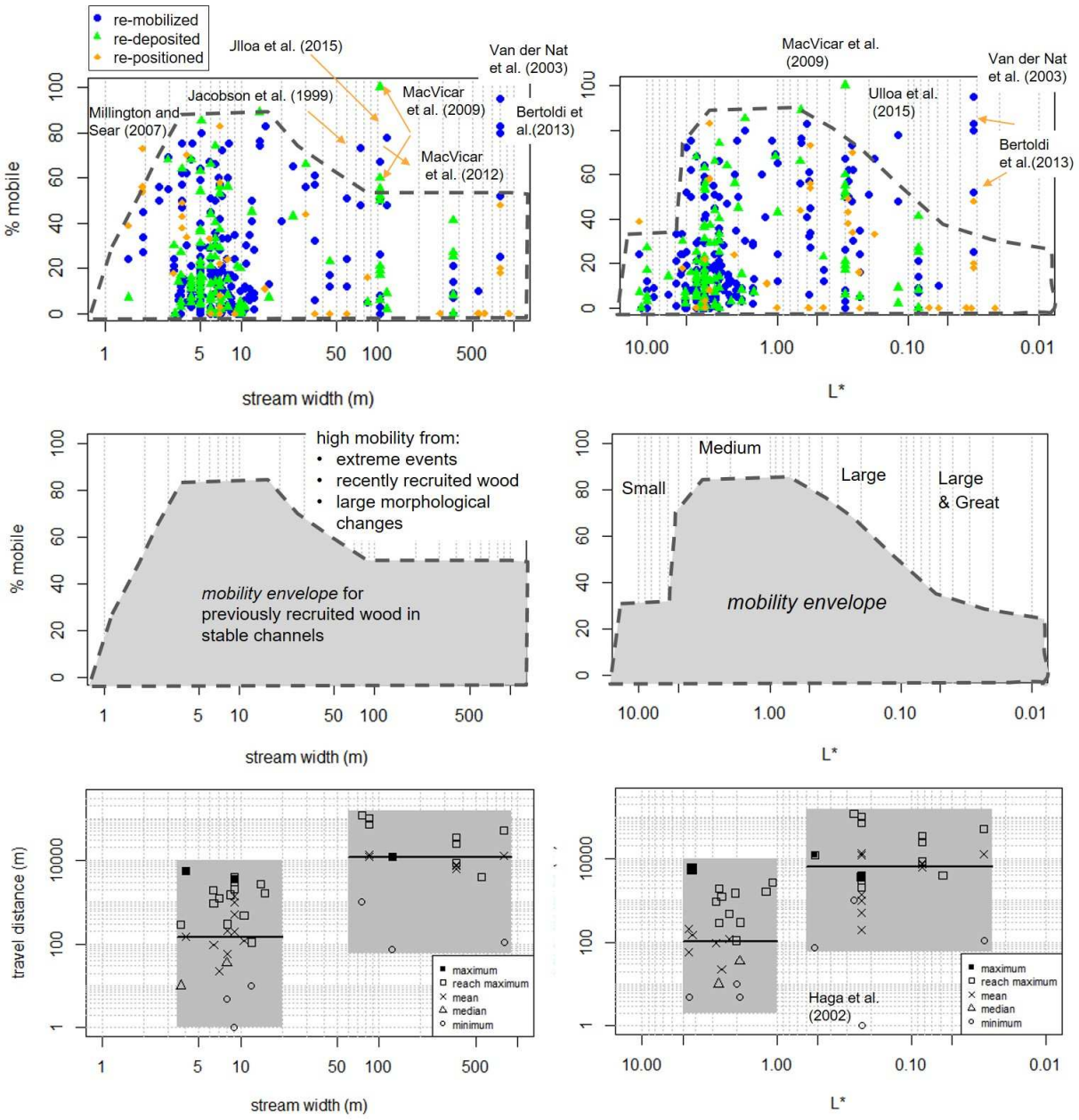

FIGURE 1.6. Mobility of wood in relation to stream size as width (Left) and dimensionless length, L^* (Right). L^* is maximum wood length in storage divided by channel width. Log scales are used to better show patterns across the wide data range. Top row: Presentation of initial mobility data; dashed lines define mobility envelopes. Middle row: Interpretation of initial mobility data. Bottom: Presentation of downstream mobility data. Solid lines mark the median transport value within each shaded grouping. Marked outliers outside of mobility envelopes are discussed in the text. Data are provided in the supplemental files *initialmobility.csv* and *distance.csv*.

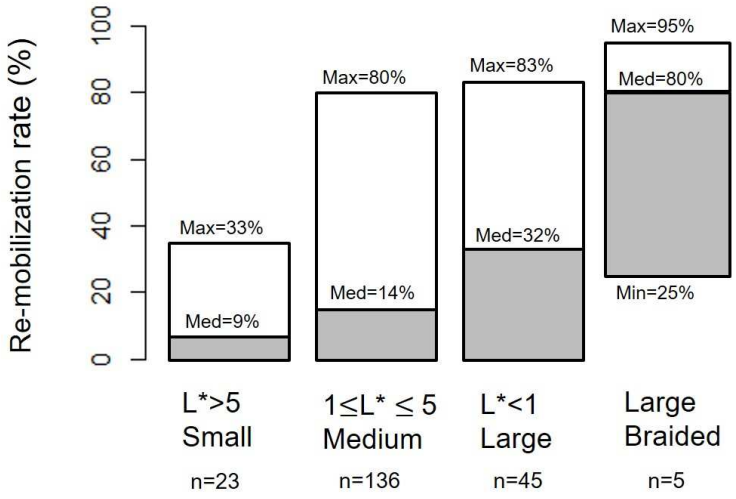

FIGURE 1.7. Re-mobilization rates by stream class. Extent of bars is the range of the data.The shaded grey portion extends from the minimum to the median values.

Even though not all wood was recovered, and thus maxima are not true maxima, transport distances appear to be about two orders of magnitude higher for large rivers than for medium rivers. The median travel distance (calculated from all reported values: max, means and mins) for each group is drawn as a solid black line on Figure 1.6 (bottom row) and is close to 100 m for small-medium rivers and one to two orders of magnitude higher for large rivers. The one outlier is from experimental release and tracking of smaller pieces of wood in a cleaned mountain channel with no obstructions (*Haga et al.*, 2002). Due to the small size of wood pieces, this study plots as a medium river when plotted by channel width, but a large river when considering the size of wood in the experiment in relation to channel width.

One analysis that we would like to conduct is to compare flow (as RI or fraction bankfull) to the ratio: L_{max} of transported wood/L_{max} of wood in storage. Unfortunately, few studies reported both the length characteristics of transported wood and the length characteristics of wood in storage in a manner that facilitated comparison. Or, studies did not include values of flows that transported wood compared to either bankfull or to the gage record. We recommend that future studies of wood mobility report size characteristics of transported wood, size characteristics of the non-transported wood, and recurrence interval or proportion of bankfull for flows.

The transition between medium and large rivers is usually placed at L^*= 1. Our plots of % mobility against L^* (Figure 1.6) reveal that most observations of mobilization have been conducted in medium sized rivers with maximum log length between two and five times channel width. Our plots of % mobility and transport distance suggest that the transition between medium and large rivers occurs between L^*=1 and L^*=0.5. Although maximum initial mobility may be maximized for medium channels (Figure 1.6), median mobility measurements increase with increasing channel size (Figure 1.7), increasing from 9% in small channels (n=23) to 14% in medium channels (n=136), 32% in large channels (n=45), and 80% in braided large rivers (although this sample size is small, n=5).

Several field studies have empirically modelled probability of movement and downstream transport and we summarize their approaches and equations in Appendix 1.A. The probability of movement is typically modelled from change in storage using logistic functions with wood characteristics as explanatory variables (*Merten et al.*, 2010; *Lassettre and Kondolf*, 2003; *Wohl and Goode*, 2008). Variables typically include length or length related to bankfull width, categorical variables for anchoring or rootwads, and diameter related to flow depth. Numerical simulations of wood flux based on physical modeling of a 10 yr flood on the Czarny Dunajec in Poland present transport ratios (the amount of wood exported divided by the amount imported) as linear functions of wood volume, effective depth, and dimensionless wood length (L^*), as well as exponential functions of wood density separately for single- and multi-thread reaches (*Ruiz-Villanueva et al.*, 2015a). Non-linear functions of transport ratios related to varying discharge are also presented in which *Ruiz-Villanueva et al.* (2015a) shows that the transport ratio response is different between more (RI <10-15 years) and less frequent events. *Iroumé et al.* (2015) found linear relationships between percent mobility of stored pieces and flow characteristics such as the unit stream power at maximum stage height and the ratio of maximum stage over bankfull stage.

Transport distance has been modelled using exponential functions to reach retention rates (*Millington and Sear*, 2007) and water depth at peak flow (*Haga et al.*, 2002). Transport distance has also been modelled as a function of jam spacing (*Lassettre and Kondolf*, 2003;

Martin and Benda, 2001), although this may have limited application to low flow conditions when jams are completely obstructing the channel and are not mobile.

Although there is some overlap in variables modeled in empirical field-derived equations for wood mobility (see Supporting Section 1.A), most of the studies listed modeled different response variables (wood velocity, percent mobile, probability of key piece mobility, travel distance) because each study was focused on different goals. To facilitate comparison of mobility between case studies and between rivers of differing size, we suggest that field scientists focus effort on empirical formulation of % mobility and travel distance. As we have shown in Section 1.3, % mobility can be calculated in many ways (e.g., % start that left, % end that came). We suggest developing equations of mobilization that predict the % of starting value that leave the reach or are re-positioned within the reach because this will facilitate estimation of wood flux from measured storage values. However, we highly recommend always reporting the raw volume or count values of changes in storage so that other researchers can re-calculate mobility in other forms.

1.4. Discussion

1.4.1. Foundational Tenets. The origin of instream wood research as a discipline can be traced back to the Pacific Northwest (Oregon, Washington, and British Columbia) during the mid 1970s to early 1990s, where government foresters and fish ecologists became interested in the role of wood for improving fish habitat. Early research into wood transport was primarily motivated by the desire to understand the stability of wood in streams because investigators thought that the longevity of instream wood influences the quality of fish habitat by creating stable pools that trap bio-available fine material and sediment (*Bilby and Ward*, 1989), creating more complex channel morphologies through bank erosion (*Keller and Swanson*, 1979; *Hogan*, 1984; *Nakamura and Swanson*, 1993), and providing nutrients through decomposition (*Anderson and Sedell*, 1979; *Harmon et al.*, 1986). We identified four primary wood transport ideas presented by early papers (e.g., *Anderson and Sedell*, 1979;

Keller and Swanson, 1979; *Harmon et al.*, 1986; *Maser et al.*, 1988) that have informed the design and interpretation of subsequent research.

(1) Channels can be classified functionally into small, medium, and large based on wood dynamics (*Keller and Swanson*, 1979; *Church*, 1992; *Nakamura and Swanson*, 1993)
(2) The pattern of wood stored in river networks reflects input and transport processes (e.g., *Keller et al.*, 1995; *Harmon et al.*, 1986).
(3) Transport of wood increases as the width of channels increases relative to the length of wood pieces (*Lienkaemper and Swanson*, 1987).
(4) Wood transfer is both regular and episodic (*Lienkaemper and Swanson*, 1987).

These tenets were developed mostly from observations in the headwaters and alluvial plains of the Pacific Northwest, which is dominated by Douglas-fir stands in a temperate rain forest with rain and snow melt hydrologic regimes. Although the original investigators recognized that their observations and inferences might not be universal, many of their ideas have since been extrapolated to diverse regions. Here, we discuss these foundational assumptions in the context of the qualitative and quantitative case study synthesis presented in Sections 1.2 and 1.3.

1.4.1.1. *Functional classification from wood dynamics.* *Keller and Swanson* (1979), *Church* (1992), and *Nakamura and Swanson* (1993) introduced the idea that channels can be classified functionally into small, medium, and large based on wood dynamics. Channels are not subdivided into these categories based solely on their size, but based on the patterns and functions of wood within them (Table 1.1, Figure 1.2). *Church* (1992) makes the point that a small river could behave like a large river if all the wood being transported is less than the width of the channel. However, this is not visually intuitive and referring to headwater reaches as large when they do not carry larger pieces of wood is confusing. Because the names of these functional categorizations are small, medium, large, and great, there will always be a propensity to classify them into these categories strictly by channel size rather than by incorporating wood dynamic process domains as originally intended.

Categorizing channels into functional wood dynamic classifications based on size generally works because, as channel size increases, the behaviour of wood also changes. In channel networks, the behaviour of wood roughly corresponds to a piece-dominated regime with rare episodic movement in steep headwaters, followed by a jam-dominated regime in medium sized, second to fourth order channels. As log lengths become shorter than channel width, channel-spanning jams are rare or non-existent and instead wood accumulates on channel margins, bars, side channels, and floodplains. In the flow-dominated regime of large rivers, wood is more regularly transported downstream or exported to the floodplain and is less dependent on large, episodic events to move wood from stable jams. Many large rivers flow into great rivers, delivering their wood into hydraulic, deposition and/or burial-dominated regimes where wood is either transported long distances downstream, is carried onto the floodplain, or is buried.

Although connecting certain process regimes to sizes of channels enables testing of general network trends, the functional wood dynamic classification fails to capture spatial and temporal network heterogeneity. For example, a small creek may have some reaches that are recruitment-dominated and others that are jam-dominated. In addition to referring to rivers by size class to convey scale, we suggest that researchers begin classifying rivers by process domains related to definable regimes of wood dynamics. Universal, succinct process domain categories are useful to facilitate comparison among studies, to explore the temporal-spatial distribution and heterogeneity within channel networks, and to identify sets of predictive equations that perform better under different regimes.

One option is to designate process domain names that refer to the dominant storage, transport, and recruitment regimes. *Davidson et al.* (2015) describe two storage regimes, a randomly distributed, newly recruited state and a self-organized jam, stable state. *Braudrick et al.* (1997) describe three transport regimes: congested, semi-congested, and uncongested flow. We suggest that primary reach-scale wood process domains are recruitment-dominated regimes, jam-dominated regimes, flow-dominated regimes, and burial/exhumation-dominated regimes. Additional process domains are also possible. For example, flash-flood-dominated

regime might be the best category for desert ephemeral channels. *Jochner et al.* (2015) present a compelling, four end-member conceptual model of wood regimes as event-driven export (continuous recruitment, episodic export), event-driven delivery (episodic recruitment, continuous export), fully episodic (episodic recruitment and export), or fully continuous (continuous recruitment and export).

Reach-scale process domains likely transition through time from one regime to another due to fluctuations in flow and changes in morphology, disturbance, or system-wide trajectories caused by regional drivers such as climate change or alterations of land use. Once a consistent set of process domains is defined, this can be used as a tool to explore and map temporal and spatial transitions between process domains.

1.4.1.2. *Storage patterns and transport processes.* Field case studies support the idea that, in rivers where most dimensionless lengths (log length/channel width or L^*) are $<$ 1, interactions between wood and reach-scale morphologic characteristics are the dominant controls on storage patterns, whereas hydraulics exert a stronger influence in larger rivers (*Ruiz-Villanueva et al.*, 2015b). However, even if patterns and general trends are distinguishable, there is commonly substantial variability caused by variations in hydro-bio-geomorphic characteristics on the reach scale that increase or decrease channel retentiveness and trapping sites both longitudinally along a river and with changing flow stage (*Bertoldi et al.*, 2013).

Stored wood characteristics have been used to develop wood budgets to infer wood flux and transport distance (e.g., *Martin and Benda*, 2001) because the pattern of wood stored in river networks is assumed to reflect input and transport processes. To a large extent this is true. When wood is clumped in jams, flows are sufficient to re-mobilize wood (*Davidson et al.*, 2015). Channels with randomly distributed wood are commonly small and wood either decays in place or is only moved during extreme events (*Keller and Swanson*, 1979). As we have shown and others have noted (e.g., *van der Nat et al.*, 2003), flows under bankfull generally transport less than 30% of the stored wood, roughly corresponding to available loose wood positioned under bankfull stage (Figure 1.4, Table 1.7). However, the linkages between

wood transport and wood storage are poorly defined and complex and thus the interpretation of wood transport only through patterns in storage is limited. Video monitoring of wood in active transport on the Ain River, a large meandering river in France, has shown that estimates of wood export derived solely from storage and recruitment characteristics may be underestimating actual wood flux by two to ten times (*MacVicar and Piégay*, 2012).

The main shortcoming is that storage characteristics only provide a snapshot of conditions based on the time interval monitored, limiting inferences regarding short- or long-term temporal fluctuations in transport from seasonal re-surveys of storage. Another problem is the existence of large reach-to-reach variability in wood mobilization. For example, *Iroumé et al.* (2010) found that, for low order, mountain headwater channels in Chile, wood movement (% pieces mobilized) only occurred in a few reaches. Also, there is a large discontinuity in wood storage and transport processes between flows that access floodplains and those that do not (*MacVicar and Piégay*, 2012; *Dixon and Sear*, 2014). Thus, when estimating wood flux from field measurements, results can be highly dependent on design and spatial and temporal extent of sampling.

The largest advances in linking transport processes to wood export and storage characteristics have been made in flumes with simplified wood and mobile banks. These flume experiments have expanded the understanding of linkages between input rates and storage regimes (*Braudrick et al.*, 1997; *Bocchiola et al.*, 2008; *Bertoldi et al.*, 2014), entrapment processes due to the interaction of channel form with wood and flow characteristics (*Braudrick and Grant*, 2001; *Bocchiola et al.*, 2006b; *Welber et al.*, 2013), and how live wood moderates and controls storage and export (*Bertoldi et al.*, 2015). Although these physical models are useful, they are simplifications of the complex interactions found in the field. The combination of infrequent, complex field observations coupled with frequent yet simplified scaled measurements in flumes and models yields the biggest advances, as in *Ruiz-Villanueva et al.* (2016a).

1.4.1.3. *Wood size, channel size, and transport of wood.* The length of wood is arguably the most important control on how wood behaves in rivers. Larger wood is harder to mobilize

than smaller pieces of wood, especially longer pieces, for all stream sizes. This is in part due to piece size, but also because larger pieces of wood are more likely to be anchored in some way. Once in motion, field data suggest that larger pieces are transported shorter distances than smaller pieces of wood in channels where $L^*< 1$ (*Berg et al.*, 1998; *Millington and Sear*, 2007; *Warren and Kraft*, 2008; *Iroumé et al.*, 2010; *Dixon and Sear*, 2014). In larger rivers, log length does not appear to significantly limit transport distance compared to smaller pieces (*Jacobson et al.*, 1999; *Schenk et al.*, 2014; *Ravazzolo et al.*, 2015a). This may result from preferential travel of longer pieces in the channel thalweg (*MacVicar and Piégay*, 2012).

There is general ignorance of the relative importance of factors influencing downstream transport due to the scarcity of studies that actually track transport of wood during floods. We found 17 studies that tracked wood via tagging, RFID, or tethered GPS boxes. Of these, only two actually tracked all wood regardless of how far each piece travelled (*Dixon and Sear*, 2014; *Ravazzolo et al.*, 2015a). Two other studies had 100% recovery for a year because they were able to recover the one piece that moved during lower-than-average flows (*Pecorari*, 2008; *Schenk et al.*, 2014). Most studies only tracked wood within designated study reaches. Thus, for most tracking studies, no absolute maximum distances were measured. Because maximum transport distances were commonly bounded by study reach lengths, reported mean transport distances do not reflect the entire transported population.

Despite the importance of rootwads for limiting both mobility and transport distances (*Wohl and Goode*, 2008; *Davidson et al.*, 2015), almost no information exists relating rootwad size, type, and shape characteristics to mobility beyond noting presence or absence. One exception is a recent flume study which suggests that shorter bole lengths on pieces with rootwads actually increases stability over longer lengths (*Davidson et al.*, 2015), but this is yet to be corroborated in the field.

In our quantitative analysis, we used L^* (length of wood/channel width) to place channels into woody dynamic size categories of small, medium, large, and great (Figure 1.6). L^* proved to be a useful dimensionless metric that allowed for easy comparison of wood mobility

metrics across stream type and size. However, as discussed in Section 1.3, more work needs to be done to determine which length of wood should be used in the L^* equation to maximize predictability of wood mobility. Should this be L_{max} or a smaller size fraction like L_{90} or L_{85}? Also, *MacVicar and Piégay* (2012) suggested using $\phi = log_2(L)$ to define wood size classes, as done by *Cadol and Wohl* (2010); *Iroumé et al.* (2010) and as used to define sediment size categories. Although this idea has not thus far garnered much support from field scientists, the base 2 log transform of wood lengths has proven useful when modelling and explaining wood mobility.

Investigators commonly assume that the transport of wood increases as the widths of channels increase relative to the length of wood and therefore larger rivers have greater transport capacity than smaller rivers. Although potential transport distance appears to be two orders of magnitude greater for channels wider than maximum log lengths (Figure 1.6), potential mobilization of wood in storage between channel sizes is nuanced. Median values of mobilization increase with increasing channel size, which suggests that larger channels do transport higher proportions of stored wood more regularly than smaller channels (Figure 1.7). However, event-based turnover of stored wood is maximized in medium channels (Figure 1.6). Lower maximum mobilization rates on large rivers compared to medium rivers seem reasonable because the stored wood in larger rivers is more likely to be partially buried or scattered on floodplains at farther distances from the main channel. Medium-sized channels are typically more confined than large or great rivers, with smaller floodplains and coarser substrate. Consequently, most of the stored wood in medium rivers is closer to the thalweg, where flow velocities are the greatest and there is less opportunity for anchoring via burial or by instream live-wood. We suggest that the live-wood growing on islands, bars, and frequently inundated floodplains likely counterbalances the increased conveyance of wood in larger rivers.

1.4.1.4. *Regular and episodic transfer of wood.* Wood transfer is both regular and episodic. *Jochner et al.* (2015) describe a four end-member conceptual model linking combinations of

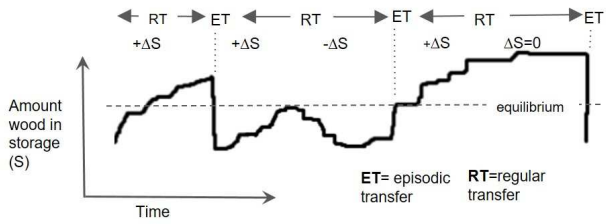

FIGURE 1.8. Conceptual model of dynamic equilibrium of wood in storage (S) through time. Stepped profile reflects alternating smaller scale regular transfer (RT) and large scale episodic transfer (ET) of wood.

continuous recruitment and export with episodic recruitment and export. Even in the Pacific Northwest, which is known for more stable logjams, there are high rates of movement, especially for the smaller fractions of large wood, such that wood flux is a constant process (*Keim et al.*, 2000). Juxtaposed on this constant flux is large scale, episodic flux of the biggest jams and largest pieces during floods with long recurrence intervals.

We have conceptualized regular versus episodic flux of wood in storage in Figure 1.8. The stepped profile of wood storage in the diagram relates to small episodic delivery and export of wood and the large steps represent rarer episodic wood fluxes. Small channels have large episodic wood flux but minimal to no yearly regular flux, whereas larger river have more frequent regular flux but smaller scale episodic flux due to the increased sites of deposition on floodplains during large flows. Plots such as Figure 1.8 for different timescales could illuminate links between wood storage and flux through time and help to characterize variability in wood storage as a function of time. Developing such plots would involve continued monitoring of known sites of wood retention via cameras (minutes to days), field re-visits (months to years), and satellite or remote imagery analysis (years to decades). Especially useful would be measuring the flow stage or discharge so that sudden changes in wood storage could be more easily linked to hydrology.

Most studies are yearly re-surveys that include multiple high flows rather than investigating the impact from one flood, which is problematic for relating wood to flow because wood movement is an episodic, flood-driven process. Thus, there is a disconnection between how mobilization is measured and the process that drives mobilization. Some studies have used cameras or GPS trackers to monitor change in storage at finer timescales (*Bertoldi et al.*,

2014; *Ravazzolo et al.*, 2015a) and others have made efforts to return to field sites during (*Schenk et al.*, 2014) or immediately after floods (*Dixon and Sear*, 2014). We recommend that more investigators attempt to differentiate wood mobility for each wood-transporting flow, rather than simply finding the yearly averaged change in storage.

Our quantitative analysis shows that when flows are sufficiently high, large amounts of wood are episodically recruited to or exported from reaches, with potential for about 80-90% turnover for re-mobilization of fluvial wood (Figure 1.4). The highest turnover rates are for new recruits and in areas with large morphological changes (see Section 1.3). However, for a typical year, there also appears to be a background flux of wood for low flows that is at maximum ∼30% of the total amount of wood in storage (Figure 1.4). Additional data collection focused on the goal of separately measuring smaller-scale yearly flux versus flux from more rare, episodic large flows with potential for high flux would be useful, as would constraining thresholds (both for volume of export and recurrence interval) between the two types of wood transfer. There may be consistent low-flow flux rates related to elevations of loose wood below bankfull that can be used universally to obtain rough estimates of background wood exported from basins. On top of this background rate, episodic flux could be estimated or modelled based on characteristics of flow, wood, and the channel reach.

All mobility rates under maximum thresholds are possible for all flows. The largest flows do not always transport the most wood from a reach and can even have zero mobility (Figure 1.4) because mobility depends not only on absolute flow magnitude but also on deposition patterns set by the sequence of prior high flows (e.g., *Haga et al.*, 2002) and reach-scale biogeomorphic characteristics. Low reach-scale re-mobilization rates can occur alongside high reach-scale re-deposition rates, or vice versa, resulting in increasing or decreasing trends in total reach wood storage. Whether a reach has net increasing or net decreasing trends in stored wood impacts wood export yields for future floods. The asymmetry towards net accumulation of wood in storage for high mobility events (Figure 1.5) could reflect larger scale patterns of global wood accumulation in rivers as a result of afforestation, effects of

disturbances such as fire on wood loads, or decreasing frequency of high peak flows due to increases in flow regulation.

Despite having high interannual variability, most systems appear to be in dynamic equilibrium with regard to wood storage and export (conceptualized in Figure 1.8). Commonly, wood mobilization studies note that wood which is mobilized out of a reach or buried is replaced with new wood so that the total storage volumes remain nearly the same with little net change from year to year (e.g., *Benke and Wallace*, 1990; *Marcus et al.*, 2002; *Wohl and Goode*, 2008). In a wood budget for the Roanoke River, *Schenk et al.* (2014) found that wood flux was in equilibrium, with inputs equaling outputs at close to 5% of the standing stock of wood. They also found that 16% percent of wood in storage was exchanged between temporary storage sites. On the Rio Tagliamento, *van der Nat et al.* (2003) noticed an apparent near-equilibrium between island formation and island erosion on a scale of a few years. In this setting, most wood is recruited during these erosive events, yet wood transport occurs regularly during much lower flows. Thus, remote sensing studies that only record changes in total volumes within a reach may report low mobility because there was little net change in volume, when in fact there was high mobility in piece exchange (*Curran*, 2010).

1.4.2. Wood transport capacity. The phrase "transport capacity" is used liberally in wood research to refer to reaches that do not store large amounts of wood. The most general definition of capacity is the original given by *Gilbert and Murphy* (1914): "the maximum load a stream can carry (35)". With regard to wood, transport capacity is determined by the effectiveness of a reach at retaining wood for a particular flow (*Marcus et al.*, 2002). At low flows, many reaches are transport limited and cannot pass wood, especially wood of large sizes. At high flows when wood transport occurs, in almost all cases, rivers can pass most of the wood supplied, so that all but small natural rivers are commonly supply limited at peak wood flux. As flood waters recede, transport capacity decreases.

The rate and timing of decreased transport capacity on the falling limb depend not only on the steepness of the falling limb, but also on reach and wood characteristics. Blanket statements that refer to reaches as having low transport capacity are not particularly helpful

because transport capacity is not a fixed quantity (*Lisle and Smith*, 2003), but is dependent on wood supply, water levels, and channel retentiveness. Much research on sediment dynamics has focused on better understanding the transition between a particle moving as bedload or suspended load, or immobile to mobile during discharge pulses in flumes and natural settings. Similarly, developing relationships between water levels and channel retentiveness for wood pieces of varying sizes as rivers transition from supply limited to transport limited on the falling limbs of floods would be useful. Basically, when and where does wood transition from immobile to mobile and back to immobile?

Borrowing from bedload research, we have constructed two conceptual models showing transport regimes of wood related to water stage. In Figure 1.9 (top), we diagram theoretical thresholds for wood movement regimes for a single log as a function of transport stage (ratio of water stage over stage at incipient motion (H_t/H_i)) on the rising limb of a hydrograph. In Figure 1.9 (bottom), we depict hypothetical mobility regimes related to discharge as a fraction of bankfull (Q_t/Q_{bf}).

Transport regimes in Figure 1.9 (top) include 1) moving in contact with the channel, 2) deflecting against channel boundaries, and 3) unimpeded floating. Mobility regimes in Figure 1.9 (bottom) include immobile, partially mobile, and fully mobile wood loads. Again borrowing from sediment research, we define immobile, partially mobile, and fully mobile as $< 10\%$, $10 - 90\%$ and $> 90\%$ mobilization of wood in storage, respectively. These categories can also be conceptualized based on downstream movement as "not moved", "locally repositioned", and "exported downstream". These conceptual models could easily be tested, developed, and refined. They can also be used for visual display of differences in threshold position as piece sizes change, or for different hydrologic or channel conditions.

The downstream transport distance of a sediment particle is commonly described as path length, which is the total lifetime stream-wise displacement of particles, composed of multiple step lengths separated by rest periods (*Haschenburger*, 2013). Analogous to this is the spiralling metaphor for wood movement introduced by (*Latterell and Naiman*, 2007) and revitalized in the recent review by *Wohl* (2016, this issue). The spiral metaphor describes

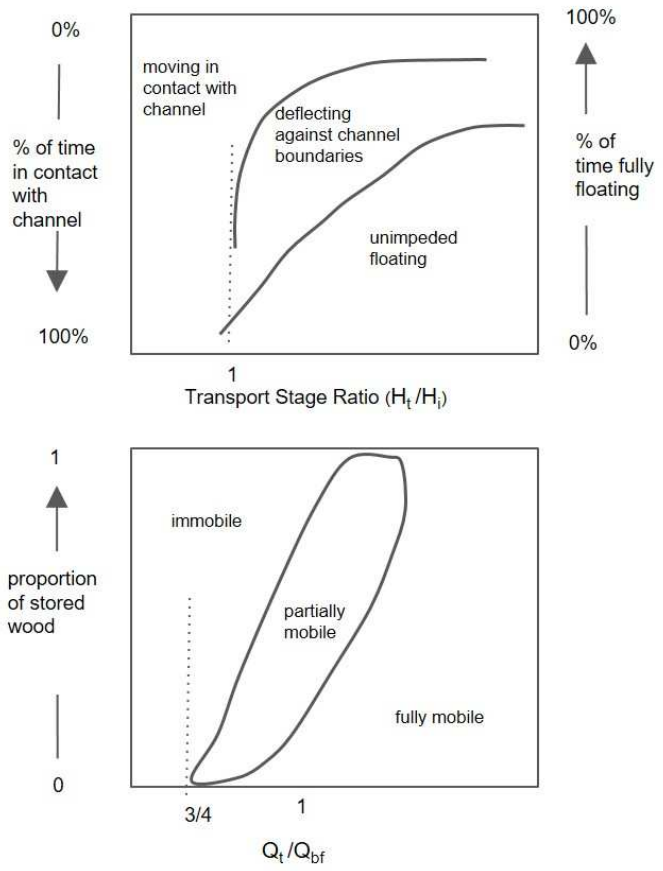

FIGURE 1.9. Conceptual transport regimes and thresholds as functions of flow. Models inspired by data supported conceptualizations of bedload particles by *Haschenburger* (2013). Top: Movement regimes of single logs as a function of transport stage (stage height at time*t* (H_t)/ stage height at initial mobilization (H_i)). At the threshold for movement (1), there is a sharp decrease in the time that wood spends in contact with the bed and the time that it spends floating starts to increase. As stage increases, wood spends more time floating and less time deflecting off of channel features. In this figure, logs do not float for 100% of the time because sometimes logs become beached for shorter amounts of time before continuing downstream. Bottom: Mobility regimes as a function of discharge at time t (Q_t) relative to bankfull (Q_{bf}). Position of thresholds depicted could change depending on patterns of antecedent floods, recruitment events, flow stage and changing channel characteristics. Mapping how thresholds change for changing conditions may be a fruitful endeavor.

the lifetime transport of wood as a series of spirals along a path: The spirals represent rest periods and the width of the spirals depict residence time. The distance between spirals is the step length between resting locations. We have conceptualized the spiral metaphor in the context of a fluvial system in Figure 1.10. The lifetime for a piece of wood from its

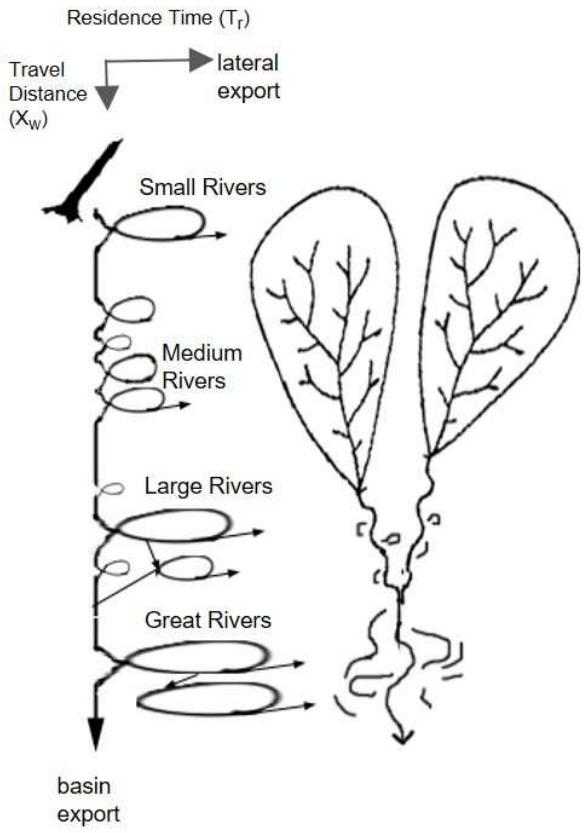

FIGURE 1.10. Conceptual model of the spiralling movement of large wood through a fluvial system. Size of loops represent residence times at a single locaiton before re-entering transport. Connected loops to the side of the main vector represent downstream transport on a floodplain. Diagram after *Latterell and Naiman* (2007) and *Schumm* (1977).

starting location in the channel to its final resting place is then the sum of all the residence times and the travel time (most likely very small compared to rest periods). The distance travelled is the sum of all the step lengths. Throughout the lifetime of the wood piece, from source to sea, the piece undergoes vertical, lateral, and downstream exchanges. Along any spiral, a piece of wood may decay in place, ending its path. Quantifying and contrasting the density functions of step lengths and rest periods for different rivers and through basin networks could be a useful manner in which to identify longitudinal and regional patterns in wood mobility.

1.4.3. A DISCONTINUOUS NETWORK - THE TRAFFIC METAPHOR. Wood dynamics are different for differently sized streams and delivery of wood from one part of a stream network

to another is a discontinuous or episodic process, as depicted in Figures 1.8 and 1.10. Thus, we propose that an apt metaphor for wood transport is vehicle traffic. Just as hydrology, wood characteristics, and bio-geomorphic reach characteristics control the movement of wood through stream networks (*Gurnell et al.*, 2015), motivation to travel, type of vehicle, and road conditions govern how people travel through road networks.

If hydrologic conditions do not meet base thresholds, there will be little to no wood flux, which is analogous to the underlying motivations that govern when and how far people will travel (i.e., wood transport mobilization and travel distance) and when and where they are stationary (i.e., wood residence time). Sometimes, special events cause extra, congested traffic. This is similar to high wood congestion due to large disturbances. More commonly, daily routines and work commutes govern traffic conditions. This is similar to regular background wood flux from normal yearly floods. Travelling at night is less common and only under special circumstances will drivers be on the road during this time. This is similar to lack of wood flux during low flows unless wood is newly delivered from a localized bank failure.

Wood characteristics can be thought of as the type of vehicle in which one is travelling. The vehicle governs which paths or road can be taken and the speed of travel. Someone on a motorized scooter will take different paths than other vehicles, just as a small piece without a rootwad may take a different path than larger pieces with rootwads. However, in some conditions, such as a traffic jam, everyone travels the same speed, which equates to fully congested wood transport.

Traffic conditions and movement are not only governed by the motivation (hydrology) and the vehicle (wood characteristics), but the state of the roads, which controls how fast or how slow a destination is reached. Road conditions are similar to how bio-geomorphic characteristics of reaches, such as presence of live-wood, degree of confinement, channel planform complexity, density of logjams, access to floodplains, and other factors that can limit or increase the distance and rate of movement of wood downstream.

We have conceptualized this metaphor in Figure 1.11 as a flow chart of stoplights. Whether a piece of wood will be moved at any given moment can be predicted by whether

the piece meets minimum mobility thresholds that allow it to go forward (green), possibly move or progress slowly (yellow), or stop (red). We first assess hydrologic conditions for transport to determine whether wood meets minimum thresholds for mobility prior to assessing wood or reach characteristics. If a piece of wood has potential to be transported based on hydrology, then the unique interactions between its characteristics and the channel are assessed. Thus, for any moment of time, a snapshot can be used to assess where individual wood pieces are located and whether they are likely to move based on the hydrologic, wood, and channel "traffic conditions" (see Figure 1.11). Assessments made over the course of a flood can be used to provide estimates of the overall efficiency of wood movement for specific floods. We recognize that this model is a simplification of the complex interactions involved. However, we consider the model a useful framework for modeling and exploring temporal variations in wood flux.

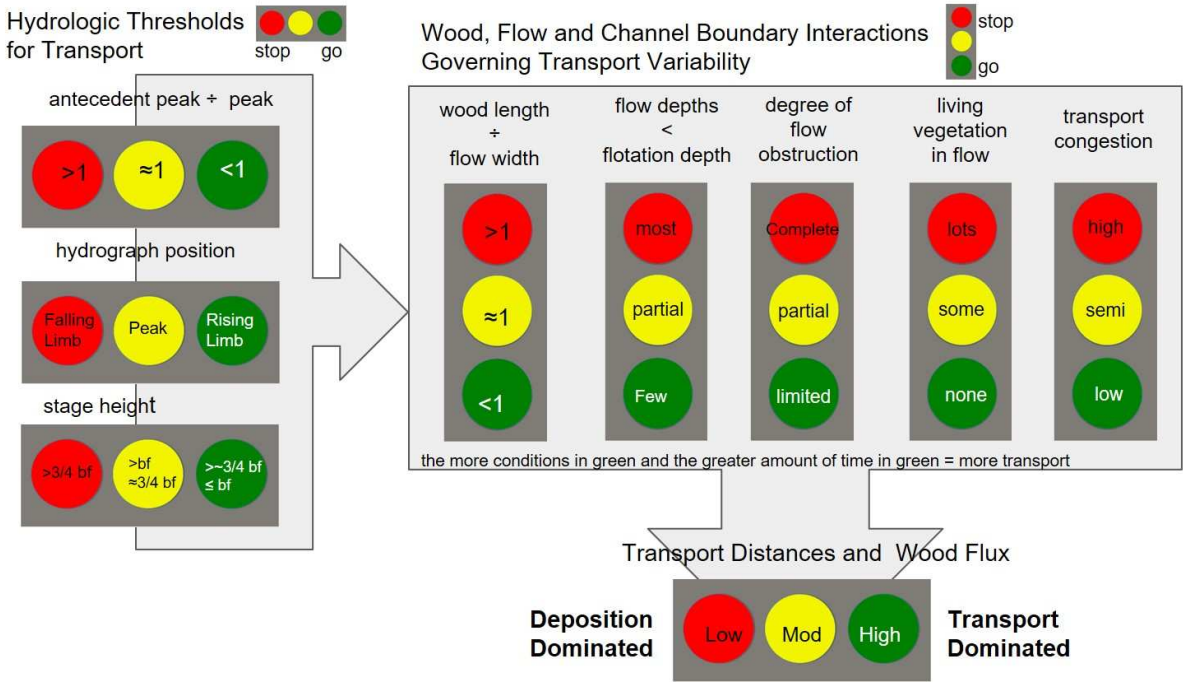

FIGURE 1.11. Conceptual model of wood movement through drainage networks as a traffic stop light metaphor. Fully described in Section1.4.3

1.4.4. MANAGEMENT IMPLICATIONS. Research into the ecology of wood in streams originates in the Pacific Northwest, where logs are large and quite stable. Thus, investigators

have assumed that stable wood is beneficial for the ecology of a stream and considerable sums of money are spent to rehabilitate wood in streams by adding anchored, engineered wood structures, even though soft engineering practices that restore natural processes of wood recruitment and transport may be more ecologically effective (*Kail et al.*, 2007). The reality is that even the largest pieces of wood and jams in natural channels move. When engineered structures are anchored in mobile systems, projects are sometimes declared unsuccessful over timeframes of 5+ years because most of the wood structures are destroyed by large floods or bank erosion (e.g., *Shields et al.*, 2006). Also, engineered logjams in Highland Water (small to medium sized meandering alluvial channel in England) were effective at trapping small wood, but did not limit the downstream transport distances of small wood, as expected (*Millington and Sear*, 2007).

Mobile rivers with high turnover of logjams and instream wood do not negate the ecological significance of wood (*Choné and Biron*, 2015). In a compelling paper on wood mobility and ecological function, *Daniels* (2006) found that although wood in a low gradient meandering river was too mobile to have more than a short-term impact on the morphology or hydraulics of the channel, wood did have a direct impact on the storage of organic material in the bed that outlasted the residence of the wood and provided valuable ecosystem services to benthic communities. They argued that wood removal from low-gradient systems substantially reduces the storage of benthic organic matter.

We speculate that high mobility of wood allows patchy deposition of nutrient-rich organic material to cover a greater spatial extent of the stream bed. If wood is always anchored in place, then organic material is limited to only those areas near anchored wood. Although rehabilitation with anchored wood may be appropriate for reaches in which wood is naturally less mobile, anchored wood is inherently flawed for reaches and rivers in which natural processes facilitate the regular and episodic transfer of wood over time periods shorter than those of desired beneficial ecological outcomes. Wood naturally moves downstream or laterally onto floodplains, so the best and most cost effective management practice is to ensure that the stream has a supply of new wood, preferably including some large pieces,

via upstream recruitment from riparian forests, and then allow the river to redistribute and repeatedly mobilize the wood (*Kail et al.*, 2007).

There is great concern that if management strategies are adopted to increase unanchored wood loads, the mobile wood will endanger instream structures and increase flood damage from clogging. This concern has merit because higher wood loads can facilitate more recruitment during floods (*Johnson et al.*, 2000). However, field evidence indicates that increased amount of wood in storage along a reach does not translate to increased wood against bridges, as presumed, but instead may decrease the hazard of wood clogging (*Lassettre and Kondolf*, 2003; *Mao et al.*, 2013).

In a study in central California, *Lassettre and Kondolf* (2003) noticed a difference between source and transport reaches: simply removing large wood from transport reaches was costly and had little or negative impact on reducing catastrophic log jamming on infrastructure downstream. Most wood comes from pieces recruited from upslope landslides and bank failures during a flood, not from previously transported fluvial wood (*Lassettre and Kondolf*, 2003; *Lucía et al.*, 2015). Higher wood loads have the potential to increase the number of instream jams (*Bertoldi et al.*, 2014) and create greater channel complexity, which in turn increases the likelihood that mobile wood will become entrapped. Thus, the common management practice of removing instream wood may actually facilitate the downstream mobility of newly recruited pieces by decreasing the likelihood that the pieces will be trapped before accumulating against structures (*Lassettre and Kondolf*, 2003; *Mao et al.*, 2013). Rather than removing wood, *Lassettre and Kondolf* (2003) recommended that the most economical option would be to replace culverts and bridges with structures designed to pass wood typical for a stream.

1.5. Conclusions

We propose that the stop and go, the jamming and unjamming, or the discontinuity of wood flux is the most important aspect of the wood regime for river morphology, dynamics, and biota, rather than wood stability. Therefore, wood transport dynamics need to

be incorporated into conceptual and quantitative models of river systems, riparian ecosystems, and nutrient routing. This requires substantial effort to obtain an equivalent working knowledge of wood transport as currently exists for sediment transport (e.g., *Haschenburger*, 2013; *Kuhnle*, 2013). This paper contributes to this effort by summarizing existing transport premises and ideas from prior studies, synthesizing quantitative results on wood transport from field studies, and presenting knowledge gaps, conceptual models, and hypotheses that can be used to design future field, flume, and modelling studies.

The main limitations to describing wood transport are inadequate observation timescales and lack of sufficient mobility data from diverse rivers and regions that also capture variability between reaches. These are similar hurdles to quantifying bedload. Bedload transport equations do not perform well for coarse-grained substrate with poor sorting because they fail to integrate spatial and temporal complexities that influence grain entrainment (*Haschenburger*, 2013).

In order to improve models of wood flux on local and regional scales, we need better characterization of average step lengths within the lifetime travel path of a piece of wood (see Figure 1.10) and we need a better understanding of how changes in storage through time are related to variability in wood flux and hydrology. Efforts to better define entrainment and entrapment conditions and thresholds will be extremely useful, especially focused on individual flows or patterns over decades. A wider range of flow observations for diverse rivers will help to link reach-scale processes with network-scale processes.

Below, we summarize some specific suggested approaches for acquiring data to achieve broader spatial and temporal coverage of wood dynamics.

(1) **Monitor wood in action.** This can be done at a station by monitoring passage via automatic video monitoring (e.g., *MacVicar and Piégay*, 2012), coarse interval timelapse cameras (e.g., *Kramer and Wohl*, 2014), or radio tags (e.g., *Schenk et al.*, 2014). The downstream movement of logs can by tracked with GPS (e.g., *Ravazzolo et al.*, 2015a) or by actively following radio tags during flooding via boat or aircraft (e.g., *Schenk et al.*, 2014).

(2) **Monitor change in storage at known retention sites at varying timescales** (e.g., *Wohl and Goode*, 2008; *Moulin et al.*, 2011; *Bertoldi et al.*, 2013; *Schenk et al.*, 2014; *Boivin et al.*, 2015).

(3) **Use wood characteristics to fingerprint wood source.** This can help identify wood-contributing subbasins and travel distances. *Moulin and Piégay* (2004) were very successful in making inferences about wood flux at basin scales based on the characteristics of wood trapped in a reservoir.

(4) **Quantify the amount of buried wood**. There has been some success identifying buried wood using acoustic bathymetry (*White and Hodges*, 2003) and ground penetrating radar (*Kramer et al.*, 2012), but values of wood buried in stream beds are largely unquantified. Buried wood is an important component of wood flux because, in rivers with sediment loads capable of easily burying wood, at least the same amount or more that is exported may be buried. For example, three-quarters of the wood exported from the Lower Roanoke River to the ocean in North Carolina was buried or decomposed en route *Schenk et al.* (2014).

(5) **Use remote sensing techniques** to assess change on larger spatial and longer temporal scales (e.g., *Bertoldi et al.*, 2013; *Atha*, 2014; *Ulloa et al.*, 2015; *Kramer and Wohl*, in review)

(6) **Conduct stratigraphic and/or other analysis of wood deposited in basins and floodplains** to obtain long term (decade to millennial scale) records of wood flux from watersheds (*Seo et al.*, 2008; *Guyette et al.*, 2008; *Seo and Nakamura*, 2009; *Fremier et al.*, 2010; *Boivin et al.*, 2015; *Kramer and Wohl*, 2015)

(7) **Use already existing data from unconventional sources.** There are hidden data within government agencies, individual scientists, or private companies that

have never been published or otherwise made easily available but that can be acquired if requested. (*Heidorn*, 2008) calls these "dark data". For example, *Moulin and Piégay* (2004); *Seo et al.* (2008); *Fremier et al.* (2010) successfully used reservoir debris extraction records to indirectly estimate basin wood flux. In addition to finding and using dark data, a vast amount of unconventionally collected data is freely available on the internet. Wood researchers have yet to take advantage of this. There are numerous photos and videos of rivers worldwide that include wood and that could be utilized to expand the geographic extent of studies. There are many videos of wood transport, especially wood transport from ice-jam flooding, flash flooding in deserts, and catastrophic flooding. These videos could be analyzed to estimate wood flux during rare events. Some internet contributors have YouTube (www.YouTube.com) channels devoted to chasing flash floods. Also, with the increased use of small waterproof action cameras, outdoor recreation enthusiasts are posting to the internet continuous footage of their excursions down sections of rivers in remote regions. Reports of changes in wood are commonly and regularly posted to online whitewater kayaking forum boards on sections of rivers that are commonly navigated. Finding ways to automatically and easily curate and utilize these data is a worthy research endeavour.

(8) **Participate and use Web 2.0 and create and utilize citizen science initiatives.** Web 2.0 refers to the part of the internet that is interactive, such as social media and citizen science platforms (e.g., www.citsci.org, www.crowcrafting.org). Citizen science refers to the use of non-scientists to help collect, process, or analyze data. Although citizen science initiatives have been utilized in ecology, medicine, and astronomy (e.g., bird surveys, gene mapping, star classification), they have been underutilized by large instream wood researchers (we came across none). In a short review of the use of citizen science, (*Silvertown*, 2009) made the point that " Almost any project that seeks to collect large volumes of field data over a wide geographical area can only succeed with the help of citizen scientists (469)." Citizen science could

be used, not only to collect data from diverse regions, but also to validate and train automatic image processing routines.

Web 2.0 not only opens up real-time interaction between scientists and non-scientists, but can facilitate data collection and curation from diverse individual scientists globally to reduce the amount of "dark data" and facilitate synthesis between studies. This has already been done in medical fields to advance treatment for particular diseases by synthesizing and collecting information on case studies from doctors practicing independently (e.g., *Butzkueven et al.*, 2006). A large but highly rewarding project would be to develop an online interactive river wood data platform where field scientists and managers could add and contribute their data while interacting with each other. This would facilitate better curation of metadata, common reporting of metrics, access to dark data, and international collaborations across disciplines.

(9) **Compile quantitative reviews** that integrate case study information for basin- and reach-scale wood flux, wood recruitment rates, residence times, and storage patterns.

A general approach that will lead to efficient quantification of wood transport is to design studies to constrain thresholds between transport regimes for different channel sizes, channel morphologies, hydrology, and wood characteristics. Until recently, most field studies that included wood transport data treated wood transport as a secondary study goal after description of wood storage, wood recruitment, or ecological impact. As more researchers make wood movement their primary focus, these thresholds will be rapidly identified. We have presented several conceptual frameworks that may prove useful to guide such work (Figures 1.9-1.11).

In an era in which new remote technologies and new sources of data are increasingly accessible and applicable to research on wood in river corridors, we anticipate that studies

of wood transport in rivers are poised to yield significant insights on wood dynamics and river ecosystem management.

Recognition of Support

This research was funded by the Warner College of Natural Resources, Colorado State University and Colorado Water Institue Student Grant (National Institutes for Water Resources (NIWR) Fund #5328011.) We would like to thank Dan Scott for review and feedback as well as the rest of the CSU Fluvial Geomorphology graduate research lab. We would also like to thank two anonymous reviewers who greatly improved the manuscript.

SUPPORTING INFORMATION FOR CHAPTER 1

Introduction. This supplemental information contains a summary of field equations on wood mobility and explanation of variables in accompanying digital datasets stored in the Colorado State University digital repository at `http://hdl.handle.net/10217/100436`.

1.A. Field Equations of Wood Mobility

Transport distance based on exponential scaling by reach retention rates (*Millington and Sear*, 2007).

$$P_d = P_0 e^{-kd}$$

where, P_d= # pieces that moved distance d in meters, P_0 = initial # of pieces introduced, k = per meter retention rate. $1/k$ represents the mean travel distance in m. Equation used in experimental addition of small dowels ($\leq$ 1.06 m in length and $\leq$ .035 m in diameter) were released in Highland Water, a small, meandering, natural channel in England

Transport distance as an exponential function of water depth at peak flow (*Haga et al.*, 2002).

$$y_1 = 0.52e^{12.75x}, R^2 = 0.58(n = 60)$$

$$y_2 = 0.45e^{13.01x}, R^2 = 0.65(n = 37)$$

$$y_3 = 0.26e^{13.97x}, R^2 = 0.71(n = 9)$$

$$y_4 = 3.84e^{8.32x}, R^2 = 0.61(n = 15)$$

where y_i is travel distance for a series of flow events and x is an estimate of water depth at peak flow. Equations derived from experimental release of logs (Length=1.7 m $\pm$ 0.4 Diam=14 cm $\pm$ 4) stripped of irregularities in a 5500-m-long section of the gravel-cobble bedded Oyabu Creek in Japan with no boulders or instream wood to block travel; bankfull width= 9 m; gradient= 4.0; size of released logs not representative of maximum riparian

heights (20-30 m); riparian tree species beech (*Fagus crenata*),oak (*Quercus mongolica*), Japanese cherry birch (*Betura grossa*), fir (*Abies firma*), and hemlock (*Tsuga sieboldii*)

Transport distance as a function of jam spacing (*Martin and Benda*, 2001).

$$\xi = L_j \frac{T_p}{T_j} \beta^{-1}$$

where, ξ is the transport distance over a lifetime of a piece of wood, L_j is the distance between transport obstructing jams, T_p/T_j is the longevity of wood over longevity of jams and β is the transport-obstructing effectiveness of jams. Theoretical quantitative equation based on inter-jam spacing and degree of channel obstruction for 28 reaches ranging from 3.3 to 23 m in width within the Game Creek watershed in southeast Alaska; assumed that transport distance is limited to interjam spacing, did not directly measure distance; tree species are western hemlock (*Tsuga heterophylla*), Sitka spruce (*Picea sitchensis*), Sitka alder (*Alnus sinuate*), and salmonberry (*Rubus spectabilis*)

Stochastic models of travel distance and mobility of individual pieces (*Lassettre and Kondolf*, 2003).

$$T_d = L_j MF[ln(RI)]$$

$$P_m = m_1 + m_2 MF + m_3[ln(RI)]$$

$$MF = \frac{1}{1 + e^{m_1 + m_2 \frac{L}{w_{bkf}} + m_3 \bar{D} + C_1 + C_2 + C_3 + C_4 + C_5}}$$

where, MF is a mobility factor with values between 0 and 1, P_m is probability of movement and T_d is travel distance. RI is recurrence interval, m_1, m_2 and m_3 are constants, L is the length of a piece of wood, $\bar{D}$ is average diameter of a piece of wood, w_{bkf} is the channel width at bankfull, and C_i are categorical variables of decay class by species, species, stability by type, rootwad presence, and cut. Empircal equations developed for individual pieces of wood in central California in meandering sections of Amaya Creek ($w_{bkf} = 6m$) and East Branch Soquel Creek ($w_{bkf} = 12m$) characterized by channel-spanning log jams; stream

wood included big leaf maple (*A. macrophyllum*), red alder (*A. rubra*), tanoak (*Lithocarpus densiflora*), coast redwood (*S. sempervirens*), and Douglas-fir (*Psuedotsuga menziesii*); maximum log length was 60 m; assumed wood moved only the average jam spacing (L_j) for yearly occurring floods; travel distance was adjusted upwards for more mobile pieces and to account for the fact that wood could pass jams by a multiple of MF and the natural log of the return period (RI)

Empirical logistic model of key piece mobility based on wood characteristics (*Wohl and Goode*, 2008).

$$P_m = 1/(1 + e^{-x})$$

$$x = 1.4 + 0.52L^*_{log} + 0.05D^*_{log} - 0.02C_1 - 0.13C_2 + 0.20C_3, R^2 = 0.47$$

Where P_m is probability of key piece mobility, L^* is the piece length divided by average reference channel width and D^* is the dimensionless annual peak flow depth divided by piece diameter. Categorical variables C_1, C_2 and C_3 are whether a key piece is a bridge, unattached or ramped, respectively. Developed using five high elevation streams of the Rocky Mountains in Colorado after 10 years of repeat surveys; channel widths ranged from 4.3 to 6.5 m, maximum wood length was 18 m and in-stream wood was mostly conifers: Engelmann spruce (*Picea engelmannii*), subalpine fir (*Abies lasiocarpa*), and lodgepole pine *Pinus contorta*.

Empirical linear relationships for percent mobility based on flow characteristics (*Iroumé et al.*, 2015).

$$M_{\%} = -4.2 + 0.0065\omega[H_{max}], R = 0.62(n = 17)$$

$$M_{\%} = -14,514 + 20(H_{max}/H_{Bk}), R = 0.60, (n = 17)$$

Where $M_{\%}$ is percent mobility, $\omega[H_{max}]$ is unit stream power for maximum stage height in N/m^3, and H_{max}/H_{Bk} is ratio of maximum stage height over stage height at bankfull. Fitted for forested mountainous headwater rivers in Chile; channel widths range from 5 to

13 m, maximum length of instream wood was 25 m, and wood type is dominated by native coihue (*Nathofagus dombeyi* and *nervosa*) and tepa (*Laureliopsis philippiana*), as well as plantations of eucalyptus (*Eucalyptus globulus* and pine (*Pinus sp.*); results showed wide scatter, with increasing variance among higher values of the explanatory variable.

Empirical exponential relationship between wood volume and wood velocity (*Ravazzolo et al.*, 2015a).

$$v_w = 0.71V_w^{0.22}, R^2 = 0.87(n = 5)$$

where v_w is wood velocity in m/s and V_w in m^3 is wood volume. Equation were developed using data from five logs with GPS tags and tracked during a flood in the large, 800 m wide, bar-braided Rio Tagliamento in northeastern Italy; in-stream wood is at maximum 25 m in length and primarily alder (*Alnus incana*), poplar (*Popoulas nigra*), and willow (*Salix Alba*).

Logistic model of mobilization based on wood characteristics (*Merten et al.*, 2010).

$$P_{mob} = e^x/(1 + e^x)$$

$$x = 0.39 - 2.64\beta_1 + 0.86\beta_2 - 1.52\beta_3 - 0.77\beta_4 - 0.80\beta_5 - 0.09\beta_6 - 1.59\beta_7$$

$$n = 865, P < 0.001, Nagelkerkes R^2 = 0.39$$

where P_mob is the probability of mobilization, β_1=burial, β_2=effective depth, β_3=length ratio, β_4=bracing, β_5=rootwad presence, β_6=downstream force ratio, β_7=draft ratio. Developed using data from instream large wood within the channel from nine forested streams draining into the north shore of Lake Superior, Minnesota; piece lengths 3.8 ± 3 m and diameters $0.18 \pm .13$ m; no tree species specified; flow depths ranged from .53-2.48 m, velocity from .86-1.92, stream power from 15-252 N/m*s, slopes from .001-.02, bankfull widths from 3.4-24 and peak flow from 2.1-54.7 m^3/s; data collected during year of extreme drought.

Transport ratio as a function of wood characteristics and discharge for single thread (T_{rS}) versus multi-thread (T_{rM}) reach (*Ruiz-Villanueva et al.*, 2015a). :

as a function of wood Volume (V_w);

$$T_{rS} = 0.31V_w^{-0.29}, R^2 = 0.56$$

$$T_{rM} = 0.03V_w^{-1.25}, R^2 = 0.33$$

as a function of wood diameter (D_w) and mean water depth (W_{depth});

$$T_{rS} = -0.18(D_w/W_{depth}) + 0.32, R^2 = 0.93$$

$$T_{rM} = -0.49(D_w/W_{depth}) + 0.58, R^2 = 0.94$$

as a function of wood length (L_w) and channel width (w);

$$T_{rS} = -2.19(L_w/w) + 0.92, R^2 = 0.91$$

$$T_{rM} = 2.40(L_w/w) + 0.12, R^2 = 0.82 \text{ for } L_w/w < 0.12$$

$$T_{rM} = -2.91(L_w/w) + 0.77, R^2 = 0.73 \text{ for } L_w/w > 0.12$$

as a function of wood density (ρ_w);

$$T_{rS} = 3.278e^{-3.89}\rho_w, R^2 = 0.98, n = 4$$

$$T_{rM} = 1.036^{-1.83}\rho_w, R^2 = 0.84, n = 5$$

as a function of discharge (Q);

$$T_{rS} = -0.12 + 0.004Q, R^2 = 0.91, \text{ for } Q < 100, RI = 10$$

$$T_{rS} = -0.25 + 0.001Q, R^2 = 0.44, \text{ for } Q > 100, RI > 10$$

OR

$$T_{rS} = -1.96 + .35Q^{0.11}, R^2 = 0.91$$

$$T_{rM} = -0.17 + 0.005Q, R^2 = 0.97, \text{ for } Q < 110, RI < 15$$

$$T_{rM} = 0.3 + 0.001Q, R^2 = 0.55, \text{ for } Q > 110, RI > 15$$

OR

$$T_{rM} = -2.12 + 1.32Q^{0.13}, R^2 = 0.95$$

The transport ratio, T, is the amount exported divided by the total amount imported to the reach. These series of equations developed from numerical simulation using *Woody Iber* computer model and simulating wood and channel characteristics from field data collected from the Czarny Dunajec River in the Polish Carpathians; simulated both multi and single thread reaches; tree species included large alders (*Alnus incana*), large willows (*Salix fragilis* and *S. alba*) and young willows (*S. purpurea* and *S. eleagnos*); wood lengths ranged from 1-18m, mean=12.5, widths from .05-.8 m, mean=0.23 and density from 0.4-0.95 g cm^{-1}, mean=0.56; results from equations from simulation of 10 yr flood (Q=105 m^3/s) and using mean values except for the variable for which the relationship was modelled.

1.B. Datasets

These datasets can be accessed via the Colorado State Digital data repository under Research Project "Big River Driftwood in Northern Canada" (`http://hdl.handle.net/10217/100436`)

Data Set S1 *changeinstorage.csv*. These data provides a compilation of wood mobility from change in storage measurements from previous studies around the world. Presented in Section 1.3.

Study	Full citation provided in bibliography of dissertation
River	River name
Lmax	Maximum Length of wood found in stream in meters
W	Width of stream. If range given, median was used.
TimeInterval	Length of time between monitoring storage
ReachL	Length of reach under investigation in meters
FbankfulpeakQ	fraction bankful of peak discharge between site visits. Either reported, estimated based on text descriptions or calculated based on reported discharges.
RI	Recurrence Interval of highest discharge between site visits. Reported or estimated based on text descriptons
Units	Specifies what was measured
Start	value for amount at beginning of time interval
Came	imported wood into reach during time interval
Went	exported wood from reach during time interval
Stayed	wood that Remained within reach -includes internally mobile pieces.
External	wood that moved through reach in time interval- imported and exported with little to no residence time in storage
Internal	Wood that was repositioned within the reach
End Value	The final value of wood in the reach at end of time interval
%EndthatCame	Reported or Calculated as came/end*100
%StartthatLeft	Reported or Calculated as left/start*100
%StartthatRepositioned	Reported or Calculated as internal/start*100
%TotalMobility	Calculated as (came+left)/(came+left+stayed)

Data Set S2 *transportdistance.csv*. These data provides a compilation of travel distance of wood from previous studies around the world. Presented in Section 1.3.

Study	Citation for study. Full Reference in dissertation
river	Name of river
location	Location of river
Start	Start year or date when wood was monitored
End	End year or date whne wood was monitored
Interval	Time interval as year(s) or fraction year that the distance measurement covers
OneFlood	Factor "Y/N" indicating that the measured travel distance is due to one high flow (Y) or undifferentiated mulitple (N)
FloodLevel	Factor w/3 levels "low" ,"moderate" or "high" indicates qualitatively whether transporting flows were likely below bankful (low), about bankful (moderate) or above bankful (high) based on descriptions in reporting article.
transported	reports the number of pieces in study that monitored and transported.
recovered	reports the number of pieces that were recovered and distances estimated
recoveryrate	fraction of wood moved that was also recovered
streamwidth	reported stream width in m. When ranges were given this was estimated to be the median.
Tmin	Minimum travel distance (m) reported
Tmed	Median travel distance (m) reported
Tmean	Mean travel distance (m) reported
Tsd	reported standard deviation (m) on mean travel distance
Tmax	reported maximum travel distance or maximum monitoring reach size when pieces were transported longer distances than contained within the study area.
TrueMax	Factor w/2 levles "Y/N" which specifies if the maximum reported is a true max or if it simply the bounds of the study reach.

CHAPTER 2

Estimating fluvial wood discharge using timelapse photography with varying sampling intervals

Summary

Monitoring large wood (LW: width $>$ 10 cm, length $>$ 1 m) in transport within rivers is a necessary next step in the development and refinement of wood budgets and is essential to a better understanding of basin-wide controls and patterns of LW flux and loads. Monitoring LW transport with coarse interval ($\geq$ 1 min) timelapse photography enables the deployment of monitoring cameras at large spatial and long temporal scales. Although less precise than continuous sampling with video, it allows investigators to answer broad questions about basin connectivity, compare drainages and years, and identify transport relationships and thresholds. This paper describes methods to: (i) construct fluvial wood flux curves, (ii) analyze the effects of sample interval lengths on transport estimates, and (iii) estimate total wood loads within a specified time period using coarse interval timelapse photography. Applying these methods to the Slave River, a large volume (10^3 cms), low gradient (10^{-2} m/km) river in the subarctic (60° N), yielded the following results. A threshold relationship for wood mobility was located around 4500 cms. More wood is transported on the rising limb of the hydrograph because wood flux rapidly declines on the falling limb. Five- and 10-minute sampling intervals provided unbiased equal variance estimates of 1-minute sampling, whereas 15-minute intervals were biased towards underestimation by $5-6\%$, possibly due to periodicity in wood flux. Total LW loads estimated from the 1-minute dataset and adjusted for a 15% mis-detection rate from July 13th through Aug 13th are: 1600 ± 200 # pieces, 600 ± 200 m^3 and on the order of 1.3×10^5 kg carbon. The total wood load for the entire summer season is probably at least double this estimate because only the second half of the summer flows were monitored and a large early summer peak freshet was missed.

2.1. Introduction

In-stream large wood plays an important and necessary role in the geo-eco-socio functioning of river corridors, coastlines and depositional basins. The presence of wood within channels is increasingly recognized as a contributing factor to large scale change in fluvial forms and processes (*Corenblit et al.*, 2011; *Collins et al.*, 2012; *Polvi and Wohl*, 2013). In-channel wood facilitates complex channel flow, enhances hyporeic flow and creates more pool and backwater areas; thus its presence enhances the biogeochemical cycling of carbon by increasing residence times of particulate organic matter and dissolved organic carbon (*Battin et al.*, 2008; *Wohl et al.*, 2012; *Skalak and Pizzuto*, 2010). Export of wood to the oceans and storage of wood along riparian corridors, lake shores, in basins are important for food webs and biodiversity (*Gonor et al.*, 1988; *Everett and Ruiz*, 1993; *Naiman et al.*, 2002; *Gurnell et al.*, 2005). Artificial introduction of wood for stream rehabilitation projects is a common management strategy (*Beechie et al.*, 2010). Large wood accumulations deposited during floods are considered when designing in-stream structures such as dams, weirs and bridges (*Ruiz-Villanueva et al.*, 2014). Coastlines are stabilized from erosion by the presence of wood (*Heathfield and Walker*, 2011). And lastly, human communities often depend on driftwood as a fuel to heat their homes. (*Jones et al.*, 2013).

Although many studies quantify, either in the field or via remote sensing, the potential stock of wood available for transport along streams and rivers (*Abbe and Montgomery*, 2003; *Moulin et al.*, 2011; *West et al.*, 2011), little effort has been employed in monitoring and quantifying wood in transport as it happens. The buoyancy of wood makes the use of imagery ideal for monitoring wood transport. Just as sediment gages are integral for developing basin-wide sediment budgets, wood gages, in the form of cameras, could be used alongside stream gages to generate wood transport data to inform basin-wide wood budgets. At the most basic level, a wood budget is a change in wood storage along a reach equal to the inputs (from the hillside, bank and upstream) minus the outputs (export downstream or to long term permanent storage on the floodplain). Previous attempts at generating wood budgets have focused on estimating recruitment volumes and changes in storage and then back-calculating

wood export (*Benda and Sias*, 2003). However, this approach may be underestimating actual wood export by as much as a factor of ten (*MacVicar and Piégay*, 2012). Recently, *Schenk et al.* (2014) tracked individual logs in transport using radio telemetry and combined those results with data from aerial photographs and on-site wood surveys to develop the first basin-wide wood budget on the low gradient Roanoke River in North Carolina.

A first attempt at creating a wood transport curve used video monitoring of floods on the Ain River in France in 2011 (*MacVicar and Piégay*, 2012). The study focused on high temporal resolution (continuous recording at 5 fps) video data over hydrograph peaks and then analyzed subsamples via an automated MatLab program. Three major conclusions were: wood transport begins at a threshold value of two thirds bankfull discharge, wood discharge increases linearly with water discharge up to the bankfull discharge, after which it becomes much more variable as the flood plain is inundated, and wood transport rates are four times higher on the rising limb than the falling limb (*MacVicar and Piégay*, 2012).

Whilst video monitoring provides high temporal resolution data useful for computing rates of transport and fine scale relationships between wood and water discharges, timelapse photography allows a researcher to sample at broad spatial and long temporal scales. Investigations at broad scales that answer questions about basin connectivity are integral as river scientists attempt to quantify system resilience and make recommendations for managers in an increasingly uncertain future. Sampling at long intervals (minutes) is also extremely advantageous for studies with small budgets which seek to install networks of cameras to be left up for months. This is especially true for remote areas where access, travel costs, or project costs limit the practicality of video monitoring.

This study is part of a larger study investigating wood transport in large rivers and export of LW to the Arctic from the Mackenzie Basin, Canada. Part of the larger study involves basin-wide questions of wood connectivity, differences in transport thresholds between tributaries and relationships between wood export and ice jam processes. Prior to installing a network of eight remote cameras to be left up for months in a basin which drains 20% of Canada, this study was conducted to develop procedures to: estimate LW fluxes and

total loads during high flows with non-continuous coarse data and; identify unbiased, equal variance coarse sampling intervals with the overall goal to select the coarsest sampling interval possible in order to minimize post-processing time, on-site power usage, and memory storage.

2.2. The Slave River Study Site

The Slave River begins at the confluence of the Peace River with the Athabasca Delta and flows north for 430 km, providing 74% of the inflow to the Great Slave Lake (*Gibson et al.*, 2006), one of the world's deepest lakes and the origin of the Mackenzie River. The Slave River drains approximately 6×10^5 km^2, with much of its water originating from the melting of mountain glaciers and snowpack in the Canadian Rockies in Southern Alberta. The Slave River freezes every winter and there are generally two hydrograph peaks: the first corresponds to ice break-up and the second is a freshet peak related to runoff from snowmelt. However, not all years have a large ice break-up flooding event because it is dependent on river flows and the formation and location of ice jams (*Beltaos et al.*, 2006). In some years, large releases from the W.A.C Bennet Dam (built 1963-1968, filled by 1971) on the Peace River and/or large summer rain events can cause late summer secondary peaks.

The Slave River flows through boreal forest and recruitable trees along the river corridor are predominantly fairly small ($<$ 30 cm diameter) aspens and white spruce. However, it is common to find driftwood tree boles of poplars and conifers $30-80$ cm in diameter (without bark) and $10-20$m in length (many snapped) in the vicinity of the field site (unpublished data). This suggests long (10^2-10^3 km) travel distances of in-stream wood recruited from the Northern Alberta plains and mountainous forests of the Southern Canadian Rockies where trees are larger. Although not addressed in this study, ice processes likely play a large role controlling annual flux of wood from the Slave and other Northern rivers. Trees which fall into the river via bank failure or are stranded by high flows are routinely transported by ice jams and associated floods.

A camera was installed next to the 'Slave River at Fitzgerald' gage 7NB001 operated by Water Survey Canada (1921-present). Based on a cross-section surveyed on May 12, 2011 by Water Survey Canada, the cross-sectional area is around 4000 m^2 with bottom depths from $8 - 12$ m and a surface width of 400 m. The upstream gradient is 10^{-2} m/km and the gross drainage area is 6.06×10^5 km^2. Summer flows generally range from $2000 - 6000$ cms and the highest recorded flow was 11200 cms on May 5th in 1974 during an ice break-up event. The 1.5 year flood is 5700 cms based on 45 years of data from 1966 to 2011. Ice break-up occurs in May, freshet peaks occur in June and July, baseflows are reached by September and freeze-up occurs in November.

The 10 cm in diameter and 1 m in length cutoff for LW commonly used in instream wood studies (*Naiman et al.*, 2002), and the 20 cm in diameter and 3 m cutoff used by *Schenk et al.* (2014) are both reasonable approximate size thresholds for the Slave River based on analysis of size distributions of logs measured in downstream jams (Fig. 2.1). For this site, the upper threshold was adjusted to 0.23 m in diameter based on a natural break in the data (Fig. 2.1). Following convention, all pieces greater 10 cm in diameter and 1 m in length are considered as LW with pieces smaller than this identified as small wood. An extension to this categorization is that LW pieces less than 0.23 cm and 3 m are considered medium LW and pieces greater than 0.23 cm, 3 m are considered large LW. The point jam ratio of small:medium:large was 25:4:1. Using a simple formula for a cylinder (tree boles are usually stripped of branches are fairly straight) and ignoring rootwads, the average LW piece volume was 0.35 m^3, $s^2 = 0.31$ for $n = 127$. Most of the variance in LW volumes comes from the variance of large LW which had a mean volume of 1.01 m^3, $s^2 = 0.52$ for $n = 35$. In comparison, the mean volume for medium LW was 0.09 m^3, $s^2 = 0.01$ for $n = 92$. These are minimum estimates because they do not include rootwad volumes. Approximately one third of the LW logs measured from point jams had rootwads. More work needs to be conducted to develop root wad volume relationships with easily measured metrics.

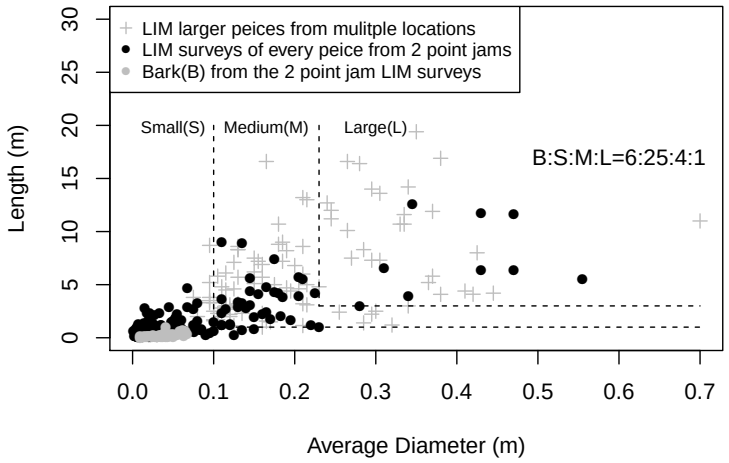

FIGURE 2.1. LW size thresholds from point jams. Wood pieces were measured along transects using the line intersect method in jams within 20 km downstream of the camera location in 2012. Transects were laid along the entire length of the jam perpendicular to piece orientation. Any piece crossing the line was measured for its length and two end diameters. The x-axis in this plot is the average of the two end diameters. For two transects, lines were drawn with spray paint and any piece with paint on it, no matter how small, was counted. These two surveys are represented as filled circles, black denotes sticks or logs while grey denotes bark(B). The grey plus signs represent logs from transects from which only logs $>$ 10 cm in diameter(d) and $>$ 1 m in length(l) were measured. The dashed lines are drawn at two thresholds dividing the log pieces into three categories: small(S) $< d =$ 10 cm, $l =$ 1 m $\leq$ medium(M) $< d =$ 23 cm, $l =$ 3 m $\leq$ large(L). Using these thresholds, the point jam piece size ratio was 6(B):25(S):4(M):1(L).

2.3. Data Collection

In the summer of 2012, an Olympus X560WP camera connected to an intervalometer captured photos at one minute intervals for 32 days from July 13th through August 13th. Not all days were monitored within the study period. The camera was not functioning July 18th, July 23th through the 27th and from August 1st through August 8th. The camera was placed on the outside of a bend constricted by a bedrock point and looked out across the river ($59°51'48"N, 111°35'28"$, 120° azimuth).

For the majority of the channel and the majority of the flows, it took close to, or longer than, one minute for a log to traverse the field of view. Therefore, the 1-minute dataset is assumed to represent the true count of logs during the sampled periods. The thalweg

transported most wood (90% based on an hour of on-site observation) closer than 100 m to the bank with downstream transport distances of $20 - 100$ m in the field of view. The channel length captured by the camera for the far shore is around 400 m. The average velocity calculated by dividing discharge by cross-sectional area ranged from $40 - 60$ m/min throughout the study period. Surface velocities measured by Water Survey Canada on May 12, 2011 during a discharge of 4700 cms ranged from $12 - 150$ m/min. The peak flow during the study period was 5000 cms, the average flow was 4000 cms, and the minimum flow was 3400 cms.

A total of $12,761$ photos were manually analyzed for presence/absence and number of easily identifiable pieces of LW such as tree boles, rootwads, and larger branches. If present, the number of pieces in each photo were tallied. If a log was circulating in the eddy near the shore or if it was at the top of one frame and the bottom of the next, it was not counted more than once. In total, 652 logs were counted and 7% of them had rootwads. This task was not automated because the human eye performs better than automated object identification schemes and the goal of the study is to analyze the effects of sampling at coarser intervals, not the detection of error rates for automated techniques.

In order to obtain an idea of error associated with mis-counted logs in images, an hour was spent on-site viewing and recording logs in transport in 2013. When wood floated by the camera, the time, distance from shore (close < 60 m or far > 60 m), and approximate size (small, medium or large) were noted. Small pieces included sticks and branches estimated to be under the 10 cm in diameter and 1 m in length cutoff for LW. Medium and large pieces were tree boles or large branches. Large pieces were estimated to be greater than 23 cm in diameter and 3 m in length based on piece size distributions measured from downstream jams (Fig. 2.1). During the hour, a total of 102 pieces were counted and the ratio of small:medium:large pieces was 20:3:1. This ratio is similar to the ratio of 25:4:1 obtained from jams, thus the average piece size on point jams is likely a good approximation of average piece size for logs in transport. Counted logs were then compared to wood identified on photos taken during the same time period at intervals of 30 seconds. Small pieces were

generally not seen in the images. Twenty LW pieces (medium or large) were counted with an success rate of 85% (17/20). Thirteen of the 20 logs were correctly counted while 4 of 17 logs were made-up. All of the logs that were missed were medium sized logs marked as far from shore. There was 100% recognition of large logs and medium logs close to shore. From on-site field observations of floating wood, most logs were not waterlogged and floated high on the surface, thus error rates due to sunken logs are assumed to be negligible.

2.4. Wood Flux as a Probability

2.4.1. Statistical Methods. Calculating wood flux as probability of occurrence (proportions of photos) is very advantageous because it does not depend on wood size or count, effectively eliminating large uncertainties with calculating these metrics. It also allows for easy comparison across drainages with different wood sizes and facilitates quick post processing of photos. In order to calculate a wood flux as a probability, only presence/absence needs to be noted. An additional level would be to include several quick categorizations (e.g. absent, single, sparse, clumped, congested or carpet) and the probabilities of each. During this study, there was only sparse wood transport so categories were not utilized.

Unlike monitoring water discharge, it is impossible to ever obtain complete absolute values of wood flux because there will always be data gaps at night when it is too dark to capture good imagery. Additionally, there are often data gaps when equipment is not working or not installed. Stratification of proportion estimates (by time, by discharge, or by any other scheme) allows comparison between strata categories with unequal number of photos and extrapolation of data into unsampled time periods. Precision will always be increased when stratification is used if variance within strata is minimized while variance between strata is maximized (*Scheaffer et al.*, 2012).

For the Slave River case study, both stratification by day and stratification by discharge were utilized. Daily proportions are the probabilities, for any given moment, in any given day, of seeing wood in transport. Discharge proportions are the probabilities of seeing wood in transport for specified ranges of flows. Stratification by day was used to obtain insights

into how LW flux relates to water discharge. Stratification by discharge was used to estimate total LW loads despite data gaps of more than one day.

Proportions, $\hat{p}$, and variances, $\hat{V}(\hat{p})$, were estimated based on systematic sampling of a finite population (*Scheaffer et al.* (2012), pg. 228).

$$\hat{p} = \sum_{i=1}^{n} \frac{y_i}{n} \qquad \hat{V}(\hat{p}) = \frac{\hat{p}\hat{q}}{n-1} fpc \tag{1}$$

Where $\sum_{i=1}^{n} y_i$ is the total number of photos with logs present, n is the total number of photos sampled (sample size), $\hat{q}$ is $1-\hat{p}$, fpc is the finite population correction factor $\frac{(N-n)}{N}$, and N is the finite population, the total minimum number of frames needed to uniquely capture the entire wood load within a period of interest. If the entire period of interest was sampled at intervals equal to the amount of time for a log to travel across the frame, then you would be calculating the proportion exactly ($\hat{V}(\hat{p}) = 0$). For $n << N$ the fpc approaches 1 and $\hat{V}(\hat{p})$ approaches the equation for an infinite population. For this study, 1-minute intervals were used to estimate N since this was the approximate amount of time that it took a log to traverse the field of view during sampling periods (see Data Collection).

If stratification was desired, $\hat{p}$ and $\hat{V}(\hat{p})$ were estimated using double sampling for stratification.

$$\hat{p}_{st} = \sum_{i=1}^{L} \hat{w}_i \hat{p}_i \qquad \hat{V}(\hat{p}_{st}) = \frac{fpc}{n-1} \sum_{i=1}^{L} \hat{w}_i \hat{p}_i \hat{q}_i + \frac{1}{n^2} \sum_{i=1}^{L} (1-\hat{w}_i) \hat{p}_i \hat{q}_i \tag{2}$$

Where L is the number of strata and $\hat{w}_i = N_i/N$, the weight for each stratum. Weights were calculated post sampling as the proportion of the population (total # of intervals) in each stratum. $\hat{p}_i$ was calculated using Eqn 1 for each stratum and 95% confidence intervals were constructed using a bound of $2\sqrt{\hat{V}(\hat{p}_{st})}$. $\hat{V}(\hat{p})$ is the sum of two terms. The first term is the variance of the sampling, while the second term penalizes for choosing strata after the fact (the number of samples within each stratum was not known prior to sampling). In most cases, the second term rapidly approaches zero as n increases and can be considered negligible (this study included).

2.4.2. Slave River Results. Within this 32 day study (July 13th-Aug 13th), LW flux ($\hat{p}$) ranged from zero to just under 20% and peak values corresponded well with a freshet peak in mid July (Fig. 2.1, top). The estimated probability from sampled images over the entire study period was near 4% (Table 2.1). Precision on this estimate was increased by 6% and 9% if stratification by day and by discharge were utilized (Table 2.1). Strata by discharge included two groups: $Q < 4500$ cms and $Q > 4500$ cms based a transport threshold identified by comparing daily water discharges to daily wood fluxes (Fig. 2.1, bottom).

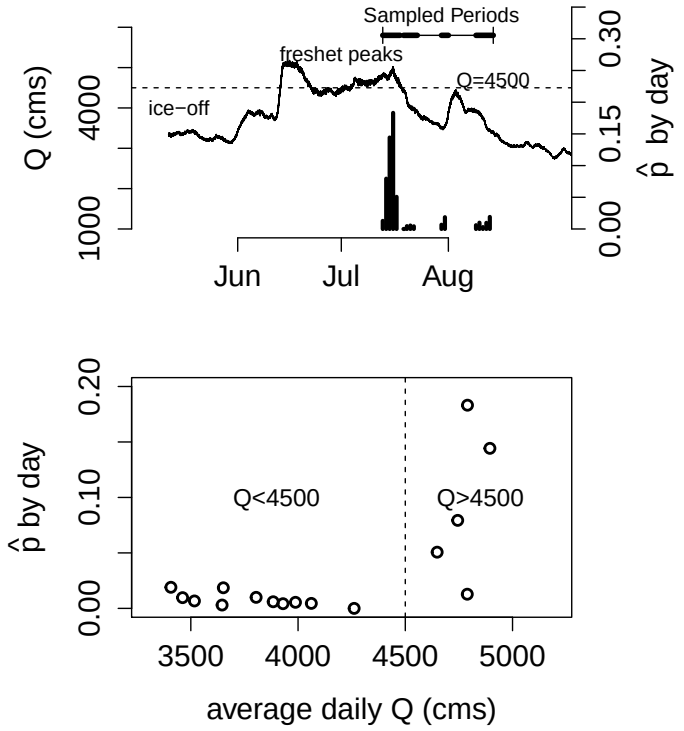

Figure 2.1. Wood flux and transport thresholds, Summer 2012. Top: Comparison of wood flux as daily probabilities (as bars) to water discharge (Q) over the study period. The horizontal line segment at top of graph shows the time period (July 13-Aug 13) over which the total wood loads were estimated. Sampled periods are depicted as thicker bars. Unfortunately due to a camera malfunction, data were not gathered over the apex of the humped peak in late August. For this year, ice-off occurred May 8th without ice jam flooding. However there were two prominent freshet peaks. Camera installation occurred after the first peak, but captured the second. Bottom: daily probabilities of seeing wood in transport versus discharge. A transport threshold of $Q = 4500$ cms is identified and shown in both graphs.

TABLE 2.1. Comparison of stratification versus nonstratification on $\hat{p}$ and its precision for the complete 1-minute dataset from July 13th through August 13th. The finite population total was estimated to be the number of possible frames taken at 1-minute intervals within these 32 days ($N = 46,080$). Q was stratified based on a 4500 cms threshold for transport (Fig. 2.1). Refer to Eqn. 1 for the calculations of $\hat{p}$, $\hat{V}(\hat{p})$, and *Bound*. $\%\Delta$ *Precision* were calculated as change in $1/\hat{V}(\hat{p})$ from no stratification.

	$\hat{p}$	$\hat{V}(\hat{p})$	*Bound*	$\%\Delta$ *Precision*
no stratification	$4.14E^{-2}$	$2.23E^{-6}$	$3.00E^{-3}$	—
stratified by Q	$4.14E^{-2}$	$2.11E^{-6}$	$2.91E^{-3}$	+6.25
stratified by Day	$4.14E^{-2}$	$2.06E^{-6}$	$2.87E^{-3}$	+9.10

2.5. Analysis of Sampling Intervals

2.5.1. Statistical Methods. In order to examine the effects of sampling interval on LW flux and load estimates, The data were split into sub datasets at fixed 5-, 10- and 15-minute intervals. Because the intervals are fixed, there were five 5-minute datasets, ten 10-minute datasets and fifteen 15-minute datasets. Henceforth, each dataset within a sampling period will be referred to as a trial. Variances were calculated with the population total N equal to the 1-minute dataset rather than total number of 1-minute photos possible over the entire study period (see Eqn. 1 and Table 2.1). This was done to use the collected 1-minute data as the known true population, p, when comparing the effects of sampling at coarser intervals. Errors of estimation were calculated daily and for the whole time period as $\hat{p} - p$, where $\hat{p}$ is the estimate of p obtained from the 5-, 10- and 15-minute trials. When the error of estimation is negative, $\hat{p}$ underestimates and visa versa.

To compare variances and bias between sampling intervals, it is necessary to make the sample size of each trial over all sampling intervals equal via bootstrapping. A simple random sample of size $n = 100$ for each 5-, 10- and 15-minute trial was repeatedly sampled $10,000$ times. The mean $\hat{p}$ and $\hat{V}(\hat{p})$ were calculated for each trial, and the average of all the trials within each time interval $\hat{\bar{p}}$ was compared to the population value p from the 1-minute data.

2.5.2. Slave River Results. Non-stratified proportions of photos with wood present were calculated for each trial using Eqn. 1. While the 5- and 10-minute intervals provided

unbiased estimates of the 1-minute proportion ($+10^{-4}\%$), the 15-minute dataset was biased towards underestimating the actual value by about 5% (Fig. 2.1 and Table 2.1).

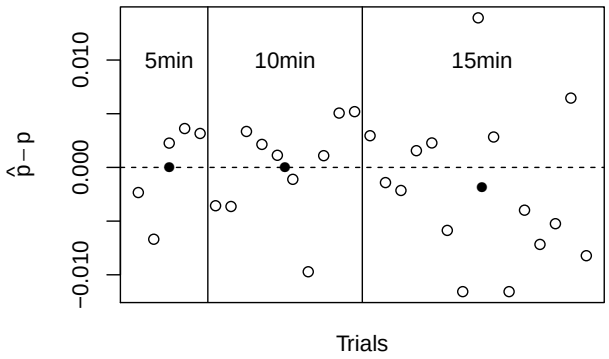

FIGURE 2.1. Error of estimations for all trials. Open circles represent errors from the 1-minute data calculated for each trial, closed circles are the average error of all trials for each interval and the dashed. Circles plotted on the dashed line show very little to no difference relative to the 1-minute dataset.

TABLE 2.1. Mean errors over all trials for each interval. $\hat{p}$ is the estimated proportion of photos with wood over the entire sampling period for each interval and p was estimated from the 1-minute data to be $4.14E^{-2}$.

	5 min	10 min	15 min
$\hat{p} - p$	$2.34E^{-7}$	$3.58E^{-7}$	$-2.20E^{-3}$
$\%difference$	$5.67E^{-4}$	$8.66E^{-4}$	-5.30

All daily estimates of proportions for 5-, 10- and 15-minute trials in relation to the 1-minute data are shown in Figure 2.2 for the freshet peak mid July. Proportions have much more variability on the rising limb than the falling limb for all trials. Most trials capture the peak in the 1-minute data, but the 15-minute trials appear to consistently underestimate peak values and do a poor job characterizing the steep falling limb. The daily errors of estimations confirm this pattern. While the 5- and 10-minute datasets appear to be evenly split between under and overestimating the true proportion, the 15-minute data consistently underestimate. In addition, the errors are 2-3 orders of magnitude larger for the 15-minute data compared to the 5- or 10-minute data, most notably near peak wood transport.

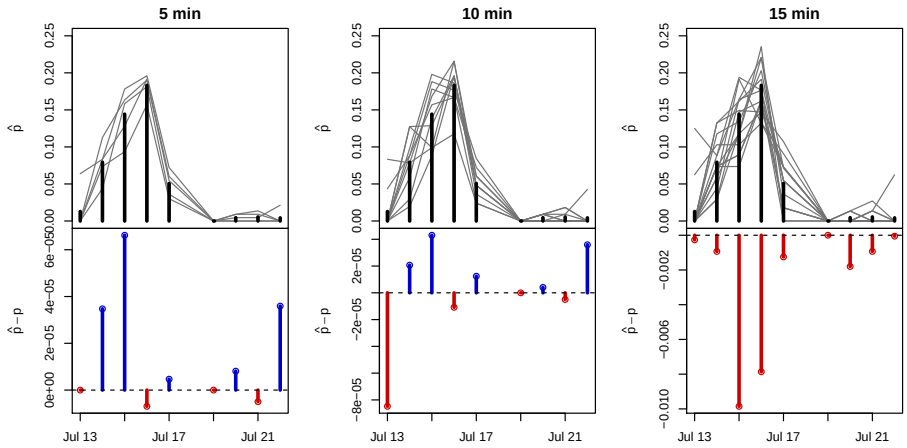

FIGURE 2.2. Timeseries of each trial over the freshet peak with daily errors. Solid bars show p from the 1-minute data while grey lines are the $\hat{p}$ estimates from each trial. Solid error bars were calculated by averaging the errors from each trial and then by subtracting from the 1-minute dataset.

Although the 15-minute trials are biased towards underestimation, bootstrap sampling clearly demonstrates that the variance is stable across all sample intervals (Fig. 2.3). Although not shown, the data were unbiased up to 14 minutes. This sudden bias at 15 minutes suggests that there may be some periodicity in the data. This idea is somewhat supported by a slight jump in the number of instances corresponding with a 15-18 minute lag between wood presence in images (Fig. 2.4).

2.6. Calculating Total Wood Loads

2.6.1. Statistical Methods. The following equations calculate, in steps, the estimates for total wood loads (count and volume) within a period of interest. By calculating in steps, imprecision for each component can be clearly compared to other components. Sampling strategies can be employed to focus efforts on reducing variability in the most efficient manner by addressing components with the most imprecision.

For each stratum of interest, estimate:

(1) total number of frames that logs are present

$$\hat{T}_f = N\hat{p} \qquad \hat{V}(\hat{T}) = N^2\hat{V}(\hat{p}) \tag{3}$$

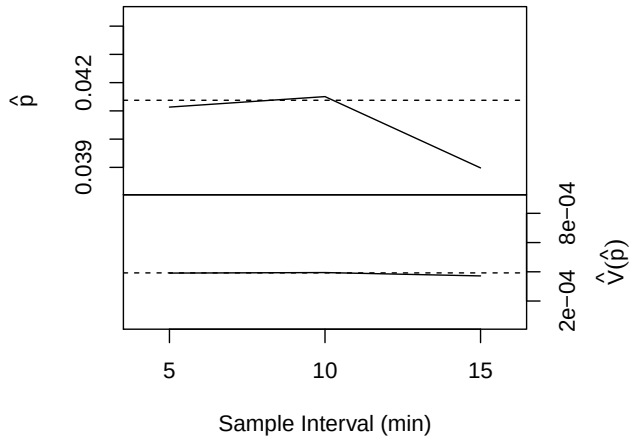

FIGURE 2.3. Comparison of proportions and variance across sample intervals using bootstrap sampling to achieve equal n. Each trial was sampled for $n = 100,\ 10,000$ times and averaged. All trials were then averaged to obtain an estimate for each sample interval. Dashed lines represent values from the 1-minute dataset.

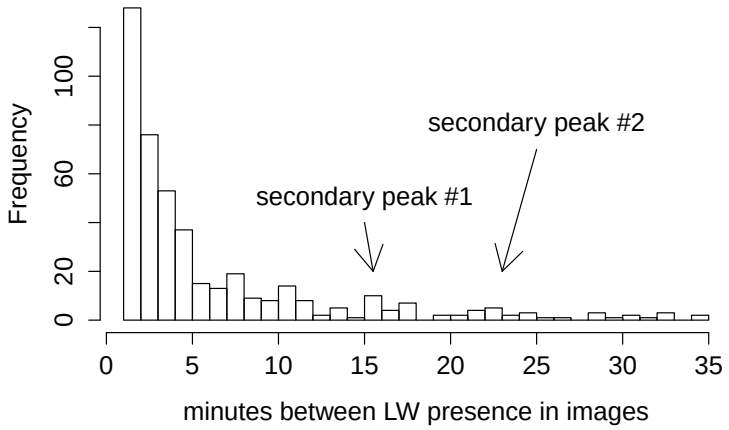

FIGURE 2.4. Frequencies of lag times between LW presence in images. Time between presence decays fairly rapidly and evenly from 1 minute to about 14 minutes. This is expected since most wood is transported within 4 days of the 32 day study period (Fig. 2.1). After the curve decays to near zero at 14 minutes, there appears to be secondary jump in the number of instances corresponding with a 15-18 minute lag between wood transport. A second, yet more gradual, peak occurs between 20 and 25 minutes.

Where N is the number of frames within a set time interval it takes a log to traverse the field of view and $\hat{p}$ and $\hat{V}(\hat{p})$ are computed using Eqn. 1. N is essentially the minimum number of frames (moments in time) needed to capture the entire

LW population within a stratum in a study period. For the Slave River, N was estimated to be the number of one minute intervals within each stratum for the 32 day study period (see the Data Collection section for justification). However, N could be adjusted to account for changing velocities. This may be useful for rivers with rapidly varying flows or narrower rivers with shorter transport distances.

(2) total count of logs

$$\hat{T}_c = \hat{T}_f \bar{c} \qquad \hat{V}(\hat{T}_c) = \hat{T}_f^2 \hat{V}(\bar{c}) + \bar{c}^2 \hat{V}(\hat{T}_f) \tag{4}$$

Where $\bar{c}$ is the average number of logs in a photo when logs are present, s is the sample standard deviation, and $\hat{V}(\bar{c}) = s^2/n\, fpc$. For this study, the entire sample was used, but $\bar{c}$ could also be computed using a subsample, which could greatly increase processing efficiency. Within any population smaller subsamples will be less precise than larger ones. If a population has high variance, more samples will need to be included to achieve the same precision as a population with low variance.

(3) total volume of logs

$$\hat{T}_v = \hat{T}_c \bar{v} \qquad \hat{V}(\hat{T}_v) = \hat{T}_c^2 \hat{V}(\bar{v}) + \bar{v}^2 \hat{V}(\bar{c}) \tag{5}$$

Where $\bar{v}$ is the average volume per log and $\hat{V}(\bar{v}) = s^2/n$. The average volume per log could be calculated from a sample of the captured images, estimated, or measured from jams downstream. If $\bar{v}$ is measured directly from the sampled images, a finite population correction factor should by applied to the variance, as in Eqn. 1.

To compute total LW loads over an entire period of interest sum over all strata and compute a bound. For the equation below, T_i denotes any of the above totals from a single stratum.

$$\hat{T} = \sum_{i=1}^{L} \hat{T}_i \qquad \hat{V}(\hat{T}_i) = \sum_{i=1}^{L} \hat{V}(\hat{T}_i) \qquad Bnd_{95\%CI} = 2\sqrt{\hat{V}(\hat{T}_v)} \tag{6}$$

A carbon load can be calculated by multiplying the total volume estimate by an average density and then multiplying by the of fraction carbon.

2.6.2. Slave River Results. Three main assumptions were made during the calculation of wood loads for the Slave River: (i) the sampled periods are good representations of the unsampled flows, (ii) a log traverses the field of view at about 1-minute intervals for the duration of the study, and (iii) logs measured in jams are representative of the size distributions of large logs captured on the images. The first assumption is reasonable because most of the unsampled flows occurred beneath the 4500 cms transport threshold and wood transport under this threshold had low variance (Fig. 2.1, bottom). Based on on-site observation, the unsampled peak in late August transported wood at similar rates as sampled periods under 4500. Wood available for transport is likely stored along banks higher than the bankheight for flows < 4500 cms.

The second assumption that a log traverses the field of view at about 1-minute intervals for the duration of the study is reasonable based on image analysis and an analysis of velocity ranges (see Data Collection). Although more rigorous estimation of the total number of frames needed to uniquely characterize the wood load is possible by accounting for changes in velocity, using an approximation based on one minute intervals was deemed acceptable for the goals of this study: outline methods for using timelapse photography to investigate the effects of sampling at coarser resolutions and to obtain first order estimates of wood flux and loads. Uncertainty due to this factor was not included in the estimate of total wood loads. An improvement to the techniques presented here would be to rigorously estimate the minimum number of theoretical frames needed to capture the entire population of drift logs by incorporating changes of velocity. Due to variability in velocities in wood transport paths, uncertainty in river cross-sections, and variability in channel length in the field of view this is actually quite challenging to do. Future work comparing timelapse at short time intervals to continuous video monitoring may help to constrain these estimates.

The third assumption that logs measured in jams are representative of logs captured in images is also reasonable. The size ratio of small:medium:large logs from jams (25:4:1), is similar to the ratio derived from on-site monitoring of wood in transport (20:3:1) (see Data Collection). Jams were measured the first season after a large wood flood in 2011

deposited them and were positioned above the high water level for 2012. Thus, little to no winnowing of smaller pieces had occurred prior to measurement. Jams were also not re-organized by ice because no ice jamming events were recorded by the upstream gage in 2012. Measuring logs directly from images has large uncertainties given distortion from oblique viewing, submergence of parts of logs, and uncertainties of widths. The characterization of distribution volumes of large logs in temporary storage may provide a valuable proxy to measuring logs directly from images.

Wood loads from July 13th through August 13th were calculated based on proportion estimates stratified by discharge (Table 2.1). 28% of the study period was sampled. During peak transport ($Q > 4500$ cms), 53% was sampled. Although stratifying by day increased precision more than stratifying by discharge, it was not used to estimate total LW loads because not all days were monitored (Fig. 2.1). Ice break-up and the first major freshet peak were not monitored, thus the wood loads presented are not the total estimate for the year, just for the second half of the summer. Because the majority of wood transport likely occurred during the first freshet peak mid June (Fig. 2.1), the total yearly wood load for 2012 is probably more than double the values summarized below.

The total LW loads, estimated from the 1-minute data, are 1406 ± 119 # pieces ($\hat{T}_c$), 492 ± 120 m^3 ($\hat{T}_v$) and on the order of 1.1^5 kg carbon. The mis-detection analysis presented in the Data Collection section suggests a detection rate of 85%, meaning that these estimates are underestimating actual load by about 15%. The wood loads, adjusted to take this mis-detection into account and rounded so that more precision than present is not implied, are: 1600 ± 200 # pieces ($\hat{T}_c$), $600 \pm 200 m^3$ ($\hat{T}_v$) and on the order of $1.3E^5 kg$ carbon. The bounds for $\hat{T}_c$ and $\hat{T}_v$ were both rounded up instead of down in order to include any additional unaccounted for uncertainties. For this study, amount carbon was estimated assuming an average density of 450 kg/m^3 (the main tree species are: poplar, aspen, white spruce, birch and larch) and a 0.50 fraction of carbon. The carbon estimate does not include a bound because uncertainties associated with the density or fraction of carbon were not included.

TABLE 2.1. LW load estimates for the study period (July 13th through Aug 13). Estimates were calculated from the 1-minute data using Eqns. 1-6. Estimates include a 95% confidence interval of $\pm 2\sqrt{Variance}$

	n	N	n/N	$\hat{p}$
$Q \leq 4500$	8643	38322	0.23	$0.08E^{-1} \pm 0.02$
$Q > 4500$	4118	7758	0.53	$1.11E^{-1} \pm 0.09$
$Q = All$	12761	46080	0.28	$0.41E^{-1} \pm 0.03$

	$\hat{T}_f$	$\bar{c}$	$\hat{T}_c$	$\hat{T}_v$
$Q \leq 4500$	306 ± 66	1.01 ± 0.03	310 ± 68	109 ± 39
$Q > 4500$	864 ± 73	1.27 ± 0.04	1096 ± 97	384 ± 114
$Q = All$	1170 ± 98	1.24 ± 0.04	1406 ± 119	492 ± 120

n is the total number of frames sampled.
N is the total number frames needed to uniquely characterize the wood load.
n/N is the proportion of the population sampled.
$\hat{p}$ is the estimated poportion of time LW was present (Eqn.1 or 2).
$\hat{T}_f$ is the total estimated population of frames with LW present (Eqns.3 & 6).
$\bar{c}$ is the average number of LW pieces per frame.
$\hat{T}_c$ is the total estimated count of LW (Eqns.4 & 6).
$\hat{T}_v$ is the total estimated volume of LW in m^3 (Eqns.5 & 6). An estimated average piece volume of $\bar{v} = 0.35$ $m^3, V(\bar{v}) = 2.4E^{-3}$ was used (See Data Collection and Fig. 2.1).

The total count of logs, $\hat{T}_c$, from the 1-minute data is more precise than the total volume, $\hat{T}_v$ (Table 2.2). After comparing variance contributions in Eqns. 3-6 it was determined that the imprecision in the $\hat{T}_v$ estimate is largely due to imprecision in average volume per log ($\bar{v}$). Most of the variance in $\hat{T}_v$ originates from variance in $\bar{v}$ (86%) rather than the variance in $\hat{T}_c$. The variance in $\hat{T}_c$ mostly originates from variance in $\hat{p}$ (92%) rather than variance in the average number of pieces per frame ($\bar{c}$).

TABLE 2.2. Comparison of LW load estimates between sampling intervals. Estimates for each sample interval were computed by averaging the results for for the trials within that sampling interval (see Fig. 2.1). Load estimates were obtained stratifying by Q, as shown in Table 2.1. $\%Error = (bound/estimate) \times 100$.

	1 min	5 min	10 min	15 min
Total Count				
$\hat{T}_c$ (m^3)	1406 ± 119	1406 ± 287	1406 ± 409	1314 ± 482
$\%Error$	9	20	29	37
Total Volume				
$\hat{T}_v$ (m^3)	492 ± 120	492 ± 151	492 ± 183	460 ± 200
$\%Error$	24	31	37	44

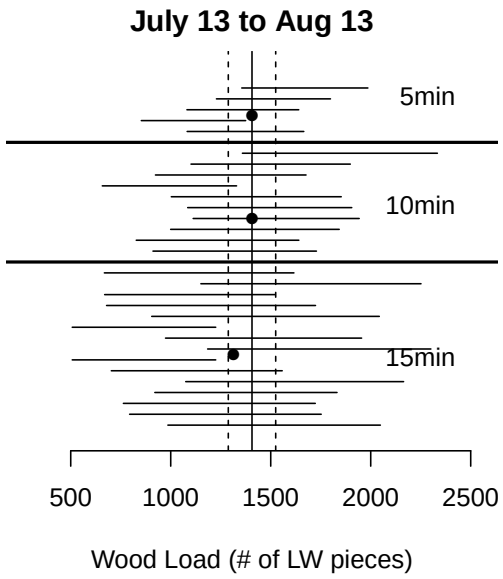

FIGURE 2.1. Horizontal lines are the 95% confidence intervals in total wood load for each trial. The solid vertical line and two dashed lines mark the estimate from the 1-minute data and its 95% confidence interval. Filled points mark the average estimate over all trials for each sampling interval summarized in Table 2.2.

Precision and accuracy of LW load estimates are compared across sampling intervals in Table 2.2 and Figure 2.1. While the 5- and 10-minute data are unbiased compared to the 1-minute data, the 15-minute data underestimates by about 6.5%. When bounds are compared to the 1-minute data, the 5-, 10- and 15-minute data are 2.4, 3.4 and 4 times less precise for the total count and are 1.3, 1.5 and 1.7 less precise for the total volume, respectively. By comparing % error between count and volume, the 1- 5-, 10- and 15-minute count estimates are 2.7, 1.5, 1.3, and 1.2 times as precise as volume, respectively. Figure 2.1 shows the 95% confidence intervals about the total count estimate for each trial. All trials for the 5- and 10-minute data plot within the confidence interval of the 1-minute data while 13% of the 15-minute trials plot outside the 1-minute confidence band (dashed lines).

Based on these results, a network of 8 cameras were installed in 2013 on major tributaries of the Mackenzie River, Canada and set to take pictures every 10 minutes. The Olympus X560WP camera connected to an intervalometer was not used. Although the pictures were excellent, it was found that this set-up used too much power to be practical without regular

access. Instead, A Brinno TLC200 timelapse camera ($150) with waterproof housing was connected to a 6V Energizer battery. Although this set-up captured lower resolution photographs, wood could still be reliably seen on images. Photographs captured at 10 minute intervals from March 17th to July 9th in 2013 used $0.15V$ and only $1G$ of memory. Images with this camera are stored as a movie file with a user-defined framerate. During periods of wood transport, individual frames can be exported from the movie for detailed analysis.

2.7. Discussion

The methods presented are a good way to gather broad spatial and long temporal wood transport data. Although imprecise, these methods can be very useful to examine trends along a drainage network and trends through time, to help constrain wood and carbon budgets, and to show general relationships between water flux and wood flux. Sampling at coarse intervals extends the amount of time cameras can be left without maintenance by saving memory space and battery usage. When project budgets are too tight to install fully equipped monitoring stations with solar panels and automatic downloads, the use of coarse resolution timelapse photography sampling provides a cost-effective way to monitor and estimate wood loads. Coarse interval sample also greatly reduces the amount of post-processing time by reducing the number of photos to analyze.

For the Slave River, timelapse sampling at less than fifteen minute intervals provides imprecise, unbiased, equal variance estimates of 1-minute data (Tables 2.1 & 2.2). Periodicity in wood flux will bias results for regular interval sampling if sampling interval is close to the wavelength of the periodic flux. There may a slight periodicity in flux for the this site around 15-18 minutes (Fig. 2.4) which may be the cause of the underestimation bias in the 15-minute dataset. Future work should focus on analyzing wood flux periodicity and relating it to drivers such as water and/or recruitment fluxes.

Appropriate sampling intervals to achieve unbiased estimates may be related to hydrograph and wood recruitment regimes. For rivers similar to the Slave River, characterized

by less variable hydrographs (rise and fall of a peak flow takes many days) and wood recruitment driven by hydrology rather than upslope processes, sampling at 5 or 10 minute intervals should be adequate to achieve unbiased estimates of wood load. For drainages with short event durations, it is likely that 5-10 minute sampling intervals may no longer provide unbiased estimates due to undersampling compared to rates of change.

Although caution should be used when applying results from this study to drainages with flashier hydrographs and/or more episodic wood recruitment dominated by landslides, the statistical and estimation methods discussed here can be used to determine appropriate sampling intervals. Additional analyses from many basins need to be conducted to determine if there exist universal thresholds or predictable relationships for sampling intervals which yield unbiased, equal variance estimates of finer sampling intervals and to illuminate processes and patterns of wood flux across regions. Analysis of wood flux, sampling interval, and rates of change in water discharge between locations, events, and years would be an interesting future endeavor.

A valuable outcome of monitoring wood fluxes using timelapse cameras is the rapid identification of transport thresholds. *MacVicar and Piégay* (2012) identified a threshold for transport near 2/3 bankfull. The 1.5 year flood event (a proxy for bankfull) for the Slave River is 5700 cms and two thirds of that is 3800 cms. A 3800 cms LW transport threshold seems to be a tad high for the Slave River (Fig. 2.1, bottom), but is close since there was less than 1% probability of transport for flows less than 4500 cms (Table 2.1). The 4500 cms threshold identified in this study is interesting for its similarity to a 4000 cms threshold for ice jam flooding on the Slave River's primary tributary, the Peace River (*Beltaos et al.*, 2006).

Estimates of total LW loads are useful for refining and computing LW or carbon budgets. After a 15% upwards adjustment for mis-detection errors, the total loads for the Slave River between July 13th through August 13th were estimated to be 1600 ± 200 # pieces, 600 ± 200 m^3 and on the order of 1.3×10^5 kg carbon. These estimates of total load depend on how well unsampled flows are represented by sampled flows, estimation of the total number of frames

(population total) required to uniquely capture wood load, and the estimation for average volume per log. To help refine the methods presented in this paper, future work should focus on analyzing the impacts of data gaps, comparing video monitoring to timelapse photography in order constrain estimates of population totals, and comparing log size measurements from imagery to jams downstream. These wood load estimates are minimum estimates for the time period because they do not include sunken logs or rootwad volumes. Rootwad volumes were not calculated due to difficulties in estimating volumes and because only a small (7%) of LW monitored had rootwads. Future work that focused on developing relationships to easily estimate drift rootwad volumes would be valuable for estimating total LW volumes and carbon mass from drift logs.

Precision decreased as sampling interval length increased due to smaller sample sizes (Table 2.2). For example, the percent error for total wood count increased from 9% for 1-minute data to 37% for 15-minute data. Thus, determining an interval at which to sample becomes a balance between precision desired and equipment, access and post-processing time constraints. Precision can be increased by computing estimates using stratification schemes such as stratifying by day or discharge (Table 2.1). Total count estimates are more precise than total volume estimates (Table 2.2) due to large uncertainties in the average volume per log. The most gain in precision will be achieved by future work that focuses on reducing the variance in average volume per log. This can be done by experimenting with sampling strategies and increasing the sample size.

It is important to reiterate that the total loads presented here are not estimates of the total seasonal load for the Slave River in 2012 because only the second half of the summer was monitored. Actual wood loads are likely more than twice these values since the larger first freshet peak of the season was not monitored. In 2012 there was no ice-jam flood event. In years with ice-jam flooding, wood transport is likely much higher due to the bulldozing effect of ice and sudden failure of ice jams that release waves of water downstream. Multi-year analysis needs to be conducted to determine if these values are typical for any given year.

2.8. Conclusion

This study is part of a larger study investigating wood transport dynamic in large rivers and export of large wood to the Arctic from the Mackenzie Basin, Canada. Prior to the installation of the network of cameras, this study was initiated to determine the longest sampling interval that achieved unbiased equal variance results and to develop methods to compute wood fluxes and loads from the data. Specifically, this study developed methods to: (i) construct fluvial wood flux curves, (ii) analyze the effects of sample interval lengths on transport estimates (both flux and load), and (iii) estimate total wood loads within a specified time period from coarse interval ($\geq$ 1 minute) timelapse photography.

There are many strengths to using timelapse photography to monitor wood fluxes and loads. It is a low cost, low maintenance, power efficient method. It can be used to extrapolate into data gaps, such as night time. It produces conservative, first order estimates of minimum wood loads. And, it allows easy comparisons of wood flux to hydrographs on long spatial and broad temporal scales. However, it is good to keep in mind its limitations. Estimates are imprecise. In order to obtain wood loads, it relies on making several assumptions about representative sampling, log travel times, and average log size. And, it is limited to large pieces and has a limited range (approximatly $<$ 60 m for logs $>$ 10 cm in width and 1 m in length; and $<$ 300 m for logs greater than $>$ 20 cm in width and 3 m in length). As mentioned in the Discussion, future work should focus on improving precision, analyzing the effects of data gaps, estimating rootwad volumes, estimating sunken log transport, comparing timelapse to video monitoring, and identifying intervals that produce unbiased estimates for a variety of drainage sizes, hydrograph regimes, and recruitment processes.

Recognition of Support

This project was primarily funded by the Edward M. Warner Graduate Grant awarded by the CSU Geoscience Department with an additional donation from Charles Blyth. Special thanks to Robin Reich for his knowledge and support and to Water Survey Canada, The Yellow House and the Smith's Landing Band of Fort Smith for logistics, field support and

data. Edward Schenk and one anonymous reviewer greatly improved this manuscript and we are deeply grateful for their constructive and well thought out reviews. National Geographic Research Grant 9183-12 funded the acquisition and deployment of a network of cameras in 2013.

SUPPORTING INFORMATION FOR CHAPTER 2

2.A. Dataset

This dataset can also be accessed via the Colorado State Digital data repository under Research Project "Big River Driftwood in Northern Canada" (`http://hdl.handle.net/10217/100436`)

Data Set S1 *FF2012_wood.csv*. This dataset is a compilation of presence and number of wood pieces in each minute timeframe moving past the Fort Fitzgerald Gauge on the Slave River, Alberta from July 13th 2012 to August 10th 2012. Gauge and camera located at 59.872222 N, 111.583333 W. Data were used to analyze appropriate sampling intervals to monitor wood flux in Chapter 2 "Estimating fluvial wood discharge using time-lapse photography with varying sampling intervals" (Kramer and Wohl, 2014- DOI: 10.1002/esp.3540).

time	(year-month-day H:M:S). year is 2012
rootwads	integer specifying # of rootwads in photo frame
logs	integer specifying # of logs in photo frame
Qwood	integer specifying estimated interpolated discharge at time of photo.

CHAPTER 3

Driftcretions: The legacy impacts of driftwood on shoreline morphology

Summary

This research demonstrates how biotic communities interact with physical processes to govern landscape development, with multiple feedbacks among biota and landforms. We quantify and describe interactions between driftwood, sedimentation and vegetation for Canada's Great Slave Lake, which is used as proxy for shoreline dynamics and landforms before deforestation and wood removal along major waterways. We introduce the term driftcretion to describe large, persistent concentrations of driftwood that interact with vegetation and sedimentation to influence shoreline evolution. We report the volume and distribution of driftwood along shorelines, the morphological impacts of sustained driftwood delivery throughout the Holocene and rates of driftwood accretion. We conclude that driftcretions facilitate the formation of complex and diverse morphologies that increase biological productivity and organic carbon capture, and buffer against erosion. Driftcretions and associated landforms should be common on shorelines which receive a large wood supply and have processes which store wood permanently.

3.1. Introduction

Interactions between wood, sediment and vegetation in rivers lead to major alterations of physical and ecological states (*Corenblit et al.*, 2011; *Dietrich and Perron*, 2006). One of the most striking examples of this is the co-evolution of vascular plants with river meandering in the Carboniferous (*Gibling and Davies*, 2012). Other examples include wood jams forcing multi-thread channels in low gradient mountain valleys (*Polvi and Wohl*, 2013), beaver dams controlling sedimentation and sustaining meadow wetlands (*Westbrook et al.*, 2011), in-stream wood on gravel bars initiating stable vegetated islands in anabranching rivers (*Gurnell and Petts*, 2002), large in-stream wood facilitating the expansion of alluvial old

growth forests on floodplains (*Collins et al.*, 2012), log rafts forcing avulsions and forming semi-stable, multi-thread distributary channels in deltas (*Phillips*, 2012), sunken logs on the deep ocean sustaining biological hotpots (*Knudsen*, 1970), and shoreline driftwood supplying a steady food source and creating habitat patchiness in coastal and mid-ocean ecosystems (*Maser et al.*, 1988).

Driftwood plays a major role in distributing water-borne nutrients and organic particulates, including carbon, into broader areas than would otherwise be reached (*Wipfli et al.*, 2007). However, research that investigates the long term storage and decay of drift piles and their legacy impact on landforms, trophic cascades and carbon cycling is limited. Global shorelines, especially in the temperate zone, are severely wood-impoverished relative to their condition prior to intensive human settlement (*Wohl*, 2014a). Thus, landforms along recently wood-impoverished river corridors and lakes may reflect past processes when driftwood was more abundant. Studying these processes and connecting vestige landscapes to driftwood are difficult in the absence of contemporary wood recruitment to shorelines.

A few large river catchments remain largely forested and unregulated. The Mackenzie River of Canada still exports large amounts of driftwood to the Arctic Ocean (*Eggertsson*, 1994). We use Great Slave Lake as a natural, wood-rich laboratory to study the legacy of driftwood over time scales of $10^1 - 10^3$ years, including: the morphological impacts of high wood loads along shorelines, rates of landscape change, and rates of fluvial driftwood export. This site provides a proxy for shoreline dynamics and landforms for marine and terrestrial depositional basins before widespread historical deforestation and wood removal along major waterways.

3.2. Methods

We used a combination of field and remote sensing techniques to investigate driftwood processes in Great Slave Lake. We circumnavigated the lake margin in a small aircraft, taking oblique air photos to record the distribution and type of driftcretions. Ground-based field visits facilitated process observations, topographic surveys, driftwood measurements,

and tree coring. Knowledge of current onshore driftcretion processes from these methods was used, along with satellite imagery of lake margins in Google Earth and results from scientific literature, to infer the large spatial and long temporal impact and shoreline processes associated with high wood loads on shorelines. Expanded methods and links to data are provided in the supporting information document.

3.3. Driftcretions

We use the term driftcretion to refer to large concentrations of driftwood that promote sedimentation and interact with vegetation to influence shoreline morphology and evolution. Driftcretions are persistent rather than transitory landscape elements, and over time interact with vegetation and sediment to influence landscape form and function. Large log accumulations can become driftcretions if they become stabilized and vegetated until they are buried or decay in situ. We argue that driftcretions and their geomorphological impacts have three main broad-reaching implications. Driftcretions 1) increase the biological productivity of shorelines by facilitating habitat patchiness and by providing a base food source to food webs, 2) provide shoreline protection from erosion by waves, and 3) facilitate the long term capture and storage of carbon, both as buried wood and by increasing the amount of stable offshore standing water bodies which can capture carbon from the atmosphere (*Tranvik et al.*, 2009).

We classify driftcretions into three types: berms, mats and a piecewise matrix. Berms are raised ridges of driftwood that form parallel to the shoreline when waves or ice push driftwood into linear piles. Mats are large, relatively flat, imbricated accumulations of driftwood composed of a mix of large and small pieces. A piece-wise matrix is driftwood interspersed or layered in sediment. More detailed descriptions of berms, mats and matrices are in the Supporting Information. Figure 3.1 shows photographs of these three forms of driftcretions as well as shoreline morphologies facilitated by driftcretion. Figure 3.2 illustrates typical deposition of driftcretions along idealized transects for protected and exposed shorelines. These

idealized transects are useful for understanding how driftcretions influence the appearance and evolution of the lakeshore.

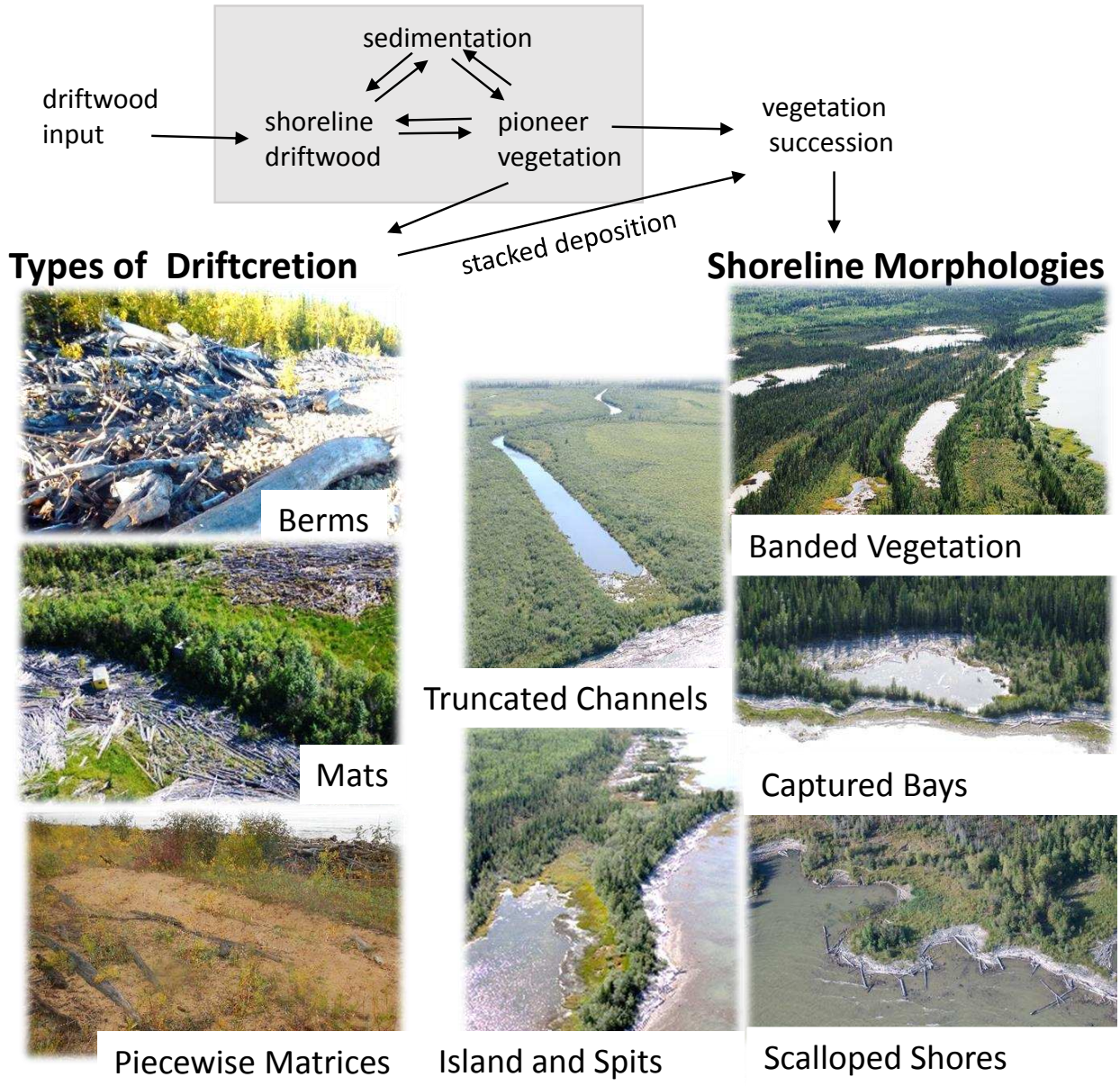

FIGURE 3.1. Conceptualization of processes which retain and facilitate driftwood to form driftcretions with examples of types and resulting shoreline morphologies. The three main impacts of driftcretions on shores are increased biological productivity and diversity due to increased habitat patchiness and food availability for trophic cascades; carbon capture in onshore water bodies and wetlands; and protection of shorelines from wave, ice and flood disturbances.

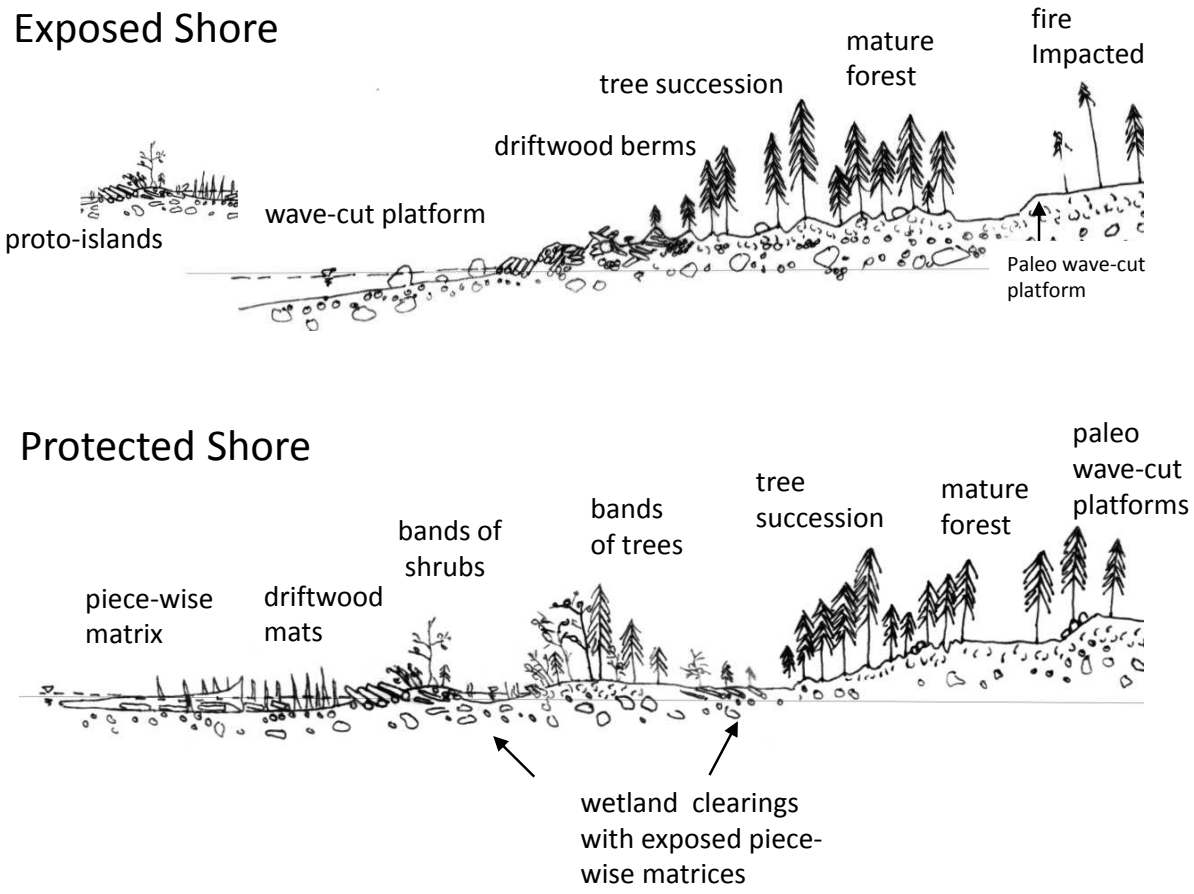

FIGURE 3.2. Two idealized cross-sections which demonstrate the typical morphology of exposed and protected shorelines and relation to driftwood based on field observations and topographic surveys. Topography drawn with 15x vertical exaggeration. Vegetation is not to scale. Cross-sections are approximately 200 m in length. Note the tree succession on topographic berms on the protected shoreline. Berms only form on high exposure shores, so the presence of this sequence reflects past conditions when the shore was more heavily exposed. This occurred before vegetation established on the mats and piece-wise matrices in front of the berms. This pattern demonstrates how the growth of islands and spits protect shorelines and facilitates rapid sedimentation.

In the Great Slave Lake, driftcretions impact progradation rates of shorelines and facilitate the infilling of the lake. This occurs through the successive and continued accretion of drift piles and their subsequent decay and vegetation. The mechanisms for accretion are caused by lake level changes on timescales spanning days to thousands of years. Driftwood

is episodically delivered to the lake with ice break-up and river high flows and distributed by surface currents. Driftwood becomes a driftcretion after it is hydrologically disconnected and vegetated. Hydrologic disconnection occurs mechanically when lake level fluctuations from ice, storm waves or large seiches (lake tsunamis, see (*Gardner et al.*, 2006)), push or strand large piles of driftwood farther inland than can be reworked by lake processes before vegetation establishment. Hydrologic disconnection can also occur when driftwood and shoreline grasses facilitate increased local sedimentation, eventually decreasing local lake depth enough that pioneer species like willow, alder and poplar can grow. These pioneer species then act as nets which capture and retain large drift piles floated or pushed into them by waves and ice, further facilitating land progradation. In addition to episodic delivery and storage, yearly flux of driftwood is buried in bottom sediments. If there is a regional drop in lake level, large expanses of driftwood-laden sediments become exposed and vegetated. Regional lake level may drop due to hydrologic alterations from human development of the river corridor, climate change or isostatic rebound.

Figure 3.3 conceptualizes relationships between time scales, amount of land accretion, driftcretion types and shoreline morphologies for various mechanisms that change shoreline positions. Additional descriptions, photos and analyses that were used to develop and constrain and this conceptual model are provided in the Supporting Information. The next sections further discuss shoreline morphologies, distribution and amount of stored driftwood, rates of driftwood accretion and implications.

3.4. Shoreline Morphologies

Berms, mats, and piece-wise matrices work in concert and in succession to build large scale landscape elements, such as truncated channels, banded vegetation, islands and spits, scalloped shores and captured bays (Figure 3.1, also Supporting Information). Morphological features similar to those on modern shorelines, especially vegetative bands and enclosed bays, are visible on satellite imagery up to about 70 km inland. Lake levels have changed over the last 8000 years due to draining of Glacial Lake McConnell, isostatic rebound, and

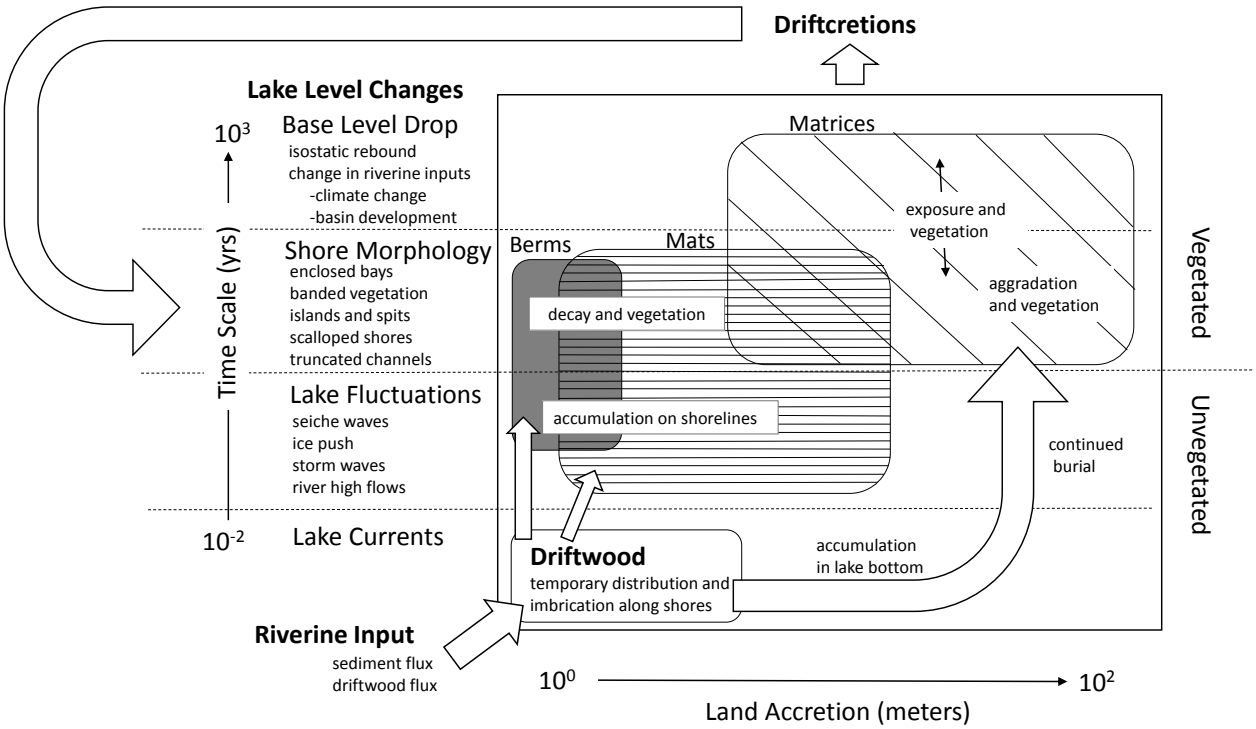

FIGURE 3.3. Conceptualization of driftcretion formation driven by changes in lake level at local and regional scales and on short and long timescales. Note the feedback between driftcretion and shoreline morphology. For example, if driftcretions facilitate bay capture, this will impact local lake levels by hydrologically disconnecting part of the lake, which in turn facilitates more driftcretions as large events float wood into these bays and buried matrices are uncovered.

infilling of the Slave River Delta in a now buried southern arm of the lake (*Smith*, 1994; *Vanderburgh and Smith*, 1988). Given driftwood supplies to the lake basin throughout this time period (*Vanderburgh and Smith*, 1988), it is not surprising that the morphological impacts of driftcretions are still evident so far inland.

3.4.1. TRUNCATED CHANNELS. Distributary channels can be cut-off at their mouths by mats of driftwood originating, not from the channel, but from drift along shorelines. If the influx of shoreline wood and associated sedimentation is greater than the ability of the distributary channel to keep its path to the lake clear, the wood effectively truncates the channel, forming a bridge across the mouth. This facilitates sedimentation and vegetation

establishment. If more wood comes down the channel. it is jammed behind the bridge. Eventually, new shoreline builds outward in front of the channel and the channel starts to fill.

3.4.2. Banded Vegetation. Vegetation banding along shorelines reflects the episodic delivery of large amounts of driftwood. During a year of exceptional driftwood delivery (about every 20-50 y), large deposits of driftwood become permanently stored and converted into driftcretions linear to the shore. Vegetation preferentially establishes on decaying logs. Thus, sequential bands of vegetation parallel to the shore not only reflect past shoreline locations, but the recurrence interval of large driftwood inputs.

3.4.3. Islands and Spits. Shallow shoals that become vegetated commonly create linear islands, spits and peninsulas that protect the main shore from large waves and other disturbances. Behind the protection of these woody shoals, sedimentation, capture of smaller floating wood and pulp, and accumulation of piece-wise matrices occur at increased rates. On shores with extensive land spurs and islands, the amount of shoreline (distance of land in contact with the main body of the lake) is increased by an average 2.7 times. In one location, the amount of shoreline increased by a factor of 8.

3.4.4. Scalloped Shores. Scalloping develops on shorelines with high wood loads that are positioned perpendicular to wind direction. The average sinuosity of scalloped shores is 1.5 m/m. These shorelines have increased potential for biological productivity due to the increased length of land-water interface.

3.4.5. Captured Bays. When scalloped shorelines and spits expand, they can enclose shoreline embayments. In regions with many bay enclosures, a mottled offshore landscape of standing water bodies and clearings is created that resembles a karst landscape with a high density of sinkholes.

3.5. Amount and Distribution

Based on an analysis of stratified random sampling of oblique aerial photos from imagery covering the circumference of the lake (link to dataset), the average visible surface area of wood in mats or berms per meter of linear shoreline distance is $0.20 - 13$ m^2/m for eleven shoreline regions (Figure 3.1). Wood-rich shorelines average $10 - 13$ m^2/m of wood, but as much as 50 m^2/m of wood can be present locally (see Supporting Information for methods and calculations). Mats are present along all shoreline regions, but berms are only present along steeper shorelines that are approximately perpendicular to the predominant wind direction. Visible individual wood pieces were included in the total area estimation, but form less than 2% of the total area calculated. Piece-wise matrices are not visible on photographs and were not included in the analysis.

The largest amount of wood accumulates on the southern shore due to proximity of major wood-supplying tributaries (Slave and Hay Rivers) and perpendicular orientation to wind. Negligible amounts of wood are supplied by northern and eastern tributaries because these areas either drain channels that flow through Canadian Shield bedrock or small basins of very low relief with disconnected, lake-rich channel networks that retain wood. Surface currents distribute wood entering from the major wood-supplying southern tributaries to the northern shore. Northern shorelines with the most wood are either perpendicular to wind direction and/or parallel with stronger currents. The eastern shorelines do not accumulate wood due to high relief, rocky shorelines (Supporting Information). Surface currents bypass the lake outlet to the Mackenzie River, where almost no wood is found. Great Slave Lake is a wood sink and does not source appreciable amounts of wood to the Mackenzie River, as corroborated by timelapse photography of the Mackenzie River at Fort Providence and local knowledge.

We estimate the total surface area of visible wood stored along the lake margins to be $4.6\text{x}10^6 \pm 0.7\text{x}10^6$ m^2 (see Supporting Information for calculations). Estimating volumes for drift piles can be imprecise due to large uncertainties and variances in the fraction of wood in jams and heights of jams. Thus, we report wood volumes and mass of carbon as a reasonable

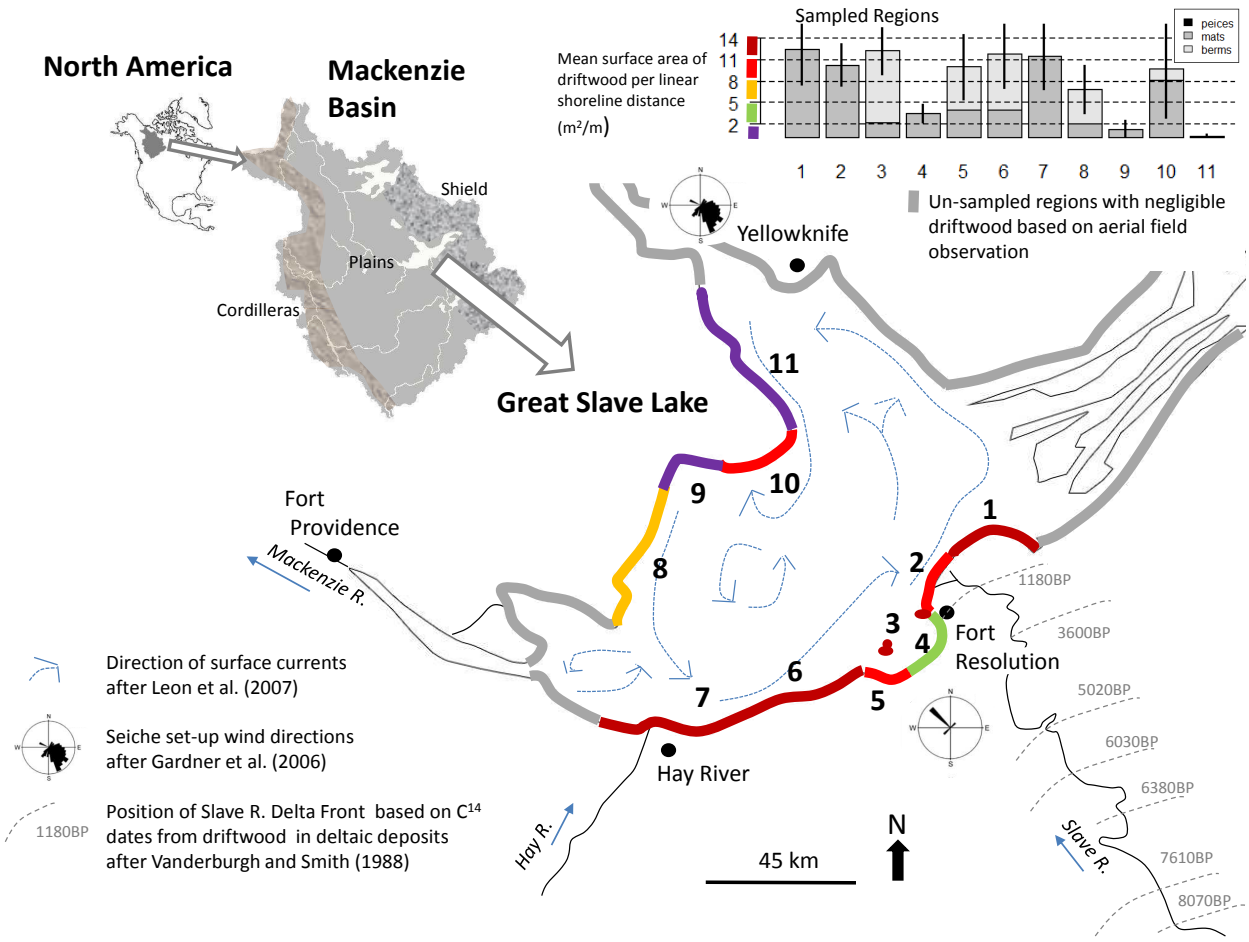

FIGURE 3.1. Driftcretion distribution around the Lake. The colored bars shows high to low driftcretion volumes stored along lake margins based on estimated driftcretion area divided by shoreline length as displayed in the bar graph in the upper right. Numbers in bar graph relate to numbers drawn on the map. Seiche rose diagrams (*Gardner et al.*, 2006), lake surface currents (*León et al.*, 2007) and Slave River delta progradation positions (*Vanderburgh and Smith*, 1988) were adapted from previous literature.

range rather than a bounded estimate. If we use conservative ranges of values for average height ($0.5 - 1.5$ m), fraction of wood ($0.20 - 0.80$), fraction of carbon (0.5) (*Lamlom and Savidge*, 2003), and density of wood (450 kg C m^{-3}, then the average volume per shoreline distance is on the order of 10^{-1} to 10^{0} m^3/m and the average mass carbon per shoreline distance is on the order of 10^2 to 10^3 Mg C/m. These estimates are minima since the buried wood in piece-wise matrices was not included. These volume and mass estimates reflect 50 years of accumulation, after which driftcretions become vegetated and unrecognizable by air.

3.6. Rates

There is currently much interest in quantifying 1) rates of landscape change due to biotic-physical interactions (*Dietrich and Perron*, 2006; *Reinhardt et al.*, 2010), 2) instream wood budgets (*Benda and Sias*, 2003; *Boivin et al.*, 2015; *Schenk et al.*, 2014), and 3) the amount of carbon, as wood, recruited and exported from river networks to the oceans (*West et al.*, 2011; *Eglinton*, 2008). In most field areas, calculation of only one or two of these metrics is possible due to the episodic and transitory nature of wood movement in channels and/or due to the depletion of wood from human activities. Great Slave Lake is unique in preserving a long record of transport volumes for discrete events.

Wood input into the lake today is similar to that in the historic past due to minimal development of the 6.8×10^6 km^2 wood-contributing drainage basin. Flow regulation impacts only around 10% of this area and most of the riparian corridor remains intact. Driftwood decays slowly because it is frozen for more than half the year, thus it is still recognizable as wood 100 years after deposition. Vegetative bands record wood depositional events up to the typical age of old-growth white spruce, around 300 years (*Timoney and Robinson*, 1996). Rates of export can be calculated by coring living trees growing from wood piles in various stages of decay and distances inland (see Supporting Information for details).

Table 3.1 summarizes and compares rates of land accretion, and wood storage, recruitment and transport metrics from this and other studies. Wood recruitment values over the basin are 1-2 orders of magnitude less than reported values for headwater channels, basins in Japan and steep tropical catchments. This seems appropriate, because this study averages recruitment over an entire drainage in which large areas likely are not directly supplying wood to the channel. The average transport rates for this site are very similar to or slightly higher than rates reported in Japan and Québec. Wood delivered to oceans from tropical storms may deliver more wood than an average wood transport event on the Slave River.

We used the distribution of germination ages derived from a tree-ring analysis of cores to compare driftcretion deposition rates to rates of driving processes such as ice-push, river discharge and seiches (Figure 3.1). More of the trees germinated after 1950, especially on

TABLE 3.1. Summary of landscape metrics, storage, recruitment and transport of driftwood.

Landscape Metrics	This Study	
Accretion per event	berms&mats: $4-10$ m/event, matrices: $14-23$ m/event	
Accretion per year	berms&mats: $0.1-0.4$ m/y, matrices: $0.6-1.4$ m/y	
Event recurrence	$20-40$ y	
Storage Metrics	This Study	
time period (t)	50 y	
events (n)	$2-3$ events	
Shore distance (X)	$6\text{x}10^5$ m	
Area (A)	$4.6\text{x}10^6 \pm 0.7\text{x}10^6$ m^2	
Volume (V)	10^5-10^6 m^3	
Carbon (C)	10^8-10^9 Kg C	
Recruitment Metrics	This Study	Other Studies
Drainage area (DA)[a]	$6.8\text{x}10^5$ km^2	
Stream length (L)[a]	$1.7\text{x}10^5$ km ($> 3^{rd}$ order)	
$C/DA/n$	10^1-10^3 Kg C/km^2	$2.4\text{x}10^4$ Kg C/km^2 as wood, vegetation and soil from the Rio Chagres Panama during a tropical storm (*Wohl and Ogden*, 2013)
$V/L/t$	10^{-4}-10^{-3} m^3/km/y	$0.2\text{-}5.1\text{x}10^{-1}$ m^3/km/yr (*King et al.*, 2013) Upland headwater streams in British Columbia.
$C/DA/t$	10^1-10^2 Kg C/km/y	$82-5168$ Kg C/km^2/y from reservoir storage of wood from drainages of varying sizes in Japan (*Seo et al.*, 2012).
Transport Metrics	This Study	Other Studies
C/n	10^5-10^6 Kg C/event	3.8-8.4 x 10^9 Kg C as wood soil and vegetation delivered to oceans from coarse wood during a tropical storm that triggered landslides in Taiwan (*West et al.*, 2011).
V/t	10^3-10^5 m^3/y	$1.93\text{x}10^3$ m^3/y based on $25,000$ m^3 of wood trapped as rafts in the Saint-Jean River, Gaspé (Québec, Canada) over 50 yrs from 1963-2013 (*Boivin et al.*, 2015)
C/t	10^6-10^7 Kg C/y	10^5-10^9 Kg C/yr measured from wood removed from reservoirs in Japan (*Seo et al.*, 2008)

a.wood-contributing drainage area and stream length. Sections of basin on the Canadian Shield that do not contribute driftwood were not included.

mats and matrices. This bias towards more recent events is because older mats and exposed matrices are located farther inland than the length of sampling transects and, unlike berms, decayed mats and vegetated matrices with wood no longer visible or buried lack topographic expression to distinguish discrete events.

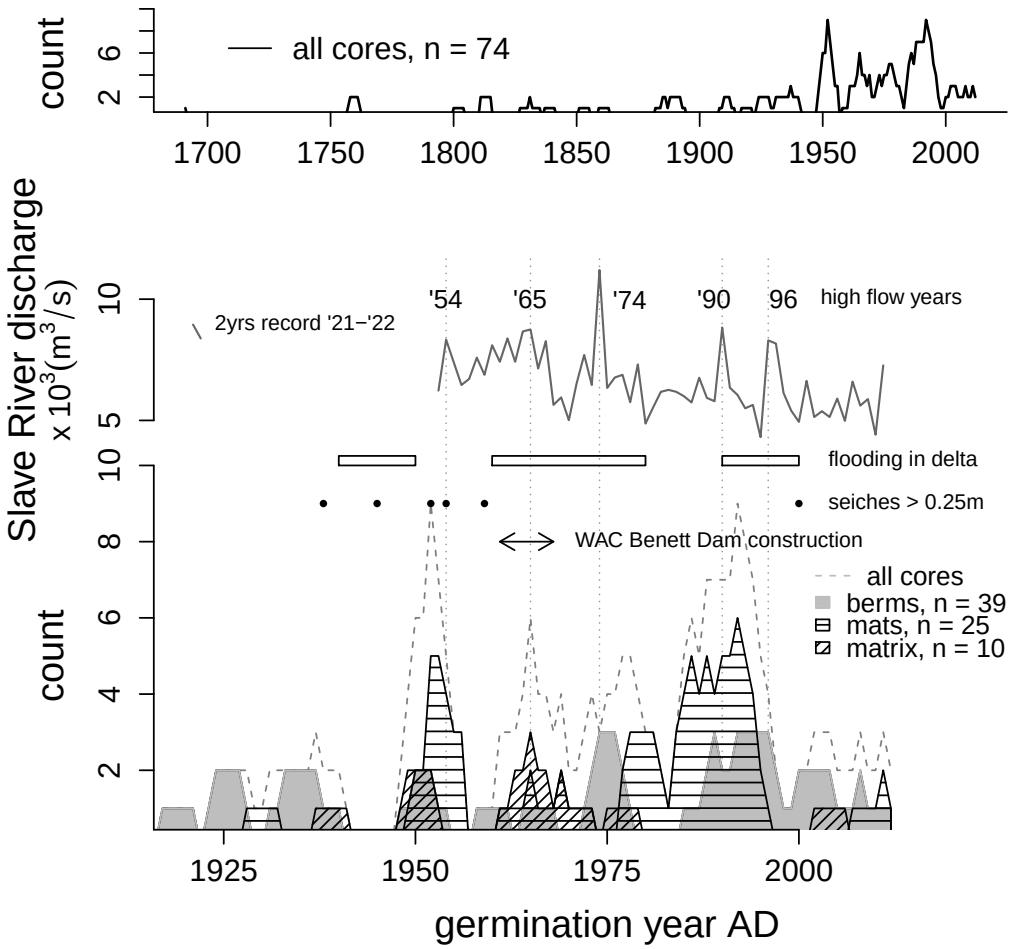

FIGURE 3.1. Counts of white spruce germination year for living trees growing on driftcretions. All cores are shown in the top graph. The bottom graph is a detail of the past 100 years and highlights relationships between germination year, peak yearly river flow (Water Survey Canada, Slave River at Fort Fitzgerald gauge 7NB001), flooding of delta lakes (*Brock et al.*, 2010), large seiche events (*Gardner et al.*, 2006) and construction of the WAC Bennett Dam. Germination year was smoothed using a five year window in order to portray uncertainty.

Driftcretions accumulate episodically, generally coinciding with or lagging years of high river flows (Figure 3.1). This pattern is expected because high flows deliver a supply of wood that can later be pushed into berms. Large ice-push events occur along exposed shores during years of high Spring river flows simultaneous with lake ice-off (*Bégin*, 2000; *Philip*, 1990). Large seiche events typically occur in the late summer (*Gardner et al.*, 2006). Mat deposition is more closely tied to the timing of high wood delivery than is formation of berms because

berm formation may not coincide directly with high flow but rather large ice or seiche events. This lag between high flow and berm germination is apparent for the 1974 and 1990 peak flows (3.1). Spruce germination around 1950 probably correlates with unrecorded high flows in the late 1940s or with a period of multiple large seiches during 1930-1950. Development of an ice-push event chronology using ice-scar chronologies on lakeshore trees and shrubs, as done for large northern lakes in Quebec (*Bégin*, 2000; *Lemay and Bégin*, 2012), would greatly augment understanding of relationships between flow, ice-push and berm formation.

After construction of the W.A.C. Bennett Dam in 1967, Great Slave Lake levels decreased during the summer months (*Gibson et al.*, 2006). The high density of germination on piece-wise matrices during construction of the dam reflects vegetation establishment on newly exposed sunken wood (Figure 3.1).

Large scale wood export is episodic and associated with peak river flows that follow periods of low flows during which driftwood accumulates along river corridors. On the Slave River, a very high peak flow in 1990 followed 16 years of lower flows (Figure 3.1). Germination on driftcretions peaked a few years after 1990, especially on mats. The lack of germination on driftcretions following the subsequent 1996 event may reflect the fact that the 1990 flow had already cleared much of the standing stock of wood on river banks and much less wood was delivered in 1996. In midsummer 2011, very large amounts of wood were delivered to the lake with flows just above 7000 cubic meters per second. During our 2013 and 2014 sampling, new spruce had not yet germinated on the newly deposited driftcretions from 2011. This suggests at least a three-year lag between driftcretion deposition and vegetation establishment.

3.7. Implications

A complex mosaic of habitats and sinuous shorelines exists along Great Slave Lake because of the length of time over which abundant driftwood has been supplied to the lake. Enclosed bays, land spurs and wind-protected shores support large expanses of marsh that trap additional driftwood and sediment and provide valuable habitat for fish, migratory

birds and mammals. Offshore standing water bodies resulting from bay capture and channel truncation are important sites of carbon capture (*Tranvik et al.*, 2009; *Mongeon*, 2008). Driftcretions protect shorelines from wave and ice processes and facilitate backshore sedimentation which promotes shoreline progradation into the lake.

Driftcretions and their resulting landforms should be common on shorelines which receive a large wood supply and store wood permanently. Descriptions strikingly similar to drifcretions were reported on the coastal shores of Graham Island, British Columbia where they were noted as an important component of the beach-dune system that facilitated vegetation, impacted shoreline morphology and limited erosion (*Walker and Barrie*, 2006). Using Google Earth, we found evidence of driftcretion in: 1) protected embayments along marine coastlines (e.g., Montague Island south of Anchorage, Alaska) , 2) portions of freshwater lakes at high latitudes (e.g., Great Bear Lake; ozero Keta and ozero Khantayskoye in Siberia east of the Yenisei River, Lake Ladoga and Lake Onega in the Karelian portion of Russia), 3) portions of reservoirs (e.g. Vilyuyskoye Vodokhranilishsche in the Sakha region of Russia), and 4) marine deltas (e.g. Yukon River delta). Steep shoreline topography, removal of wood by humans, no substantial point source of wood, and locations above treeline limit driftcretion elsewhere. Abundant preserved wood accumulations in Pliocene sediments along the Arctic coast were deposited when global climate was $2-3^{\circ}$ warmer and boreal forests grew within 10° latitude of the North Pole (*Davies et al.*, 2014). These deposits suggest that as modern tree-lines migrate northward, driftcretions may increase along Arctic shores barring intensive deforestation of river corridors in Siberia and northern Canada or loss of boreal forest during fires.

The Arctic coast is now recognized as being at risk of erosion due to increased wave action, melting permafrost, and rising sea levels (*Forbes*, 2011). If river basins draining to the Arctic are extensively developed for hydropower and/or old growth forests along riparian corridors disappear to land use change, driftwood supply will drastically decrease. Our study suggests that if driftwood supply to shorelines decreases, Arctic coasts may lose buffering capacity offered by driftwood and related landforms, exacerbating coastal erosion.

Most instream wood research has focused on zones of wood production (mostly headwater channels) or wood transfer rather than zones of wood deposition. This study demonstrates that driftwood in depositional zones can profoundly impact the landscape as well as record long histories of wood export. We encourage others to investigate these landscapes. Of particular interest is understanding how driftwood-based landscapes are utilized by biota and how depletion of wood from river corridors by humans reduces ecosystem functions in formerly wood-rich depositional basins.

Recognition of Support

Data can be accessed at the Colorado State University Data Repository (`http://digitool.library.colostate.edu/R/?func=collections&collection_id=5307`). This study was supported by National Geographic Research CRE Grant #9183-12 by the Committee for Research and Exploration, Geological Society of America Graduate Grants and the Warner College of Natural Resources, Colorado State University. Special thanks to Dave Oleson of Hoarfroast River Huskies Ltd. and Sean Buckley of Great Slave Lake tours for field support. Special thanks Brett C Eaton and Francesco Comiti for their assistance in evaluating this paper.

SUPPORTING INFORMATION FOR CHAPTER 3

Introduction. This supporting information contains four parts. S1 is a description of data collection. S2 (pg 128) provides detailed descriptions of driftcretions along with eight figures of field and oblique aerial photo compilations. S3 (pg 139) describes the methods and calculations used to map wood distribution and estimate wood storage. S4 (pg 155) describes methods associated with tree coring and estimating year of germination from the cores. Each section of text has figures and datasets associated with them. Explanation of accompanying digital datasets are provided at the end.

3.A. S1. Data Collection

3.A.1. oblique aerial photos. On August 29, 2014, oblique aerial photographs were taken of shorelines from a small Husky 2-seater float plane. Figure 3.A.1 shows the flight path. Three cameras were used: a Nikon D7000 DSLR camera with either a Nikor 35mm f1.8 fixed lens or a Nikor 80-200 f2.8 zoom lens; a wide angle Contour 2+ action camera attached to the wing of the aircraft; and a wide angle GoPro HD2 action camera hung inside the plane looking out the window. All photos from the flight and a datasheet with their coordinates can be downloaded from the Colorado State University Digital Data Repository (`http://hdl.handle.net/10217/172976`).

3.A.2. field sites. In 2013 and 2014, eighteen sites were visited on the southern shore of the lake. At these sites, driftwood size was measured, observations were made along transects from the shore inland, and spruce trees growing out of driftcretions (or along linear features associated with past driftcretions) were sampled by collecting a section (entire slice of the trunk of the tree) for small trees or cores for large trees. Driftwood size was measured for each piece larger than 1 m in length and 10cm in diameter for every piece that crossed a line laid on the ground with a measuring tape. Figure 3.A.2 shows the locations of each transect and Table 3.C.1 summarizes the coordinates, the number of wood pieces measured, and the number of cores from each site used for analysis.

FIGURE 3.A.1. The flightpath is shown as the blue line. North is to the top of the page.

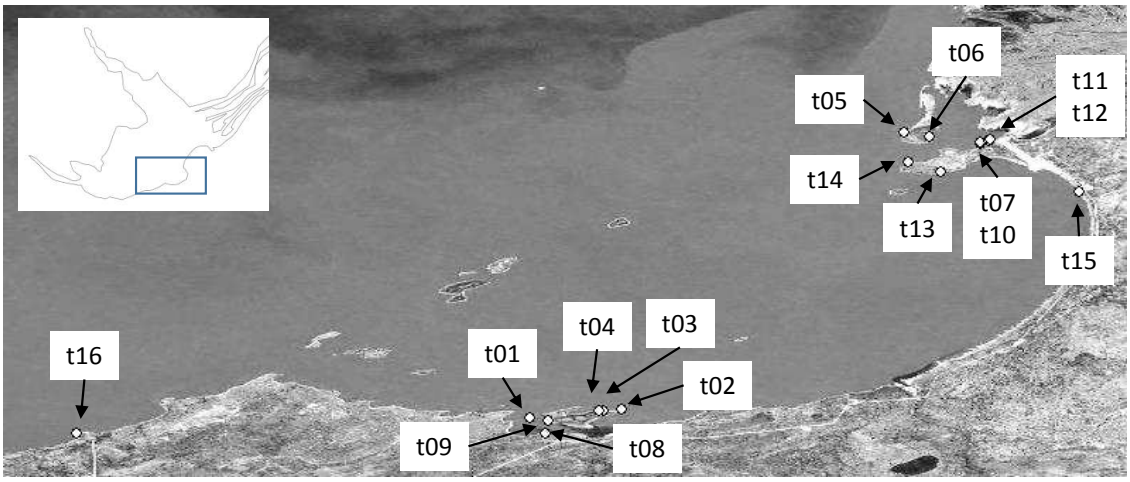

FIGURE 3.A.2. The location of field transects. Information about each trasect is located in Table 3.C.1.

3.B. S2. DRIFTCRETION

In this section, we first describe driftcretions and how they are formed and then present a photo tour of driftcretions and landforms from around the lake that highlight relationships between sediment, wood and vegetation. Figures 3.B.1 to 3.B.7 show compilations of both

field and oblique aerial photos highlighting relationships between sediment, wood and vegetation from various locations around the lake. The large scale landscape features that these interactions produce are quite impressive.

3.B.1. TYPES.

3.B.1.1. *berms.* Berms are raised ridges of driftwood that form parallel to the shoreline when seiches or ice push wind-imbricated driftwood along shorelines into linear piles. Berms form on high energy windy shores with gravel or cobble beaches and higher topographic relief (2+ m). Berms can be fairly small (< 0.5 m in height) to quite large (> 2 m in height). A berm can be either predominantly gravel and cobbles with a driftwood drape, or driftwood intermixed with gravel, cobbles and boulders. A berm with a driftwood drape forms when ice or waves create a linear beach ridge and wood is rafted and draped by waves on the top and shoreward side. Similar wood-draped gravel berms occur in New Zealand *Kennedy and Woods* (2012). Wave-formed berms are typically $0 - 1$ m of relief with driftwood oriented parallel to shore. In contrast, a berm with intermixed gravel, cobbles and boulders forms when ice bulldozes shoreline wood, along with shoreline substrates into a poorly sorted ridge with driftwood randomly oriented with respect to the shore. These berms can reach heights that exceed 2 m.

Cobble beach ridges are present up to the maximum extent of the lake during the last deglaciation *Lemmen* (1990) about 70 km inland. These cobble ridges likely also had driftwood either on top or within them when they formed because driftwood $1,000 - 8,000$ y in age is abundant in buried Slave River deltaic sediments *Vanderburgh and Smith* (1988), implying that driftwood has remained an important flux into the lakeshore system throughout the Holocene.

Berms are stacked in parallel lines such that the newest berm is closest to the shore . The wood on each successive berm inland is progressively more decayed. Spruce, alder, and poplar germinate on berms with decaying wood, but no trees germinate on berms that lack wood. Even-aged lines of spruce correspond to topographic expression of old berms so that

an inland progression across these berms crosses successively older lines of spruce trees up to a mature forest (> 300 y) or fire-impacted terrain ($50 - 100$ m inland).

Within the mature forest, the forest floor is covered by thick springy moss, but topographic undulations corresponding to linear berms remain apparent. Lichen-covered boulder erratics, similar to those offshore on wave cut platforms and within modern ice-pushed berms, dot the forest floor. Underneath the moss, mineral soil is absent, with only cobbles similar to those found on the modern beach.

3.B.1.2. *mats.* Mats are large, relatively flat accumulations of driftwood composed of a mix of large and small pieces, usually imbricated against each other parallel to the lake shore. Mats can be quite large (20+ m wide and 2+ m thick) or fairly small (< 5 m wide and < 0.5 m thick). Pieces of bark, smaller twigs and branches drape on top or are layered between larger logs. Mats are generally found on shorelines with low relief, sand to silt substrate, and low exposure to wind or ice push. On windy, exposed shores, mats are found in protected bays or trapped on low-lying proto islands. The largest mats are located near river deltas or in large bays. Smaller mats are found in small pocket bays along irregularly shaped shorelines or trapped in reeds.

Most mats are deposited when large seiches strand driftwood mats higher onto shores and farther into reeds and bays than can be removed with normal variations in lake level. Mats also form during periods of large riverine wood inputs when floating rafts become lodged along shorelines near deltas and then stranded as high flows recede. Mats on sandy shorelines are common and can continually accumulate as waves transport driftwood onto beaches, where the wood becomes trapped in sediment on top of, or next to, previously deposited wood.

Driftwood mats effectively raise the vertical elevation of the land. In places, large mats that appear to be underlain by solid, dry ground are in fact wood suspended above shallow water. Bands or clumps of shrubs and trees are commonly associated with decaying mats. In some areas, shoreline growth is more rapid than mat decay and large expanses of decaying mats are visible tens of meters inland.

3.B.1.3. *piece-wise matrix.* A piece-wise matrix forms when driftwood is interspersed or layered in sediment, providing structural support in an otherwise unstructured medium. Large and small driftwood can become part of a piece-wise matrix. On both protected and exposed shores, rootwads anchor large driftwood boles into shallow shoals and sand bars, pioneering new areas for increased sedimentation and establishment of plants. Protected shores are ideal sites for trapping driftwood. In areas with abundant reeds and sedges, driftwood sinks to the bottom, thus forming an underwater carpet of wood that facilitates more reed growth, sedimentation and capture of more wood, eventually leading to establishment of shrubs and trees *English et al.* (1997).

When shallows with underwater wood carpets become disconnected from lake hydrology, exposure of previously sunken logs supply nutrients and dry germination sites in saturated environments

On sandy shores, piece-wise matrices accumulate when wood is delivered and subsequently buried by sediment transport from longshore drift and wind. Driftwood near the surface stabilizes sand, provides germination sites for seeds and protects emerging vegetation from burial. Buried driftwood promotes vegetative growth long after vegetation establishment by supplying nutrients to roots and retaining moisture, similar to the role of driftwood in creating moist, organic-rich microhabitats in large ephemeral rivers *Jacobson et al.* (1999). Discrete, long lines of trees parallel to the shoreline resulting from this process correspond to prior shoreline positions.

3.B.2. FORMATION. Formation of driftcretions is intertwined with sedimentation and vegetation establishment. Sedimentation creates depths shallow enough for colonization by marsh grasses such as horsetails and sedges. Grasses then facilitate further sediment deposition and capture floating smaller pieces of wood, which sink and join a sediment-wood matrix. Over time the lake bottom builds up, until pioneer species such as willows and alders establish. Large mats of driftwood become captured by the emergent vegetation and provide a substrate for the establishment of poplar and spruce. Drift logs are then caught up on vegetated shores. On high exposure shores (shores with high exposure to wind), ice

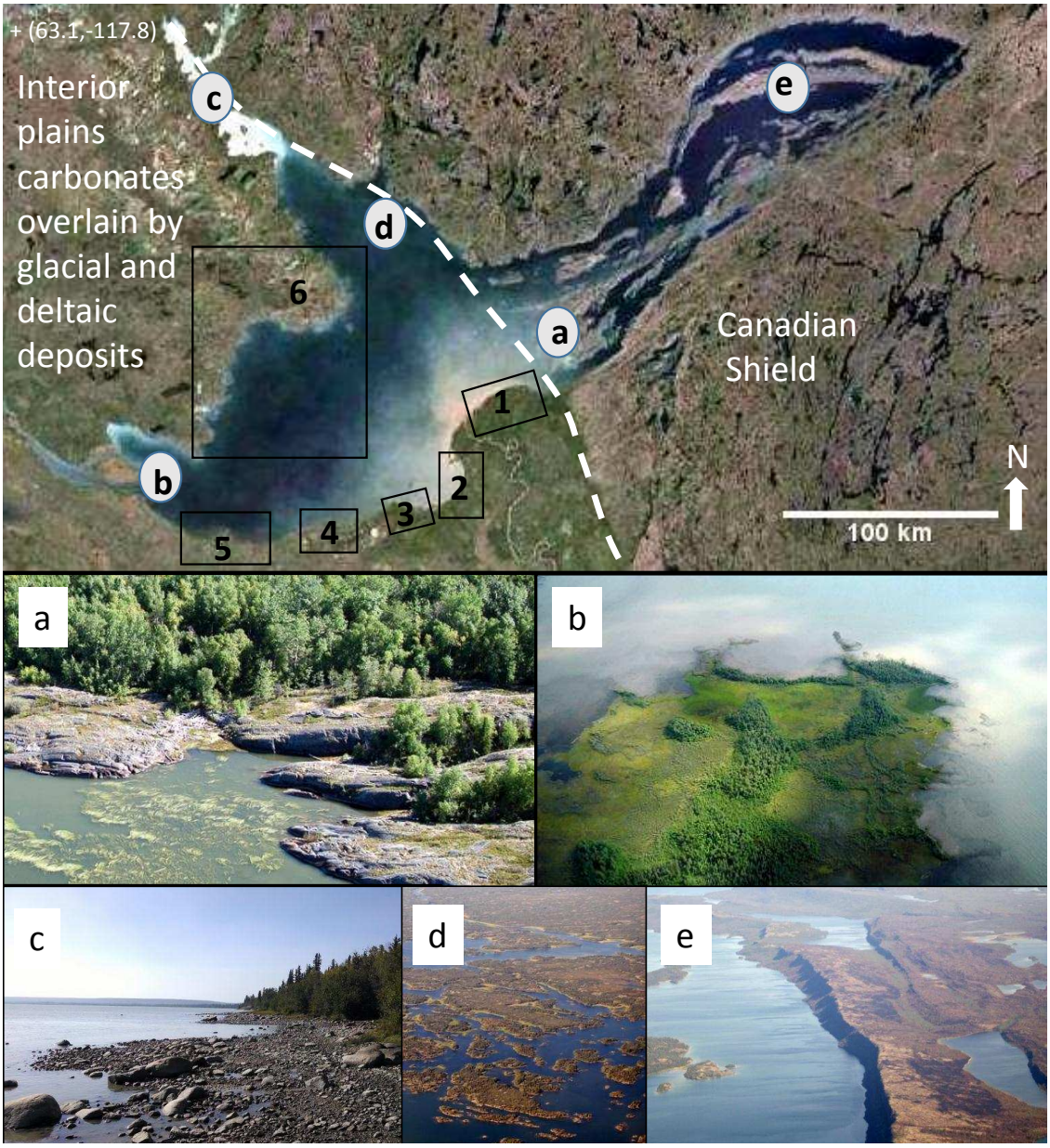

FIGURE 3.B.1. Index figure showing the locations of the next six figures (boxes) as well as some photos from locations with little to no driftwood (a-e). The boxes labelled 1 through 6 correspond with Figures 3.B.2 through 3.B.7 and are locations with lots of driftwood. Due to abrupt shoreline relief, little to no wood is stored along shores of Canadian Shield bedrock (a,d,e). Although hard to see, along bedrock shores near the Slave River Delta, small pockets of wood can be stored in bedrock crevices (a). There is an abrupt transition to little to no wood near the start of the Mackenzie river (b). Little to no wood is delivered from streams draining the Canadian Shield as evidenced by no wood high in the North Arm of the lake (c)

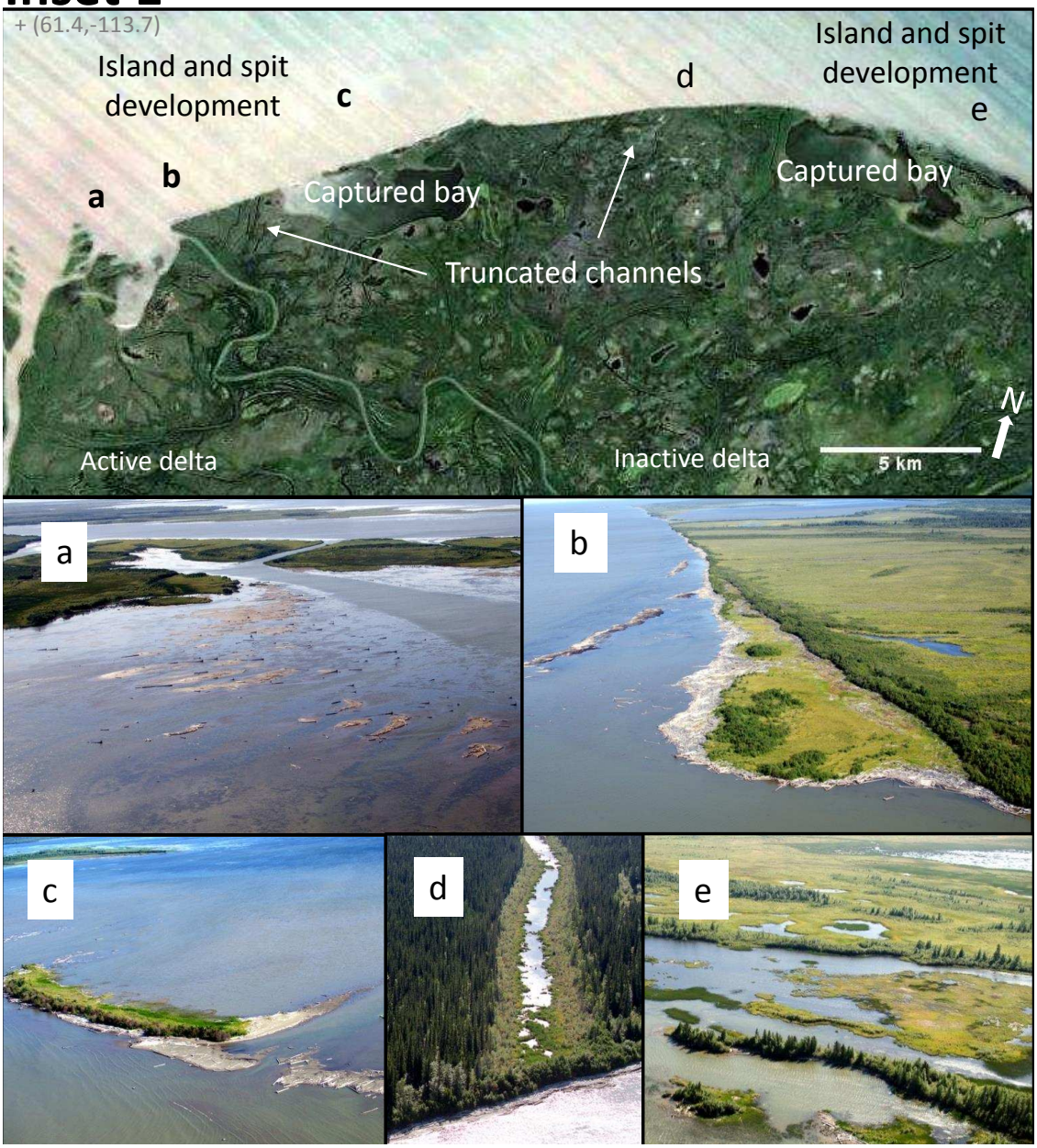

FIGURE 3.B.2. The Slave River delta stores large amounts of driftwood on its shorelines. In front of the active main distributary channel, large logs become lodged, pioneering new sandbars that will later turn into vegetated land (a). Logs are also crucial for extending and stabilizing off-shore spits and bars (b, c, e) that play a role in enclosing bays. Wood accumulates along linear shorelines, truncating old distributary channels that no longer have the power to flush the wood from their outlets (d). These channels eventually become vegetated. Linear lines of trees are associated with old decaying drift piles (e).

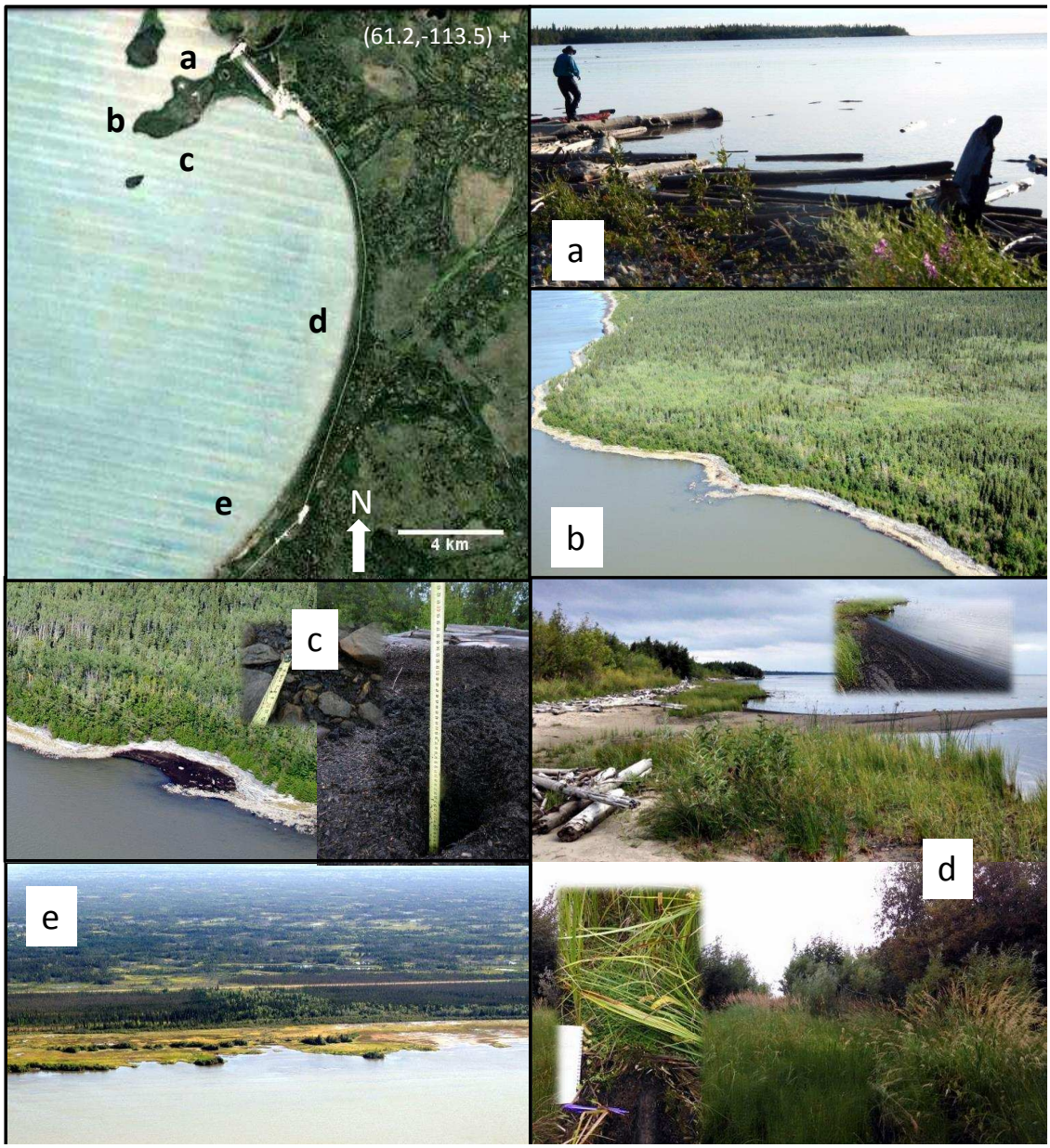

FIGURE 3.B.3. During calm spells of no wind, driftwood that is not yet pushed high onto the land from ice or wind floats back into the lake and drifts along shorelines on surface currents (a). Along windy cobble beach shorelines, driftwood is pushed away from the waters edge and piled in ridges by ice (b) and in thick wood pulp accumulates in protected pockets and fills the interstices between cobbles (c). Along sandy, protected shores, dritwood is not clearly visible by air (e) but upon visiting these sites on the ground (d) it is apparent that there are large amounts of buried driftwood (d lower inset) and pockets of driftwood pulp (d upper with inset). Lines of shrubs and trees correspond to driftpiles (e) and inland meadows are underlain by carpets of wood (d lower with inset).

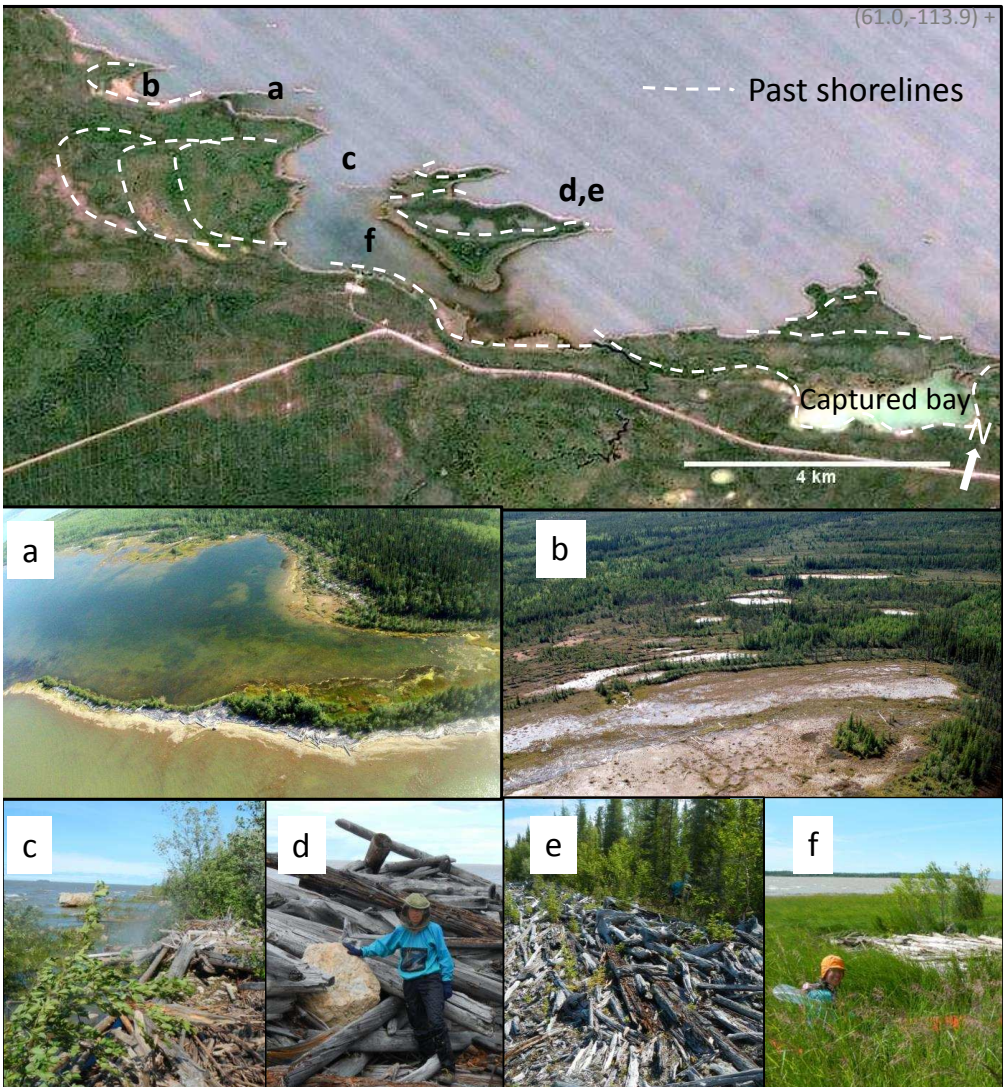

FIGURE 3.B.4. Shores approximately obliquely perpendicular to the predominant wind direction develop elongate islands and spits that enclose bays (a). Before total enclosure, bays collect wood and fill with sediment. Linear lines of trees corresponding to drift piles in these bays record the progression of infilling (b). Spits are expanded when large logs with rootwads become lodged in shallow areas, pioneering new proto islands that eventually become connected to larger spits and islands. These proto islands capture large wood mats on their windward side that increase the elevation of the islands just enough to facilitate the establishment of willow, alder and poplars (c). Along the windward side of large islands and the mainland, ice pushes driftwood mixed with cobbles and boulders into large piles parallel to the shore (d) that then decay, providing nursery sites for spruce germination (e). On the leeward side of islands reeds and sedges trap driftwood both at the surface and under the water. Willows and alders take root near trapped piles (e).

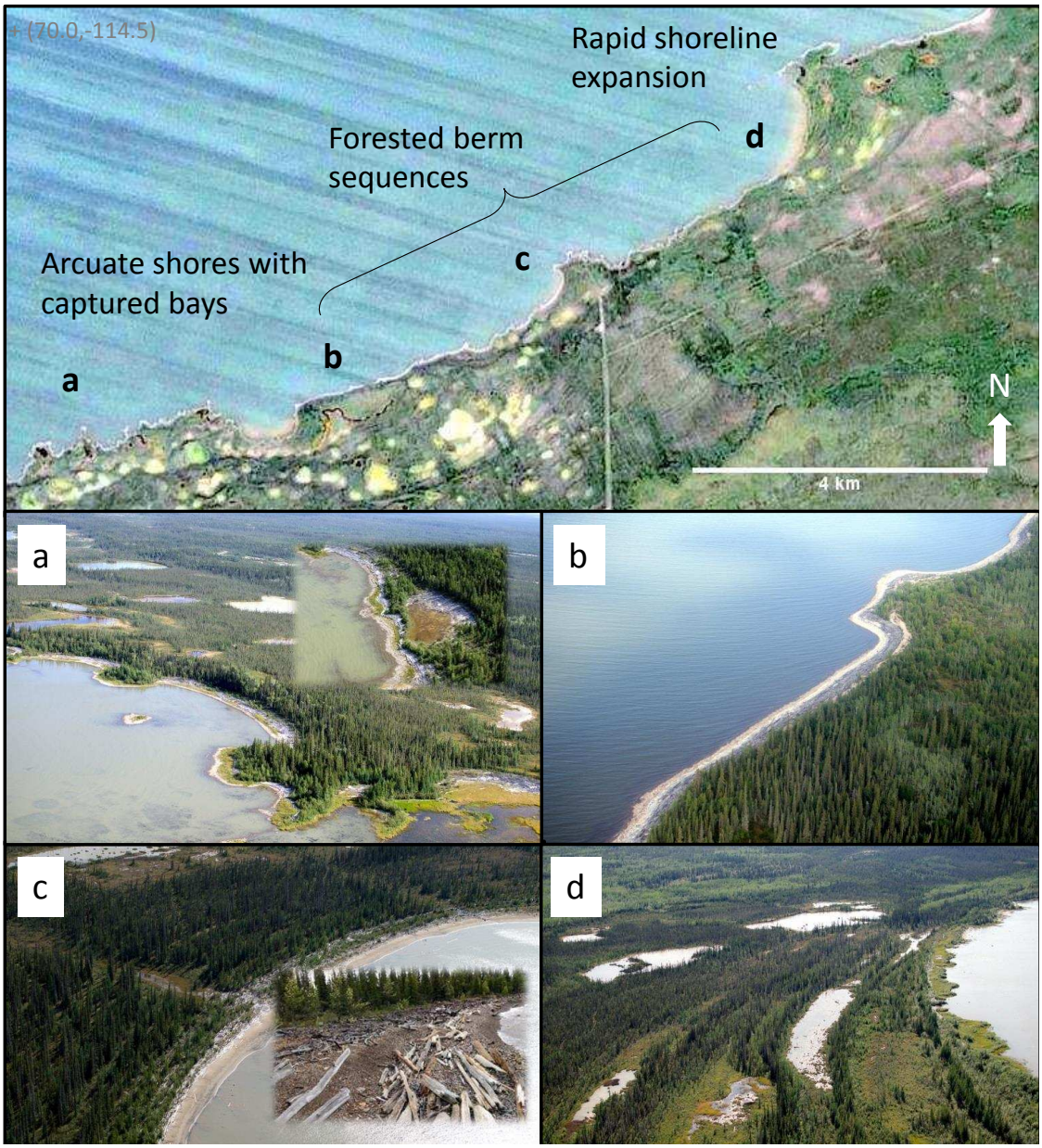

FIGURE 3.B.5. Wood-rich shorelines are often scalloped with small enclosed embayments (a and inset). Over time as the land progrades into the lake, a zone of enclosed bays creates a mottled offshore landscape of standing waterbodies and clearings resembling a karst landscape (a and overview image). Along linear shorelines, driftwood is easily discernable as a constant grey strip, generally between 15 and 30 meters wide (b). On windy shores, heavy wave action can create gravel cobble berms that are draped with drifwood on their backslopes (c inset). Shoreline expansion rates are much slower for shorelines exposed to high winds than along protected shores. Spruce trees grow in closely spaced linear lines on shores positioned perpendicular to high winds (c) while they grow in more widely spaced linear lines along shorelines that are protected from the wind (d). The lines of trees correspond with decaying driftwood piles.

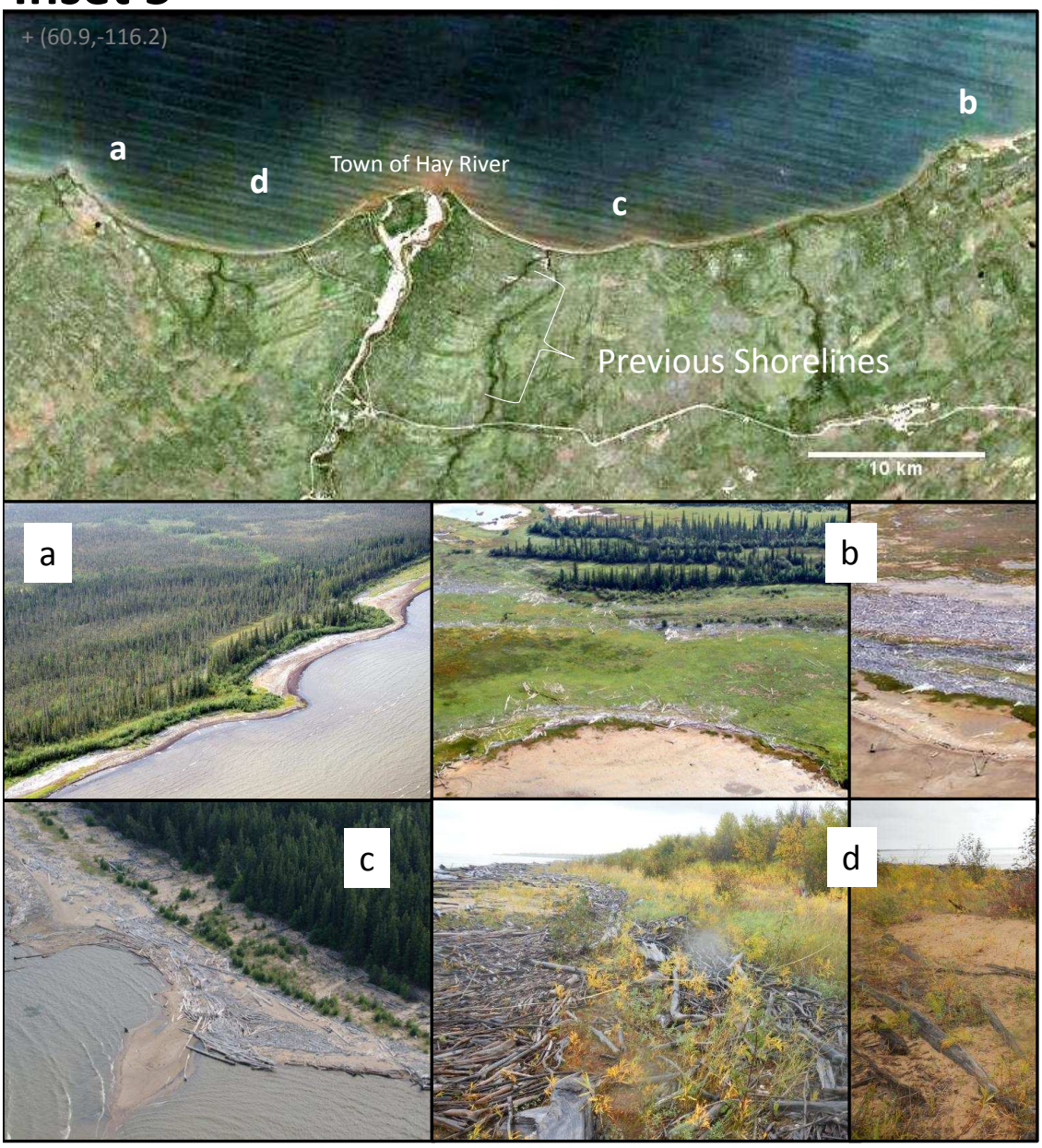

FIGURE 3.B.6. The south shore in the vicinity of Hay River is much sandier and shallower than the rest of the lakeshores due to the high sand loads that this river deposits. As a result, instead of tall berms driftwood is jammed against the shore and subsequently buried. Vegetation bands grow on bands of buried wood in the sand (a,b,c,d) which can be seen kilometers inland on satellite imagery (overview map). Larger driftlogs appear to be posistioned at the beach (c) while smaller branches and logs are piled on the back shore where they become incorporated into a piece-wise matrix. The buried logs help to retain moisture in the beach sands and provide nutriends and germination sites.

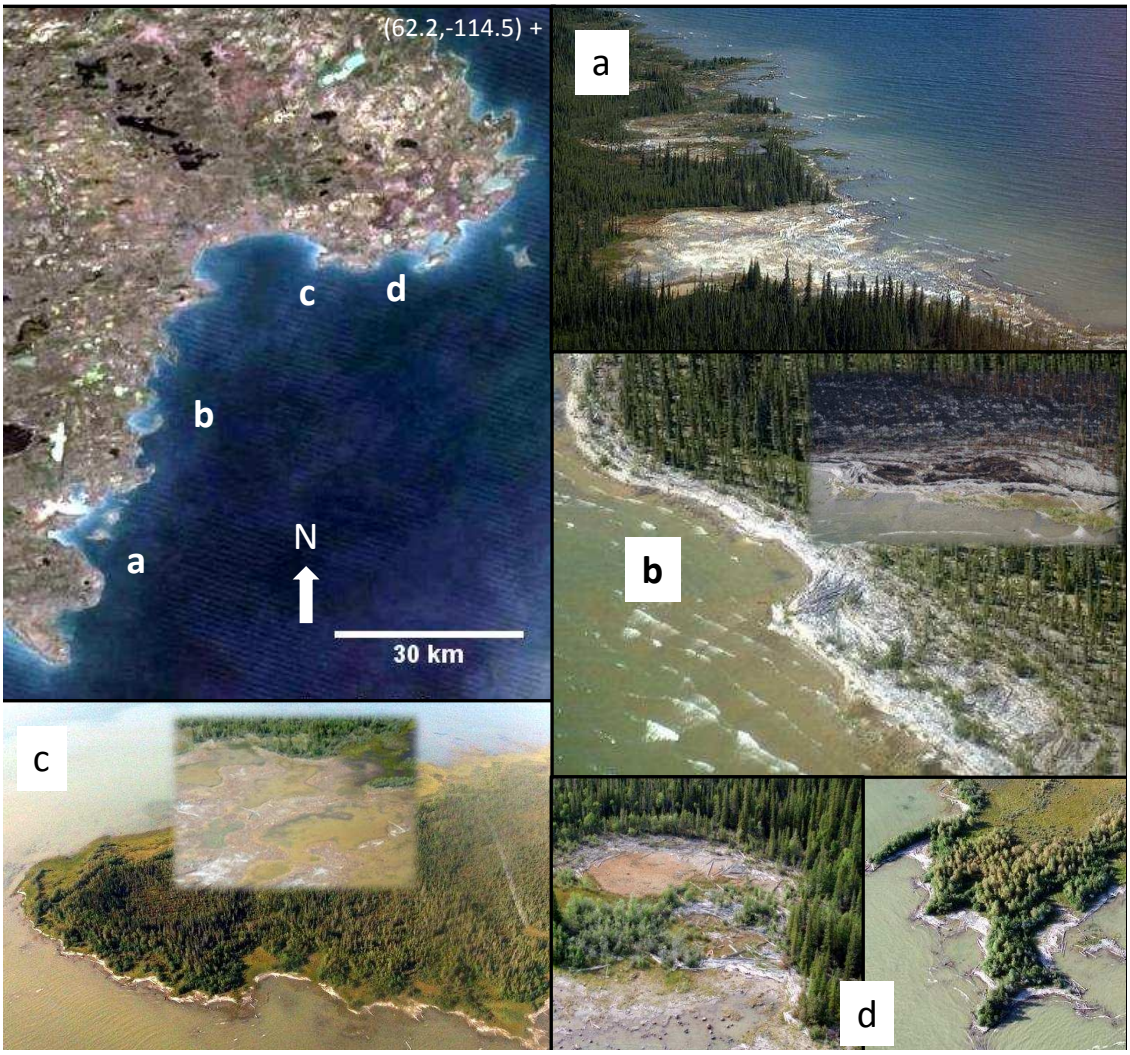

FIGURE 3.B.7. The north shores derive all their wood from lake currents transporting wood from rivers draining into the south shore. Even though overall there is less wood on the north shores, there is still an appreciable amount. Large embayments on this shore align with glacial features and can become filled with mats of wood (a) however, many large embayments are oriented such that they are protected from the wind and recieve little to no wood (inset c). On shores that do recieve wood, smaller scale scalloped shores and land spurs are superimposed on top of the glacial embayment template (c,d) and sometimes capture mini-bays (d). It is quite common to see wood-rich scalloped shores on the windward side of peninsulas and calm shallow bays lacking wood on the leeward (c). On shorelines aligned approximately perpendicular to heavy winds, berms and associated lines of trees are common (b). In 2014, there were extensive stand replacing forest fires in the Northwest Territories. One of the regions hit hard was the north shore of the Great Slave Lake. In many places the fires burned all the way to the shore (inset b, taken in 2014, matches the location in b, taken in 2013). The severity and extent of these fires was unprecedented in historic memory. Shoreline trees and forest characteristics prior to the 2014 fires, showed no evidence of previous fires at the lakeshore.

and large waves push drifted logs into piles which later decay and support establishment of more woody vegetation.

Shoals that become vegetated often create linear spits and peninsulas, thus forming strings of islands that protect the main shore from large waves and other disturbances. They also grow outwards from the land creating a scalloped shoreline that protects mini bays and pockets. Behind the protection of these woody shoals, sedimentation of fines and capture of smaller floating wood and pulp occurs at increased rates. Eventually, backwater areas fill in with woody sediment and the shoreline expands outward to join the string of protecting islands or shoals. The emergent backshore is rich in nutrients and is quickly established by plants. The windward side of coastlines continue to grow when ice-pushed drift berms and seiche rafted driftwood mats provide additional substrate for plant colonization. At this point, new shoals form a new line of protection and the process begins anew.

3.C. S3. Wood Distribution Methods and Analysis

Figure 3.C.1 is a synthesis schematic showing the sampling and analysis of driftcretions around the Great Slave Lake.

3.C.1. sampling. In order to estimate the amount and distribution of driftwood around the Great Slave Lake, lake shores with appreciable amounts of driftwood were stratified into 11 shoreline regions based on observed differences in shoreline appearance or known differences in processes impacting the shore. Almost the entire shoreline of interest was photographed with overlapping wide-angle photos taken during the flight described on page 127. The complete dataset of all photos can be accessed via the Colorado State University Data Repository (`http://hdl.handle.net/10217/172976`). Data were gathered by randomly selecting and analyzing 10 non-overlapping oblique aerial photos from each of the 11 regions (Figure 3.C.1). If a photo was randomly selected that overlapped with a previously analyzed photo, that photo was discarded and another photo was randomly chosen.

3.C.2. image analysis. Photo distortion from the wide angle lens was corrected using software PTlens (http://epaperpress.com/ptlens/). The horizon was used as a guide for

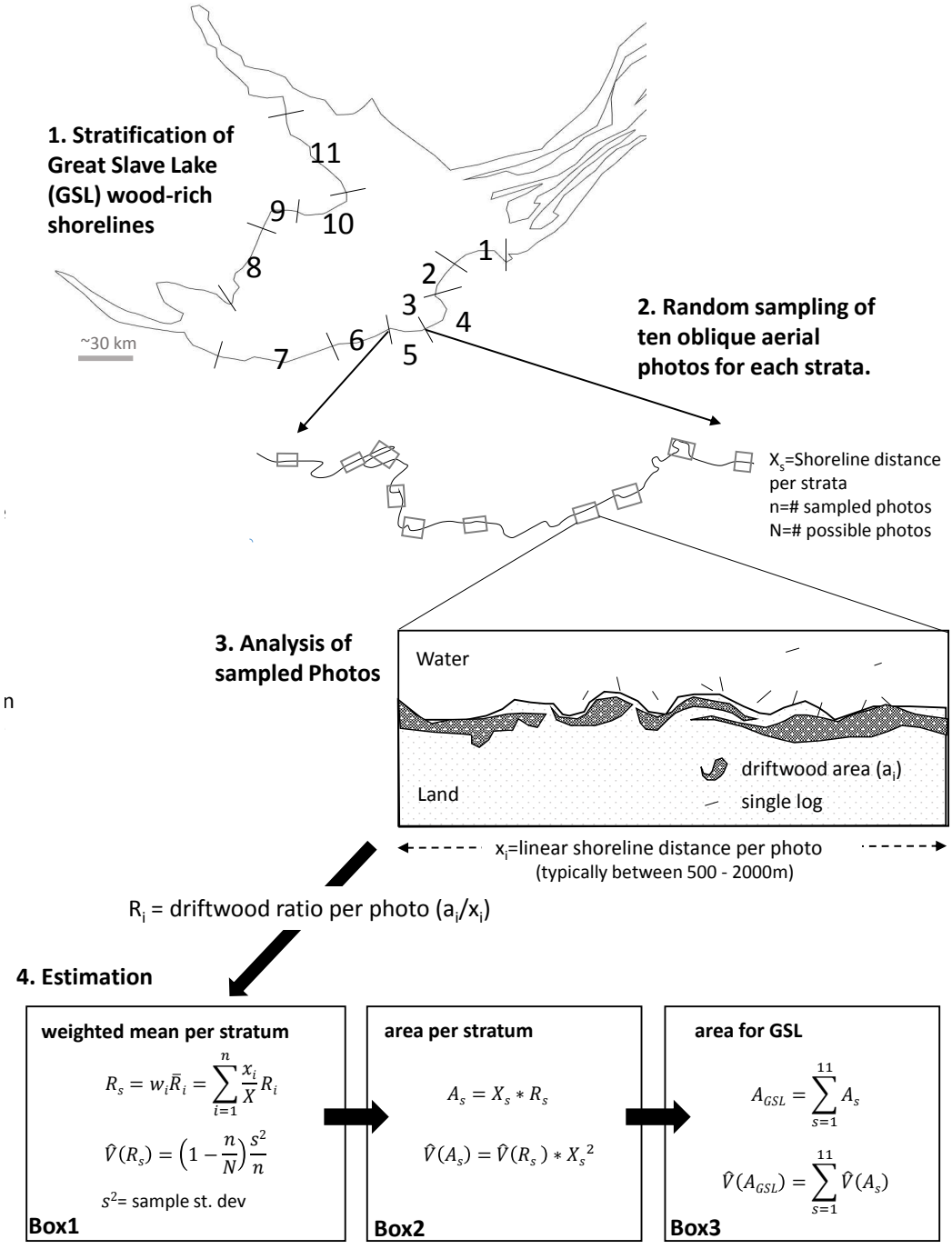

FIGURE 3.C.1. Sampling scheme and process for the estimation of driftcretion from oblique aerial photos

correction (Figure 3.C.2). After distortion was corrected, photos were cropped and loaded into ImageJ, an open source software platform for image analysis (http://imagej.nih.gov/ij/). The horizontal scale and pixel ratio were set using distances between identifiable landscape

features measured on Google Earth. Only correcting for scale distortion in two directions (width and height of pixels) was sufficient because most photos were taken so that the shoreline, and thus drift piles, were aligned with the image width. Polygons were drawn around areas of visible wood and lines were drawn over each individual log distinct from driftwood piles. The curved shoreline distance and the linear shoreline distance were also measured on each photo.

Total area of land covered by driftwood was calculated for berms, mats and individual logs. The area of land covered by individual logs was calculated by multiplying the total log length per photo by 0.23 m. This value is the mean diameter logs measured in the field which had lengths that were within one standard deviation of the average length of logs measured on the photos (Figure 3.C.3). Field measured data of log length and width is included in Supporiting Information Data Set (explanantion of variables on page 143).

TABLE 3.C.1. Transect Information.

TranID[a]	Date Visited	Start Coord (WGS84)	X(m) [b]	#logs [c]	#cores [d]
t01	7/13/2013	60.97863 -114.0576	15	9	–
t02	7/13/2013	60.98483 -113.9883	25	17	2
t03	7/14/2013	60.98416 -114.0018	102	15	6
t04	7/15/2013	60.98413 -114.0048	136	64	4
t05	7/16/2013	61.19497 -113.7748	118	13	6
t06	7/16/2013	61.19076 -113.7555	165	–	4
t07	7/16/2013	61.18597 -113.7169	27	–	2
t08	7/17/2013	60.96742 -114.0461	93	–	5
t09	7/17/2013	60.97661 -114.0440	132	–	8
t10	8/17/2014	61.18677 -113.7167	62	–	6
t11	8/17/2014	61.18858 -113.7103	52	–	5
t12	8/17/2014	61.18865 -113.7096	59	–	6
t13	8/18/2014	61.16502 -113.7464	31	–	3
t14	8/18/2014	61.17243 -113.7709	28	–	4
t15	8/18/2014	61.14939 -113.6422	188	–	4
t16	8/19/2014	60.96727 -114.4001	36	–	7
t17	9/15/2012	60.84083 -115.8822	13	19	–
t18	9/15/2012	60.84121 -115.8808	17	14	–

a. All transects are located in Figure 3.A.2 except for t17 adn t18 which are located just west of the Hay River Delta.
b. X is the length of the transect in meters.
c. The number of driftwood logs measured for size.
d. The number of trees cored or sampled for age.

Each driftwood area was normalized by the measured linear distance of the shoreline in the photo and reported as a ratio. This was done to minimize error comparing values between photos based on uncertainty in setting the photo scale. This metric also makes intuitive sense because it is the average distance inland that driftwood covers (width of driftpiles) per meter of shoreline. A measure of shoreline irregularity was calculated by taking the shoreline distance and dividing it by the linear distance. The derived data for each photo is included in Supporting Data Set, S2 (explanantion of variables on page 154). Table 3.C.2 briefly describes each shoreline region and summarizes the results by region.

FIGURE 3.C.2. Photo on the left shows the original fish-eye distortion and the photo on the right shows the photo corrected for distortion, cropped and ready for analysis.

3.C.3. ESTIMATION.

3.C.3.1. *areas.* The total area of visible driftcretions for the lake was calculated by multiplying the total shoreline distance (X_s) by the mean driftcretion ratio (R_s) for each region and then summing the regions (Table 3.C.2 and Figure 3.C.1). The variance each region was calculated using the standard equation of variance for total estimates from ratio estimators. The variance for the lake total was calculated from the sum of the variances for the regions. Bounds were estimated as two times the square root of the variances. The total estimate for area covered by non-vegetated, non-buried driftwood is $4.6 \pm 0.7x10^6$ m^2.

3.C.3.2. *volumes and mass carbon.* A volume of wood on the order of 10^6 to 10^7 m^3 is estimated for the Lake. This value was calculated by multiplying the total area by a reasonable range for average accumulation heights ($0.5 - 1.5$ m) and a reasonable range for accumulation porosity (0.5 to 0.8 fraction of wood). Porosity was highly variable in Great Slave Lake drift piles, depending on the degree of imbrication and amount of smaller branches, twigs and wood pulp draped on top. To estimate mass carbon, volume of wood

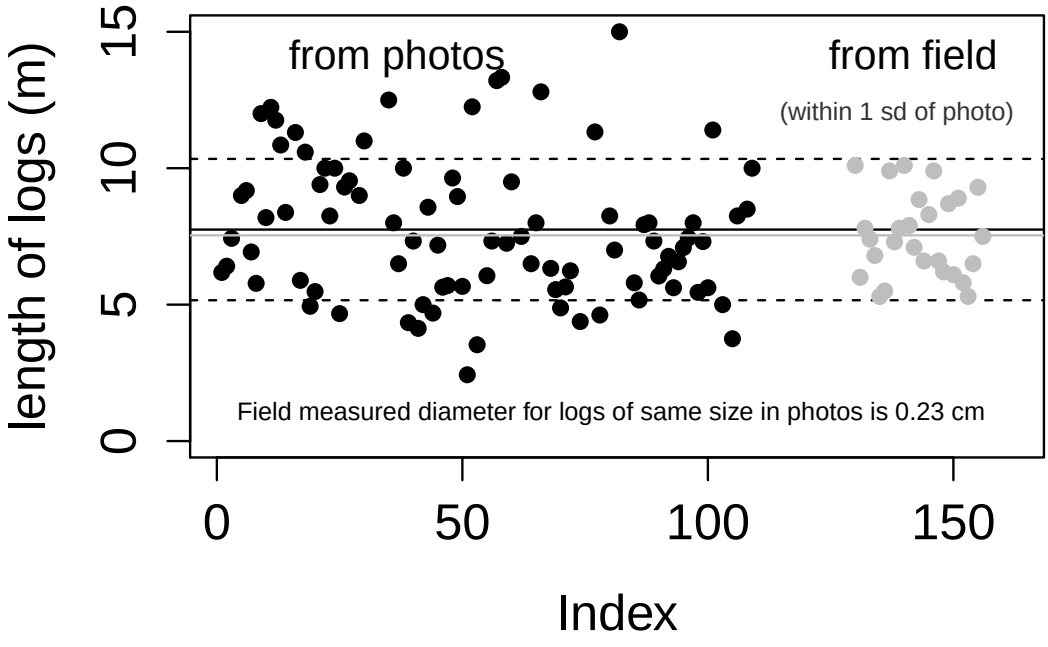

FIGURE 3.C.3. Log lengths from field measurements (grey dots) within one standard deviation of the average length of individual logs from photos (black dots) were used to estimate the average diameter of logs on photos, 0.23 m

TABLE 3.C.2. Description of shoreline regions and results. View concurently with Figure 3.C.1.

Region Descriptions	X_s [a]	R_s [b]	C [c]	bfrac [d]	mfrac	pfrac
1. Inactive Slave River Delta	47.9	12.4 ± 4.6	1.1	0.00	0.99	0.01
2. Active Slave River Delta	26.5	10.2 ± 2.5	1.9	0.00	0.99	0.01
3. Chain of windy exposed islands	46.8	12.2 ± 3.1	1.2	0.83	0.17	<0.01
4. Protected curved shore near Fort Resolution	23.2	3.5 ± 1.0	1.3	0.00	>0.99	<0.01
5. Windy shore with many elongate land spurs near Paulette Island	31.0	10.0± 4.1	1.1	0.61	0.38	0.01
6. Very windy arcuate shores near Pine Point	36.9	11.8 ± 5.1	1.2	0.68	0.32	<0.01
7. Straight sandy shores near Hay River	80.4	11.5 ± 5.3	1.1	0.00	>0.99	<0.01
8. North-south trending North Shore	103.7	6.8 ± 2.6	1.2	0.70	0.29	0.01
9. Protected large bay on North Shore	37.4	1.2 ± 0.2	1.5	0.00	0.99	0.01
10. East-west trending North Shore	64.8	9.6 ± 6.2	1.7	0.16	0.84	<0.01
11. West shore in the North Arm	99.5	0.2 ± 0.3	1.3	0.44	0.54	0.02

a.X_s is the total shoreline distance within each region in kilometers.
b.R_s is ratio of driftwood area over linear shoreline distance.
c. C (for Complexity) is a measure of the small scale (10^1 m) irregularity of the shoreline. It is calculated like a sinuosity, but also includes distances around islands and spits close to shore Complexity and R_s are average values from ten randomly sampled photos from each region.
d. bfrac, mfrac, and pfrac report the fraction of area within each region covered by berms, mats or individual logs, respectively.

was mulitplied by 450 kg/m^3 (which is a reasonable estimate of the density of wood for the tree species present: poplar, aspen, birch, white spruce and larch), and then divided by two (wood is only about one half carbon *Lamlom and Savidge* (2003)). The error on the volume and carbon estimates are reported as ranges that are based on the small and large end members corresponding to the ranges of probable heights and porosities.

In order to facilitate comparison of values across regions, volume or mass carbon are often normalized by contributing drainage area (which is useful for basins with wood recruitment dominated by upslope mass wasting), total basin stream length (which useful for basins with wood recruitment dominated by bank failures), or total length of shoreline (which is useful for thinking about wood storage). For this site, contributing basin area is 6.8 x 10^5 km^2, total stream length (3rd order or higher) is 1.7 x 10^5 km, and length of shoreline is 6 x 10^5 m. These values were to normalize results for comparison to other studies in other regions.

Currently, there is no consistent reporting protocol for large wood rates and volumes. To facilitate broader synthesis of wood and carbon budgets, we propose that studies reporting metrics related to driftwood or instream wood include: contributing drainage area and stream length, length of shore or bank surveyed, total volume (with explanation of methodology and assumptions for porosity and height), total carbon (with assumptions for fraction carbon and density), time frame, and sampling situation. Not included in this list is the total surface area of logs within jams, which is of particular interest for ecologists (*Wallace and Benke*, 1984), but not a practical field measurement for large scale spatial studies. Surface area of wood can be calculated based on relationships developed between wood volume and surface area (*Manners et al.*, 2007). Consistently reporting these values will allow researchers to synthesize field data from across disciplines and spatial scales to help constrain wood and carbon budgets in fluvial networks, which is needed to refine global carbon fluxes (*Aufdenkampe et al.*, 2011).

3.D. S4. Tree Core Methods and Analysis

A dataset of of the cores used in this analysis is provided as Supporting Information datafile DS3 and Table 3.E describes the variables in the dataset. In addition to the height of the core and the distance inland, the decay class (see Figure 3.D.4) of the driftcretion upon which the tree is growing and the number of driftcretion between the location of the tree and the shoreline were noted. For berms and mats, the term driftcretion event is used to describe discrete driftwood piles in varying levels of decay that were probably deposited during or within a few years of a year of high wood delivery to the lake. For piece-wise matrices, an driftcretion event relates to when a large segment of woody sediment was exposed and vegetated.

3.D.1. Estimating Germination Year.

The age of each sampled tree was calculated by counting rings and then adding the number of years missed if the core was off-center and the number of years missed by coring at some height off of the ground. Germination year was calculated by subtracting the estimated age from the year the sample was collected.

3.D.1.1. *estimating years on cores by counting rings.* Core and cross-section samples were mounted, sanded and rings were counted under a microscope. The quality of the cores ranged from excellent to poor. In 2013, many cores were twisted and broken. In 2014, a new corer was bought and most cores were of excellent quality. The poorer quality cores from 2013 were still used since it was still possible to count rings for a minimum age and this study was interested in general decadal scale trends in germination rather than a precise analysis of year to year tree widths and growth. Conservative errors were assigned to each core ranging from 1-10 years based the quality.

3.D.1.2. *estimating years missing on off-center cores.* Some cores did not go through the exact center of the tree. The number of rings missing due to missing the center was estimated by aligning a transparency of concentric circles with the curvature of rings near the middle of each core and then measuring the distance from the edge of the core to the center and multiplying it by the average ring width near the center of the core. Measurement error associated with the distance to the center and with the average center ring widths were estimated and used to estimate error.

3.D.1.3. *estimating years missing from germination to core height.* Age-height relationships were developed by slicing twelve juvenile white spruce trees into cross-sections every 5 centimeters from the top of the root to 20-60 cm up. Years since germination were recorded by subtracting the number of rings counted at each interval by the number of rings counted at interval 0 (the section just above the roots). This analysis was done to obtain prediction estimates for the number of years missed by coring larger trees at some height above ground level, usually between 20 and 40 cm off of the ground. Data from this analysis in included as Supporting Information data file "ageheight.csv", and Table 3.E describes the the variables in this dataset.

Age-height relationships were developed for three categories of ring widths (rw): small ($< 0.07cm$), medium (0.07 cm $\geq$ rw $<$ 0.14 cm), and large (rw$\geq$ 0.14 cm). For each tree the average ring width for the cross section at height=0 was clasified into one of the three categories. Figure 3.D.1 shows the age-height relationships for each of the three categories.

the y axis, "years", corresponds to the variable $yrsbfr$ in Table 3.E and represents the number of years elapsed, or age, before a tree grows to a particular height. The resulting models for the three categories of ring widths are:

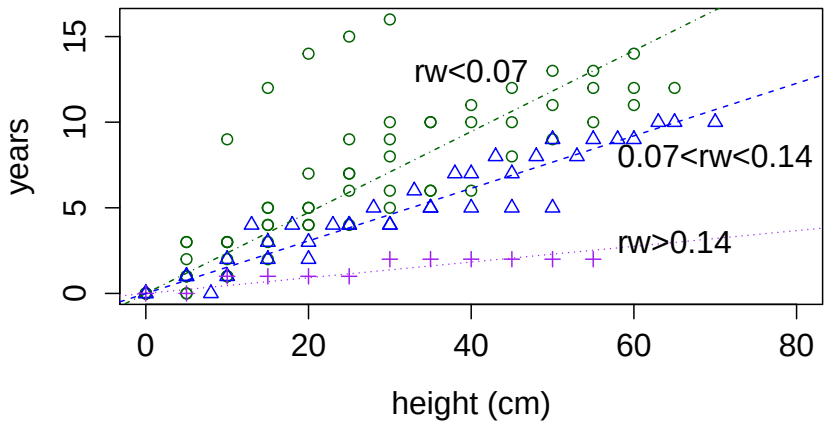

FIGURE 3.D.1. Regressions to determine years since germination at some height for three category of ring widths (rw). Ring width values are in centimeters. Model coefficients and fit are reported on page 147.

(1) small rings: rw < 0.07 cm

$$Years = 0.24 * Height(cm), RMSE = 3, R^2 = 0.87$$

(2) med rings: 0.07 cm$\geq$ rw < 0.14 cm

$$Years = 0.15 * Height(cm), RMSE = 1, R^2 = 0.98$$

(3) large rings: rw≤ 0.14 cm

$$Years = 0.05 * Height(cm), RMSE = 0.3, R^2 = 0.95$$

Average ringwidths near the center of each core in the main dataset (described on page 155) were measured then grouped into the three categories of ring widths. The regression equations on page 147 were applied to the core height to obtain an estimate of years from germination to core height. 95% Prediction confidence on the years from germination to core height were were estimated by $\pm 2 * RMSE$. In the cases where the lower confidence limit

extended below zero,values were truncated to zero since a tree can never be negative years old.

The years and their errors estimated from this step were then added to the estimated age at the height of the core as described previously. The resulting ranges of germination for each core are shown in Figure 3.D.2. Uncertainty increased with age and with the quality of cores. Most of the cross-sections with germination year after 1950 are cross-sections rather than cores and are much better constrained.

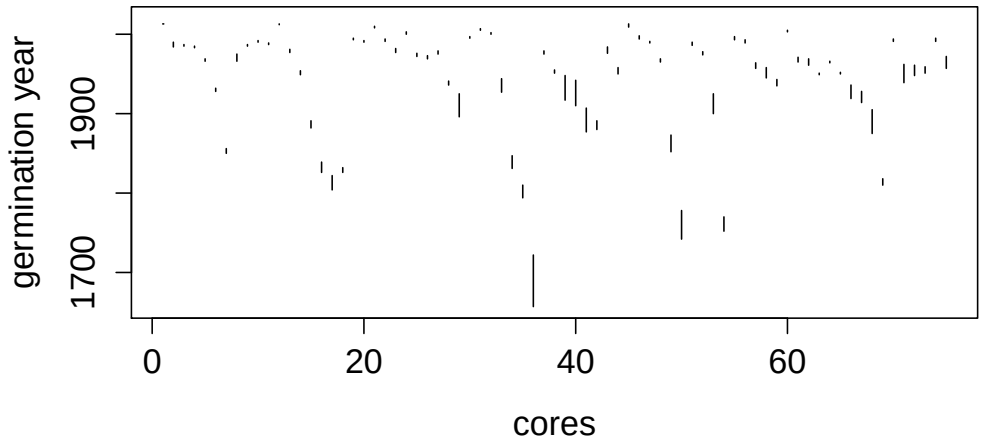

FIGURE 3.D.2. Estimated ranges of germination year for each core. Cores are ordered along the x axis by their index, which is the order that they appear on "cores.csv". The vertical bars represent the uncertainty in the germination age for each core.

3.D.2. RESULTS.

3.D.2.1. *decay rates.* We estimated decay rates by subtracting the median ages of trees sprouting out of driftcretions for each decay class. Figure 3.D.4 shows photographs of each decay class. Rounding values to the nearst tens place, it takes approximately 20 years to decay from class 2 to 3, 40 years from class 3 to 4 and 60 years from class 4 to 5 (Figure 3.D.3 Driftwood piles take just over 50 years to become fully vegetated (class 4 is fully vegetated) and thus unrecognizeable as wood in aerial photographs.

3.D.2.2. *driftcretion rates.* Rates were computed by calculating the rates between each individual core along a transect, as shown in Figure 3.D.5. This was done in order to capture

FIGURE 3.D.3. Age of spruce trees growing out of driftcretions at varying states of decay. Each decay class is very significantly greater (p-values < 0.01 at $\alpha = 0.05$) than the class before it using two sample t-tests. The approximate time between classes noted were calculated by substracting the means of each class and rounding to the nearest ten.

the variability of rates through time. In addition to calculating an average rate as a distance over time, we also calculated rates per event. It is useful to think about rates per event since driftcretions are deposited episodially rather than continually. Cores collected in the field were excluded from the Data Set S3 and the rate analysis if it was determined that the tree germinated within a mature forest rather than coincident with driftcretion deposition. This was detected by plotting age versus distance inland and looking for age reversals. An example of this is shown in Figure 3.D.5.

A total of 50 paired cores growing out of berms, mats and piece-wise matrices were used to estimate rates. The Supporting Information Data Set S5 contains the rate data and page 155 describes the variables in this dataset. Figure 3.D.6 graphically shows the data in a scatterplot shaded by driftcretion type and Figure 3.D.7 compares boxplots between the three driftcretion types.

Generally, more time passes and less land is accreted for berm events and the most land is accreted in the shortest amount of time for piece-wise matrices. Mats are somewhere in-between, but more closely align with berm than matrices. However, for all driftcretion types,

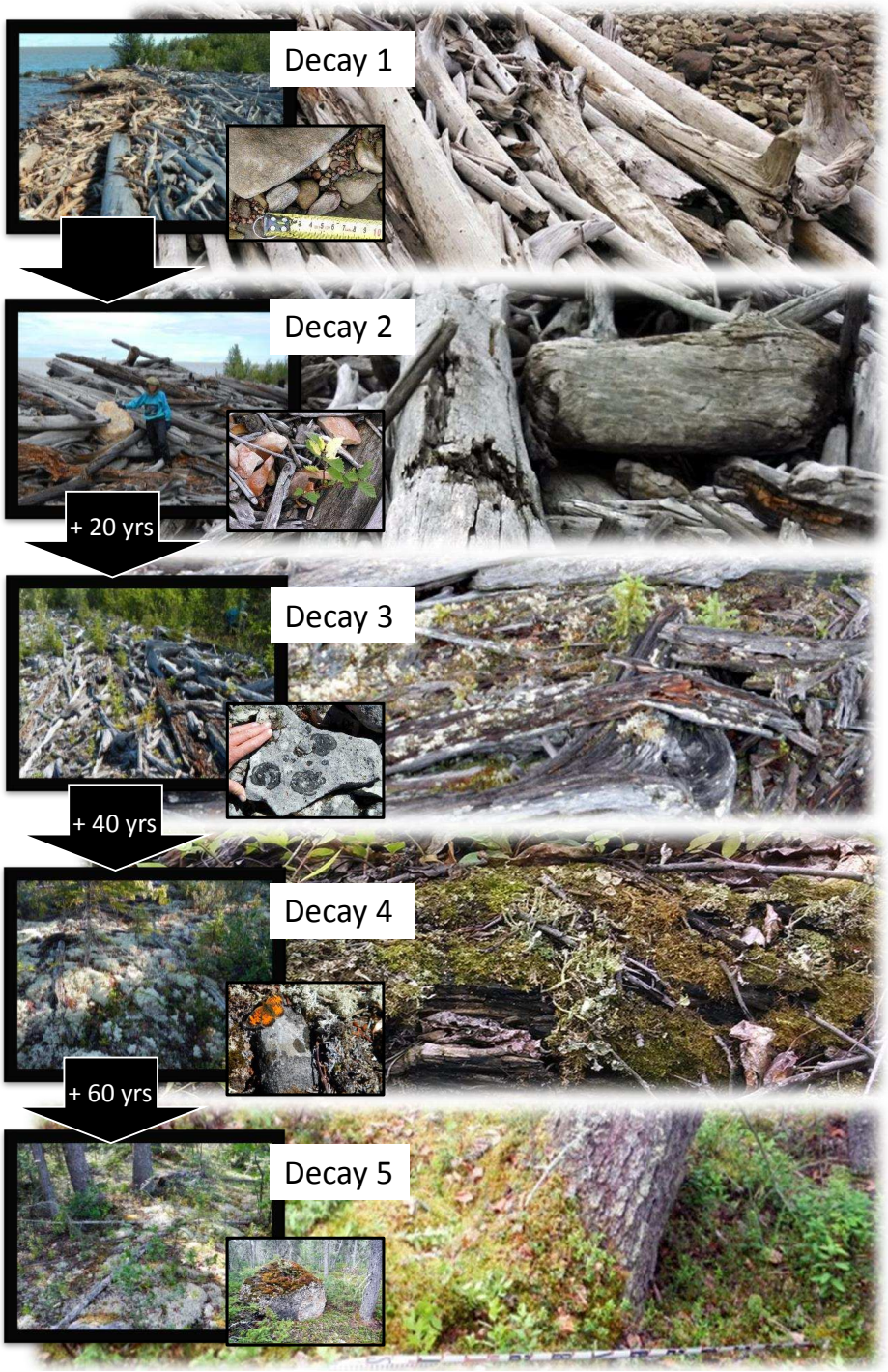

FIGURE 3.D.4. Decay classes. The background images show the conditions of logs. The leftmost image shows how the driftpiles appear in the landscape and the small inset photos show the growth of lichen, moss and other fungi on boulders and cobbles associated with each decay class.

mean years between events are similar (pvalue>0.05). Based on a rounded interquartile range for all the data, driftwood accumulates episodically about every 20-40 years (rounded to the

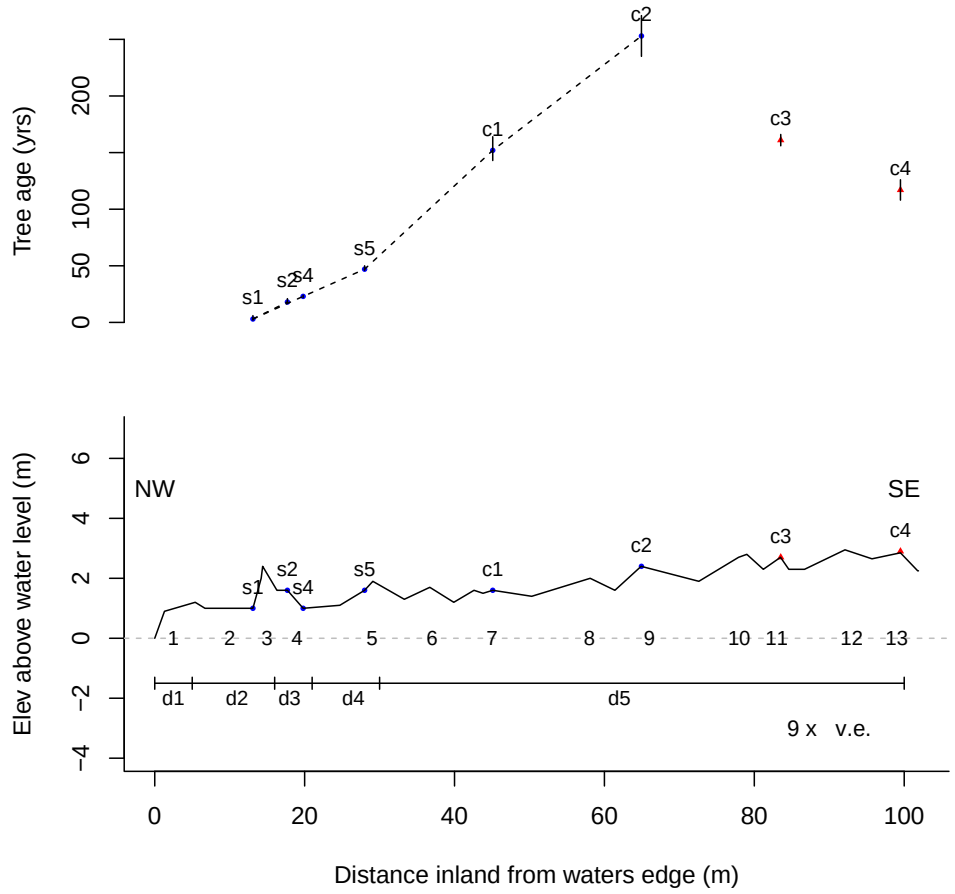

FIGURE 3.D.5. Computing rates from cores ages along transects. The top figure shows dashed lines representing rates between cores sampled along the profile "t03" (Refer to Figure 3.A.2 for the location). This transect was on a high exposure shore with a sequence of parallel berms. Due to age reversal after c2 and because c2 is near 300 years old, a recognized upper limit for the age of white spruce in forests (*Timoney and Robinson*, 1996), c3 and c4, shown in red, were discarded from the dataset. It is likely that c3 and c4 germinated within a mature forest rather than on a driftcretion. The numbers along the bottom count the number of discrete driftcretion events identified in the field based on wood or topography. The segmented bar at the bottom annotates regions of discrete decay classes (see Figure 3.D.4 for a visual guide to decay classes). The average rates between cores for this transect ranged from 0.16 m/yr (s5 to c1) to 0.34 m/yr (s4 to s5). The number of years between events ranged from 15 yrs (s1 to s2) to 52 years (s5 to c1). The distance of land accreted per event ranged from 4 m (s1 to s2) to 10 m (c1 to c2).

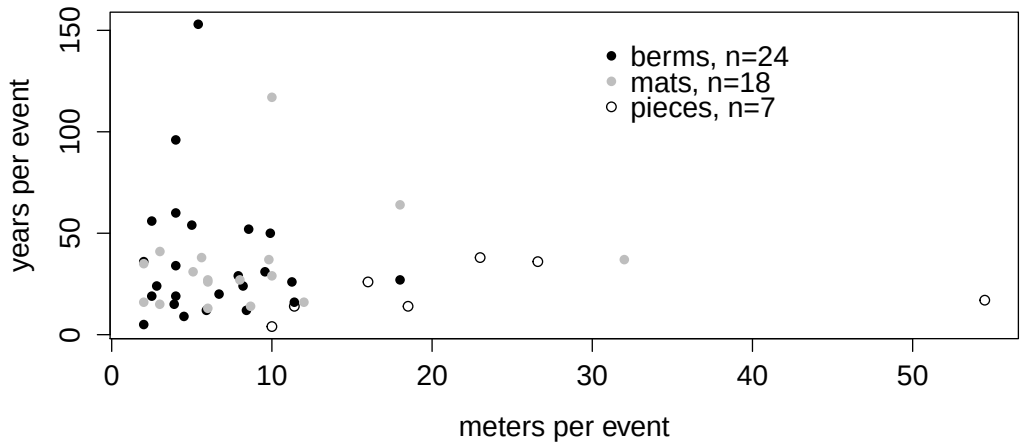

FIGURE 3.D.6. Scatterplot of rate data classified by berms, mats and pieces.

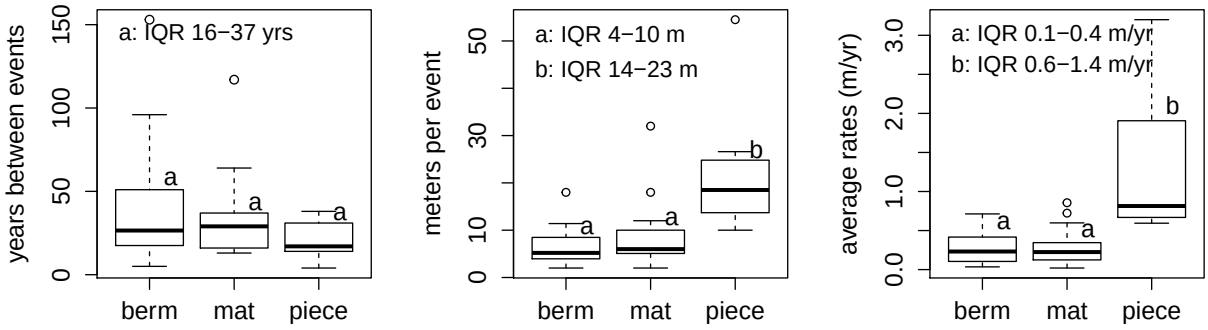

FIGURE 3.D.7. Distribution of rate data by driftcretion type. Letters denote statistically significantly different groups using pair-wise t-tests at $\alpha = 0.05$. Data from types with no statistical difference were combined and the interquartile range for each grouping is noted at the top of each graph.

nearest ten). Berms and mats accrete similar amounts of wood per event, between 4-10 m, while matrices accrete between 14-23 m. Average rates of accretion for berms and mats are lower than for matrices (0.1-0.4 m/yr compared to 0.6-1.4 m/yr).

Berms are formed with ice pushes shoreline wood up into compact linear ridges. This is a spatially and temporally discontinuous process that may not align with wood delivery, thus the time between events could be large and quite variable, which is what is shown in both Figures 3.D.6 and 3.D.7 (left). Most piece-wise matrices form in shallow embayments or between actively growing spits and the main body of land. If the embayment accumulates

enought sediment or becomes hydrologically disconnected from the main lake body, then a vast area of formerly buried driftcretions (10-50 m) may become exposed and vegetated in a short period of time, which is supported by our data.

3.D.2.3. *germination timing and variability in growth.* Most white spruce seedlings in boreal forests germinate early to mid July in hummocky litter and decaying logs *Berger* (2002). Survival through winter is greatest for seedlings rooted in logs because they provide a stable moisture supply and water temperatures and because roots become easily established in the porous structure of log. Logs also provide protections from smothering by leaf litter. Thus, the shoreline wood provide prime conditions for the establishement and survival of spruce seedlings on new driftwood mats and berms. The mature forest within 20-50m of the shoreline provides a steady source or viable seeds. Thus it is likely that a new band of spruce becomes established within 3-10 years of wood deposition.

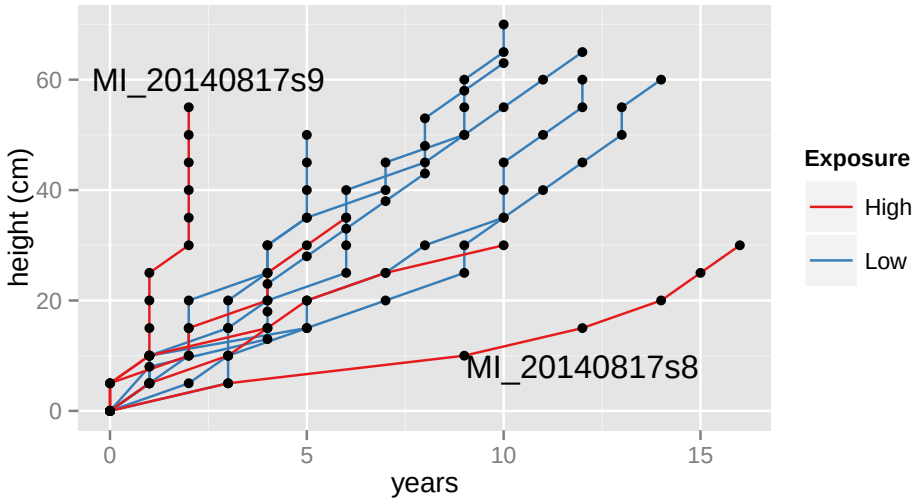

FIGURE 3.D.8. Growth trends of White Spruce on high exposure versus low exposure shorelines

We used the data from Data Set S4 (155) to investigate the impact that site exposure has on growth trends of spruce. Figure 3.D.8 plots height versus years of growth. Height is plotted on the y axis so that the growth curves easily interpretable; the steeper the curve the more height was gained per year, the flatter the curve the more stunted the upwards growth. Trees are color coded with whether they germinated along high exposure (red lines) or low

exposure (blue lines) shore. Along low exposure shores with less wind and ice disturbances, growth appears to be fairly consistent between samples while in along high exposure settings growth can be quite variable. For example MI_20140817s8 grew very quickly even though it was physcially adjacent MI_20140817s9, which grew very slowly. The explanation for this is that MI_20140817s8 germinated within the hollow of a decaying rootwad resulting in protection from wind and a ready supply of nutrients. We conclude that germination site greatly impacts growth trends on high exposure shores. The implication for our study is that on windy shores, the larges trees in a grove of similar aged trees may not be the oldest.

3.E. Datasets

All data files described here can be accessed at `http://hdl.handle.net/10217/100436`.

Data Set S1 Field measured driftwood size, explanation of variables (see section

TranID	Unique transect identifier
Dm	The median diameter in meters as an average of the small and large end diameters
L	The length excluding the rootwad

Data Set S2 Driftcretion data per sampled photograph, explanation of variables

RegionID	Unique identifer for each of the 11 regions
Photoname	Name of the photo used
Long	Longitude of photo (WGS84)
Lat	Latitude of photos (WGS84)
lineardist	The linear distance of the shoreline in m
weight	The proportion of region shoreline covered by photo (X_s/lineardist)
shoredist	The shoreline distance in m
Complexity	shoredist / linear distance
pieces	of individual logs counted
lengthpiece	the total length of individual logs counted (m)
avglog	the average length of individual logs counted (m)
matarea	the total area of mats (m^2)
bermarea	the total area of berms (m^2)
Ri	the total area per linear distance (matarea+bermarea)/lineardist

Data Set S3 Data per core, explanation of variables (See section 3.D.1 for details).

CoreID	Unique identifier for 73 cores
TranID	15 levels: Transect identifier
Type	3 levels: "berm", "mat", "piece"
X	Distance of core inland from shoreline in meters
Decay	5 levels for decay where 1 is least decayed and 5 is completely decayed.
Event	The number of discrete driftcretion events between the core location and the shoreline
yrsamp	The year the core was collected
h	The height from the ground at the location of the core in cm
d	The diameter of the tree at the height of the core in cm
age	Age estimate
ageplus	Upper bound on age estimate
ageminus	Lower bound on age estimate
germyr	Estimate of the year of germination (yrsamp+age)

Data Set S4 Spruce age-height dataset, explanatation of variables (see section 3.D.1.3 for usage).

ID	Unique identifier for 12 tree samples
exp	3 levels: "High", "Low",or "Med" shoreline exposure
h	The height in cm
d	The diameter in cm at a particular height
agech	The cored age of a tree at a particular height
yrgrowth	The year that the tree starting growing at a particular height
yrsbfr	The number of years elapsed before the tree reached a particular height
avgring	The average ring width in cm/yr at a particular height
tavgring	The average ring width in cm/yr measured at height=0

Data Set S5 Rate dataset derived from data S3, explanation of variables (See section 3.D.2.2 for usage).

CorePairs	lists which cores were compared
TranID	unique transect identifier
type	Three levels: "berm","mat","piece" based on what the tree was rooted within.
xperevent	The distance accreted per event in meters.
yrbtwnevent	The number years between events. Calculated by taking the age between two adjacent cores divided by the number of events recored between them.
rate	Average rate of driftcretion in m/yr. Calculated by taking the change in distance between two adjacent cores and dividing them by the difference in age between them.
ratemin	The lower bound for rate calculated using the largest possible difference in core ages from core age bounds.
ratemax	The lower bound for rate calculated using the smallest possible difference in core ages from core age bounds.
yrbtwneventmin	The lower bound for yrbtwnevent calculated using the largest possible difference in core ages from core age bounds.
yrbtwneventmax	The upper bound for yrbtwenevent calculated using the smallest possible difference in core ages from core age bounds.

CHAPTER 4

The Pulse of Driftwood for Multiple Timescales in a Great Northern River

Summary

In order to better plan for hazards associated with wood and to better model nutrient paths through river systems, we must have a better understanding of the processes which govern the magnitude of wood discharge during floods. This study presents a thorough and intriguing case study of large wood (>10 cm diameter and >1m length) transport on the great Slave River in northern Canada (Q=10^3 m^3s^{-1}, DA=60^5 km^2, width >300 m) with the objective to better understand the variability in pulsed wood fluxes from forested catchments with continuous recruitment processes. We use field characterization of wood, historical anecdotes, repeat aerial imagery of stored wood, and time-lapse imagery of wood in transport to assess daily to decadal variability in wood flux, identify transport thresholds and processes, and estimate recurrence intervals of massive episodic large wood floods. Pulsed wood export on the Slave River is not an artefact of episodic recruitment from major up-basin disturbances, but rather reflects decadal- to half-century-scale discharge patterns that re-distribute wood continually recruited from channel migration and bank slumping. We suggest that the multi-year flow history is of paramount importance for estimating wood flux magnitude, followed in declining importance by the yearly sequence of peaks and the magnitude and characteristics of the rising limb of individual floods. This study shows that repeat monitoring of known sites of temporary storage with new or historic imagery is a very useful tool for constraining wood flux histories.

4.1. Introduction

The processes governing recruitment, storage, and transport of large wood (*Wohl*, 2016) are referred to as wood dynamics. The main drivers behind research into wood dynamics in rivers are: to understand the role that wood plays in the ecology and health of riparian

corridors (*Harmon et al.*, 1986; *Gurnell et al.*, 2005); to understand the influence wood has on shaping the morphology and sediment regime of channels (*Keller et al.*, 1995; *Iroumé et al.*, 2010; *Wohl*, 2013b); to better constrain global biogeochemical cycles by describing how large wood influences nutrient fluxes from the land to the oceans (*Sedell et al.*, 1988; *Hilton et al.*, 2008; *Sutfin et al.*, 2016); and to predict and plan for hazards associated with wood clogging of engineered structures during debris flows and floods (*Rigon et al.*, 2012; *Ruiz-Villanueva et al.*, 2014; *Piton and Recking*, 2015). Transport processes have arguably received the least attention by river scientists compared to recruitment and storage (*Kramer and Wohl*, in review; *Wohl*, 2016).

In this paper, we assess temporal variability in driftwood flux from the Slave River, which we characterize as a great river (*Kramer and Wohl*, in review), to the Great Slave Lake. By focusing on the outlet of a large basin rather than headwater catchments, we assess the cumulative patterns of wood flux from the entire basin through time. We center our paper on understanding a wood flood (atypical massive, congested, downstream transport of floating wood) that we witnessed in 2011.

Congested wood transport occurs when input rates of wood exceed some threshold (*Braudrick et al.*, 1997; *Bertoldi et al.*, 2014) and is often directly related to episodic wood recruitment from large scale forest disturbance (*Davidson et al.*, 2015), usually due to extreme storms, tectonic activity and/or landslides and windthrow (*Phillips and Park*, 2009; *West et al.*, 2011). In large rivers, export of wood is generally assumed to occur continuously because 1. recruitment processes are continual (meandering bank failures and mortality), and 2. high discharges can easily transport all sizes of logs at a variety of flows (*Jochner et al.*, 2015).

Despite continual recruitment processes, wide channels (>200 m) and high discharges ($>10^3$ m^3s^{-1}), both the Slave and Mackenzie Rivers have event-driven export regimes (defined in *Jochner et al.* (2015) as episodic transport with continual recruitment). Although several studies allude to the importance of flow history on magnitude of wood mobilization and flux (*Johnson et al.*, 2000; *Haga et al.*, 2002; *Bertoldi et al.*, 2013; *Jochner et al.*, 2015),

this is the first study that we know of to directly address it on timescales longer than one year. There is also currently no discussion in the literature about how re-mobilization of previously recruited wood in large rivers result in congested transport. In this study we seek to answer the question: "what are the processes controlling pulsed export of large wood in rivers with continual recruitment processes?"

In order to answer this question, we explore wood transport across different timescales using a variety of methods. We use wood characterization to glean information about transport processes based on the size, type, and condition of wood. We use historical imagery and anecdotes to constrain recurrence intervals and estimate magnitude of rare, massive, wood flux events. We use repeat aerial imagery (1933-2014) of change at storage sites to assess decadal patterns of change in storage in relation to yearly peak freshets and ice jams. We use time-lapse imagery to capture wood in transport for multiple years (2012-2015) with the goal of assessing variability and defining thresholds between wood flux and discharge.

After a brief introduction to the study site (Section 4.2), we have organized this paper into four main sections: wood characterization (Section 4.3), magnitude and recurrence of wood floods (Section 4.4), decadal to seasonal patterns of wood flux (Section 4.5), and yearly to daily patterns of wood flux (Section 4.6). Detailed methods and results are included within each section. Wood characterization is presented first to provide a base understanding of wood transport and recruitment processes for the river. This is followed by progressing from our methods and results from low (decadal) to high (daily) temporal resolution and from long (half-century) to short (daily) timescales.

Unless otherwise noted, large wood is defined to be greater than 10 cm in diameter and 1 m in length. We also use the term "driftwood" as well as "large wood" (LW) because we discuss floating wood in a lake and along a very wide river that is about 15 to 30 times wider than the longest pieces of wood. In these situations, wood is drifting through the water and washing up on shorelines, thus the term driftwood is appropriate. The terms large wood and driftwood are more universally applicable to rivers and lakes than the commonly used "instream wood".

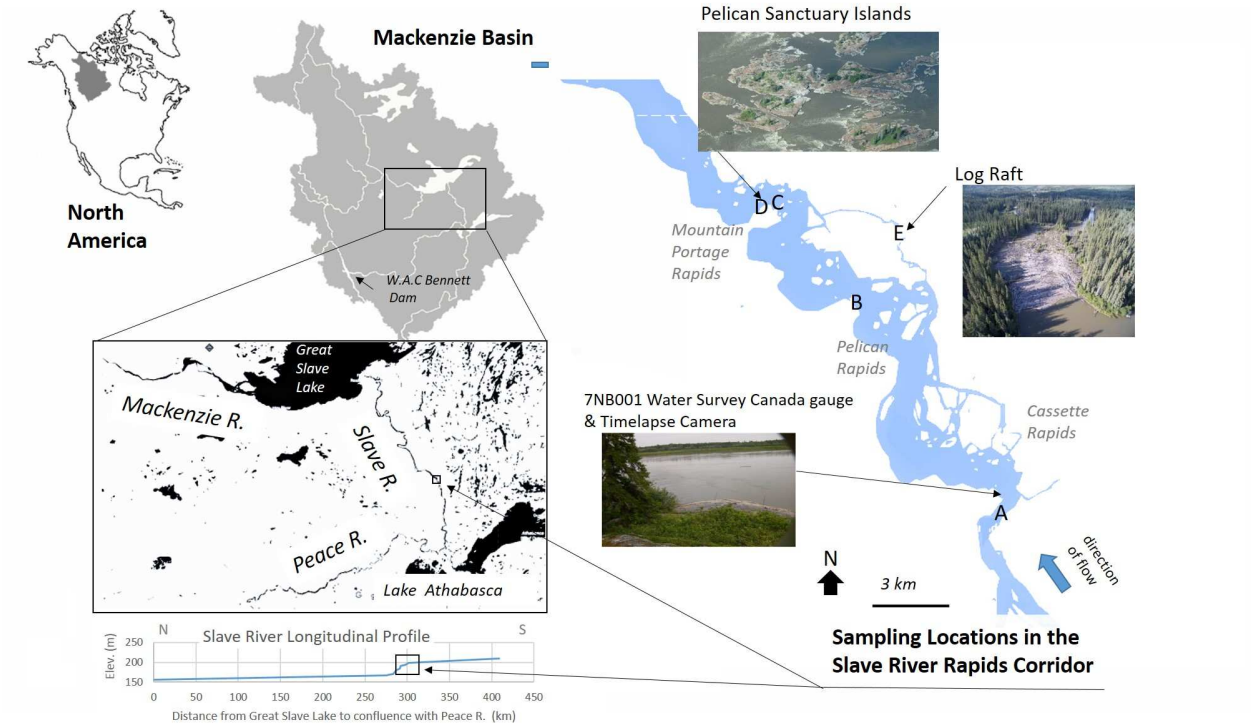

FIGURE 4.1. Study sites in the Slave River Rapids Corridor, Canada. Letters A-E correspond to location of photos in Figure 4.1.

4.2. STUDY SITE

The Slave River drains approximately 6x10^5 km^2 and connects the Peace and Athabasca rivers to the Great Slave Lake (Figure 4.1) in northern Canada. The water from the Great Slave Lake flows into the Mackenzie River and eventually out to the Arctic Ocean. Study sites were located within the Slave River Rapids Corridor, which is on the 60°N parallel on the border between Alberta and the Northwest Territories. The Slave River Rapids Corridor drops 32 m of elevation in 26 km. This is a unique stretch of river characterized by split flow and powerful hydraulics around bedrock islands of polished Canadian Shield granite. Within the corridor, there are four main sets of steep rapids split by lower gradient reaches between them. We had field sites in the three sets of upstream rapids: Mountain Portage, Pelican and Cassette (Figure 4.1).

Downstream of the rapids, the river meanders for 276 km through incised Great Slave Lake deltaic deposits that date to 8000 BP at Fort Smith (downstream end of the rapids) to 1000 BP at the start of the modern delta (*Vanderburgh and Smith*, 1988). Upstream of the

rapids, the river is fairly straight and flows north along the contact between the Canadian Shield to the east and Interior Platform sedimentary rocks to the west. Channel widths upstream and downstream from the rapids are about 500 m, whereas widths in the rapids sections widen to as much as 2000 m. Channel gradients are distinct for the three sections. The gradient is 0.1 m/km upstream of the rapids, 1.3 m/km for the rapids corridor, and 0.04 m/km downstream of the rapids (Figure 4.1).

Just upstream of Cassette rapids, Water Survey Canada has operated the "Slave River at Fitzgerald" gauging station, 7NB00l, from 1921 to present (see Figure 4.1 for location). Base flows are approximately 2000 m^3s^{-1} and summer flows commonly reach 6000 m^3s^{-1}. The Slave River freezes every winter (November) and there are generally two hydrograph peaks: the first corresponds to ice break-up (May) and the second is a freshet peak (June-July) related to runoff from snowpack and glacier melt from the southern Canadian Rockies. The highest recorded flow of 11,200 m^3s^{-1} was associated with an ice break-up event in May 1974. Ice break-up events do not occur in all years because they are dependent on river flows and the formation and location of ice jams. In recent years, ice break-up events appear to be less common (*Beltaos et al.*, 2006). As the climate warms and glaciers recede, we expect that the Slave River will start to experience more mid to late summer hydrograph peaks from large rainstorms and earlier spring melt.

In the mid-1960s, the large, earthen W.A.C. Bennet Dam was built on the Peace River approximately 1000 km upstream from the Slave River Rapids Corridor (Figure 4.1). Flow regulation from operation of the dam has greatly altered river hydrology, ice processes, and flooding on the Peace River and the Peace-Athabasca delta (*Beltaos et al.*, 2006). Impacts of flow regulation on the Slave River are buffered by discharge from the unregulated Athabasca River, but an analysis of gauge records indicates that the Slave River, since construction of the dam, has had higher baseflow, lower magnitudes for 1-20 yr recurrence intervals (Figure 4.2), decreases in break up and freshet peak magnitudes, and increases in the number of late summer secondary peaks due to releases. Several large-capacity hydropower projects are currently under negotiation and study for the Peace, Athabasca, and Slave Rivers. At the

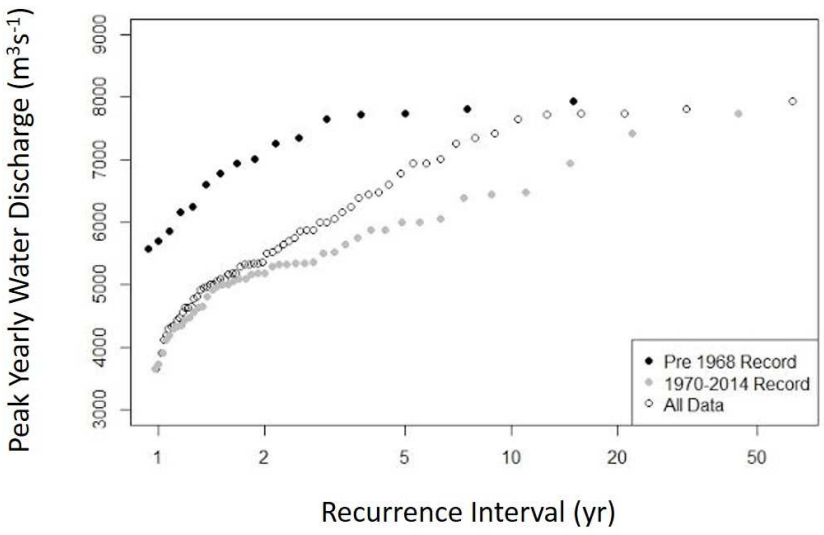

FIGURE 4.2. Recurrence interval at Fort Fitzgerald gauge, 7NB001, before and after construction of the W.A.C. Bennett Dam.

time of this study, less than <10% of the Slave River drainage is upstream of dams. Thus, our data provide a baseline for wood dynamics in a great river prior to extensive development of the river corridor because wood is not halted by reservoirs from greater than 90% of the basin area.

The Slave River is an ideal location to study the variability of wood flux through time because it has a rich history of river use for shipping and travel, the rapids contain many islands that temporarily, yet regularly, trap wood in transport, we could easily install readily accessible cameras to record the yearly movement of wood, and once delivered to the Great Slave Lake, wood is stored in age distinct accumulations that can be dated. We realized that at this location we could obtain snapshots of wood storage and transport through time at different temporal resolutions, enabling us to assess the variability and history of wood flux near the outlet of a great river.

4.3. WOOD CHARACTERIZATION

4.3.1. BACKGROUND. Most of the wood transported through the Slave River is sourced from the Peace River and deposited along the shores of Great Slave Lake (*Kindle*, 1919),

where the wood interacts with sediments and vegetation to create complex shoreline morphologies (*Kramer and Wohl*, 2015). The wood delivered to the Slave River from the Peace River basin is mostly sourced from bank failures along meander bends in the boreal plains rather than mountainous regions because the wood from the Canadian Rocky Mountains is likely trapped behind the W.A.C Bennet Dam before reaching the plains. Thus, wood dynamics on the Slave River reflect continual up-basin recruitment of wood by bank failures and lateral migration into riparian forests rather than episodic loading from landslides in mountainous regions.

Some wood is locally sourced from the boreal riparian forests along the banks of the Slave River. Recruitable trees are fairly small (<30 cm diameter) aspens, poplars, and birch (*Populus* spp.), alders (*Alnus* spp.), willows (*Salix* spp.), and white spruce (*Picea* glauca). Banks are easily erodible and there is active slumping of hillslopes that regularly recruit wood to the river. Based on our observations, trees that enter the river via bank failure or stranding of drift logs on banks by high flows appear to be routinely transported by ice jams and associated floods in subsequent years.

Field reports from the early 1900s of the Slave River upstream of the rapids note large amounts of wood sourced from banks that become caught up in vast driftwood piles on mid-river, small, bedrock knobs. If flows do not re-distribute these piles before vegetation establishes, then the piles form the nuclei for stable mid-channel islands and commonly grow to become interconnected (*Kindle*, 1919). We have seen similar driftwood-based vegetation in the steeper rapids corridor. Wood-initiated, mid-river, vegetated islands and log rafts are not unique to the Slave River. This process and resulting landforms have been well documented elsewhere on other large rivers draining forested catchments in North America, Europe, and Africa (*Hickin*, 1984; *Triska*, 1984; *Jacobson et al.*, 1999; *Gurnell and Petts*, 2002; *Collins et al.*, 2012; *Boivin et al.*, 2015).

The 2011 wood flood completely re-organized wood and deposited fresh wood accumulations in the Slave River Rapids Corridor. Figure 4.1 shows type deposition sites including

point jam, bay, raft and racked piece accumulations. In the winter of 2013, fluvially deposited wood piles from 2011 were again re-organized, this time by ice push during break up. Ice-pushed jams were usually deposited on the lee side of islands and appeared to be more densely packed and randomly oriented than fluvially deposited jams. A short video about driftwood in the Slave River and Great Slave Lake is provided as a supplemental file (*ms01_WoodResearchVideo.mp4*) and is particularly useful for gaining an appreciation for the great scale of the place, system, and processes that we describe in this paper.

4.3.2. Wood Metrics.

4.3.2.1. *Methods.* Useful information can be gained about transport processes and wood provenance by characterizing wood size and condition (*Moulin and Piégay*, 2004). We characterized the size distribution and characteristics of wood that had been transported by the 2011 wood flood by conducting line intersect transects laid across two flood deposited point jams, one raft, one racked piece accumulation, and two bay accumulations (see Figure 4.1 for representative photos and descriptions). Along most line intersects, large wood (LW) (>10 cm in diameter on the largest end and >1 m in length) that intersected the line were measured and characterized. For a smaller subset of intersects, all pieces, no matter how small were measured. The wood accumulations measured were chosen based on accessibility. Since wood characteristics are not the focus of this paper, herein we only include basic results on wood size for ease of comparison with other studies and insights into wood provenance and transport history gleaned from wood type and condition. A more complete description of methods and thorough analysis of the data for all wood metric surveys are supplied in the Supporting information for this chapter (page 188).

4.3.2.2. *Results.* For ease of comparision with other studies, we summarize basic basin, river and wood characteristics in Table 4.1. Large wood measured from line intersect surveys (n=187) had a mean length of 6.1 m with a standard deviation of 4.4 m, a median of 4.7 m and a maximum of 19.4 m. Representative diameters (average of end diameters) had a mean of 0.21 m with a standard deviation of 0.11 m, a median of 0.18 m, and a maximum of 0.7 m. We found that point accumulations were enriched in shorter pieces and had a significantly

FIGURE 4.1. Wood accumulations in the Slave River Rapids Corridor resulting from the 2011 wood flood. Arrows denote general direction of flow. A: Photo of congested wood transport during the wood flood taken with a wide angle lens at Fort Fitzgerald; discharge=7,200 $m^3 s^{-1}$, channel width=500 m. B: This point jam was one of the largest jams that was deposited during the three-day wood flood. By 2013, the point jam was mostly gone, scraped clean by ice break ups. C: Typically, bays collect very large rootwads and numerous small wood pieces, such as bark and small branches, whereas point jams collect more mid-size pieces. C: This photo of racked pieces shows split flow around bedrock islands typical of the river (upstream flow width=60 m) which, at this location, is just a fraction of the 1000 m wide river. D. The dashed yellow line on the raft indicates new wood delivered in 2011 to a small side channel, east of Pelican Rapids, channel width=50 m. Locations of photos are marked by letter on Figure 4.1.

TABLE 4.1. Site and wood characteristics summary

Site Characteristics	
Latitude	60 deg N
Elevation	$\sim$ 200 m asl
Drainage Area	6x10^5 km^2
Gradient	$0.04 - 1.3$ m km^{-1}
Discharge	2000-11,200 m^3 s^{-1}
Magnitude RI $_{1.2yr}$[a]	$\sim$ 4200 m^3 s^{-1}
LW Size : mean, sd, med, max	
Length (m)	7.4, 5, 6.1,19.4
Diameter (m)	0.23, 0.12, 0.21, 0.7
Coniferous V_r^{*b} (m^3)	1.2, 1.3, 0.8, 7
Deciduous V_r^{*b} (m^3)	0.9, 1.2, 0.4, 5
LW type and condition	
%Coniferous: Deciduous[c]	58:42
%Coniferous: Deciduous[d]	42:58
%Sound:Decay	84:16
%No Bark: Bark Present	81:19
%Abraded: Limited Abrasion	94:6
%Beaver Chew	5
%Rootwads	32

a. RI is recurrence interval. This value reflects yearly recurrence interval post-dam. See Figure 4.2

b. V_r^* is the air-wood rootwad volume which is the volume of a box that completely encloses the rootwad (*Thevenet et al.*, 1998)

c.proportions based on all pieces surveyed.

d.proportions based on only pieces with rootwads and may more accurately represent recruitment because deciduous are more likely to break and contribute more large pieces per tree to overall wood loads.

different size distribution than all other accumulation sites (Supporting section 4.A, Figures 4.A.1 and 4.A.2, Table 4.A.3). We attribute this to preferential trapping of smaller pieces on point jams. Thus, data from log rafts, bays and racked accumulations are likely more representative of the size of wood in transport than wood in point accumulations. When point jam data is extracted from the dataset, mean and median lengths increase by about 1 m and mean and median diameters by about 2 cm. Without the point jam data, mean wood length is 7.4 m with a standard deviation of 5 m and a median wood length of 6.1 m; mean diameter is 0.23 m with a standard deviation of 0.12 m and median diameter of 0.21 m.

Based on proportions of wood as bark, small wood (length <1 m or diam <10 cm), medium LW, and large LW (length $\geq$3 m and diam $\geq$0.23) measured along a complete line intersect survey in a bay, we estimate that the Slave River carries 2680 pieces of bark

per 407 pieces of small wood per six pieces of medium LW per 1 piece of large LW (see Supporting section 4.A for explanation of estimates and Supporting Figures 4.A.1-4.A.3 and Tables 4.A.3-4.A.4 for size distributions and summaries by size class). Further work should be conducted to more precisely and accurately constrain distributions of wood size that include small wood. If this is done then, it becomes possible to better understand how fluvial processes impact size distributions by comparing in stream wood size distributions to riparian tree distributions, as suggested by *Turowski et al.* (2013).

The bulk of LW pieces on the Slave River are smooth boles with no bark and sound wood (Supporting Section 4.A, Figure 4.A.4, Table 4.A.5). Overall, 84% of wood is sound compared to 16% decayed; 19% of wood contains bark versus 81% with no bark; and 6% of wood shows limited abrasion whereas 94% of pieces are abraded. This indicates that wood in transport has travelled long distances (highly abraded), has spent time in the water (no bark), but has not spent a long time rotting in place on floodplains (sound wood rather than decayed). A high percentage (35%) of wood contained rootwads, confirming that recruitment is likely dominated by bank erosion.

About 5% of LW wood from line intersect surveys is beaver chew. There were no large differences in wood condition between coniferous and deciduous trees. We also found that deciduous trees enrich size distributions with smaller lengths of wood, most likely because they contribute greater quantities of larger snapped off branches than coniferous trees. When all the data is considered, 58% are deciduous and 42% are coniferous. However, if we select the data to include only trunks with rootwads, the percentages reverse to 42% deciduous and 58% coniferous. Further analysis of rootwad size and shape is provided in Supporting Section 4.A, Figures 4.A.5 and 4.A.6, and Tables 4.A.6 and 4.A.7.

4.4. Magnitude and Recurrence of Wood Floods

4.4.1. The 2011 Wood Flood. The wood flood we witnessed on the Slave River in 2011 was a swath of congested wood transport about 20-100 m wide that lasted 3 days. It looked like one long, continuous snake of driftwood moving down river. Uncongested

transport continued for weeks afterward. The scale of wood movement downstream was impressive and strikingly similar (albeit smaller) to a 1919 wood flood described by *E.M. Kindle* (1921) on the Mackenzie River:

> "The immense volume of this floating mass of travel-scarred tree trunks and forest debris greatly exceeded anything seen or imagined. In general it formed a nearly continuous mass of a mile or more in width...Walking over this driftwood was often more feasible than canoeing through it... The closely packed phase of this particular exodus occupied about four days in passing a given point. (53)"

The water discharge during the 2011 wood flood was about 7,200 m^3s^{-1}. Flow depths at the Fort Fitzgerald gauge (Figure 4.1) range from 8-12 m and channel width is close to 400 m. Using an estimate for cross-sectional area of 4000 m^2, the mean velocity during the flood was about 1.8 m/s. This matches well with surveyed ranges of surface velocities at lower discharges at the gauging station from 0.2 m/s at the banks to about 2 m/s in the thalweg (Water Survey Canada, pers. communication G. Lennie, July 2013). If we assume complete congestion of a 50-m-swath of logs 0.15 m thick (median diameter of all large wood measured in this study) moving at 1.8 m/s, then the wood discharge rate was 20 m^3/s^{-1}. This amounts to 5x10^6 m^3 of wood transported by the river over the three days and 2x10^6 m^3 over one day. In addition to this volume, there was also sparse transport of wood for weeks after the main body had passed. After conducting an uncertainty analysis by adjusting the width, thickness, and velocity, we consistently estimate 3-day flux volumes over 10^6 m^3. This is 10^4 times the 492 $\pm$ 120 m^3 total seasonal background flux volume estimated for same location between July 13th and August 13th in 2012 (*Kramer and Wohl*, 2014).

When delivered to the Slave River Delta, the wood from the 2011 event completely clogged the Nagle distributary channel and boat launch (Supporting Figure 4.B.1). Residents of Fort Resolution who regularly use this channel for travel spent several days clearing the wood. Failure to clear this channel would have likely caused avulsion and re-positioning of the channel. Much of the wood in 2011 was delivered to the delta front in massive mats and large driftwood berms (Supporting Figure 4.B.1). Succession of driftwood deposits from large wood floods like 2011 are a primary driver of outer deltaic morphology and vegetative

patterns (*Kramer and Wohl*, 2015). Tree core dates growing out of drift piles suggests that discrete driftwood berms are deposited every 30-50 years (*Kramer and Wohl*, 2015).

4.4.2. A Historical Perspective. In a write-up of a field excursion in 1917, *Kindle* (1919) writes "there is probably no lake in North America which receives anything like the amount of driftwood which is poured into the Great Slave Lake, chiefly through the Slave River" (pg 358).

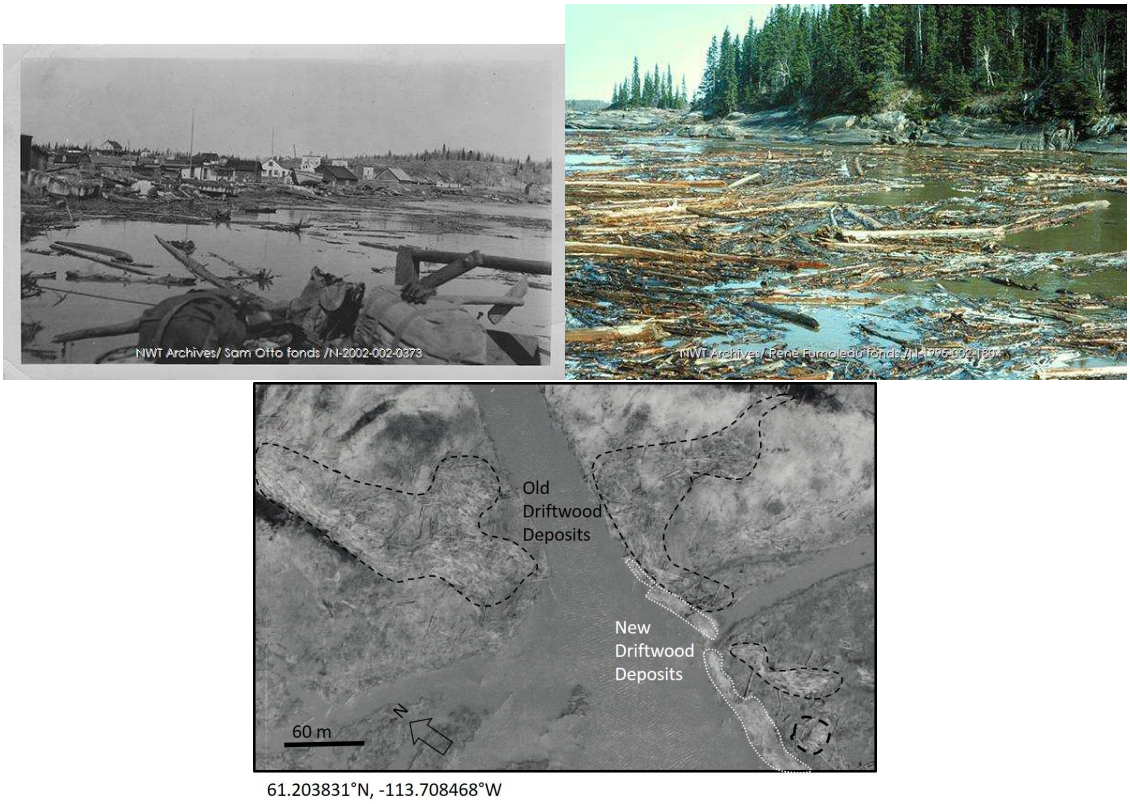

Figure 4.1. Historic photos of wood transport. Photos are from the NWT archives http://www.nwtarchives.ca/. Left: River driftwood at Fort Fitzgerald upstream of the rapids, photo by Sam Otto Fonds, accession number N-2002-002, item number 0373. Right: River driftwood at the bottom of Mountain Portage rapids, photo by Rene Fumoleau Fonds, accession number N-1995-002-1804. Bottom: Driftwood deposits in the Slave River delta, May 29, 1972. National Air Photo Library (NAPL) Roll #A22708, photo #20

To gain a sense of the recurrence interval for wood floods, we spoke with local residents of Fort Smith and Fort Fitzgerald and searched historic archives for evidence of past wood floods. Many residents expressed that the event in 2011 was unique in their experience. Some

residents who frequent the river mentioned that driftwood is common every year, especially near ice break up, but the magnitude and late summer timing of the event in 2011 was unusual. After a search of the NWT Archives (`http://www.nwtarchives.ca/`), we found photographs of congested wood transport in 1933 and in 1975 (Figure 4.1-Top). Wood floods appear to be important recurring events on the Slave River. Historic air photos of the Slave River delta in 1972 show distinct new and old wood deposits on the delta front (Figure 4.1-Bottom).

4.4.3. Log Raft - Evidence for Recurring Wood Floods.

4.4.3.1. *Methods.* In August 2015, we visited a log raft clogging a side channel in the Slave River Rapids Corridor (located at 59.95530°N -111.65456°W and annotated on Figure 4.1. Additional photos of the raft are presented (Supporting Figure 4.C.1). This same log raft is mentioned in Alexander Mackenzie's journals circa 1789 during his quest to find a route to the Western Ocean through Canada (*Mackenzie*, 1793). We hypothesized that the position of the front of the raft was migrating upstream with episodic forward growth due to additions from wood floods such as the one in 2011. To test this hypothesis, we gathered as many historic aerial photographs of the raft as possible and mapped the progression of the jam front. A photomosaic of aerial photos used in the analysis (Supporting Figure 4.C.2) and table with source information for each air photo (Supporting Table 4.C.1) are presented in the Supporting Section 4.C.

We georectified each photo in ArcGIS (v 10.3.1) to a 2004 Google Earth screen capture with first-order polynomial transformations. Residual error for tie points was <7 m. The average residual error was about 2% of the total length under study and is smaller than distance gained from episodic large additions to the front of the raft (45 to 143 m). We measured the distance along the center of the channel between two adjacent time periods. A negative distance is recession of the log front downstream and a positive distance is advancement of the log front upstream. In 1930, the log raft was split into a primary jam and a secondary jam farther upstream. Therefore for 1930, we measured from the front of the primary, downstream jam.

4.4.3.2. *Results.* Between 1930 and 2015, the log front progressed a total of 260 ± 5 m upstream (Figure 4.2). This progression upriver is not uniform in time. Three large advances of 98 m, 143 m, and 45 m occurred during 1930-1950, 1950-1966, and 2004-2013, respectively. One minor advance of 19 m occurred between 1982-1991. The jam advance between 2004 and 2013 was due to the 2011 wood flood. Although we do not have the temporal resolution to constrain exactly when jam advances occurred between 1930-1950 and between 1950-1966, jam progression upstream was probably caused by episodic wood floods like 2011, rather than continuous additions. Since there were three large advances in a the 82 year study period, we estimate a wood flood recurrence interval of 27 years, which is close to the 30-50 year recurrence interval estimate for wood floods based on dates of vegetated driftwood deposits along the margins of the Great Slave Lake (*Kramer and Wohl*, 2015).

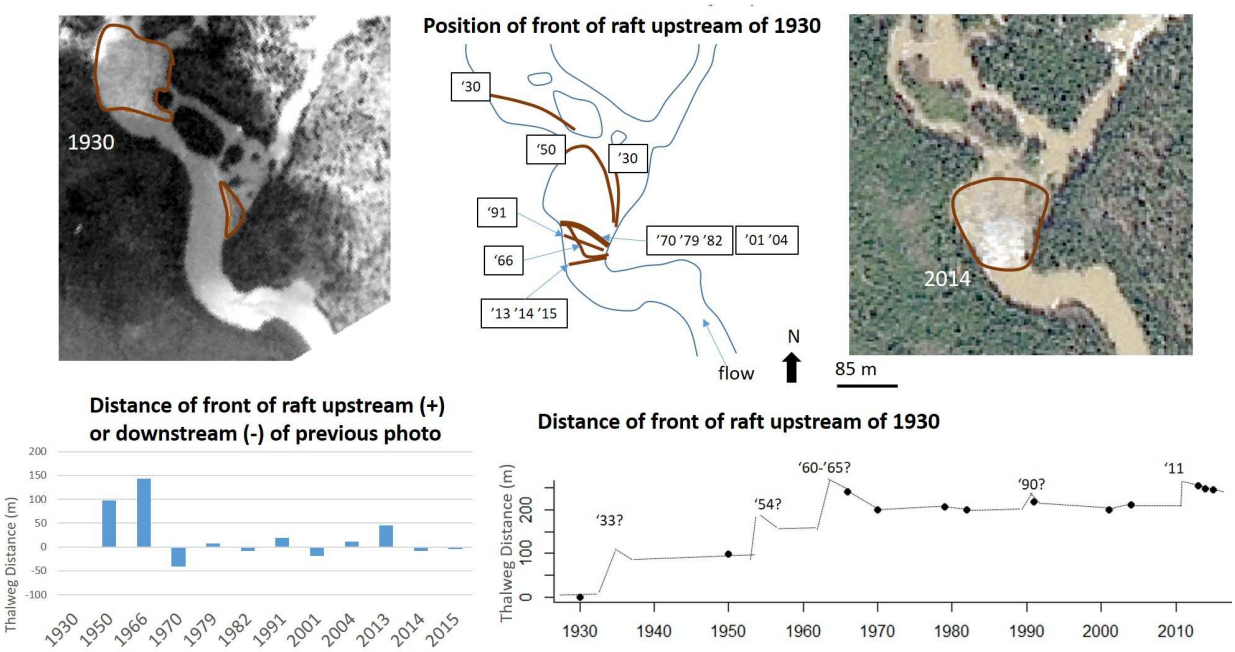

FIGURE 4.2. Log raft evolution from 1930 to 2015.

The newer deposits of driftwood deposited on the Slave River delta front in 1972 (Figure 4.1-Bottom) are likely associated with a wood event recorded by advance of the log raft between 1950 and 1966 (Figure 4.2). The older piles are likely associated with one or multiple wood events between 1930 and 1950. The 1933 event captured in historic imagery (Figure

4.1) could correlate with the advance of the front of the log raft between 1930 and 1950 (Figure 4.2) and the older driftwood deposits in the 1972 photo of the delta front (Figure 4.1-Bottom).

There is not a corresponding increase in the raft front related to the historic photo from 1975 (Figure 4.1). There could be at least three reasons for this. First, the wood captured on camera could be local re-mobilization of de-stabilized wood by ice push and ice jam flooding in 1974 (the highest recorded discharge on record) rather than regional transport of new wood coming from upstream. Second, we only analyzed the log raft in 1970 and again in 1979, so we may have missed changes to the log front in the middle of the decade. Third, it could be that the 1975 photo date is in error.

We have depicted a stepped progression for the jam in Figure 4.2 that is representative of the episodic process of infrequent wood events causing sudden raft progression upstream. We have placed hypothetical wood events at 1933, 1954, 1960, and 1990 and a known wood event in 2011. We placed a wood event at 1933 because a historic photo shows wood in transport during this date. We chose 1954 because this was a high water year, coupled with evidence from the Great Slave Lake that large amounts of drift piles germinated in the early 1950s (*Kramer and Wohl*, 2015). We chose 1960 because this was the first year of high flows after five years of a decreasing pattern of flows similar to the pattern preceding 2011 (see section 4.5). The minor jam advance in 1991 was likely caused by a wood event in 1990, which was a year with a flashy breakup preceded by lower water years.

Large raft advances are usually followed by smaller raft recession. Between 1950 and 1966, the raft grew the most and part of the front was even with the 2015 raft front. But, by 1970, just four years later, the raft front had receded downstream 41 m. This pattern of large advance followed by smaller scale recession is caused by bank erosion expanding the width of the channel as well as compaction of the raft in years following wood delivery.

In general, the average rate of raft progression was much faster prior to construction of the W.A.C Bennett Dam (7 m/yr compared to 1 m/yr). Also, the stasis of the jam from 1970 to 1990 corresponds with the period of lower wood storage noted on the Pelican Islands

from 1983-1990 (see Section 4.5). Thus, there was less wood in transport during this time period, which may reflect blockage of wood from the mountainous regions of the catchment by the dam, or could be part of the natural variability in wood fluxes on longer timescales than covered by our data.

4.5. Decadal to Seasonal Patterns of Wood Flux

4.5.1. Methods. In order to relate wood flux to flow history, we graphically compared change in storage of wood on mid-channel islands to patterns of flow and discharge magnitudes on decadal and seasonal timeframes. We used 30 years of repeat photographs of the Pelican Sanctuary islands (59.97116°N, 111.74853°W) and records from the Fort Fitzgerald gauge (7NB001, Water Survey Canada, 59.868923°N 111.582301°W) to compare change in wood storage to highest recorded discharge between photos. We hypothesized that higher peak discharges would relate to greater changes in wood storage on the islands. Figure 4.1 annotates the general location of the islands and gauge. A more detailed inset location image with photos of the islands and gauge are provided in Supporting Figures 4.D.1 and 4.E.1.

We obtained the historical aerial photo record of the islands from the Pelican Advisory Circle, a local citizens group that has been monitoring a White Pelican colony continually since 1975 to assess number of nests and chick survival rates. Photos were taken obliquely by pointing a camera outside a window of a fixed wing aircraft two to four times each summer. Flights were, and still are, funded by Environment Natural Resources, Government of Canada. Due to a lack of overview photos that cover the entire set of islands prior to 1983, we only used photos from 1983-2014. Prior to 2005, photos were stored on slides, whereas from 2005-2014 photos were stored digitally. We were only able to obtain low resolution scans of the pre 2005 slides (<800 pixels per side). We obtained high resolution copies of the digital images (>3000 pixels per side).

The photographs were georectified using spline transformations with greater than 50 tie points per image. High resolution images were then brought into eCognition and segmented, wood was semi-manually classified, and wood polygons were exported as shapefiles. Low

resolution images did not segment well and so were brought straight into ArcGIS where polygons were drawn around wood manually using the ArcEditor toolset. A more thorough description of how the images were prepared for analysis is provided in Supporting Section 4.D. The supplemental digital file (*ms02_PIanimation_2fps.avi*) is an animation of the entire resulting dataset through time.

We analyzed shapefiles of wood areas in ArcGIS in two different ways; we analyzed change within the same common area between all the photos from 1983 to 2014 (Dataset 1, *ds05_D1areas.csv*) and we analyzed the change between adjacent photos in time from 1988-2014 (Dataset 2, *ds06_D2change.csv*). Dataset 2 was subset to start in 1988 rather than 1983 due to many missing adjacent timeframes from inadequate coverage of the islands prior to 1988. For Dataset 1, we simply summed the total area of wood within the common area of interest for all photos. For Dataset 2, we estimated areas of wood that overlapped in adjacent photos ("stayed"), that were present in the second photo but not the first ("came"), and that were present in the first photo but not the second ("went"). Fractions were then calculated for each time period as each category divided by the total amount of wood that passed through storage in the interval (came+went+stayed). For example, fraction of wood that stayed equals stayed/(came+went+stayed). The highest peak discharge within the time period under scrutiny was extracted from the discharge records for comparison. See Figure S11 for flow chart of methods and example datasets.

We used Dataset 1 to graphically assess the change absolute total area of wood through time, which enabled us to identify timeframes when wood was accumulating on the islands versus when it was being removed. We used Dataset 2 to investigate inter- and intra- annual variability in wood imports versus exports and to identify patterns and thresholds for wood change in relation to discharge. Because of the unique, high temporal resolution of these repeat photographs (two to four photos per summer for 30 years), we were also able to assess the relative influence of ice jam flooding compared to freshet flooding on wood storage.

4.5.2. Results. To test our hypothesis that the amount of change in storage increases with increasing discharge, we plotted the fractions of wood that came, went, or stayed from

Dataset 1 against discharge and visually assessed relationships. There is clear threshold behavior between change in storage and discharge (dashed line on Figure 4.1). Less than 50% of wood changes position below 4200 m^3s^{-1}. For discharge above this transport threshold, there is a linearly increasing threshold for maximum amount of change up to around 6800 m^3s^{-1}, when a trapping limit is reached as the islands become flooded. However, underneath the stepped upper threshold for amount of change possible (dashed line on Figure 4.1), there is great variability and higher discharges do not always equate with greater amounts of change. There are many events that experience high flows, but wood is not changing position very much. There is also evenly dispersed scatter in the amount of wood that either went or came. No pattern between discharge and type of change indicates that import and export of stored wood are equally likely at all flows.

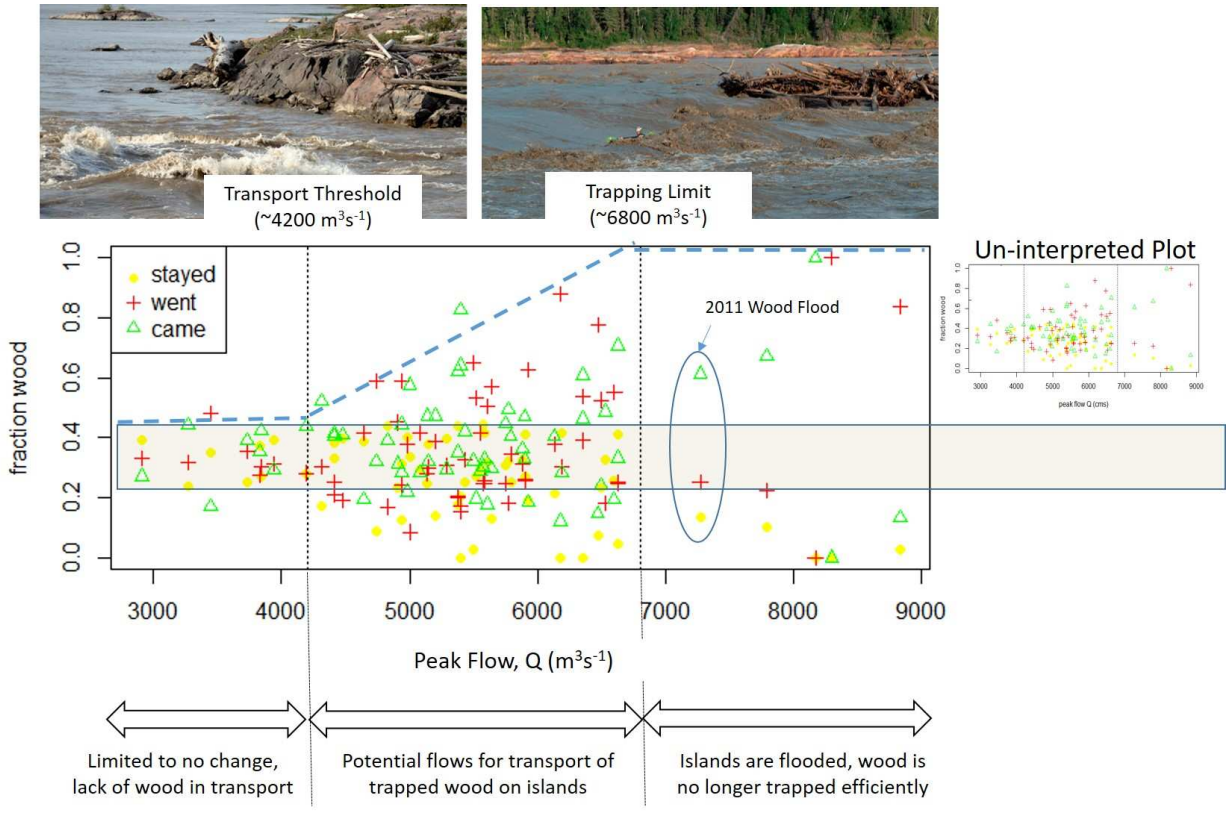

FIGURE 4.1. Flow thresholds for change in storage on the Pelican Islands. High values of wood that stayed indicate little to no change on the islands.

When interpreting fraction wood values in Figure 4.1, it is important to recognize that because it was impossible to line up wood polygons exactly between years (due to the obliquity and variability in the source photographs), the dataset contains noise. For example, a piece that should be 100% stationary based on visual inspection of location on photographs will always have some portion of its area that came or went due to slight mis-alignments and slightly different shapes (see example in Supporting Figure 4.D.3). The error is greatest only for years with little to no change. To constrain this noise for years with little change, we have interpreted Figure 4.1 to include a band to indicate events that have limited impact on wood storage. The band was defined from 0.2-0.4, based on a consistent upper threshold for highest fractions stayed, the lower data limit for fractions less than the transport threshold, and visual inspections of photographs.

In order to assess how patterns in yearly and decadal hydrograph regimes might impact storage, we plotted the summer (April through September) hydrographs against total wood in storage through time (Dataset 1) and fractions of change in storage between adjacent time periods (Dataset 2) (Figure 4.2). The islands fluctuate between low, moderate, and high wood loads on a decadal time scale (6-12) years (Figure 4.2-A).

Flows between 1983 and 1990 were consistently between the transport threshold and trapping limit. Thus, despite some data gaps, we think that wood in storage was likely in equilibrium at the moderate levels, as bracketed by the 1983 and 1988 data. In 1990, water levels spiked well above the 6800 m^3s^{-1} trapping limit, which resulted in clearing the islands of wood (Figure 4.2-B). Wood levels remained in a low equilibrium for about one decade until 2001, when late summer freshets peaked just below the trapping limit and re-loaded the islands. Flows then again hovered at or under the transport threshold for the next five years and wood slowly accumulated until 2007, when ice break up flows rose to just below the trapping limit and flushed wood from the islands, setting wood loads back to moderate levels. Rather than staying in equilibrium, wood loads from 2007 to 2014 have fluctuated.

A four-year-hydrograph sequence with each year peaking just below the year before occurred from 2007-2010. Wood loads responded by increasing each year as new wood was

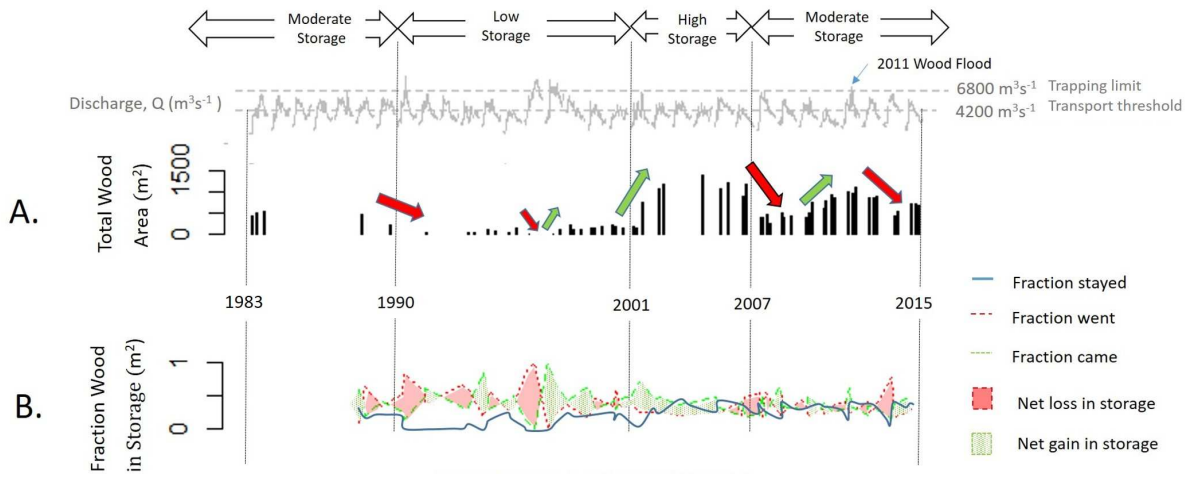

FIGURE 4.2. Decadal patterns in wood storage. Only summer flows (April-Sept) are shown A. Plots of volume of total wood stored within a common area (Dataset 1) from 1983 to 2014. Bars are located at photo date. All photos had wood in them except for 1996, when no wood was present. Arrows indicate general periods of wood loading. B. Lines represent the fraction of wood in storage (Dataset 2) that came (green small dashed line), went (red long dashed line) or stayed (solid blue line). Regions that are shaded with stippled green indicate periods when more wood was recruited than exported, whereas regions shaded solid red indicate periods when more wood was exported than recruited. Sharp downward spikes in fraction stayed indicate time periods with large changes in storage. There were large proportions of change between 1990 and 2001 due to the extremely low wood loads, making it possible for a few pieces to greatly impact the fractions that went, stayed, or came.

deposited at lower elevations than the prior year (Figure 4.2-A). River levels during 2010 were record setting lows. In 2011, the year of the wood flood, the levels spiked in a late summer freshet to above the trapping limit for the first time in 14 years. The combination of the prior four years of decreasing flows that loaded banks and islands with wood, along with the high flows, probably precipitated the wood flood.

What is interesting is that, despite high volumes of wood moving down the river, there was only a slight increase in total wood storage after the flood (Figure 4.2-A). This is probably because high amounts of wood were already in storage on the island before the flood and the wood that was there may have simply been replaced, resulting in little net change. Supporting Figure 4.D.4 shows distribution of wood on the islands before and after the 2011 wood flood. The sharp downward spike in wood that stayed (Figure 4.2-B) in 2011 supports the idea that, while there was little net change in total stored area 4.2-A), there

were large changes in the positioning of wood, with overall net gain of new pieces in new places (Figure 4.2-B). In the two years following the wood flood, there have been ice jamming and flooding, which have flushed wood from the islands and decreased wood loads (a field observation supported by Figure 4.2).

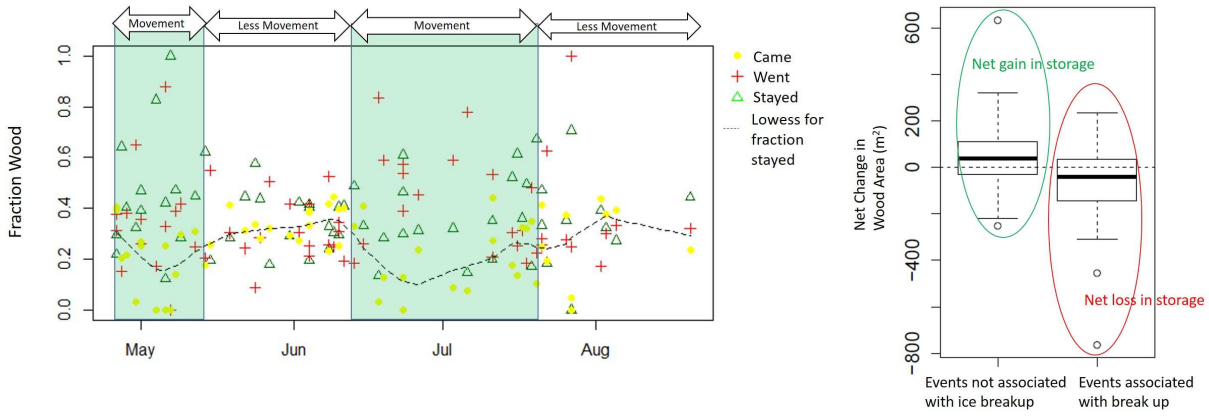

FIGURE 4.3. Seasonal patterns in wood storage. Left: Low values of fraction stayed and separation between fraction stayed and the rest of the data indicate timeframes of greater change. Right: Flushing versus storage for ice break up and freshet events. After conducting one sample, one sided t-tests, we are 90% confident that the mean change in storage is less than zero for ice break up (n=18, pval=0.10) and greater than zero for freshet peaks (n=35, pval=0.04)

Thus, wood floods are not just associated with high magnitude flows, but are highly dependent on the magnitude of wood in storage preceding the event. This is highlighted by the fact that, although 1996 and 1997 were two years of exceptionally high flows, they occurred in years with low wood storage, and no wood floods are associated with these years in historical documents, the log raft or the memory of local people.

Whether high flows tend to reduce or build wood storage is partly dependent on the type of high flow. Patterns of change by month (Figure 4.3-Left) show that change in storage on the islands occurs either in late April to mid-May in association with ice break up, or mid-June to early July in association with spring freshet. Although there is some variability, on average, flashier ice break up events tend to flush wood, resulting in loss of wood in storage, whereas later summer freshets tend to build wood in storage (Figure 4.3-Right).

4.6.0.1. *Methods.* A Brinno TLC200 camera was installed next to the Slave River at Fitzgerald gauge 7NB001 (located at 59.868923°N 111.582301°W and annotated on Figure 4.1). Following methods from *Kramer and Wohl* (2014), we collected photos of the river every 10 minutes from April through August in 2013 and 2014. Images are stored as a video file and frames were extracted for periods when wood was present. The camera was placed on the outside of a bend and most wood was carried within 100 m of the camera (*Kramer and Wohl*, 2014). The extracted images were 96 dpi (1268 x 760 pixels). Images were categorized as congested transport, clumped transport, or sparse transport. Sparse transport was defined as one to several pieces of wood that could be counted at a glance. Clumped transport was defined to be more than a few pieces, commonly with groupings of two or more pieces touching. Congested transport was large amounts of wood jumbled together such that it would be very difficult to count all the pieces.

Again following methods from *Kramer and Wohl* (2015), we estimated the proportion of photos from one day that contained floating wood ($\hat{p}$). Thus, $\hat{p} = 1$ means that there is wood floating past the camera 100% of the day, whereas as $\hat{p} = 0$ means that no wood passed the camera that day. There are several advantages to using $\hat{p}$ to characterize wood flux. It avoids uncertainty from wood volume estimates due to flotation depth and estimating sizes at variable distances in the frame of view. It is quick to obtain. And, it allows for an estimate of wood flux to incorporate data periods with missing samples, such as night. Although we did not estimate flux volumes, estimates of $\hat{p}$ were proved useful for comparing basic shapes and patterns of wood flux to water discharge.

In addition to the 2013 and 2014 data, we also included in our analysis July 13-August 13, 2012 data from *Kramer and Wohl* (2014) as well as estimates of $\hat{p} = 1$ for July 16-18, 2011, which correspond to the wood flood. We conducted a graphical analysis of $\hat{p}$ relative to daily discharge and yearly hydrographs. Raw time-lapse data can be accesses at `https://dspace.library.colostate.edu/handle/10217/100436`. Derived datasets are provided as Supporting digital file *ds07_FFwoodphyatQ.csv*

4.6.0.2. *Results.* We compared wood flux ($\hat{p}$) to water discharge for 2011 through 2014 (Figure 4.1). Although we did not take any photos for 2011, we marked $\hat{p} = 1$ for the three-day wood flood (July 16-18). Within a year, wood peaks generally correspond with hydrograph peaks. Wood flux only reaches above $\hat{p} = 0.5$ for rapid and large changes in discharge (increases of about 2000 m^3s^{-1} within a few days). Although these larger events usually occur in May due to ice jamming, as in 2013 and 2014, they can also happen later in the summer due to rapid melt of heavy snowmelt, torrential up-basin rainstorms, or large releases from the W.A.C. Bennet Dam (1996).

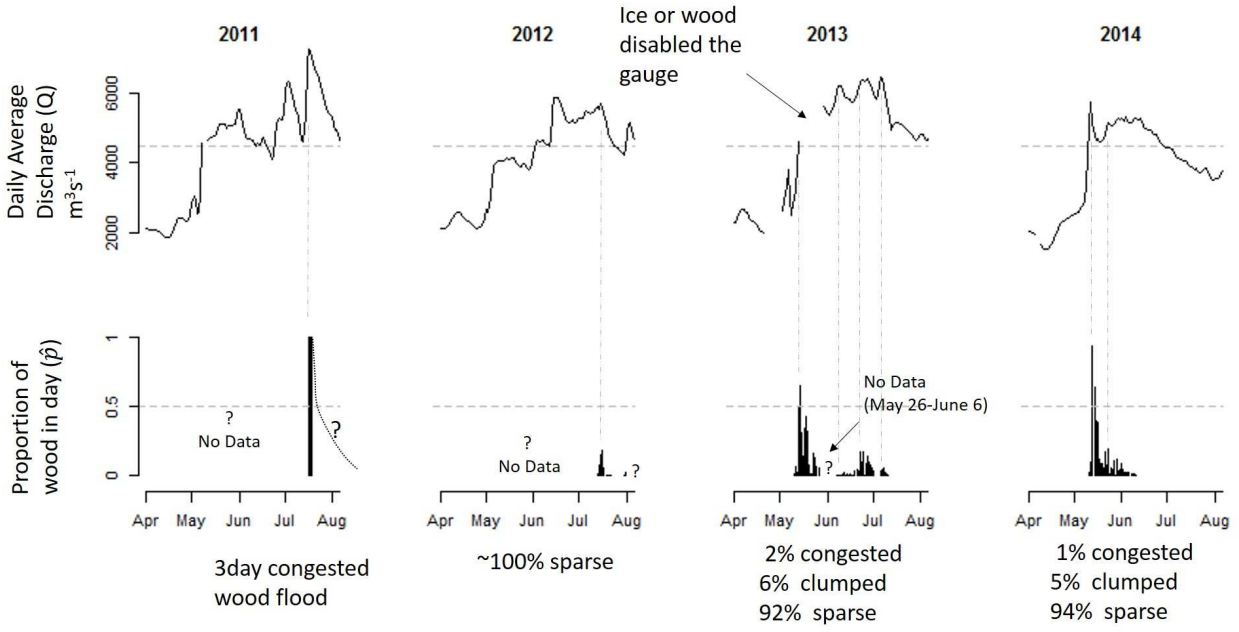

FIGURE 4.1. Wood discharge compared to water discharge 2011-2014. 2012 data from (*Kramer and Wohl*, 2014). Horizontal guidelines drawn at $\hat{p} = 0.5$ (wood in 50% of photos for the day) and at Q=4500 m^3s^{-1}, a transport threshold identified in Figure 4.2. Vertical guidelines are drawn to connect hydrograph peaks with wood graphs. Within the time period between July and August 13th, 2012, *Kramer and Wohl* (2014) estimated 1600 pieces 600 $\pm$ 200 m^3, 1.3 x 10^5 kg C.

The 2011 hydrograph is distinct due to the double-humped, late summer, steeply rising freshet peaks. In 2011, Alberta had the highest snowpack in over a decade coupled with a warmer than average summer. The wood flood occurred during the second, not the first, peak. Although there was some wood transport during the first peak (field observation), it

was not nearly the quantity during the second peak. The steeply rising second peak likely crossed some threshold above 6000 m^3s^{-1} (about the) that enabled access to large amounts of stored wood at higher elevations in a short enough time to instigate congested transport.

In 2012, there was no ice jamming. Instead, there was a stepped ice-off. Although there are no data at the beginning of the summer, wood movement from the second freshet was minimal, peaking around $\hat{p} = 0.2$, with most photos containing only a single log. Within the rapids corridor, the wood deposited in 2011 remained essentially undisturbed. The wood that was being transported appeared to be the wood that was stranded at the tail end of the 2011 event.

In 2013 and 2014, ice jamming was captured by the camera. Supporting movie file, *ms03_FF2013051314_10min5fps_breakup.avi*, is a video time-lapse of break up and wood transport over two days in 2013. Supporting Figure 4.E.2 shows a photo time series of ice jamming using frame captures from the video. The river first thermally melts and is largely ice free. Then, quite suddenly, an ice jam moves through the site for about two hours. Wood is jumbled within the ice jam, and large clumped mats of driftwood follow in its wake. About half a day to a day behind the major ice jam, there is increased semi to congested wood transport. Wood accumulations within the rapids corridor were re-positioned from ice push (field observation). These patterns are also seen in 2014, but the ice jamming was smaller and less dramatic.

The magnitude of wood flux is not directly related to the magnitude of water discharge (Figure 4.2). For any given discharge, we found that there could be either high or low wood flux. However, there is a transport threshold at ~ 4500 (m^3s^{-1}). Below this threshold there is minimal wood transport, whereas above this discharge there is the potential for appreciable wood flux. Whether the potential is reached likely depends on the sequence of peaks as well as multi-year fluctuations in elevations and availability of stored wood for transport.

Further evidence for this threshold effect is the shape of the wood flux curves. Generally, wood flux (on the timescale of a day) does not gradually increase but jumps quickly to max

flux and then has a longer trailing tail (Figure 4.1). This pattern appears to be true for both the larger steeply rising events as well as smaller later summer events.

4.7. Discussion

Although we did not directly evaluate fluctuations in up-basin recruitment, the characteristics of wood temporarily stored in the Slave River Rapids Corridor indicate that wood mostly originates from banks and travels long distances, moving from one temporary storage site to another. The high amount of abrasion and lack of bark suggest non-locally sourced wood, whereas the lack of appreciable decay suggests that wood in active transport does not remain long enough in one place to become decomposed by organisms. At high latitudes, more wood from up-basin may cumulatively travel longer distances in good condition because the wood decays more slowly. In an Alaska stream at similar latitude, *Murphy and Koski* (1989) found that the mean age for trees with bark and limbs attached was 4.5 years and that residence time for wood with solid centers but with extensive surface rot was 125 years. Since the majority of the wood on the Slave River was solid, yet lacked limbs and bark (Table 4.1), residence times are likely greater than 4.5 years and less than 100. The large proportions of trees with rootwads and the up-basin meandering stream morphology

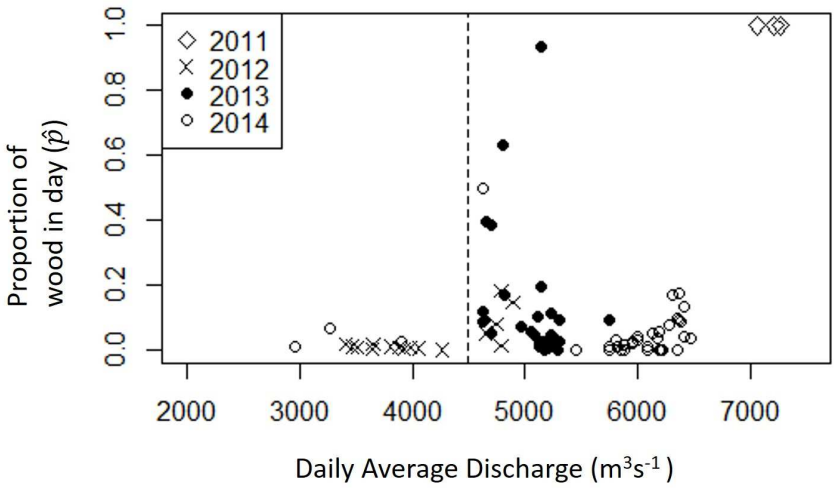

Figure 4.2. Identification of a wood transport threshold

of the Slave River suggest that the bulk of the wood originates from channel migration and localized slumping and failure of banks, rather than hillslope failures.

Wood on the Slave River is transported episodically on varying time frames and at varying magnitude, despite evidence for continual recruitment from banks. Although recruitment processes govern the total amount of wood available for transport, it is the flow regime that governs the timing and volume of wood flux as wood is transported through the fluvial system. Across diverse drainage basins, large scale recruitment events such as massive hurricanes (*Phillips and Park*, 2009) will increase the amount of wood available for transport, which will increase overall wood loads and fluxes. But, depending on the location and type of wood recruitment, there may be some lag time or dissipation of volumes between input and export response.

Correspondence between different lines of evidence for "return interval" of wood floods on the Slave River suggests that episodicity in wood flux is real and not an artefact of a particular dataset or method of analysis. The 2011 wood flood delivered massive new mats and piles of wood to the Slave River delta and deposited them shoreward of distinct, older vegetated deposits of varying ages (*Kramer and Wohl*, 2015). Using dates of germination on vegetated driftwood in the Slave River Delta and on the shores of the Great Slave Lake, *Kramer and Wohl* (2015) estimated a recurrence interval for large wood floods between 30-50 years. Vegetated drift piles were clumped around the 1930s, early 1950s, mid 1960s, late 1970s, and early 1990s. These dates correspond well with evidence from the Pelican Islands, log raft, and historic photos in this study. The two very large advances of the log jam front between 1930 and 1950 and again between 1950 and 1966 (Figure 4.2) correlate with the early 1950s and mid 1960s vegetated driftwood dates from the lake. Although there was no recorded change in the raft position for the mid-1970s, wood transport and delivery to the lake occurred in the early to mid-1970s based on the historic photos and dates of lake driftwood. The vegetated 1990s deposits in the lake relate well to the raft moving forward in 1991, likely from the same high flows that removed wood from the Pelican Islands (Figure 4.2) during ice break up.

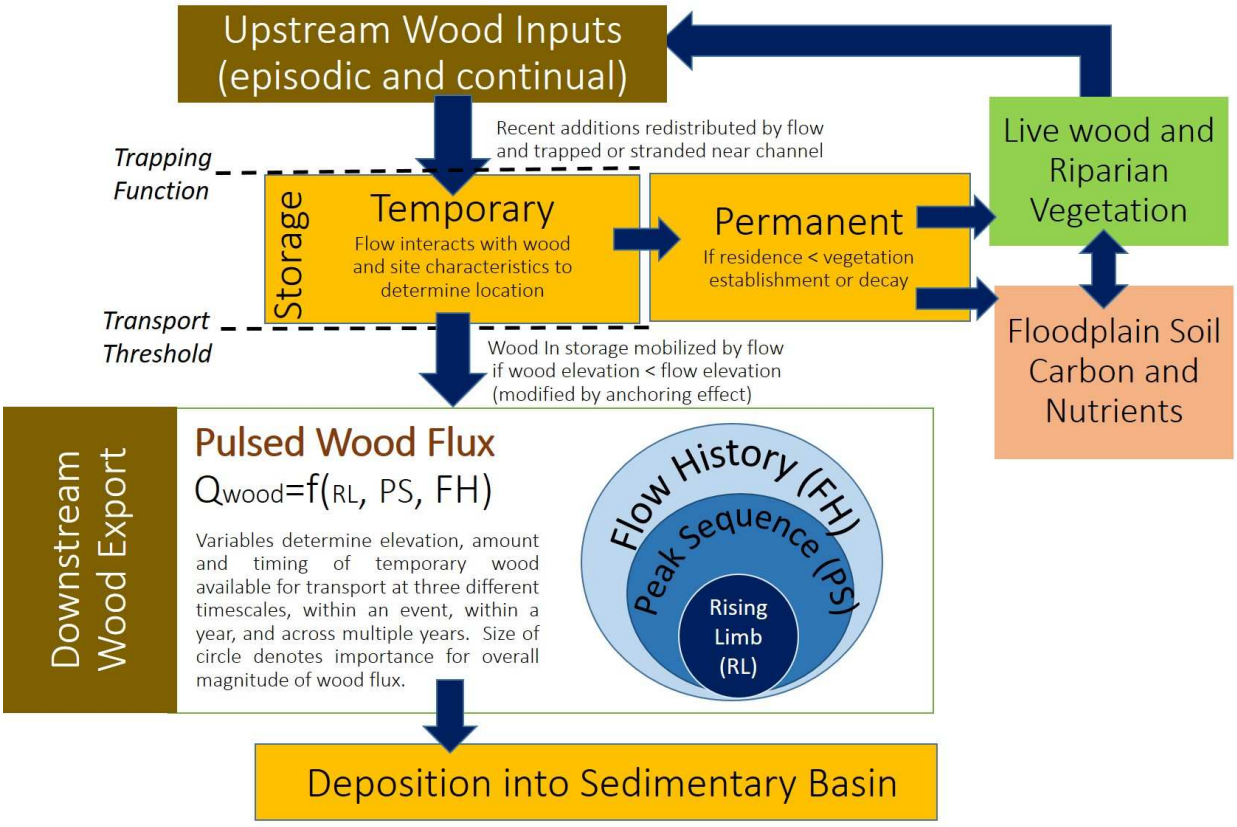

FIGURE 4.1. Conceptual model of pulsed wood export from drainage basins

In Figure 4.1, we present a conceptual model to explain the processes by which wood is exported downstream in pulsed fluxes of varying magnitude despite conditions imposed by different recruitment regimes. This model works for explaining how both massive and continual recruitment are routed through river systems. Where and when newly recruited wood is deposited depends upon the interactions among flow, wood characteristics, and channel characteristics (*Kramer and Wohl*, in review; *Ruiz-Villanueva et al.*, 2015a): we call this the trapping function. If the wood decays or is vegetated before it can move again, then it has become laterally exported and is in permanent storage. When wood is deposited in locations that are accessible by subsequent flows, it is in temporary storage.

At some point, wood that is in temporary storage is re-mobilized when the elevation of flow surpasses the elevation of the wood (*Bertoldi et al.*, 2013), modified by an anchoring effect. We define the anchoring effect to be anything that limits mobilization when flow elevation equals wood elevation. Factors that limit wood mobilization include larger piece

sizes, partial burial, rootwad presence, contact with other pieces, bracing against channel boundaries, protection by larger pieces, and channel irregularities (*Wohl and Goode*, 2008; *Merten et al.*, 2010; *Kramer and Wohl*, in review). Wood is often stranded at a narrow range of elevations from a flood (*Bertoldi et al.*, 2013), therefore the mobilization threshold for one piece of wood is also the mobilization for many, resulting in a rapid increase in wood flux over some reach-scale discharge threshold. After the threshold is crossed, we suggest that the magnitude of the wood flux is mostly a function of three nested processes operating on three different timescales (Figure 4.1): 1. the characteristics of the rising limb during one flood, 2. the sequence of flows during run-off season and 3. multi-year to multi-decadal flow history.

On the rising limb of wood-transporting floods, wood transport increases rapidly, peaks with water discharge (on a day-averaged timescale) and then decays more slowly as flows recede, resulting in a skewed distribution with a heavy positive, or right tail (Figure 4.1). Studies that have examined wood fluxes on timescales of minutes or less have found that wood flux peaks before water discharge (*MacVicar and Piégay*, 2012; *Kramer and Wohl*, 2014). Flashier hydrographs are known to mobilize and tranport more wood (*Ruiz-Villanueva et al.*, 2016a). We also found that large changes of magnitude in short amounts of time (steep rising limbs) associated with ice jamming or flashy freshet peaks create larger magnitude wood fluxes that are more likely to have congested transport. This finding is supported by flume experiments which indicated that the rate at which dowels were introduced is the dominant explanatory variable behind whether the dowels were transported as congested, semi-congested, or uncongested (*Braudrick et al.*, 1997).

The discharge magnitude of an event specific wood transport threshold can vary between floods because it is highly dependent on the elevation at which the preceding flood deposited wood (*Haga et al.*, 2002; *Bertoldi et al.*, 2013). If the rise in water levels does not sufficiently increase enough to access wood on the banks, no wood will be transported, no matter how steep the rise. Thus, the sequence of peaks within a year governs the location and availability of wood, whereas the rising limb dictates whether the wood is accessed. We have shown

that the highest wood fluxes occur as infrequent, episodic congested wood floods within the context of flow history. The largest wood floods happen when there are multiple years of decreasing peak discharges that strand wood at successively lower elevations, followed by an exceptional year with a flashy peak that is of sufficient magnitude to quickly recruit wood stranded from multiple years.

Over time for a given flow regime, consistent thresholds can be identified below which wood transport is almost always negligible (*Ruiz-Villanueva et al.*, 2016a). *MacVicar and Piégay* (2012) found that a transport threshold is reached at 3/4 bankfull depth. *Ravazzolo et al.* (2015a) found that wood was transported when flow was above a 10-20% exceedance probability. *Ruiz-Villanueva et al.* (2015a) found different threshold responses in wood transport related to bankfull discharge between headwater multi-thread and single thread channels. In this study, using multiple methods, we found a consistent Slave River threshold for transport between 4,200 and 4,500 m^3/s^2 which is between a 1 and 2 year recurrence interval.

For the Slave River, we found a sharp inflection in post-dam discharges at a recurrence interval of ∼1.2 yr. This inflection occurs at 4200 m^3s^{-1} which is the same as the transport threshold identified using data from the Pelican Sanctuary Islands in Section 4.5, and is close to the transport threshold we identified monitoring wood in transport with time-lapse cameras in Section 4.6. Although recurrence intervals converge between pre- and post-dam data for infrequent (>20 year) floods, events with less than <10 year recurrence were 1.5 times higher before construction of the dam (Figure 4.2). Thus, wood transport thresholds could have been higher pre-dam when the flow regime had higher peak magnitudes and more frequent ice jamming. Interestingly, just upstream on the Peace River,*Beltaos et al.* (2006) found that a minimum of 4000 m^3s^{-1}, which is strikingly similar to our wood transport threshold, is needed in the Spring for mechanical, rather than thermal, icebreak up to occur.

Although we have shown the re-mobilization of wood occurs as a threshold response to discharge of common rather than rare floods, it is important to recognize that this is a time averaged threshold below which wood transport is typically negligible, it is not a threshold above which wood transport always occurs. In Figures 4.2 and 4.1, we have shown that not

all years or events that exceed the identified threshold result in wood transport, thus crossing the discharge threshold does not imply that there will be transport, only that transport is possible. Whether transport happens and the magnitude of the wood flux depends on the flow history.

4.8. Conclusion

We found that the magnitude of wood flux is strongly influenced by the shape and patterns of water discharge at varying timescales: 1. the rate of rise on the rising limb, 2. the sequence of peaks within a year and 3. flow history that sets decadal patterns of wood storage. Within the framework of recruitment and wood availability, we argue that flow history is the most important variable for prediction of the magnitude of wood flux, followed by decadal patterns and the rate of change during the rising limb.

Previous studies that have examined change in wood storage have focused on mobilization only from single events or a run-off season along a reach (*Berg et al.*, 1998; *Cadol and Wohl*, 2010; *Dixon and Sear*, 2014; *Iroumé et al.*, 2015; *Young*, 1994). Generally, all wood is counted and then after a year (or one flood), wood is tagged and counted again. Although this approach provides a general sense for average percentage of wood that moves in one year or one flood, it is inherently limited for understanding variability of wood export and transport thresholds as it does not account for change in thresholds due to sequence of flows or flow history.

Known temporary trapping sites that have high turnover of wood, such as channel constrictions, channel spanning jams, and mid channel bars and islands, are ideal locations to study wood transport through time and can be analyzed with historic imagery or actively monitored with time-lapse cameras. Other ideal locations are sites of continued and permanent deposition such as log rafts (*Boivin et al.*, 2015), lakes and reservoirs (*Moulin and Piégay*, 2004; *Seo and Nakamura*, 2009), and delta fronts (*Kramer and Wohl*, 2015).

We suggest replication of our approach of monitoring known sites of temporary or permanent storage through using repeat imagery or surveys coupled with active monitoring of wood

in transport with video or time-lapse photography. This would facilitate further exploration of the relative importance of discharge/transport thresholds, sequences of flows, influence of wood trapping sites, and influence of wood recruitment in natural rivers of differing size and type.

Mapping or surveying relative abundance of wood volumes at varying elevations at chosen monitoring sites could be used as a hazard management tool to understand when banks are becoming loaded with wood versus when they are losing wood. Similar to earthquake hazards, risk increases when more time elapses between wood flushing events because banks may become more heavily loaded with wood. Picking monitoring plots through drainage networks could also help to understand how waves of wood from mass recruitments propagate downstream.

Recognition of Support

This project was primarily funded by the Edward M. Warner Graduate Grant awarded by the CSU Geoscience Department with an additional donation from Charles Blyth and grant from the Colorado Water Institute. Field work was supported by National Geographic Research CRE Grant #9183-12, Geological Society of America Graduate Grants. Special thanks to the Pelican Advisory Circle and John McKinnon for allowing access to their pelican survey records and to Gen Cote, John Blyth, Chuck Blyth and Adam Bathe for camera field support. Several undergraduates were involved with varying aspects of data collection and/or analysis: Brooke Hess-Homeier (coauthor), Jay Merrill, Cole Conger-Smith, Madeline Egger, Matthew Suppes, Eva Hanlon, Landry Brogdon, Jake McCane, Aaron Brown and John Harris. All datasets presented here can also be accessed via the Colorado State Digital data repository under Research Project "Big River Driftwood in Northern Canada" (`https://dspace.library.colostate.edu/handle/10217/100436`)

SUPPORTING INFORMATION FOR CHAPTER 4

Introduction. This supporting information includes an extended presentation of methods and results from surveys of wood size and condition in the Slave River Rapids Corridor as well as extended methods for image conditioning of oblique aerial photos of the Pelican Sanctuary prior to analysis. Also, in order to better orient the reader to field sites, we provide several detailed location figures for our repeat photographic analyses at the log raft, Pelican Island Sanctuary and at the Fort Fitzgerald timelaspe camera. Geodatabase of feature datasets from analysis of the Pelican Sanctuary including: wood, land and image footprints as well as the ruleset used in eCognition to segment images can be accessed via `http://hdl.handle.net/10217/100436`.

Herein, we also provide full descriptions of variables in uploaded datasets (.csv files) and captions for the three uploaded supporting video files. All datasets presented here can also be accessed via the Colorado State Digital data repository under Research Project "Big River Driftwood in Northern Canada" (`http://hdl.handle.net/10217/100436`).

4.A. Wood Metrics

4.A.1. Text S1. Wood Metric Data Collection. We measured wood accumulations in the Slave River rapids at several sites, chosen by accessibility. We analyzed the data using exploratory data analysis, graphical analysis, and basic summary statistics to provide estimates of wood size classes and to provide insights into wood provenance and transport history. We characterized the size distribution and characteristics of wood that had been transported by the 2011 wood flood by conducting line intersect transects laid across two flood deposited point jams, one raft, one racked piece accumulation, and two bay accumulations. Along most line intersects, large wood (LW) (>10 cm in diameter on the largest end and >1 m in length) that intersected the line were measured and characterized. For a subset of the line intersects (two point jams and one bay transect), all pieces, regardless of size, were measured. For these complete surveys, the line was spray painted and all pieces that

TABLE 4.A.1. Table of location and dates of wood metric surveys

SiteID	Survey Date	Lat , Long (WGS84). Description
Src1	Aug 10, 2012	59.88975°N -111.61385°W. Line intersect survey of just LW at main jam on Rollercoaster island
Src2	Aug 15, 2012	59.88991°N -111.61349°W. Line intersect survey of all wood sizes across secondary smaller point jam on Rollercoaster island
Src3	Aug 16, 2012	59.88998°N -111.61401°W. Survey of all scattered large pieces with rootwads on main Rollercoaster Island
Src4	Aug 15, 2012	59.88991°N -111.61349°W. Survey of all scattered large pieces on the smaller Rollercoaster Island near Src2 jam
Src5	Aug 7, 2013	59.88998°N -111.61401°W. Survey of all scattered large pieces with rootwads on Rollercoaster Island different than 2012.
Smn1	Aug 8, 2012	59.97399°N -111.72672°W. Line intersect survey of all wood sizes at the main point jam on portage island at "Molly's Nipple" rapid
Smn2	July 27, 2013	59.97419°N -111.72638°W. Survey of all scattered large pieces with rootwads on the chutes and shore to the right of the portage island at "Molly's Nipple" rapid
Sei1	Aug 28, 2012	59.96904°N -111.74867°W. Line intersect survey of just LW across racked pieces on the upstream end of "The Edge" kayaker viewing island river right.
Sec1	Aug 14, 2012	59.96747°N -111.74003°W. Line intersect survey of just LW across accumulated pieces in "English Channel" Bay
Sec2	Aug 14, 2012	59.96747°N -111.74003°W. Line intersect survey of all wood sizes across accumulated wood in "English Channel" Bay
Spi1	Sep 14, 2012	59.97116°N -111.74853°W. Survey of large identifiable pieces for size calibration with aerial images on the "Pelican Islands".
Slr1	Aug 10, 2015	59.95530°N -111.65456°W. Line intersect survey along at the front end of a channel spanning raft. Due to difficulty walking on the raft, the short and end diameters were not measured, just the middle diameter.

had paint on them were used in the sample. The line intersects did not have a set length but extended the entire length of the accumulation, oriented perpendicular to most logs. Table 4.A.1 surmmarizes location, dates and codes for field locations. Table 4.A.2 summarizes and provides detail on the wood metrics measured for each piece during wood metric surveys. Accessory files *ds01_Largewood.csv*, *ds02_Smallwood.csv*, and *ds03_Rootwads.csv*, described later in this file, are the resulting datasets from this fieldwork.

A summary of variables measured for each peice of large wood is provided in Table 4.A.2. The length (L) and end diameters (D) of each piece were measured. A representative diameter (D_m) was calculated as the average of the small and large end diameters. D_m could be less than 10 cm because only the largest end needed to be greater than 10 cm to be counted. Volumes of boles (V) were estimated assuming a cylindrical shape ($L * \pi(D_m/2)^2$). If rootwads were present, the length of the rootwad (L_r) from the top of the flare in the bole

to the longest down-growing root was measured, as well as the widest basal diameter ($W1_r$) and the basal diameter perpendicular to $W1_r$ ($W2_r$). Following methods from (*Thevenet et al.*, 1998), air-wood volumes for rootwads ($V*_r$) were calculated as L_r*$W2_r$*$W3_r$, which represents the box that completely encloses the rootwad. To increase the sample size of rootwads, additional surveys were conducted on large logs scattered on or near Molly's Nipple island, Rollercoaster island, and the Pelican Sanctuary islands (see Figure 1 in the main document).

Additional categorical variables were also measured to describe the condition and type of wood. Wood was categorized by type (coniferous or deciduous), type of end (snapped, beaver chew, anthropogenic, root, and unbroken tip), amount of bark present, and four levels of amount of bark, decay, and abrasion (see explanation of dataset *ds01_Largewood* and Table 4.A.2). Many studies use one category for decay that incorporates aspects of abrasion and amount of bark present. We found that it was too difficult to accurately describe the condition of wood with just one variable. Most wood was sound (not decayed), but had high amounts of abrasion. On some pieces, all the bark was removed, but the tree still had most of its small twigs and branches. This occurs wherever riparian trees fall into slow current but remain attached to the bank. Over time, the bark falls off and the rest of the tree remains intact. Similar separation of decay from abrasion was recommended by (*King et al.*, 2013). Because most wood did not have bark, we did not attempt to identify tree species. Conifers were easily distinguishable from deciduous trees by the branching patterns, wood grain, general shape, and rootwad appearance.

TABLE 4.A.2. Descriptions of wood metric data.

Large wood bole dimensions and categorical variables	
L	Length of the bole from small end to bottom end or top of flare in rootwad
D_l	Diameter of the large end. Measured at the top of the flare if rootwad present.
D_s	Diameter of the small end.
D_m	Representative diameter $(D_l + D_s)/2)$
V	Volume modeled as $L * \pi(D_m/2)^2$
Wood Type	
D	Deciduous
C	Coniferous
End Types	
S	snapped
T	un-snapped tip
R	rootwad
B	beaver chew
A	anthropogenic, such as saw cuts
Decay Classes	
1	Sound
2	Heartwood sound, sapwood decayed but cannot be pulled apart
3	Sapwood can easily be pulled off
4	Log cannot support weight but retains shape
Bark Classes	
1	Most or all bark remains
2	Partial bark retained
3	Remnants of bark
4	No bark present
Abrasion Classes	
1	Most branches present, including smaller ones
2	Most branches snapped off
3	Branch stubs
4	Smooth
Rootwad dimensions	
L_r	Length of rootwad measured from top of flare along the axis of the bole
$W1_r$	Widest basal footprint width
$W2_r$	Width of basal footprint perpendicular to $W1_r$
$V*_r$	Air-wood volume of rootwad modeled as $L_r * W1_r * W1_r$
Small wood dimensions	
L_{sw}	Length of the small piece
D_{sw}	Middle diameter of the small piece
V_{sw}	Volume modeled as $L_{sw} * \pi(D_{sw}/2)^2$
L_{bk}	Longest length of a piece of bark
W_{bk}	Width, or intermediate length of a piece of bark
H_{bk}	Height, or shortest length of a piece of bark
V_{bk}	Volume modeled as $L_{bk} * W_{bk} * H_{bk}$

4.A.2. Text S2. Size distributions of Slave River Driftwood. Distributions of large wood size were similar for accumulations sampled from racked pieces, bays, and rafts, whereas point jams were enriched with large wood < 5 m in length compared to all other trapping sites (Figure 4.A.1, see Figure 2 in main article for images of accumulation types). Based on the density functions and cumulative distributions presented in Figure 4.A.1, we hypothesized that the two point jam surveys represent one population and that the other surveys represent another population. We used the Kruskal -Wallace rank sum to test the null hypotheses that 1) length and diameters of wood from the two point jams come from the same distribution and 2) all other sites come from the same distribution but separate from the point jams. In both cases, we did not reject the null hypothesis, so we grouped all the point jam data into one dataset and all the other sites into another dataset that we call "other". Wilcox rank sum tests were performed on the untransformed data and t-tests on the log_2 transformed data (to normalize the distributions) to determine whether these two data groups were significantly different from each other. Both tests resulted in rejection of the null hypothesis with 95% percent confidence. There was a very significant difference between point jams and the other sites ($p < 0.001$ in all cases).

Table 4.A.3. Summary statistics for large wood >10 cm in diameter and >1 m in length.

	Min.	1st Qu.	Median	Mean	3rd Qu.	Max.	sd
Wood Length (L) in meters							
Point	1.0	2.3	3.9	4.6	5.9	16.4	3.0
Other	1.1	3.3	6.1	7.4	11.3	19.4	5.0
All	1.0	2.9	4.7	6.1	8.3	19.4	4.4
Wood Length in $\phi = Log_2(L)$							
Point	0.0	1.2	1.9	1.9	2.6	4.0	0.9
Other	0.1	1.7	2.6	2.5	3.5	4.3	1.1
All	0.0	1.5	2.2	2.2	31)	4.3	1.1
Wood Representative Diameter (D_m) in meters							
Point	0.07	0.12	0.15	0.19	0.21	0.56)	0.11
Other	0.08	0.13	0.21	0.23	0.30	0.70	0.12
All	0.07	0.12	0.18	0.21	0.28)	0.70	0.11

Data were separated into "Point" (n=86) and "Other" (n=100) as a result of analyses presented in section 4.A.2 and Figure 4.A.1."Point" (n=86) includes line intersect surveys from transects from two different point jams. "Other" (n=100) includes line intersect surveys from one racked accumulation (n=25), two bay transects (n=35), and one raft accumulation (n=41). "All" combines the data (n=187).

Thus, wood pieces deposited in point jams are likely less representative of the size distributions of floating wood downstream. This may be because point jams are efficient at capturing and entrapping smaller floating pieces and/or because large pieces are less likely to become entrapped in point jams: when large pieces hit the point jam, more of the large piece is extended into the current and it is less likely to stay in place.

Table 4.A.3 summarizes the untransformed data for length and diameter as well as the log_2 transformed wood length, ϕ, recommended by *MacVicar and Piégay* (2012). Histograms

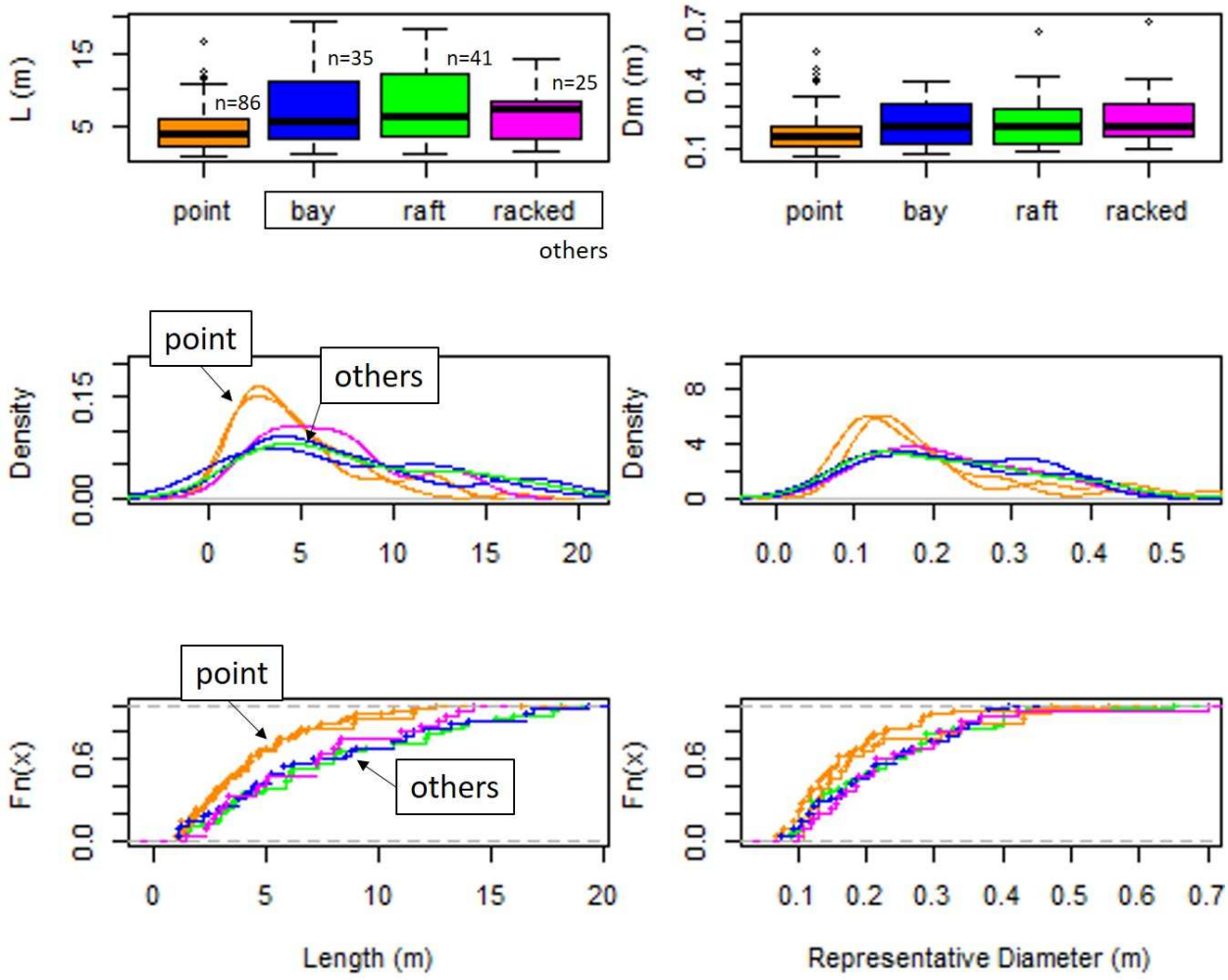

FIGURE 4.A.1. Size distributions of LW from study sites. Columns from left to right show size distributions for length (L), representative diameter (D_m), and estimated volume (V). Rows from top to bottom show boxplots, density functions, and cumulative distributions by collection site type. Summary statistics are provided in Table 4.A.3.

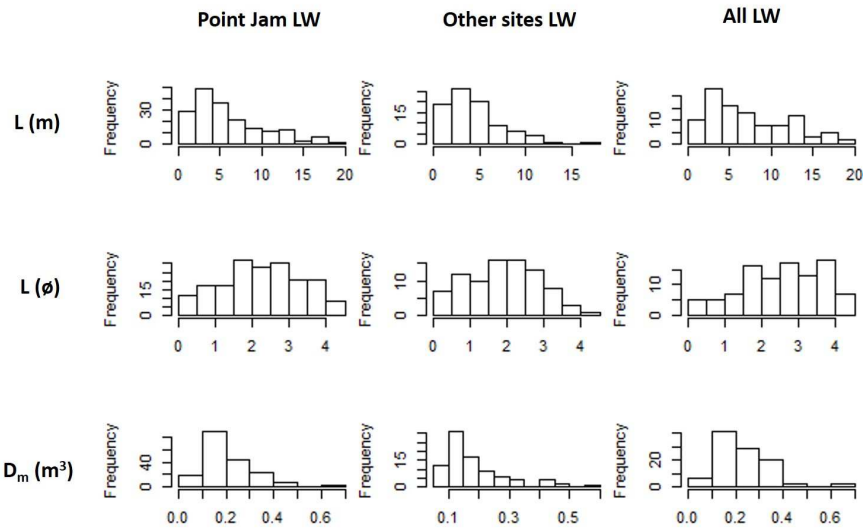

FIGURE 4.A.2. Size distributions of LW from study sites. Rows from top to bottom show size distributions for length (L) in meters, length in ϕ and representative diameter (Dm). Columns from left to right present present data for all sites, point jams, and non-point jams (other). Summary statistics are provided in Table 4.A.3 in the main text.

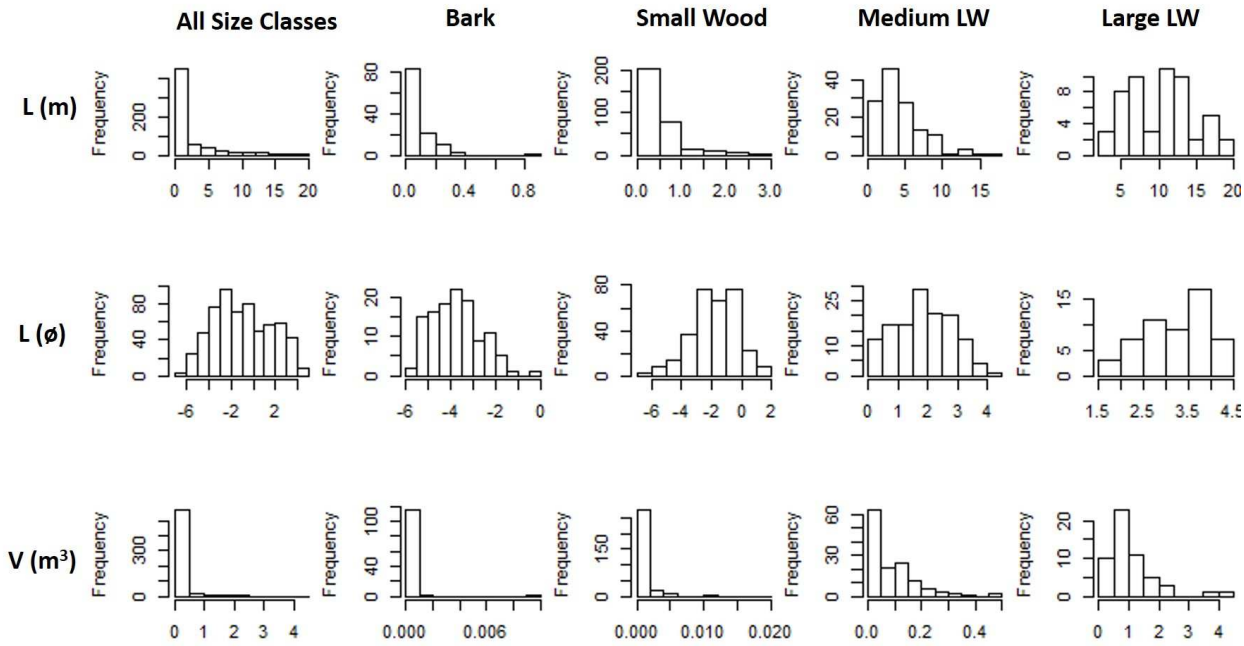

FIGURE 4.A.3. Histograms of LW by size categories.Rows from top to bottom show size distributions for length (L) in meters, length in ϕ and estimated volume (V). Columns from left to right present present data for each size class. Summary statistics are provided in Table 4.A.4 in the main text.

of these data are provided in Figure 4.A.2. Reporting lengths on a log_2 scale, as done in sedimentology, is advantageous because this normalizes and linearizes wood lengths. It is also particularly useful for LW studies that define the lower length threshold at 1 m, which is zero on the log_2 scale. Any lengths longer than 1 m will be positive.

Many studies on larger rivers, only measure the largest logs (*Schenk et al.*, 2014), rather than the 10 cm diameter, 1 m length threshold for large wood (LW) common for reach-scale studies in smaller rivers and streams. Thus, knowing the ratio of medium to large logs is important for connecting wood dynamics from the headwaters to large rivers and for estimating mass wood budgets from remote sensing of only the largest logs. Also, *Turowski et al.* (2013) have recently shown that there may be consistent relationships between the proportions of small wood smaller than 1 m length and 10 cm in diamter to large wood that could prove useful for estimating wood fluxes in rivers. We provide a summary of the length and volume for each size category: bark, small wood, medium LW and large LW in Table 4.A.4 and histograms by these size classes are provided in Figure 4.A.3.

In a preliminary analysis of the same point jam data presented here, *Kramer and Wohl* (2014) found that the relative proportions of medium to large LW were fairly similar between point jam line intersect surveys (4:1) and observed floating wood (3:1). *Kramer and Wohl* (2014) used a cutoff of $D_m = 0.23$ m and $L = 3$ m between medium and large LW based on a natural break in the data. We confirm that the medium LW:large LW ratio for point jams is 4:1 and for the other accumulation sites we estimate a ratio of 2:1. Some LW studies in big rivers use a cutoff of 0.20 m and 3 m (*Schenk et al.*, 2014, e.g). Following these criteria, the ratio of medium to large LW is 2.7:1 for point jams and 1.2:1 for the other accumulations.

Kramer and Wohl (2014) also characterized the proportions of bark:small wood:medium LW:large LW as 6:25:4:1 based on two complete point jam line intersect surveys that measured all wood. For comparison, we calculated the bark:small wood: medium LW: large LW ratio for one complete survey in a bay to be 20:11:2:1. Most notably, the bay accumulation was enriched in bark and contained smaller amounts of small wood compared to the point jam. However, it is important to note that these data were collected along a line intersect

only the width of a spray-painted stripe and may not represent actual ratios of wood loads because large logs are much longer than small pieces of wood.

TABLE 4.A.4. Length and volume summary statistics by size category from line intersect surveys.

	Min.	1st Qu.	Median	Mean	3rd Qu.	Max.	sd
Wood Length (L) in meters							
Bark	0.02	0.04	0.08	0.10	0.18	0.87	0.10
Small Wood	0.01	0.15	0.29	0.47	0.65	2.87	0.50
Medium LW	1.0	2.3	3.5	4.4	5.8	16.6	3.0
Large LW	3.0	6.2	10.7	10.2	13.2	19.4	4.4
Wood Length in $\phi = Log_2(L)$							
Bark	-5.64	-4.64	-3.70	-3.74	-3.09	-0.20	1.06
Small Wood	-6.80	-2.74	-1.79	-1.80	-0.62	1.52	1.56
Medium LW	0.00	1.20	1.81	1.84	2.54	4.05	0.94
Large LW	1.59	2.64	3.42	3.20	3.72	4.28	0.71
Volume in cubic meters							
Bark	$4.9e^{-7}$	$3.3e^{-6}$	$1.4e^{-5}$	$1.6e^{-4}$	$6.0e^{-5}$	$9.8e^{-3}$	$9.2e^{-4}$
Small Wood	$7.1e^{-}8$	$2.0e^{-5}$	$6.8e^{-5}$	$7.8e^{-4}$	$4.9e^{-4}$	$2.0e^{-2}$	$2.1e^{-3}$
Medium LW	0.01	0.03	0.05	0.09	0.13	0.47	0.09
Large LW	0.20	0.55	0.92	1.03	1.25	4.23	0.76

Volumes is estimated using representative diameter and length assumuing a cylinder. ϕ is a log_2 transform of the data. Sample sizes are: n=119 for bark, n=312 for small wood, n=133 for medium LW, n=54. To qualify for large LW, wood had to be both $\geq$ 0.23 m in diameter and $\geq$ 3m in length.

We suggest that the true ratios of wood sizes can be estimated by taking the line intersect ratios and multiplying each category by the number of pieces in that category necessary to equal the average length of large LW. For example, using median lengths in Table 4.A.4, 134 pieces of bark, 37 pieces of small wood, and 3 pieces of medium LW would be the equivalent length of 1 piece of large wood. Thus, the ratio 20:11:2:1 that we measured along a line intersect in a bay becomes 2680:407:6:1. If we multiply each category by the median volumes from Table 4.A.4, then the ratio of total wood volume per size class becomes 25:19:0.3:0.9. Following this procedure for point jams, the ratio of pieces 6:25:4:1 becomes 612:925:12:1, with a volume ratio of 6:42:0.6:0.9. We used the median instead of the mean because the median provides a better estimate of the central tendency data that are not normally distributed.

We recognize that these represent first-order approximations and that the accuracy and validity of this thought experiment could be tested by comparing this method to a complete

survey of an accumulation. We suggest this as a future endeavor. However, these values suggest that small wood and bark likely contribute >30 times the volume of large wood to wood loads in great rivers. These comparisons do not include the volumes from rootwads, but rather only the boles, loose sticks, and bark. In the next section, we examine rootwad sizes and types more closely.

4.A.3. Text S3. Condition and Type of Slave River Driftwood. We summarize the results of the categorical variables in Table 4.A.5. Of all the wood from LW line intersect surveys, 58% is deciduous and 42% is coniferous. However, if we select the data to include only trunks with rootwads, the percentages reverse to 42% deciduous and 58% coniferous. Deciduous trees are more likely to have forks, split trunks, and larger branches. These branches break off, thus increasing the overall number of pieces that are deciduous. If only pieces without rootwads are calculated, this effect is quite apparent. Under this scenario, the percentage of deciduous increases to 67%, with coniferous dropping to 33%.

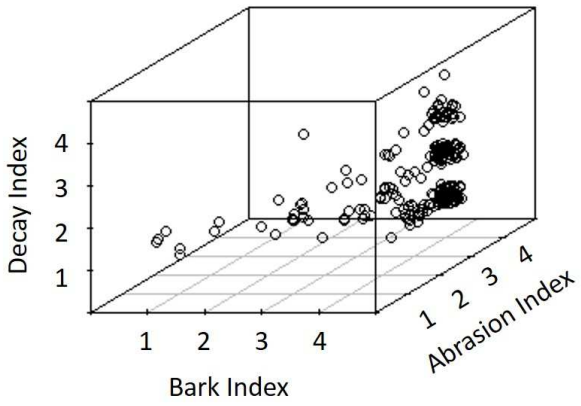

Figure 4.A.4. Jittered scatterplot of wood condition classes. See Table 4.A.2 for a description of classes. Higher numbers indicate longer amounts of time in the river or floodplain. The bulk of wood is located at (4,4,1), which corresponds to no bark, smooth boles, and sound wood.

TABLE 4.A.5. Wood characteristics summary.

	"All" Line Intersect LW					
Category	n	#:#	%:%			
deciduous:coniferous	169	98:71	58:42%			
rootwads yes:no rootwads	187	65:122	35:65%			
beaver chew yes:no	145	7:137	5:95%			
anthropogenic yes:no	145	1:144	<1:100%			
not snapped:snapped top	145	7:137	5:95%			
sound:decayed	185	156:29	84:16%			
bark present:bark absent	185	35:150	19:81%			
limited abrasion: abraded	184	11:74	6:94%			
	Pieces with rootwads			**Pieces without rootwads**		
deciduous:coniferous	60	25:35	42:58%	109	73:36	67:33%
not snapped:snapped top	50	2:48	4:96%	95	5:117	5:95%
sound:decayed	65	52:13	80:20%	120	104:16	87:13%
bark present:bark absent	65	13:52	20:80%	120	22:88	18:73%
limited abrasion: abraded	65	3:62	5:95%	120	8:112	7:93%
	Deciduous			**Coniferous**		
not snapped:snapped top	73	2:71	3:97%	57	3:54	5:95%
sound:decayed	97	85:12	88:12%	71	57:14	80:20%
bark present:bark absent	97	19:78	20:80%	71	15:56	21:79%
limited abrasion: abraded	97	5:92	5:95%	71	5:66	7:93%

The counts do not always add up to the full 187 count dataset because of missing values. The "All" dataset from the line intersect surveys was used (n=187). The raft line intersect survey did not include information on beaver chew or anthropogenic markings on wood so overall percentages calculated for those categories is based off of a sample of n=145.

We plot condition classes in Figure 4.A.4. To simplify dimensions for reporting and to compare condition characteristics between coniferous and deciduous LW, we collapsed each condition class (see Table 4.A.2) into only two classes: bark present (B=1,2 or 3) versus bark absent (B=4), sound (D=1 or 2) versus decayed (D=3 or 4), and limited abrasion (A=1 or 2) versus abraded (A=3 or 4). The summary of percentages for each class is presented in Table 4.A.5. There are no large differences in deciduous and coniferous wood conditions. Overall, 84% of wood is sound compared to 16% decayed; 19% of wood contains some bark versus 81% with no bark; and 6% of wood shows limited abrasion whereas 94% of pieces are abraded.

Because of this snapped branch effect, the size distribution of LW with rootwads may be more representative of the sizes of trees being recruited from banks rather than the larger population of all measured wood. Even though ranges were about the same, mean and medians lengths for pieces with rootwads were approximately double those of pieces without

rootwads, and diameters were just over 1.5 times wider (Table 4.A.5). One sided t-tests of the log transformed data confirm that the trunks without rootwads are very significantly ($\alpha = .05$) shorter and have smaller girth than trunks with rootwads (both p values $<.001$).

A one-sided t-test of transformed data indicates that deciduous LW is slightly smaller than coniferous LW in length (p-value =0.02) and diameter (p-value=0.06) (see Table 4.A.6 for summary of sizes by rootwad and tree type). However, when the data are subdivided to compare only deciduous and coniferous LW with rootwads, we found that, with 95% confidence, deciduous trees are not significantly smaller than coniferous trees in either length (p-value=0.5) or diameter (p=value 0.95). This supports the idea that, as a result of snapping of branches and trunks, deciduous trees are contributing greater proportions of smaller sized large wood than coniferous trees.

TABLE 4.A.6. Summary of trunk sizes with and without rootwads.

	Min.	1st Qu.	Median	Mean	3rd Qu.	Max.	sd
with rootwads (n=65)							
L(m)	1.0	4.1	8.3	8.7	12.3	19.4	5.0
D_m (m)	0.07	0.18	0.28	0.28	0.37	0.70	.12
without rootwads (n=122)							
L (m)	1.0	2.4	3.9	4.7	6.1	18.1	3.2
D_m (m)	0.07	0.11	0.15	0.17	0.21	0.65	.09
Deciduous (n=98)							
L_m(m)	1.0	2.9	4.7	5.8	7.5	18.1	4.1
D_m (m)	0.07	0.12	0.17	0.21	0.28	0.70	0.13
Coniferous (n=71)							
L_m (m)	1.1	3.9	6.1	7.2	10.4	19.4	4.6
D_m (m)	0.07	0.14	0.21	0.22	0.28	0.47	0.10

Explanation for variables is provided in the supplemental and main document text

About 5% of LW wood from line intersect surveys is beaver chew. However, the impacts of beaver to wood loads may be greater because most beaver-chewed wood was close to or less than the cutoff for large wood. We suggest a future study to more fully investigate proportions of beaver chew in log accumulations at this site. There was minimal evidence (<1%) of humans introducing wood to the river either as construction waste or sawed logs. Almost all logs (95%) were snapped at one end.

4.A.4. Text S4. Characterization of Slave River Rootwads. We report the dimensions for coniferous and deciduous rootwads in Table 4.A.7. Air-wood volumes for deciduous and coniferous wood are similar despite differences in shape (Figure 4.A.5). This reflects the fact that, although deciduous rootwads are longer, coniferous rootwads are wider. Comparing basal asymmetry ratios ($W1_r/W2_r$) to elongation ratios ($L_r/\bar{W}$, $\bar{W} = (W1_r + W2_r)/2$) reveals striking patterns (Figure 4.A.5). Conifers have a threshold elongation ratio

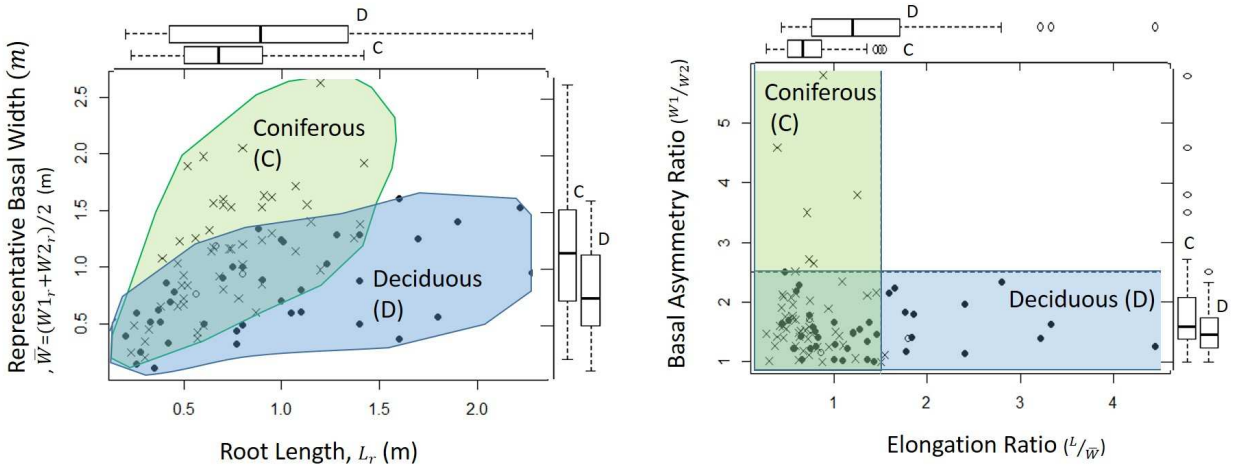

Figure 4.A.5. Rootwad shape and size between deciduous and coniferous LW. Left: Comparison of rootwad lengths and representative widths ($\bar{W}$). Right: Comparison of root elongation and basal asymmetry. Boxplots on the right and top sides of the graph show distribution of data by type per axis; scale is the same as the left and bottom axes.

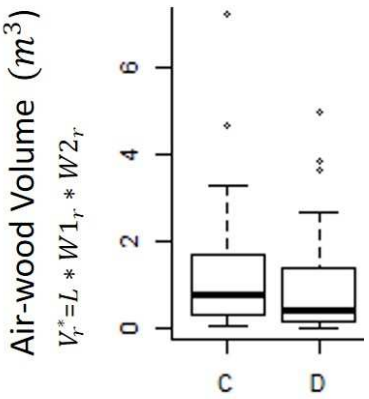

Figure 4.A.6. Comparison of rootwad air-wood volumes. Using a two-sided t-test for differences in means after log_2 transformation, p-value=0.12.

TABLE 4.A.7. Summary statistics for rootwads by tree type.

	Min.	1st Qu.	Median	Mean	3rd Qu.	Max.	sd	
Rootwad dimensions for Conifers								n=52
L_r (m)	0.2	0.5	0.7	0.7	0.9	1.4	0.3	
$W1_r$ (m)	0.2	0.9	1.3	1.4	1.9	3.6	0.7	
$W2_r$ (m)	0.10	0.5	0.8	0.9	1.2	2.0	0.4	
$V*_r$ (m^3)	$1.2e^{-2}$	0.3	0.8	1.2	1.7	7.2	1.3	
Rootwad dimensions for Deciduous								n=40
L_r (m)	0.2	0.4	0.9	1.0	1.3	2.3	0.6	
$W1_r$ (m)	0.1	0.6	0.9	0.9	1.3	2.0	0.5	
$W2_r$ (m)	0.1	0.4	0.5	0.7	0.9	1.4	0.4	
$V*_r$ (m^3)	$3.6e^{-3}$	0.1	0.4	0.9	1.4	5.0	1.2	

Explanation for variables is provided in the supplemental and main document text. Rootwad dimensions utilize an extended dataset of additional rootwads beyond those measured in the line intersect surveys.

around 1.5, with a maximum basal asymmetry of > 5, whereas deciduous rootwads have a threshold basal asymmetry around 2.5, with maximum elongation > 4. After reviewing field photos, it became apparent that as rootwads abrade in transport, conifers become asymmetrical about the base, whereas deciduous rootwads elongate. This reflects the fact that deciduous trees tend to have their longest and strongest root growing downward as a taproot, whereas conifers create a strong base by growing their strongest roots outward.

4.B. ANECTDOTES

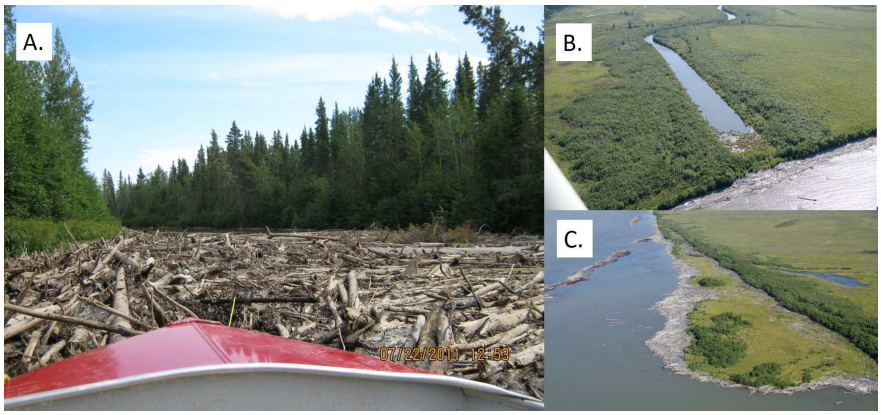

FIGURE 4.B.1. Wood in the Great Slave Lake delta. A: Wood from the 2011 wood flood completely clogs the Nagle channel in one day (photo by Eric Beck). B: Inactive distributary channel with wood clogging the outlet. C: Massive wood delivery from the Slave River is a central process regulating delta progradation and vegetation establishment. photo taken in August 2014. The bright white wood is from 2011 and the older, slightly vegetated wood marks the position of a shoreline and deposits from a past wood flood.

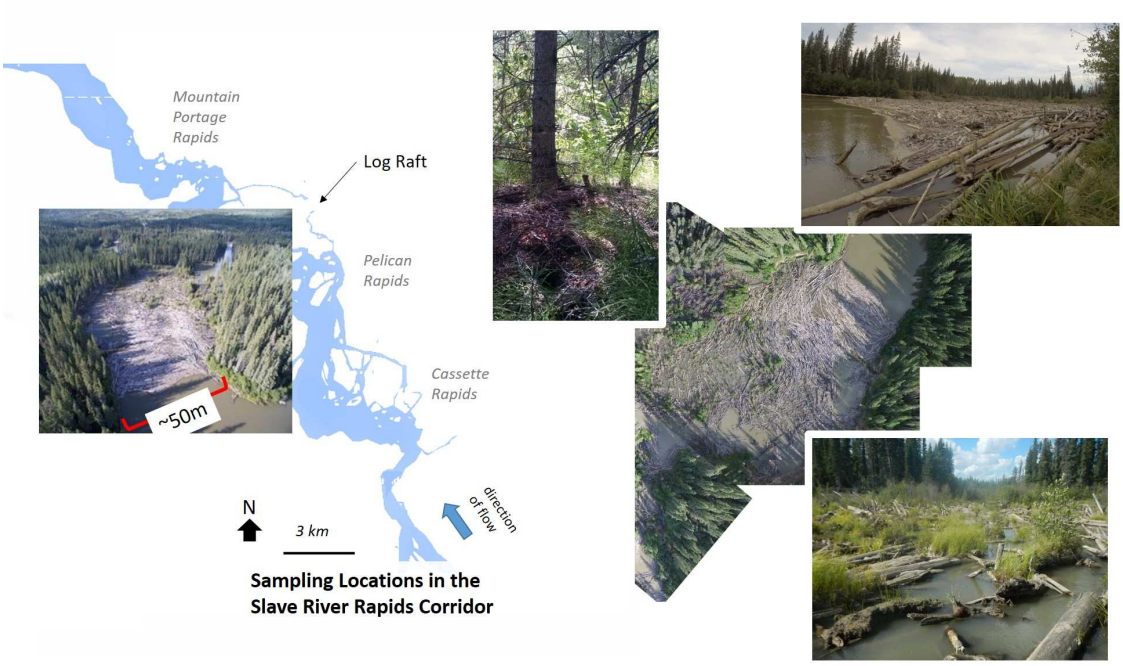

Figure 4.C.1. Location map for log raft. 59.95530°N 111.65456°W

Table 4.C.1. List of Aerial photos used in the raft analysis.

Photo Year	Photo Date	Agency	Roll#-photo#	Scale
1930	July 11	NAPL	A-2535-74	1:12000
1950	NA	APDR	NA	1:40000
1966	Sept 16	NAPL	A-30020-57	
1970	Sept 13	APDR	AS-1088-252	1:24000
1975	July 10	NAPL	A-24075-6	1:50000
1979	Sept	APDR	AS-2794-125	1:10000
1982	Oct	APDR	AS-2618-198	1:60000
1991	Aug 4	NAPL	A-27748-74	1:15000
1996	–	ENR	–	
2001	July 22	APDR	AS-2618-198	1:20000
2004	July 1	GE	DigitalGlobe	
2013	NA	GA	SPOT6	1.5m
2014	NA	GA	SPOT6	1.5m
2014	Aug 10	GA	Phantom3Drone	

NAPL is for National Air Photo Library in Ottawa, Canada . (`http://www.nrcan.gc.ca/earth-sciences/geomatics/satellite-imagery-air-photos`). APDR is for Air Photo Data Repository in Edmonton, Alberta (`http://esrd.alberta.ca/forms-maps-services/air-photos`) GE is Google Earth and GA is for Geospatial Alberta (`http://geodiscover.alberta.ca/Viewer`)

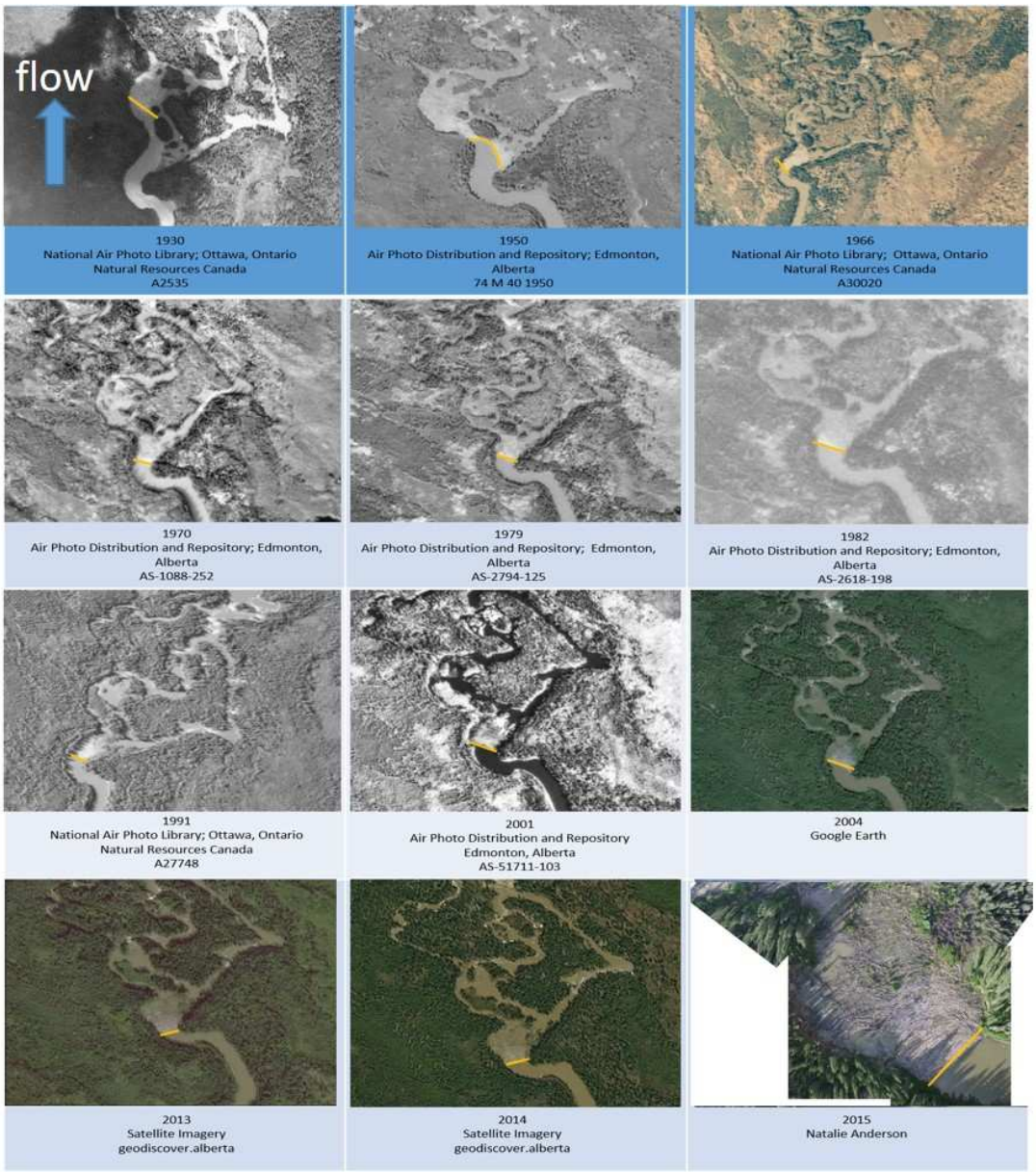

FIGURE 4.C.2. Mosaic of images used in analysis of log raft. Yellow line marks the position of the upstream edge of the raft.

4.D. Pelican Santuary

4.D.1. TEXT S5. EXTENDED METHODS ON PREPARING PELICAN ISLAND PHOTOGRAPHS FOR ANALYSIS. Figure 4.D.2 shows a flow chart of methods used to process and analyse the oblique aerial photos of the Pelican Island Sanctuary. First, we obtained a screenshot of the Pelican Sanctuary from a 2002 satellite image by Digital Globe on Google Earth. We georeferenced this image to known tagged coordinates in each corner and projected into Lambert

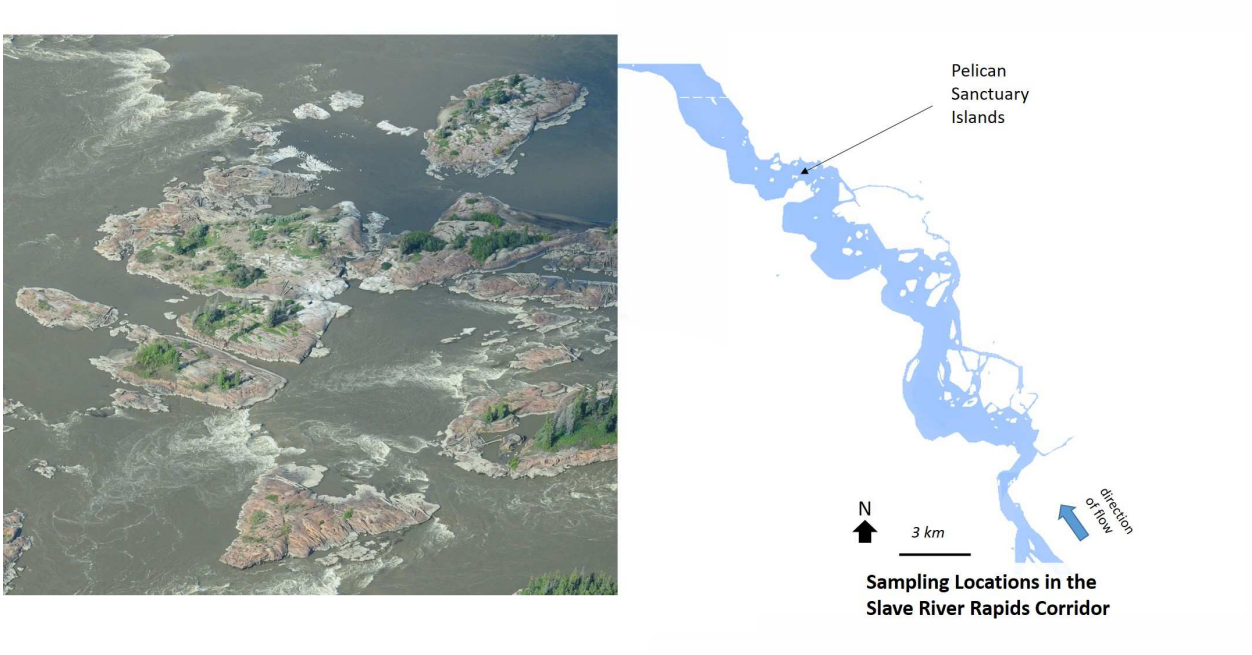

FIGURE 4.D.1. Location map for Pelican Island repeat photography. Islands located at 59.97116°N, 111.74853°W.

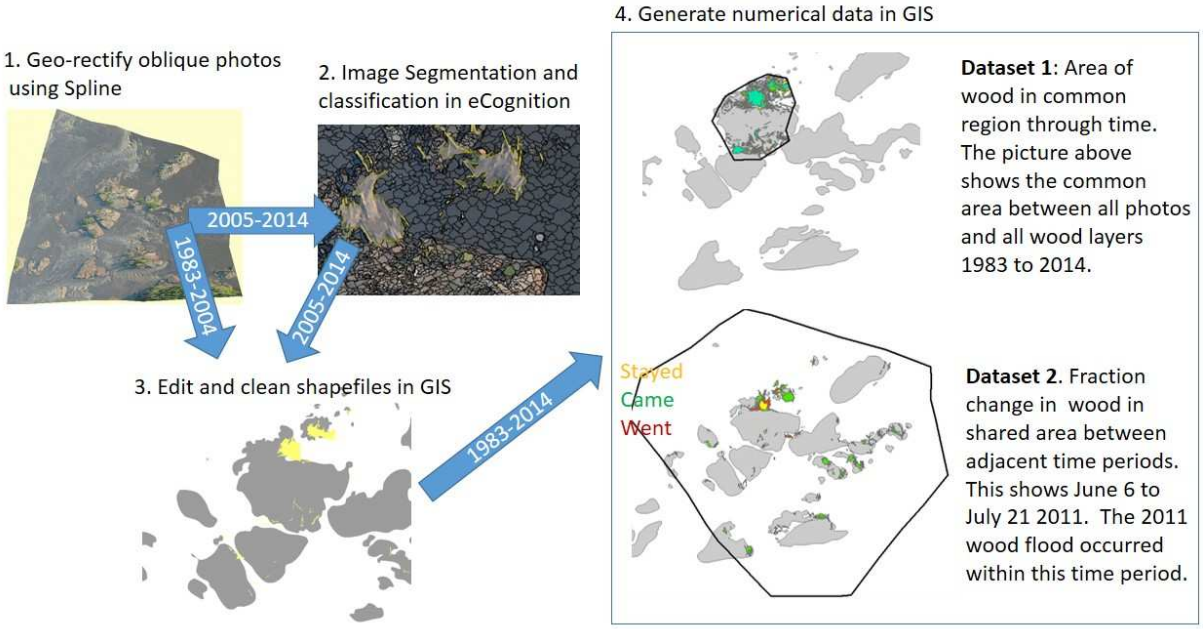

FIGURE 4.D.2. Flow chart of methods produce datasets from Pelican Sanctuary images

Conformal Conic for Canada. We then georeferenced the August 2011 oblique photo to the projected satellite image based on identifiable features. We used the high resolution August

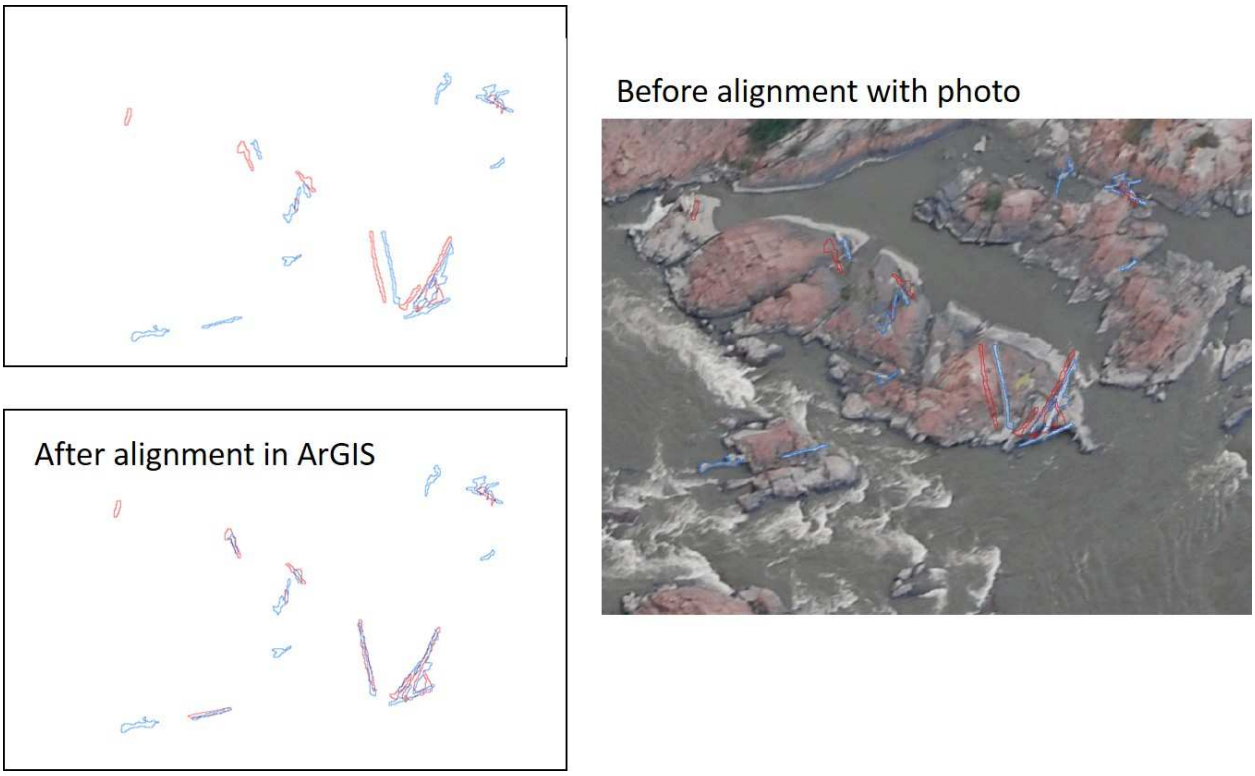

FIGURE 4.D.3. Example of subtle alignment of wood in editing phase

2011 image as a base to which all other images were georeferenced. We chose the August 2011 image as our base image because it had good overall coverage of the islands and was at a flow typical for most photos, making identifying tie points easier.

We used a spline transformation with more than 50 tie points when rectifying images. It was most important to honor points near wood on the islands rather than emphasizing overall reduction of error across the entire image. By using a spline, we ensured that wood deposits lined up as much as possible by placing more tie points near wood. We were not concerned about the accuracy of the georeferencing in the water sections where there was no wood and few to no identifiable tie points. The georeferencing for most of the digital images was conducted in GlobalMapper v.13. Due to loss of software access partway through the work, the scanned slides and 2012-2014 digital images were georectified using ESRI ArcGIS (v. 10.2) geospatial analyst toolset.

Geodatabase of feature datasets from analysis of the Pelican Sanctuary including: wood, land and image footprints as well as the ruleset used in eCognition to segment images can be

accessed via `http://hdl.handle.net/10217/100436` . Supporting movie file (*ms02_PIanimation.avi*) is an animation of the data layers through time. Figure 4.D.4 shows screenshots of two frames of the animated video from before and after the wood flood in 2011.

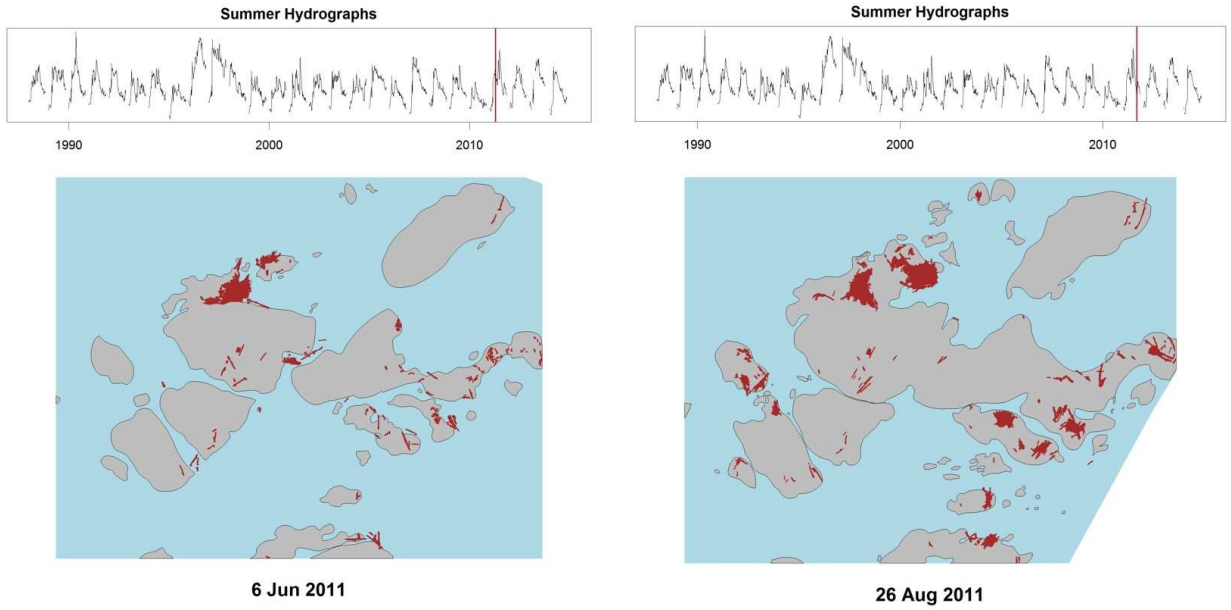

FIGURE 4.D.4. Screenshots of the animated data before and after the 2011 wood flood. Water is shaded only for regions within the footprint of the geo-referenced source image. Hydrographs show months April through September for each year of the data record. Solid line in hydrograph series indicates date of source photo. For scale, the oblong island in the upper right is about 120 m along the long axis.

The elevations, orientations, and lighting between photographs differed greatly, making automatic analysis and processing routines of the dataset impractical. We were able to use some automatic routines in eCognition to segment the high resolution 2005-2014 images. After segmentation, we manually merged, classified, and exported wood polygons as shapefiles. The automated segmentation did a poor job extracting wood on the low resolution 1983-2004 photographs, so we simply brought these photos into ESRI ArGIS (v 10.2) and manually traced wood using the ArcEditor toolset. We also created tracings of the image footprints and outlines of the islands. Prior to analysis, wood polygons were edited in ArcGIS. We edited the files by adding polygons of wood that were missed by the segmentation process,

trimming polygons that extended beyond wood, and making slight corrections in placement in order to align wood polygons that were subtly displaced (Figure 4.D.3).

We analyzed the wood shapefiles in ArcGIS in two different ways (Supporting Figure 4.D.2), we analyzed change within the same common area between all the photos from 1983 to 2014 (Dataset 1, Supporting Figure 4.D.2) and we analyzed the change between adjacent photos in time from 1988-2014 (Dataset 2, Supporting Figure S10). Dataset 2 was subsetted to 1988 due to many missing adjacent timeframes with adequate coverage of the islands prior to this date. To create Dataset 1, we simply summed up the area of wood for each date contained within the common area. To create Dataset 2, we first intersected the footprints for photographs adjacent in time, and then subtracted the polygons within the shared footprint to create a resulting shapefile that showed areas of wood that "stayed", "came", or "went" (Figure 4.D.2).

4.E. Timelapse

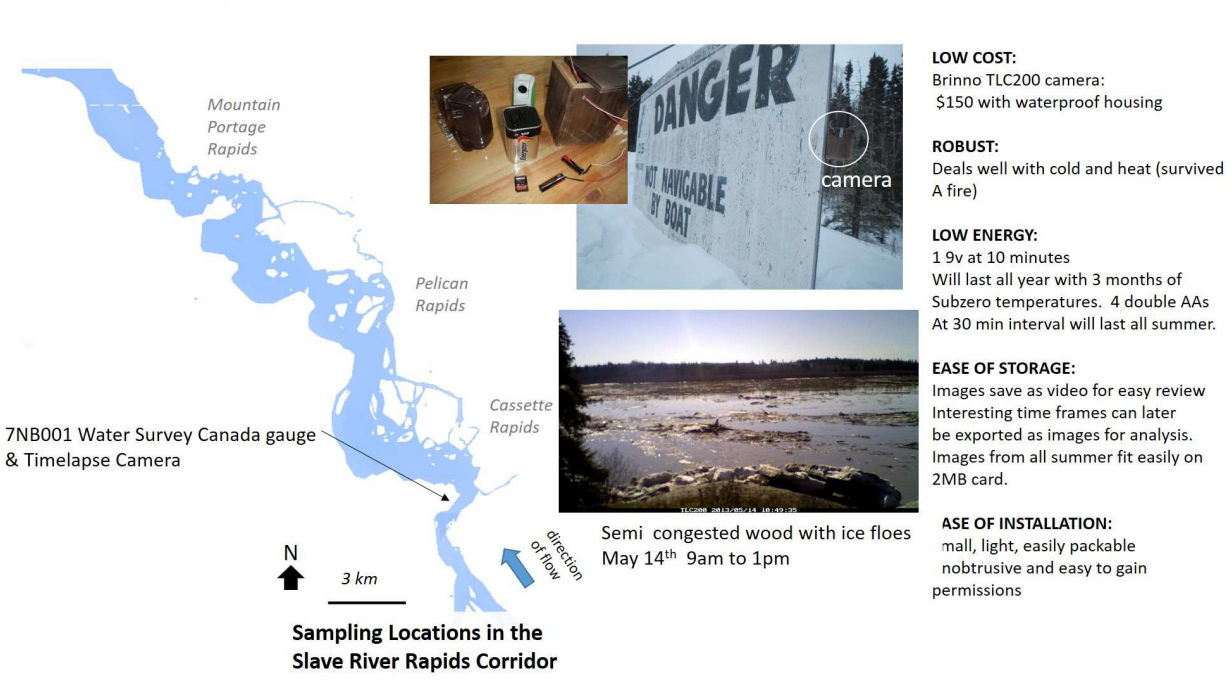

Figure 4.E.1. Location map for timelapse photography. Gauge and camera located at 59.872222° N, 111.583333° W.

FIGURE 4.E.2. Photo sequence of ice jamming with wood.

4.F. DATASETS

The following datasets and files can be accessed via the Colorado State Digital data repository under Research Project "Big River Driftwood in Northern Canada" (`http://hdl.handle.net/10217/100436`).

Data Set S1. Dataset of all measurements of wood sizes from study sites in attached file "*ds01_Largewood.csv*"

L:	Length of the bole from small end to bottom end or top of flare in rootwad in meters
Dl:	Diameter of the large end. Measured at the top of the flare if rootwad present in meters
Ds:	Diameter of the small end in meters.
Dm:	Representative diameter $(Dl + Ds)/2$ in meters)
V:	Volume modeled as $L * \pi(Dm/2)^2$ in cubic meters
Type:	D=Deciduous, C=Coniferous
Top or Bottom:	denotes type of end of the log as: S=snapped, T=un-snapped tip, R=rootwad, B=beaver chew, A=anthropogenic, such as saw cuts
D:	Decay Classes: 1=Sound, 2=Heartwood sound, sapwood decayed but can not be pulled apart, 3=Sapwood can easily be pulled off, 4=Log cannot support weight but retains shape
B:	Bark Classes: 1=Most or all bark remains, 2=Partial bark retained, 3=Remnants of bark, 4=No bark present
A:	Abrasion Classes: 1=Most branches present, including smaller ones, 2=Most branches snapped off, 3=Branch stubs, 4=Smooth
Site:	Unique site identifier
RootID:	Unique rootwad ID

Data Set S2. Dataset of small wood pieces less than 1 meter in length and 10 cm in diameter. Attached file *ds02_Smallwood.csv*

- L: Longest side of the small piece in meters
- W: Diameter or second longest side of the piece depending on shape in meters
- H: Shortest side of the piece in meters
- V: Volume of the piece in cubic meters. Estimated assuming either a cylinder ($L * \pi(W2)^2$) or a cube ($L * H * W$) depending on shape.
- type: Categorical identifying the piece as bark or stick. Beaver chew and root pieces were identified.
- site: Unique site ID.

Data Set S3. Dataset of Rootwad measurements. Attached file *ds03_Rootwads.csv*.

- RootID: Unique root identifier
- Lr: Length of rootwad measured from top of flare along the axis of the bole in meters
- W1r: Widest basal footprint width in meters
- W2r: Width of basal footprint perpendicular to W1r1 in meters
- type: D=Deciduous, C=Coniferous, U=Unknown
- Elong: Elongation Factor. L divided by the average of W1 and W2
- Symm: Base Symmetry Factor. $W1r/W2r$

Data Set S4. Data on log raft progression upstream. Attached file *ds04_logra ftposition.csv*

- Year: Photo Year
- yrchng: number of years passed since previous photograph
- distchng: meters upstream (or downstream if negative) jam front is with respect from previous photograph
- Position: upstream position of jam front in meters with respect to 1933.

Data Set S5. This is total wood storage in shared sub area from the Pelican Island Sanctuary. Data extracted from georeferenced oblique aerial photos provided by the Pelican Advisory Circle of Fort Smith. Data limited to shared area where all photos intersect. Supporting data file: *ds05_D1areas.csv*

- Date: Date, format: "year-month-day"
- Area_m2: Wood area footprint in square meters as seen from above.

Data Set S6. Change in wood storage between adjacent time periosds in the Pelican Island Sanctuary. Data extracted from georeferenced oblique aerial photos provided by the Pelican Advisory Circle of Fort Smith. Attached file: *ds06_D2change.csv*

Start:	Date "Year-month-day" of first photograph
End:	Date "Year-month-day" of second photograph
QDate:	Date "Year-month-day" of highest discharge between photographs
Qcms:	Highest averaged daily discharge between photographs in cubic meters per second.
icejam:	Factor w/ 2 levels "n","y": specifying if larges peak discharge between events was an ice break up event.
fraction:	num fraction of wood area within the time period that either came (IDnum=1), went(IDnum=-1) or stayed (IDnum=0) as identified in IDnum. For example fraction for came was calculated as came/(came +went +stayed). Shapefiles of wood are provided separately.
IDnum:	factor w/3 levels "-1", "0","1" specifying whether the entry specifies wood that went (-1) , stayed (0) or came(1)
summerindex:	day of summer with April 1=1

Data Set S7. Dataset of wood flux data derived from timelapse photos taken of the river near the Fort Fitzgerald Gauge, Slave River Slave River Rapids Corridor, Northwest Territories. The raw timelapse Photos can be accessed via `http://hdl.handle.net/10217/100436` . The derived datset is supplied as supporting file "*ds07_FFwoodphatQ.csv*"

Date:	Year-Month-Day
phat:	proportion of photos taken in that day with wood present
summerindex:	Day of summer with April 1st=1
Q:	Average daily discharge value in cubic meters per second from Fort Fitzgerald water gauge 7NB001 operated by Water Survey Canada.

4.G. Video Captions

Movie S1. Promotional research video about driftwood research in the Slave River- Great Slave Lake system, northern Canada. Attached file is *ms01_WoodResearchVideo.mp4*.

Movie S2. Animation of wood loads on the Pelican Island Sanctuary from 1980 to 2015. Location is 59.97116°N, 111.74853°W. Attached file is *ms02_PIanimation_2fps.avi*

Movie S3. Timelapse of mechanical ice break up at Fort Fitzgerald with wood transport May 13th and 14th 2013. Location is 59.868923^{c}ircN 111.582301^{c}ircW. Attached file is *ms03_FF2013051314_10min5fps_breakup.avi*.

CONCLUSIONS

The impacts of large amounts of driftwood on waterscapes - ecological and physical - are absolutely stunning both in scale and in aesthetics. In rivers draining the mostly undammed Mackenzie basin in Canada, landscape features associated with wood are abundant and reflect conditions that were likely more common in northern latitudes world-wide for the last 10,000 years up to about 200 years ago. As the world's last free flowing rivers are rapidly dammed for hydropower, I wonder: how will diminishing transport of driftwood impact the biodiversity of river corridors and marine environments? How much more at risk are wood-depleted coastlines from erosion associated with sea level rise and extreme weather? And, what impact will wood depletion have on freshwater and marine fisheries?

This dissertation is the first step in a journey to uncover the answers in that it provides new conceptual models for thinking about wood flux delivery from large basins, challenges existing assumptions, and develops new methods and approaches to quantifying wood flux. The most valuable contribution of this dissertation is the multi-temporal approach to understanding the variability of wood flux through time and linkages between transport and flow history. This research has led me to the conclusion that it is the stop and go, the jamming and unjamming, the discontinuity of wood flux, rather than wood stability, that is the most important aspect of the wood regime for river morphology, dynamics and biota.

I suggest that future studies focus on:

i. continuous or high-frequency monitoring of wood mobility;
ii. monitoring changes in wood storage at known retention sites at varying time scales;
iii. using wood characteristics to fingerprint wood sources;
iv. quantifying volumes of wood buried within channels and floodplains;
v. using remote sensing to assess changes in wood storage over large spatial scales;
vi. obtaining data from unconventional sources, such as citizen science initiatives;
vii. creating online interactive data platforms for facilitation of data synthesis; and
vii. using field and modelling data to test conceptual models and constrain transport thresholds.

BIBLIOGRAPHY

Abbe, T., and A. Brooks (2011), Geomorphic, engineering, and ecological considerations when using wood in river restoration, *Stream Restoration in Dynamic Fluvial Systems*, pp. 419–451, doi:10.1029/2010GM001004.

Abbe, T. B., and D. R. Montgomery (2003), Patterns and processes of wood debris accumulation in the Queets river basin, Washington, *Geomorphology*, *51*(13), 81–107, doi:10.1016/S0169-555X(02)00326-4.

Anderson, N. H., and J. R. Sedell (1979), Detritus processing by macroinvertebrates in stream ecosystems, *Annual Review of Entomology*, *24*(1), 351–377.

Angradi, T. R., E. W. Schweiger, D. W. Bolgrien, P. Ismert, and T. Selle (2004), Bank stabilization, riparian land use and the distribution of large woody debris in a regulated reach of the upper Missouri River, North Dakota, USA, *River Research and Applications*, *20*(7), 829–846, doi:10.1002/rra.797.

Angradi, T. R., D. L. Taylor, T. M. Jicha, D. W. Bolgrien, M. S. Pearson, and B. H. Hill (2010), Littoral and shoreline wood in mid-continent great rivers (usa), *River Research and Applications*, *26*(3), 261–278, doi:10.1002/rra.1257.

Atha, J. B. (2014), Identification of fluvial wood using Google Earth, *River Research and Applications*, *30*(7), 857–864, doi:10.1002/rra.2683.

Aufdenkampe, A. K., E. Mayorga, P. A. Raymond, J. M. Melack, S. C. Doney, S. R. Alin, R. E. Aalto, and K. Yoo (2011), Riverine coupling of biogeochemical cycles between land, oceans, and atmosphere, *Frontiers in Ecology and the Environment*, *9*(1), 53–60, doi:10.1890/100014.

Battin, T. J., L. A. Kaplan, S. Findlay, C. S. Hopkinson, E. Marti, A. I. Packman, J. D. Newbold, and F. Sabater (2008), Biophysical controls on organic carbon fluxes in fluvial networks, *Nature Geoscience*, *1*(2), 95–100, doi:doi:10.1038/ngeo101.

Battin, T. J., S. Luyssaert, L. A. Kaplan, A. K. Aufdenkampe, A. Richter, and L. J. Tranvik (2009), The boundless carbon cycle, *Nature Geoscience*, *2*(9), 598–600, doi:10.1038/ngeo618.

Beckman, N. D., and E. Wohl (2014), Effects of forest stand age on the characteristics of logjams in mountainous forest streams, *Earth Surface Processes and Landforms*, *39*(11), 1421–1431, doi:10.1002/esp.3531.

Beechie, T. J., D. A. Sear, J. D. Olden, G. R. Pess, J. M. Buffington, H. Moir, P. Roni, and M. M. Pollock (2010), Process-based principles for restoring river ecosystems, *BioScience*, *60*(3), 209–222, doi:10.1525\bio.2010.60.3.7.

Bégin, Y. (2000), Ice-push disturbances in high-boreal and subarctic lakeshore ecosystems since AD 1830, northern Québec, Canada, *The Holocene*, *10*(2), 179–189, doi:10.1191/095968300672152610.

Beltaos, S., T. D. Prowse, and T. Carter (2006), Ice regime of the lower Peace River and ice-jam flooding of the Peace-Athabasca Delta, *Hydrological processes*, *20*(19), 4009–4029, doi:10.1002/hyp.6417.

Benda, L. E., and J. C. Sias (2003), A quantitative framework for evaluating the mass balance of in-stream organic debris, *Forest Ecology and Management*, *172*(1), 1–16, doi:10.1016/S0378-1127(01)00576-X.

Benke, A. C., and J. B. Wallace (1990), Wood dynamics in coastal plain blackwater streams, *Canadian Journal of Fisheries and Aquatic Sciences*, *47*(1), 92–99.

Berg, N., A. Carlson, and D. Azuma (1998), Function and dynamics of woody debris in stream reaches in the central Sierra Nevada, California, *Canadian Journal of Fisheries and Aquatic Sciences*, *55*(8), 1807–1820, doi:10.1139/f98-064.

Berger, C. A. (2002), White spruce seed rain and germination in northwestern Alberta, Canada, Ph.D. thesis, University of Minnesota.

Bertoldi, W., A. Gurnell, and M. Welber (2013), Wood recruitment and retention: The fate of eroded trees on a braided river explored using a combination of field and remotely-sensed data sources, *Geomorphology*, *180181*, 146 – 155, doi:10.1016/j.geomorph.2012.10.003.

Bertoldi, W., M. Welber, L. Mao, S. Zanella, and F. Comiti (2014), A flume experiment on wood storage and remobilization in braided river systems, *Earth Surface Processes and Landforms*, *39*(6), 804–813, doi:10.1002/esp.3537.

Bertoldi, W., M. Welber, A. Gurnell, L. Mao, F. Comiti, and M. Tal (2015), Physical modelling of the combined effect of vegetation and wood on river morphology, *Geomorphology*, *246*, 178 – 187, doi:10.1016/j.geomorph.2015.05.038.

Bevan, A. (1948), Floods and forestry, *University of Washington Forest Club Quarterly*, US Forest Service.

Bilby, R. E. (1981), Role of organic debris dams in regulating the export of dissolved and particulate matter from a forested watershed, *Ecology*, *62*(5), 1234–1243, doi:10.2307/1937288.

Bilby, R. E., and J. W. Ward (1989), Changes in characteristics and function of woody debris with increasing size of streams in western Washington, *Transactions of the American Fisheries Society*, *118*(4), 368–378, doi:10.1577/1548-8659(1989)118⟨0368:CICAFO⟩2.3.CO;2.

Bocchiola, D., M. Rulli, and R. Rosso (2006a), Transport of large woody debris in the presence of obstacles, *Geomorphology*, *76*(12), 166–178, doi:10.1016/j.geomorph.2005.08.016.

Bocchiola, D., M. Rulli, and R. Rosso (2006b), Flume experiments on wood entrainment in rivers, *Advances in water resources*, *29*(8), 1182–1195, doi:10.1016/j.advwatres.2005.09.006.

Bocchiola, D., M. C. Rulli, and R. Rosso (2008), A flume experiment on the formation of wood jams in rivers, *Water Resources Research*, *44*(2), doi:10.1029/2006WR005846.

Boivin, M., T. Buffin-Bélanger, and H. Piégay (2015), The raft of the Saint-Jean River, Gaspé (Québec, Canada): A dynamic feature trapping most of the wood transported from the catchment, *Geomorphology*, *231*, 270 – 280, doi:10.1016/j.geomorph.2014.12.015.

Bragg, D. C. (2000), Simulating catastrophic and individualistic large woody debris recruitment for a small riparian system, *Ecology*, *81*(5), 1383–1394, doi:10.1890/0012-9658(2000)081[1383:SCAILW]2.0.CO;2.

Braudrick, C. A., and G. E. Grant (2000), When do logs move in rivers?, *Water Resources Research*, *36*(2), 571–583, doi:10.1029/1999WR900290.

Braudrick, C. A., and G. E. Grant (2001), Transport and deposition of large woody debris in streams: a flume experiment, *Geomorphology*, *41*(4), 263–283, doi:10.1016/S0169-555X(01)00058-7.

Braudrick, C. A., G. E. Grant, Y. Ishikawa, and H. Ikeda (1997), Dynamics of wood transport in streams: A flume experiment, *Earth Surface Processes and Landforms*, *22*(7), 669–683, doi:10.1002/(SICI)1096-9837(199707)22:7⟨669::AID-ESP740⟩3.0.CO;2-L.

Brock, B. E., M. E. Martin, C. L. Mongeon, M. A. Sokal, S. D. Wesche, D. Armitage, B. B. Wolfe, R. I. Hall, and T. W. Edwards (2010), Flood frequency variability during the past 80 years in the slave river delta, nwt, as determined from multi-proxy paleolimnological analysis, *Canadian Water Resources Journal*, *35*(3), 281–300, doi:10.4296/cwrj3503281.

Brooks, A. P., and G. J. Brierley (2002), Mediated equilibrium: The influence of riparian vegetation and wood on the long-term evolution and behaviour of a near-pristine river, *Earth Surface Processes and Landforms*, *27*(4), 343–367.

Brown, R. J. E. (1957), Observations on break-up in the Mackenzie River and its delta in 1954, *Journal of Glaciology*, *3*, 133–141.

Butzkueven, H., et al. (2006), MSBase: an international, online registry and platform for collaborative outcomes research in multiple sclerosis, *Multiple Sclerosis*, *12*(6), 769–774.

Cadol, D., and E. Wohl (2010), Wood retention and transport in tropical, headwater streams, La Selva Biological Station, Costa Rica, *Geomorphology*, *123*(12), 61 – 73, doi:10.1016/j.geomorph.2010.06.015.

Cenderelli, D., and E. Wohl (2003), Flow hydraulics and geomorphic effects of glacial-lake outburst floods in the Mount Everest region, Nepal, *Earth Surface Processes and Landforms*, *28*, 385–407, doi:10.1002/esp.448.

Choné, G., and P. M. Biron (2015), Assessing the relationship between river mobility and habitat, *River Research and Applications*, doi:10.1002/rra.2896.

Christoffersen, P., S. Tulaczyk, N. J. Wattrus, J. Peterson, N. Quintana-Krupinski, C. D. Clark, and C. Sjunneskog (2008), Large subglacial lake beneath the Laurentide Ice Sheet inferred from sedimentary sequences, *Geology*, *36*(7), 563–566, doi:10.1130/G24628A.1.

Church, M. (1992), Channel morphology and typology, *The Rivers Handbook*, *1*, 126–143.

Cierjacks, A., et al. (2010), Carbon stocks of soil and vegetation on Danubian floodplains, *Journal of Plant Nutrition and Soil Science*, *173*(5), 644–653, doi:10.1002/jpln.200900209.

Cohen, S. J. (1997), Mackenzie Basin impact study (MBIS): Final Report, *Tech. rep.*, Environment Canada, `http://publications.gc.ca/pub?id=9.646462&sl=0`.

Collins, B. D., D. R. Montgomery, K. L. Fetherston, and T. B. Abbe (2012), The floodplain large-wood cycle hypothesis: a mechanism for the physical and biotic structuring of temperate forested alluvial valleys in the North Pacific coastal ecoregion, *Geomorphology*, *139140*, 460 – 470, doi:10.1016/j.geomorph.2011.11.011.

Condon, W. (2013), A terrestrial biodiversity assessment for the Northwest Territories, *Tech. rep.*, Aurora Research Institute, www.nwtresearch.com.

Corenblit, D., E. Tabacchi, J. Steiger, and A. M. Gurnell (2007), Reciprocal interactions and adjustments between fluvial landforms and vegetation dynamics in river corridors: a review of complementary approaches, *Earth-Science Reviews*, *84*(1), 56–86, doi:10.1016/j.earscirev.2007.05.004.

Corenblit, D., et al. (2011), Feedbacks between geomorphology and biota controlling earth surface processes and landforms: A review of foundation concepts and current understandings, *Earth-Science Reviews*, *106*(3), 307–331, doi:10.1016/j.earscirev.2011.03.002.

Curran, J. C. (2010), Mobility of large woody debris (LWD) jams in a low gradient channel, *Geomorphology*, *116*(34), 320 – 329, doi:10.1016/j.geomorph.2009.11.027.

Daniels, M. D. (2006), Distribution and dynamics of large woody debris and organic matter in a low-energy meandering stream, *Geomorphology*, *77*(34), 286 – 298, doi:10.1016/j.geomorph.2006.01.011.

Davidson, S., L. MacKenzie, and B. Eaton (2015), Large wood transport and jam formation in a series of flume experiments, *Water Resources Research*, doi:10.1002/2015WR017446.

Davidson, S. L., and B. C. Eaton (2015), Simulating riparian disturbance: Reach scale impacts on aquatic habitat in gravel bed streams, *Water Resources Research*, doi:10.1002/2015WR017124.

Davies, N. S., J. C. Gosse, and N. Rybczynski (2014), Cross-bedded woody debris from a Pliocene forested river system in the High Arctic: Beaufort Formation, Meighen Island, Canada, *Journal of Sedimentary Research*, *84*(1), 19–25, doi:10.2110/jsr.2014.5.

Desloges, J., and M. Church (1992), Geomorphic implications of glacier outburst flooding: Noeick River valley, British Columbia, *Canadian Journal of Earth Sciences*, *29*, 551564, doi:10.1139/e92-048.

Dietrich, W. E., and J. T. Perron (2006), The search for a topographic signature of life, *Nature*, *439*(7075), 411–418, doi:10.1038/nature04452.

Dixon, S. J., and D. A. Sear (2014), The influence of geomorphology on large wood dynamics in a low gradient headwater stream, *Water Resources Research*, *50*(12), 9194–9210, doi:10.1002/2014WR015947.

Eaton, B., M. Hassan, and S. Davidson (2012), Modeling wood dynamics, jam formation, and sediment storage in a gravel-bed stream, *Journal of Geophysical Research: Earth Surface*, *117*(F4), doi:10.1029/2012JF002385.

Ecosystem Classification Group (2007), Ecological regions of the Northwest Territories: Taiga Plains, *Tech. rep.*, Department of Environment and Natural Resources, Government of the Northwest Territories, viii + 173 pp. + folded insert map.

Ecosystem Classification Group (2009), Ecological regions of the Northwest Territories: Taiga Shield, *Tech. rep.*, Department of Environment and Natural Resources, Government of the Northwest Territories, Yellowknife, NT, Canada, viii + 146 pp. + insert map.

Eggertsson, O. (1994), Mackenzie river driftwood: A dendrochronological study, *Arctic*, pp. 128–136.

Eglinton, T. I. (2008), Carbon cycle: tempestuous transport, *Nature Geoscience*, *1*(11), 727–728, doi:10.1038/ngeo349.

Elosegi, A., J. Díez, and J. Pozo (2007), Contribution of dead wood to the carbon flux in forested streams, *Earth Surface Processes and Landforms*, *32*(8), 1219–1228, doi:10.1002/esp.1549.

English, M. C., R. B. Hill, M. A. Stone, and R. Ormson (1997), Geomorphological and botanical change on the outer Slave River Delta, NWT, before and after impoundment of the Peace River, *Hydrological Processes*, *11*(13), 1707–1724, doi:10.1002/(SICI)1099-1085(19971030)11:13⟨1707::AID-HYP600⟩3.0.CO;2-O.

Everett, R. A., and G. M. Ruiz (1993), Coarse woody debris as a refuge from predation in aquatic communities, *Oecologia*, *93*(4), 475–486, doi:10.1007/BF00328954.

Forbes, D. L. (2011), State of the Arctic coast 2010: Scientific review and outlook, *Tech. rep.*, International Arctic Science Committee, Land-Ocean Interactions in the Coastal Zone, Arctic Monitoring and Assessment Programme. International Permafrost Association, Geesthacht, Germany, http://arcticcoasts.org.

Fremier, A. K., J. I. Seo, and F. Nakamura (2010), Watershed controls on the export of large wood from stream corridors, *Geomorphology*, *117*(1), 33–43, doi:10.1016/j.geomorph.2009.11.003.

Gallisdorfer, M. S., S. J. Bennett, J. F. Atkinson, S. M. Ghaneeizad, A. P. Brooks, A. Simon, and E. J. Langendoen (2014), Physical-scale model designs for engineered log jams in rivers, *Journal of Hydro-environment Research*, *8*(2), 115–128, doi:10.1016/j.jher.2013.10.002.

Gardner, J., M. English, and T. Prowse (2006), Wind-forced seiche events on Great Slave Lake: hydrologic implications for the Slave River Delta, NWT, Canada, *Hydrological Processes*, *20*(19), 4051–4072, doi:10.1002/hyp.6419.

Gibling, M. R., and N. S. Davies (2012), Palaeozoic landscapes shaped by plant evolution, *Nature Geoscience*, *5*(2), 99–105, doi:10.1038/ngeo1376.

Gibson, J., T. Prowse, and D. Peters (2006), Hydroclimatic controls on water balance and water level variability in Great Slave Lake, *Hydrological Processes*, *20*(19), 4155–4172, doi:10.1002/hyp.6424.

Gilbert, G. K., and E. C. Murphy (1914), The transportation of debris by running water, *Tech. rep.*, US Geological Survey, professional paper 86.

Gippel, C. J., B. L. Finlayson, and I. C. O'Neill (1996), Distribution and hydraulic significance of large woody debris in a lowland Australian river, *Hydrobiologia*, *318*(3), 179–194, doi:10.1007/BF00016679.

Gonor, J. J., J. R. Sedell, and P. A. Benner (1988), What we know about large trees in estuaries, in the sea, and on coastal beaches, in *From the forest to the sea, a story of fallen trees*, edited by C. Maser, R. Tarrant, J. Trappe, and J. Franklin, pp. 83–112, PNW Research Station, Portland, OR, USDA For. Ser. Gen. Tech. Rep. GTR-PNW-229.

Grant, G. E., J. E. O'Connor, and M. G. Wolman (2013), A river runs through it: conceptual models in fluvial geomorphology, in *Treatise on Fluvial Geomorphology*, edited by E. Wohl, pp. 6–21, Academic Press, San Diego, doi:10.1016/B978-0-12-374739-6.00227-X.

Gurnell, A., H. Piegay, F. Swanson, and S. Gregory (2002), Large wood and fluvial processes, *Freshwater Biology*, *47*(4), 601–619, doi:10.1046/j.1365-2427.2002.00916.x.

Gurnell, A., K. Tockner, P. Edwards, and G. Petts (2005), Effects of deposited wood on biocomplexity of river corridors, *Frontiers in Ecology and the Environment*, *3*(7), 377–382, doi:10.1890/1540-9295(2005)003[0377:EODWOB]2.0.CO;2.

Gurnell, A. M. (2003), Wood storage and mobility, in *The ecology and management of wood in world rivers*, edited by S. Gregory, K. Boyer, and G. AM, pp. 75–91, American Fisheries Society Symposium.

Gurnell, A. M., and G. E. Petts (2002), Island-dominated landscapes of large floodplain rivers, a European perspective, *Freshwater Biology*, *47*(4), 581–600, doi:10.1046/j.1365-2427.2002.00923.x.

Gurnell, A. M., D. Corenblit, D. García de Jalón, M. González del Tánago, R. C. Grabowski, M. T. O'Hare, and M. Szewczyk (2015), A conceptual model of vegetation-hydrogeomorphology interactions within river corridors, *River Research and Applications*, doi:10.1002/rra.2928.

Guyette, R. P., D. C. Dey, and M. C. Stambaugh (2008), The temporal distribution and carbon storage of large oak wood in streams and floodplain deposits, *Ecosystems*, *11*(4), 643–653, doi:10.1007/s10021-008-9149-9.

Haga, H., T. Kumagai, K. Otsuki, and S. Ogawa (2002), Transport and retention of coarse woody debris in mountain streams: An in situ field experiment of log transport and a field survey of coarse woody debris distribution, *Water Resources Research*, *38*(8), doi: 10.1029/2001WR001123.

Harmon, M. E., et al. (1986), Ecology of coarse woody debris in temperate ecosystems, *Advances in Ecological Research*, *15*(133), 302.

Harvey, A. (1984), Geomorphological response to an extreme flood : a case from southeast Spain, *Earth Surface Processes and Landforms*, *9*, 267–279, doi:10.1002/esp.3290090306.

Haschenburger, J. (2013), Bedload kinematics and fluxes, in *Treatise on Fluvial Geomorphology*, edited by E. Wohl, pp. 103–123, Academic Press, San Diego.

Heathfield, D. K., and I. J. Walker (2011), Analysis of coastal dune dynamics, shoreline position, and large woody debris at Wickaninnish Bay, Pacific Rim National Park, British Columbia, *Canadian Journal of Earth Sciences*, *48*(7), 1185–1198, doi:10.1139/e11-043.

Heidorn, P. B. (2008), Shedding light on the dark data in the long tail of science, *Library Trends*, *57*(2), 280–299, doi:10.1353/lib.0.0036.

Hickin, E. J. (1984), Vegetation and river channel dynamics, *The Canadian Geographer*, *28*(2), 111–126.

Hilton, R. G., A. Galy, and N. Hovius (2008), Riverine particulate organic carbon from an active mountain belt: Importance of landslides, *Global Biogeochemical Cycles*, *22*(1), doi:10.1029/2006GB002905.

Hogan, D. (1984), The influence of large organic debris on channel morphology in Queen Charlotte island streams, *Proceedings of the Western Division of the American Fisheries Society, Victoria, British Columbia*, pp. 263–273.

Holmes, R. M., et al. (2012), Seasonal and annual fluxes of nutrients and organic matter from large rivers to the Arctic Ocean and surrounding seas, *Estuaries and Coasts*, *35*(2), 369–382, doi:10.1007/s12237-011-9386-6.

Iroumé, A., A. Andreoli, F. Comiti, H. Ulloa, and A. Huber (2010), Large wood abundance, distribution and mobilization in a third order coastal mountain range river system, southern Chile, *Forest Ecology and Management*, *260*(4), 480–490, doi:10.1016/j.foreco.2010.05.004.

Iroumé, A., L. Mao, A. Andreoli, H. Ulloa, and M. Paz Ardiles (2015), Large wood mobility processes in low-order Chilean river channels, *Geomorphology*, *228*, 681 – 693, doi:10.1016/j.geomorph.2014.10.025.

Ives, R. (1942), The beaver-meadow complex, *Geomorphology*, *5*, 191–203.

Jackson, K., and E. Wohl (2015), Instream wood loads in montane forest streams of the Colorado Front Range, USA, *Geomorphology*, *234*, 161–170, doi:10.1016/j.geomorph.2015.01.022.

Jacobson, P. J., K. M. Jacobson, P. L. Angermeier, and D. S. Cherry (1999), Transport, retention, and ecological significance of woody debris within a large ephemeral river, *Journal of the North American Benthological Society*, *18*(4), 429–444, doi:10.2307/1468376.

Jochner, M., J. Turowski, A. Badoux, M. Stoffel, and C. Rickli (2015), The role of log jams and exceptional flood events in mobilizing coarse particulate organic matter in a steep headwater stream, *Earth Surface Dynamics*, *3*(3), 311, doi:10.5194/esurf-3-311-2015.

Johnson, S. L., F. J. Swanson, G. E. Grant, and S. M. Wondzell (2000), Riparian forest disturbances by a mountain flood - the influence of floated wood, *Hydrological Processes*, *14*, 3031–3050.

Jones, C., L. Hinzman, and K. Kielland (2013), Integrating alaskan local knowledge and science to model driftwood harvest from the yukon river in a changing climate, in *AWRA Annual Water Resources Conference*, Portland, OR.

Kail, J., D. Hering, S. Muhar, M. Gerhard, and S. Preis (2007), The use of large wood in stream restoration: experiences from 50 projects in Germany and Austria, *Journal of Applied Ecology*, *44*(6), 1145–1155, doi:10.1111/j.1365-2664.2007.01401.x.

Kang, K.-K., C. Duguay, and S. Howell (2012), Estimating ice phenology on large northern lakes from AMSR-E: algorithm development and application toGreat Bear Lake and Great Slave Lake, Canada, *The Cryosphere*, *6*(2), 235–254, doi:10.5194/tc-6-235-2012.

Keim, F., E. Skaugset, and S. Bateman (2000), Dynamics of coarse woody debris placed in three Oregon streams, *Forest Science*, *46*(1), 13–22.

Keller, E., A. MacDonald, T. Tally, and N. Merrit (1995), Effects of large organic debris on channel morphology and sediment storage in selected tributaries of Redwood Creek, northwestern California, *U.S. Geological Survey Professional Paper 1454-P*, p. 29.

Keller, E. A., and F. J. Swanson (1979), Effects of large organic material on channel form and fluvial processes, *Earth Surface Processes and Landforms*, *4*(4), 361–380, doi:10.1002/esp.3290040406.

Kennedy, D., and J. Woods (2012), The influence of coarse woody debris on gravel beach geomorphology, *Geomorphology*, *159*, 106–115, doi:10.1016/j.geomorph.2012.03.009.

Kindle, E. (1919), Notes on sedimenation in the Mackenzie River basin, *The Journal of Geology*, *26*(4), 341–360.

Kindle, E. (1921), Mackenzie River driftwood, *Geographical Review*, *11*(1), 50–53.

King, L., M. A. Hassan, X. Wei, L. Burge, and X. Chen (2013), Wood dynamics in upland streams under different disturbance regimes, *Earth Surface Processes and Landforms*, *38*(11), 1197–1209, doi:10.1002/esp.3356.

Knighton, D. (1998), *Fluvial forms and processes: A new perspective*, London.

Knudsen, J. (1970), The systematics and biology of abyssal and hadal bivalvia, in *Galathea Report*, edited by T. Wolff, pp. 7–236, Danish Science Press Ltd, Copenhagen.

Kramer, N., and E. Wohl (2014), Estimating fluvial wood discharge using time-lapse photography with varying sampling intervals, *Earth Surface Processes and Landforms*, *39*(6), 844–852, doi:10.1002/esp.3540.

Kramer, N., and E. Wohl (2015), Driftcretions: the legacy impacts of driftwood on shoreline morphology, *Geophysical Research Letters*, *42*(14), 5855–5864, doi:10.1002/2015GL064441.

Kramer, N., and E. Wohl (in review), Rules of the road: A qualitative and quantitative review of wood transport through rivers, *Geomorphology*.

Kramer, N., E. E. Wohl, and D. L. Harry (2012), Using ground penetrating radar to unearth buried beaver dams, *Geology*, *40*(1), 43–46, doi:10.1130/G32682.1.

Kramer, N., E. Wohl, S. Leisz, and B. Hess-Homeier (in submission), Pulses of driftwood over multiple timescales in a great northern river, *Water Resources Research*.

Kuhnle, R. (2013), Suspended load, in *Treatise on Fluvial Geomorphology*, edited by E. Wohl, pp. 124–136, Academic Press, San Diego.

Lamlom, S., and R. Savidge (2003), A reassessment of carbon content in wood: variation within and between 41 North American species, *Biomass and Bioenergy*, *25*(4), 381–388, doi:10.1016/S0961-9534(03)00033-3.

Lane, E. (1955), The importance of fluvial morphology in hydraulic engineering, *Journal of Hydraulics, American Society of Civil Engineers*, *81*(747), 1–17.

Larrañaga, S., J. R. Díez, A. Elosegi, and J. Pozo (2003), Leaf retention in streams of the Agüera basin (northern Spain), *Aquatic Sciences*, *65*(2), 158–166, doi:10.1007/s00027-003-0623-3.

Lassettre, N. S., and G. M. Kondolf (2003), Process based management of large woody debris at the basin scale, Soquel Creek, California, *Tech. rep.*, Department of Landscape Architecture and Environmental Planning, Berkeley, California, prepared for California Department of Forestry and Fire Protection and Soquel Demonstration State Forest.

Latterell, J. J., and R. J. Naiman (2007), Sources and dynamics of large logs in a temperate floodplain river, *Ecological Applications*, *17*(4), 1127–1141, doi:10.1890/06-0963.

Le Lay, Y.-F., B. Moulin, and H. Piégay (2013), Wood entrance, deposition, transfer and effects on fluvial forms and processes: Problem statements and challenging issues, in *Treatise on Geomorphology, Vol 12: Ecogeomorphology*, edited by J. Shroder, pp. 20–36, Academic Press.

Lemay, M., and Y. Bégin (2012), Using ice-scars as indicators of exposure to physical lakeshore disturbances, Corvette Lake, northern Québec, Canada, *Earth Surface Processes and Landforms*, *37*(13), 1353–1361, doi:10.1002/esp.3244.

Lemmen, D. (1990), Surficial materials associated with glacial lake McConnell, southern District of Mackenzie, *Tech. rep.*, Geological Survey of Canada, current Research Part D Interior Plains and Arctic Canada, Paper 90-1.

León, L., D. Lam, W. Schertzer, D. Swayne, and J. Imberger (2007), Towards coupling a 3D hydrodynamic lake model with the Canadian Regional Climate Model: Simulation on Great Slave Lake, *Environmental Modelling and Software*, *22*, 787–796, doi:10.1016/j.envsoft.2006.03.005.

Leopold, L. B., and T. Maddock Jr (1953), The hydraulic geometry of stream channels and some physiographic implications, *Tech. rep.*, US Geological Survey, professional paper 252.

Liébault, F., and H. Piégay (2002), Causes of 20th century channel narrowing in mountain and piedmont rivers of southeastern France, *Earth Surface Processes and Landforms*, *27*(4), 425–444, doi:10.1002/esp.328.

Lienkaemper, G. W., and F. J. Swanson (1987), Dynamics of large woody debris in streams in old-growth douglas-fir forests, *Canadian Journal of Forest Research*, *17*(2), 150–156, doi:10.1139/x87-027.

Lisle, T. E., and B. Smith (2003), Dynamic transport capacity in gravel-bed river systems, in *International Workshop for Source to Sink Sedimentary Dynamics in Catchment Scale*, edited by T. Araya, M. Kuroki, and T. Marutani, pp. 187–06, Organizing Committee of the International Workshop for Sedimentary Dynamics, Sapporo, Japan, http://www.treesearch.fs.fed.us/pubs/7831.

Lucía, A., F. Comiti, M. Borga, M. Cavalli, and L. Marchi (2015), Dynamics of large wood during a flash flood in two mountain catchments, *Natural Hazards and Earth System Sciences*, *15*(8), 1741–1755, doi:10.5194/nhess-15-1741-2015.

Luppi, L., M. Rinaldi, L. B. Teruggi, S. E. Darby, and L. Nardi (2009), Monitoring and numerical modelling of riverbank erosion processes: a case study along the Cecina River (central Italy), *Earth Surface Processes and Landforms*, *34*(4), 530–546, doi:10.1002/esp.1754.

Mackenzie, A. (1793), Voyages from montreal through the continent of North America to the frozen and Pacific Oceans in 1789 and 1793, Gutenberg Ebook #35658, Released March 22, 2011: journal entry Friday June 5th, 1789.

Mackin, J. H. (1948), Concept of the graded river, *Geological Society of America Bulletin*, *59*(5), 463–512.

MacVicar, B., and H. Piégay (2012), Implementation and validation of video monitoring for wood budgeting in a wandering piedmont river, the Ain River (France), *Earth Surface Processes and Landforms*, *37*(12), 1272–1289, doi:10.1002/esp.3240.

MacVicar, B., H. Piégay, A. Henderson, F. Comiti, C. Oberlin, and E. Pecorari (2009), Quantifying the temporal dynamics of wood in large rivers: field trials of wood surveying, dating, tracking, and monitoring techniques, *Earth Surface Processes and Landforms*, *34*(15), 2031–2046, doi:10.1002/esp.1888.

Manners, R. B., M. Doyle, and M. Small (2007), Structure and hydraulics of natural woody debris jams, *Water Resources Research*, *43*(6), doi:10.1029/2006WR004910.

Mao, L., A. Andreoli, A. Iroumé, F. Comiti, and M. Lenzi (2013), Dynamics and management alternatives of in-channel large wood in mountain basins of the southern Andes, *Bosque (Valdivia)*, *34*(3), 319–330.

Marcus, W. A., R. A. Marston, C. R. J. Colvard, and R. D. Gray (2002), Mapping the spatial and temporal distributions of woody debris in streams of the Greater Yellowstone Ecosystem, USA, *Geomorphology*, *44*(34), 323–335, doi:10.1016/S0169-555X(01)00181-7, geomorphology on Large Rivers.

Martin, D. J., and L. E. Benda (2001), Patterns of instream wood recruitment and transport at the watershed scale, *Transactions of the American Fisheries Society*, *130*(5), 940–958, doi:10.1577/1548-8659(2001)130⟨0940:POIWRA⟩2.0.CO;2.

Maser, C., R. Tarrant, J. Trappe, and J. Franklin (Eds.) (1988), *From the Forest to the Sea, a Story of Fallen Trees*, 83-112 pp., United States Department of Agriculture, Pacific Northwest Research Station, Portland, OR.

Massong, T. M., and D. R. Montgomery (2000), Influence of sediment supply, lithology, and wood debris on the distribution of bedrock and alluvial channels, *Geological Society of America Bulletin*, *112*(4), 591–599.

Mazzorana, B., F. Comiti, C. Scherer, and S. Fuchs (2012), Developing consistent scenarios to assess flood hazards in mountain streams, *Journal of Environmental Management*, *94*(1), 112–124, doi:10.1016/j.jenvman.2011.06.030.

Merten, E., J. Finlay, L. Johnson, R. Newman, H. Stefan, and B. Vondracek (2010), Factors influencing wood mobilization in streams, *Water Resources Research*, *46*(10).

Merten, E. C., J. Finlay, L. Johnson, R. Newman, H. Stefan, and B. Vondracek (2011), Environmental controls of wood entrapment in upper Midwestern streams, *Hydrological Processes*, *25*(4), 593–602, doi:10.1002/hyp.7846.

Merten, E. C., P. G. Vaz, J. A. Decker-Fritz, J. C. Finlay, and H. G. Stefan (2013), Relative importance of breakage and decay as processes depleting large wood from streams, *Geomorphology*, *190*, 40–47, doi:10.1016/j.geomorph.2013.02.006.

Milburn, D., D. MacDonald, T. Prowse, and J. Culp (1999), Ecosystem maintenance indicators for the Slave River Delta, Northwest Territories, Canada, in *Environmental Indices Systems Analysis Approach*, edited by R. J. L. Yuri A. Pykh, D. Eric Hyatt, EOLSS PUblishers Co. Ltd, Oxford, UK.

Millington, C. E., and D. A. Sear (2007), Impacts of river restoration on small-wood dynamics in a low-gradient headwater stream, *Earth Surface Processes and Landforms*, *32*(8), 1204–1218, doi:10.1002/esp.1552.

Mongeon, C. (2008), Paleohydrologic reconstruction of three shallow basins, Slave River Delta, NWT, using stable isotope methods, Master's thesis, Wilfred Laurier University, Waterloo, Ontario.

Montgomery, D. R., and T. B. Abbe (2006), Influence of logjam-formed hard points on the formation of valley-bottom landforms in an old-growth forest valley, Queets river, Washington, USA, *Quaternary Research*, *65*(1), 147–155, doi:10.1016/j.yqres.2005.10.003.

Montgomery, D. R., and H. Piégay (2003), Wood in rivers: interactions with channel morphology and processes, *Geomorphology*, *51*(13), 1–5, doi:10.1016/S0169-555X(02)00322-7, interactions between Wood and Channel Forms and Processes.

Moulin, B., and H. Piégay (2004), Characteristics and temporal variability of large woody debris trapped in a reservoir on the River Rhone (Rhone): implications for river basin management, *River Research and Applications*, *20*(1), 79–97, doi:10.1002/rra.724.

Moulin, B., E. R. Schenk, and C. R. Hupp (2011), Distribution and characterization of in-channel large wood in relation to geomorphic patterns on a low-gradient river, *Earth Surface Processes and Landforms*, *36*(9), 1137–1151, doi:10.1002/esp.2135.

Murphy, M. L., and K. V. Koski (1989), Input and depletion of woody debris in alaska streams and implications for streamside management, *North American Journal of Fisheries Management*, *9*(4), 427–436.

Naiman, R. J., E. V. Balian, K. K. Bartz, R. E. Bilby, and J. J. Latterell (2002), Dead wood dynamics in stream ecosystems, in *Proceedings of the Symposium on the Ecology and Management of Dead Wood in Western Forests*, pp. 23–48, USDA Forest Service Gen. Tech. Rep. PSW-GTR-181.

Nakamura, F., and F. J. Swanson (1993), Effects of coarse woody debris on morphology and sediment storage of a mountain stream system in western Oregon, *Earth Surface Processes and Landforms*, *18*(1), 43–61, doi:10.1002/esp.3290180104.

O'Connor, J., M. Jones, and T. Haluska (2003), Flood plain and channel dynamics of the Quinault and Queets Rivers, Washington, USA, *Geomorphology*, pp. 31–59, doi:10.1016/S0169-555X(02)00324-0.

Opperman, J. J., M. Meleason, R. A. Francis, and R. Davies-Colley (2008), "livewood": geomorphic and ecological functions of living trees in river channels, *BioScience*, *58*(11), 1069–1078, doi:10.1641/B581110.

Oswald, E. B., and E. Wohl (2008), Wood-mediated geomorphic effects of a jökulhlaup in the Wind River Mountains, Wyoming, *Geomorphology*, *100*(34), 549–562, doi:10.1016/j.geomorph.2008.02.002.

Parker, G., and C. M. Toro-Escobar (2002), Equal mobility of gravel in streams: The remains of the day, *Water Resources Research*, *38*(11), 46–1, doi:10.1029/2001WR000669.

Pecorari, E. (2008), Il materiale legnoso in corsi dacqua a canali intrecciati: volumi, mobilitá, degradazione ed influenza morfologica, Ph.D. thesis, Dept. Land and Agroforest Environments, University of Padova, Italy.

Pettit, N. E., J. J. Latterell, and R. J. Naiman (2006), Formation, distribution and ecological consequences of flood-related wood debris piles in a bedrock confined river in semi-arid South Africa, *River Research and Applications*, *22*(10), 1097–1110, doi:10.1002/rra.959.

Philip, A. L. (1990), Ice-pushed boulders on the shores of Gotland, Sweden, *Journal of coastal research*, pp. 661–676.

Phillips, J. D. (2012), Log-jams and avulsions in the San Antonio River Delta, Texas, *Earth Surface Processes and Landforms*, *37*(9), 936–950, doi:10.1002/esp.3209.

Phillips, J. D., and L. Park (2009), Forest blowdown impacts of Hurricane Rita on fluvial systems, *Earth Surface Processes and Landforms*, *34*(8), 1069–1081, doi:10.1002/esp.1793.

Piégay, H., and A. Gurnell (1997), Large woody debris and river geomorphological pattern: examples from S.E. France and S. England, *Geomorphology*, *19*(12), 99–116, doi:10.1016/S0169-555X(96)00045-1.

Piégay, H., Y.-F. Le Lay, and B. Moulin (2005), Les risques liés aux embâcles de bois dans les cours d'eau : état des connaissances et principes de gestion, in *Bois mort et à cavité, une clé pour des forêts vivantes*, edited by D. Vallauri, J. André, B. Dodelin, R. Eynard-Machet, and D. Rambaud, pp. 193–202, Lavoisier et Editions Tec & Doc.

Piton, G., and A. Recking (2015), Design of sediment traps with open check dams. II: Woody debris, *Journal of Hydraulic Engineering*, *142*(2), 04015,046, doi:10.1061/(ASCE)HY.1943-7900.0001049.

Pizzuto, J. (2009), An empirical model of event scale cohesive bank profile evolution, *Earth Surface Processes and Landforms*, *34*(9), 1234–1244, doi:10.1002/esp.1808.

Polvi, L. E., and E. Wohl (2013), Biotic drivers of stream planform implications for understanding the past and restoring the future, *BioScience*, *63*(6), 439–452, doi:10.1525/bio.2013.63.6.6.

Prowse, T., et al. (2006), Climate change, flow regulation and land-use effects on the hydrology of the Peace-Athabasca-Slave system; findings from the Northern Rivers Ecosystem Initiative, *Environmental Monitoring and Assessment*, *113*(1-3), 167–197.

Ravazzolo, D., L. Mao, L. Picco, and M. Lenzi (2015a), Tracking log displacement during floods in the Tagliamento River using RFID and GPS tracker devices, *Geomorphology*, *228*, 226–233, doi:10.1016/j.geomorph.2014.09.012.

Ravazzolo, D., L. Mao, B. Garniga, L. Picco, and A. M. Lenzi (2015b), Volume and travel distance of wood pieces in the Tagliamento River (Northeastern Italy), in *Engineering Geology for Society and Territory*, vol. 3, pp. 135–138, Springer.

Reinhardt, L., D. Jerolmack, B. J. Cardinale, V. Vanacker, and J. Wright (2010), Dynamic interactions of life and its landscape: feedbacks at the interface of geomorphology and ecology, *Earth Surface Processes and Landforms*, *35*(1), 78–101, doi:10.1002/esp.1912.

Rigon, E., F. Comiti, and M. A. Lenzi (2012), Large wood storage in streams of the Eastern Italian Alps and the relevance of hillslope processes, *Water Resources Research*, *48*(1), doi:10.1029/2010WR009854.

Rinaldi, M., B. Mengoni, L. Luppi, S. E. Darby, and E. Mosselman (2008), Numerical simulation of hydrodynamics and bank erosion in a river bend, *Water Resources Research*, *44*(9), doi:10.1029/2008WR007008.

Ruiz-Villanueva, V., J. Bodoque, A. Díez-Herrero, M. Eguibar, and E. Pardo-Igúzquiza (2013), Reconstruction of a flash flood with large wood transport and its influence on hazard patterns in an ungauged mountain basin, *Hydrological Processes*, *27*(24), 3424–3437, doi:10.1002/hyp.9433.

Ruiz-Villanueva, V., E. Bladé Castellet, A. Díez-Herrero, J. M. Bodoque, and M. Sánchez-Juny (2014), Two-dimensional modelling of large wood transport during flash floods, *Earth Surface Processes and Landforms*, *39*(4), 438–449, doi:10.1002/esp.3546.

Ruiz-Villanueva, V., B. Wyżga, J. Zawiejska, M. Hajdukiewicz, and M. Stoffel (2015a), Factors controlling large-wood transport in a mountain river, *Geomorphology*, doi:10.1016/j.geomorph.2015.04.004.

Ruiz-Villanueva, V., B. Wyżga, H. Hajdukiewicz, and M. Stoffel (2015b), Exploring large wood retention and deposition in contrasting river morphologies linking numerical modelling and field observations, *Earth Surface Processes and Landforms*, doi:10.1002/esp.3832.

Ruiz-Villanueva, V., H. Piegay, M. Stoffel, V. Gaertner, and F. Perret (2015c), Analysis of wood density to improve understanding of wood buoyancy in rivers, in *Engineering Geology for Society and Territory*, vol. 3, pp. 163–166, Springer.

Ruiz-Villanueva, V., B. Wyżga, P. Mikuś, H. Hajdukiewicz, and M. Stoffel (2016a), The role of flood hydrograph in the remobilization of large wood in a wide mountain river, *Journal of Hydrology*, doi:10.1016/j.jhydrol.2016.02.060.

Ruiz-Villanueva, V., H. Piégay, V. Gaertner, F. Perret, and M. Stoffel (2016b), Wood density and moisture sorption and its influence on large wood mobility in rivers, *Catena*, *140*, 182–194, doi:10.1016/j.catena.2016.02.0010341-8162.

Rundle, L., J. Morin, D. Buckley, B. S. Buckley, D. Sinclair, and A. Maurice (2005), Great Slave Lake commercial fishery recovery strategy: Setting direction for the future, *Tech. rep.*, NWT Fishermen's Federation, Hay River.

Scheaffer, R. L., W. I. Mendenhall, L. R. Ott, and K. G. Gerow (2012), *Survey Sampling*, 7th international ed., 432 pp., Brooks Cole Cengage Learning.

Schenk, E. R., B. Moulin, C. R. Hupp, and J. M. Richter (2014), Large wood budget and transport dynamics on a large river using radio telemetry, *Earth Surface Processes and Landforms*, *39*(4), 487–498, doi:10.1002/esp.3463.

Schumm, S. A. (1977), *The Fluvial System*, vol. 338, Wiley New York.

Sear, D. A., C. E. Millington, K. D. R., and R. Jeffries (2010), Logjam controls on channel: Floodplain interactions in wooded catchments and their role in the formation of multi-channel patterns, *Geomorphology*, *116*(3-4), 305–319, doi:10.1016/j.geomorph.2009.11.022.

Sedell, J. R., P. A. Bisson, F. J. Swanson, and S. V. Gregory (1988), What we know about large trees that fall into streams and rivers, in *From the forest to the sea, a story of fallen trees*, edited by C. Maser, R. Tarrant, J. Trappe, and J. Franklin, pp. 47–81, United States Department of Agriculture, PNW Research Station, Portland, OR, for. Ser. Gen. Tech. Rep. GTR-PNW-229.

Seo, J. I., and F. Nakamura (2009), Scale-dependent controls upon the fluvial export of large wood from river catchments, *Earth Surface Processes and Landforms*, *34*(6), 786–800, doi:10.1002/esp.1765.

Seo, J. I., F. Nakamura, D. Nakano, H. Ichiyanagi, and K. W. Chun (2008), Factors controlling the fluvial export of large woody debris, and its contribution to organic carbon budgets at watershed scales, *Water Resources Research*, *44*(4), doi:10.1029/2007WR006453.

Seo, J. I., F. Nakamura, T. Akasaka, H. Ichiyanagi, and K. W. Chun (2012), Large wood export regulated by the pattern and intensity of precipitation along a latitudinal gradient in the Japanese archipelago, *Water Resources Research*, *48*(3), doi:10.1029/2011WR010880.

Shields, F. D., S. S. Knight, and J. M. Stofleth (2006), Large wood addition for aquatic habitat rehabilitation in an incised, sand-bed stream, Little Topashaw Creek, Mississippi, *River Research and Applications*, *22*(7), 803–817, doi:10.1002/rra.937.

Silvertown, J. (2009), A new dawn for citizen science, *Trends in Ecology and Evolution*, *24*(9), 467–471, doi:10.1016/j.tree.2009.03.017.

Skalak, K., and J. Pizzuto (2010), The distribution and residence time of suspended sediment stored within the channel margins of a gravel-bed bedrock river, *Earth Surface Processes and Landforms*, *35*(4), 435–446, doi:10.1002/esp.1926.

Smith, D. G. (1994), Glacial Lake McConnell: paleogeography, age, duration, and associated river deltas, Mackenzie River basin, western Canada, *Quaternary Science Reviews*, *13*(9), 829–843, doi:10.1016/0277-3791(94)90004-3.

Sutfin, N. A., E. E. Wohl, and K. A. Dwire (2016), Banking carbon: a review of organic carbon storage and physical factors influencing retention in floodplains and riparian ecosystems, *Earth Surface Processes and Landforms*, *41*(1), 38–60, doi:10.1002/esp.3857.

Thevenet, A., A. Citterio, and H. Piegay (1998), A new methodology for the assessment of large woody debris accumulations on highly modified rivers (example of two French Piedmont rivers), *Regulated Rivers: research and management*, *14*(6), 467–483.

Timoney, K. P., and A. L. Robinson (1996), Old-growth white spruce and balsam poplar forests of the Peace River Lowlands, Wood Buffalo National Park, Canada: development, structure, and diversity, *Forest ecology and management*, *81*(1), 179–196, doi:10.1016/0378-1127(95)03645-8.

Tranvik, L. J., et al. (2009), Lakes and reservoirs as regulators of carbon cycling and climate, *Limnology and Oceanography*, *54*(6), 2298–2314, doi:10.4319/lo.2009.54.6_part_2.2298.

Triska, F. (1984), Role of wood debris in modifying channel geomorphology and riparian areas of a large lowland river under pristine conditions: a historical case study, *Verhandlung Internationale Vereinigung Limnologie*, *22*(3), 1876–1892.

Turowski, J., A. Badoux, K. Bunte, C. Rickli, N. Federspiel, and M. Jochner (2013), The mass distribution of coarse particulate organic matter exported from an Alpine headwater stream, *Earth Surface Dynamics*, *1*(1), 1, doi:10.5194/esurf-1-1-2013.

Ulloa, H., A. Iroumé, M. A. Lenzi, A. Andreoli, C. Álvarez, and V. Barrera (2011), Material leñoso de gran tamaño en dos cuencas de la cordillera de la costa de chile con diferente historia de uso del suelo, *Bosque (Valdivia)*, *32*(3), 235–245.

Ulloa, H., A. Iroumé, L. Mao, A. Andreoli, S. Diez, and L. E. Lara (2015), Use of remote imagery to analyse changes in morphology and longitudinal large wood distribution in the Blanco River after the 2008 Chaitén volcanic eruption, southern Chile, *Geografiska Annaler: Series A, Physical Geography*, *97*(3), 523–541, doi:10.1111/geoa.12091.

van der Nat, D., K. Tockner, P. J. Edwards, and J. Ward (2003), Large wood dynamics of complex alpine river floodplains, *Journal of the North American Benthological Society*, *22*(1), 35–50, doi:10.2307/1467976.

Vanderburgh, S., and D. G. Smith (1988), Slave River Delta: geomorphology, sedimentology, and Holocene reconstruction, *Canadian Journal of Earth Sciences*, *25*(12), 1990–2004, doi:10.1139/e88-186.

Vaux, H. J. (Ed.) (2013), *Rosenburg International Forum: The Mackenzie River Basin*, Water and Duncan Gordon Foundation, report of the Rosenberg International Forum's worshop on transboundary relations in the Mackenzie River basin. `http://thetyee.ca/Documents/2013/06/10/Rosenberg-Report.pdf`.

Walker, L., and J. Barrie (2006), Geomorphology and sea-level rise on one of Canada's most sensitve coasts: Northeast Graham Island, British Columbia, *Journal of Coastal Research*, *39*, 220–226.

Wallace, J. B., and A. C. Benke (1984), Quantification of wood habitat in subtropical coastal plain streams, *Canadian Journal of Fisheries and Aquatic Sciences*, *41*(11), 1643–1652, doi:10.1139/f84-203.

Walter, R. C., and D. J. Merritts (2008), Natural streams and the legacy of water-powered mills, *Science*, *319*(5861), 299–304, doi:10.1126/science.1151716.

Warren, D. R., and C. E. Kraft (2008), Dynamics of large wood in an eastern U.S. mountain stream, *Forest Ecology and Management*, *256*(4), 808–814, doi:10.1016/j.foreco.2008.05.038.

Welber, M., W. Bertoldi, and M. Tubino (2013), Wood dispersal in braided streams: Results from physical modeling, *Water Resources Research*, *49*(11), 7388–7400, doi:10.1002/2013WR014046.

West, A., et al. (2011), Mobilization and transport of coarse woody debris to the oceans triggered by an extreme tropical storm, *Limnology and Oceanography.*, *56*(1), 77–85.

Westbrook, C., D. Cooper, and B. Baker (2011), Beaver assisted river valley formation, *River Research and Applications*, *27*(2), 247–256, doi:10.1002/rra.1359.

White, L., and B. R. Hodges (2003), Identification of large woody debris in acoustic bathymetry data, *Tech. rep.*, Center for Research in Water Resources, University of Texas at Austin, final Report to Texas Water Development Board under Contract No. 2003-469, CRWR Online Report 03-07.

Wipfli, M. S., J. S. Richardson, and R. J. Naiman (2007), Ecological linkages between headwaters and downstream ecosystems: transport of organic matter, invertebrates, and wood down headwater channels, *Journal of the American Water Resources Association*, *43*(1), 72–85, doi:10.1111/j.1752-1688.2007.00007.x.

Wohl, E. (2011a), Threshold-induced complex behavior of wood in mountain streams, *Geology*, *39*, 587–590, doi:10.1130/G32105.1.

Wohl, E. (2011b), Seeing the forest and the trees: wood in stream restoration in the Colorado Front Range, in *Stream Restoration in Dynamic Fluvial Systems: Scientific Approaches, Analyses, and Tools.*, pp. 399–418, American Geophysical Union Press, Washington, DC.

Wohl, E. (2013a), Floodplains and wood, *Earth-Science Reviews*, *123*, 194–212, doi:10.1016/j.earscirev.2013.04.009.

Wohl, E. (2013b), The complexity of the real world in the context of the field tradition in geomorphology, *Geomorphology*, *200*, 50–58, doi:10.1016/j.geomorph.2012.12.016.

Wohl, E. (2014a), A legacy of absence: wood removal in US rivers, *Progress in Physical Geography*, *38*(5), 637–663, doi:10.1177/0309133314548091.

Wohl, E. (2014b), Time and the rivers flowing: fluvial geomorphology since 1960, *Geomorphology*, *216*, 263–282.

Wohl, E. (2016), Bridging the gaps: wood across time and space in diverse rivers, *Geomorphology*.

Wohl, E., and N. Beckman (2014), Controls on the longitudinal distribution of channel-spanning logjams in the Colorado Front Range, USA, *River Research and Applications*, *30*(1), 112–131, doi:10.1002/rra.2624.

Wohl, E., and D. Cadol (2011), Neighborhood matters: Patterns and controls on wood distribution in old-growth forest streams of the Colorado Front Range, USA, *Geomorphology*, *125*(1), 132–146, doi:10.1016/j.geomorph.2010.09.008.

Wohl, E., and J. R. Goode (2008), Wood dynamics in headwater streams of the Colorado Rocky Mountains, *Water Resources Research*, *44*(9), doi:10.1029/2007WR006522.

Wohl, E., and F. L. Ogden (2013), Organic carbon export in the form of wood during an extreme tropical storm, Upper Rio Chagres, Panama, *Earth Surface Processes and Landforms*, *38*(12), 1407–1416, doi:10.1002/esp.3389.

Wohl, E., L. E. Polvi, and D. Cadol (2011), Wood distribution along streams draining old-growth floodplain forests in Congaree National Park, South Carolina, USA, *Geomorphology*, *126*(12), 108–120, doi:10.1016/j.geomorph.2010.10.035.

Wohl, E., K. Dwire, N. Sutfin, L. Polvi, and R. Bazan (2012), Mechanisms of carbon storage in mountainous headwater rivers, *Nature communications*, *3*, 1263, doi: 10.1038\ncomms2274.

Wohl, E., S. N. Lane, and A. C. Wilcox (2015), The science and practice of river restoration, *Water Resources Research*, *51*(8), 5974–5997.

Wolfe, B. B., et al. (2007), From isotopes to TK interviews: towards interdisciplinary research in Fort Resolution and the Slave River Delta, Northwest Territories, *Arctic*, pp. 75–87.

Wyżga, B., and J. Zawiejska (2005), Wood storage in a wide mountain river: case study of the Czarny Dunajec, Polish Carpathians, *Earth Surface Processes and Landforms*, *30*(12), 1475–1494, doi:10.1002/esp.1204.

Young, M. K. (1994), Movement and characteristics of stream-borne coarse woody debris in adjacent burned and undisturbed watersheds in Wyoming, *Canadian Journal of Forest Research*, *24*(9), 1933–1938, doi:10.1139/x94-248.